Optochemical detection strategies for heavy metals in water

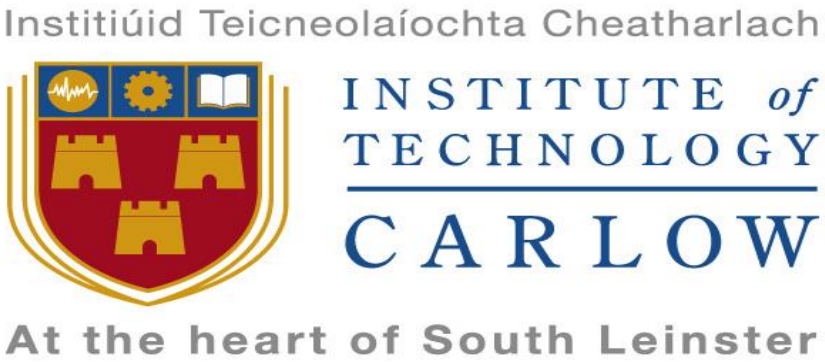

By

Annija Lace

A Thesis presented for the Degree of Doctor of Philosophy Submitted to the Institute of Technology, Carlow

Supervisors: Dr. David Ryan; Mr. Mark Bowkett and Dr. John Cleary

External Examiner: Dr. Blánaid White

Internal Examiner: Dr. Kieran Germaine

DECLARATION

I certify that this thesis which I now submit for examination for the award of PhD is entirely my own work and has not been taken from the work of others save and to the extent that such work has been cited and acknowledged within the text of my work.

This thesis was prepared according to the regulations for postgraduate study by research of the Institute of Technology Carlow and has not been submitted in whole or in part for an award in any other Institute or University.

The work reported in this thesis conforms to the principles and requirements of the Institute's guidelines for ethics in research.

Signature _____Date _____

Dedication:

To my grandparents Vija and Zigurds Ulmanis for your never ending support, encouragement and precious memories.

Acknowledgments

This thesis would not have been possible without the assistance of many people whom I want to acknowledge.

Firstly, I would like to thank my supervisor Dr. John Cleary. I am very grateful for his patience, invaluable advice and extensive knowledge which helped me throughout my journey of research. I would also like to thank Dr. David Ryan for his exceptional organisation skills, enthusiasm and help throughout my project. I would also like to thank Mark Bowkett for providing me access and assistance in TE Laboratories.

Many thanks to all members of EnviroCORE, both past and present for your help. I would also like to thank the engineers and chemists in TE Laboratory. I would especially like to thank Patrick Roche for all his time and help with the microfluidic chip work. I would also like to thank Eoin Murray for his advice and technical assistance.

I would like to take this opportunity to thank my family for their support and encouragement. I would also like to thank Navodita, Sandra, Loriane, Anusha and Ankit for the emotional support, gourmet lunch breaks, and most importantly, all the laughter. Finally, I would like to express gratitude to my fiance Christopher Finnegan for his encouragement, never ending patience and being there for me no matter the weather.

Funding Acknowledgement

This study was carried out at EnviroCORE, Department of Science and Health, Institute of Technology Carlow, Ireland. We acknowledge support from the Institute of Technology Carlow President's Research Fellowship Programme fund, Development and Research Postgraduate fund and Irish Research Council grant GOIPG/2016/301.

Abstract

Groundwater contamination by toxic heavy metals is a serious global issue, therefore, there is an increasing demand for fast, portable and reliable on site monitoring methods for heavy metals in water. Conventional laboratory based methods are not capable of meeting this demand as they require expensive instrumentation and highly trained technical staff. Consequently, cost effective and user friendly alternative methods are needed. Microfluidic detection devices have been employed for routine monitoring of water quality parameters such as nutrients, however, a limited number of commercially available techniques are available for heavy metal monitoring in water. Although numerous examples of optical methods for heavy metals have been described in the literature, only a small number of these methods have been successful in real applications.

The aim of this research was to develop an optical method for heavy metal monitoring using microfluidic detection systems, and thereby enhance the range of available techniques for water quality analysis. An extensive literature review was carried out to identify candidate optochemical based heavy metal detection methods which could be further optimised and integrated into microfluidic detection systems. Preliminary screening was carried out in the laboratory using UV-vis spectroscopy to assess different optochemical method suitability for application in microfluidic detection systems. Micro scale quartz cuvettes were used to replicate the restricted path length in microfluidic detection chip.

For chromium detection in water, a 1,5-diphenylcarbazide method was assessed. Parameters such as colour stability, reaction time, reagent stability, the effect of interfering ions, linear range, and limit of detection were investigated. Additionally, the method's effectiveness to monitor the target analyte in environmental water samples with various matrices was evaluated. A strong analytical signal was obtained from experiments carried out in micro scale quartz

cuvettes. In addition, simple reagent to sample ratio was obtained by combining the reagents, which in turn enables cost effective microfluidic detection system design. The method showed great potential for use in microfluidic detection system.

For arsenic monitoring in water, methods based on leucomalachite green, variamine blue, and molybdenum blue were assessed. Similarly to the chromium method's assessment optimum reaction conditions, reproducibility, colour stability, linear range, and limit of detection were determined for the different arsenic detection methods. The leucomalachite green method was chosen for integration into microfluidic detection systems due to its fast reaction time, strong colour development, and ability to detect arsenic in various environmental water samples. The analytical system used was based on an existing microfluidic platform developed by project partners TE Laboratories, with appropriate revisions as required to incorporate the optimised optical method.

Polymethyl methacrylate microfluidic detection and mixing chip was designed for arsenic detection using leucomalachite green method. The microfluidic detection system's design was optimised in order to enhance the reagent and sample mixing efficiency. LED and photodiode were coupled to the detection channel and served as miniaturised UV-vis photometer. Syringe pumps were used for sample and reagent introduction. A range of spiked arsenic samples were analysed using the microfluidic detection system. In addition, the effect of iron interference on arsenic monitoring was investigated. Linear range and limit of detection for the microfluidic detection method were determined. As a result, a novel arsenic determination method based on microfluidic detection was developed. Although the method's linear range was too high to be used for arsenic determination in most environmental waters, it showed a great potential for arsenic monitoring in ground or surface waters with known high arsenic concentrations as well as in waste waters.

Table of contents

List of Figures

List of Equations

List of Tables

Structure of thesis

Chapters 1-5 in this thesis are written and formatted as journal manuscripts. Each chapter contains an abstract, introduction, methodologies, results and the respective discussion and conclusion. Chapter 6 contains a conclusion and future work recommendations. Chapter 7 includes the dissemination of this thesis both nationally and internationally. Lastly, Chapter 8 presents a bibliography of the reference material used throughout this thesis.

Safety protocol

Sodium meta arsenite ($NaAsO_2$) is toxic and harmful to the environment. Potassium dichromate ($K_2Cr_2O_7$) is a strong oxidizer and is detrimental to aquatic life. Great care must be exercised when using these compounds. Additionally, appropriate control measures must be put in place to manage risks before performing the method described in this thesis. Contact with skin and eyes should be avoided when handling sodium meta arsenite and potassium dichromate. Both chemicals should be handled with nitrile rubber gloves and safety glasses should be worn at all times. Proper glove removal technique should be used and used gloves should be disposed of in accordance with good laboratory practice. Hands should be washed and dried after using the chemicals.

Unused and non-recyclable solutions of sodium meta arsenite and potassium dichromate should be sent to a licensed disposal company and disposed of as heavy metal waste in accordance with the Directive on waste 2008/98/EC. Contaminated packaging should be disposed of the same way as the unused product.

In addition, the material safety data sheets (MSDS) must be read before using the chemicals.

Key safety requirements:

- Standard solutions must be handled in a fume hood.
- Personal protective equipment must be worn when handling the substances.
- Material should be stored in tightly sealed and labelled containers away from oxidizers, acids or halogens in a cool, dry place.

Abbreviations

AAS	atomic absorption spectrophotometry
ANOVA	analysis of variance
DMF	digital microfluidics
DPC	1,5-diphenylcarbazide
DPCA	1,5-diphenylcarbazone
EU	European Union
GF-AAS	graphite furnace atomic absorption spectrometry
HG-AAS	hydrate generation atomic absorption spectrometry
ICP-MS	inductively coupled plasma-mass spectrometry
ICP-OES	inductively coupled plasma-
LED	light emitting diode
LIF	laser induced fluorescence
LMG	leucomalachite green
LOD	limit of detection
LOQ	limit of quantification
M	molar
m	slope
MG	malachite green
mg L^{-1}	milligrams per litre/ parts-per-million

PDMS	polydimethylsiloxane
PMMA	polymethyl methacrylate
PVC	polyvinyl chloride
QCM	quartz crystal microbalance
R^2	coefficient of determination
RSD	relative standard deviation
SD	standard deviation
Se	standard error
SPR	surface plasmon resonance
USB	universal serial bus
UV-vis	ultraviolet visible
v/v	volume by volume
w/v	weight by volume
WHO	World Health Organization
$ʎ_{max}$	lambda max
µPADs	paper-based microfluidic analytical devices
µg L^{-1}	micrograms per litre/ parts-per-billion

Chapter 1

A Review of Microfluidic Detection Strategies for Heavy Metals in Water

This chapter was based on the following article submitted to the Journal: Microchemical Journal

A REVIEW OF MICROFLUIDIC DETECTION STRATEGIES FOR HEAVY METALS IN WATER

Authors: Annija Lace, David Ryan, and John Cleary

1.1 Abstract

Heavy metal pollution of water has become a global issue, especially in developing countries. Heavy metals are toxic to living organisms even at very low concentrations. Therefore, effective and reliable heavy metal detection in environmental water is very important. The current laboratory based methods used for heavy metal detection in water require highly trained technicians and sophisticated instrumentation, which makes them expensive for applications such as routine heavy metal monitoring in the environment. Consequently, there is a growing demand for autonomous detection systems that could be applied for *in situ* measurements in the field. Microfluidic detection systems which are defined by their small size have many characteristics that make them suitable for environmental analysis. Some of the advantages associated with microfluidic detection systems include portability, fast sample throughput, reduced reagent consumption, increased fluid control, and reduced production cost. This review is focused on the recent developments in microfluidic detection system applications to heavy metal detection in water. The latest microfluidic detection strategies based on optical, electrochemical, and quartz crystal microbalance techniques are outlined in this review.

Keywords: *heavy metals, microfluidics, environmental monitoring, water, detection methods*

1.2 Introduction

It is estimated that around 884 million people in the world consume water from unsafe sources (Cobbina *et al.*, 2015). Heavy metal pollution of drinking water is a critical issue affecting numerous countries world wide. Heavy metals can be introduced into the environment through anthropogenic activities such as mining, improper disposal of industrial waste and use of heavy metal containing pesticides and fertilisers. Additionally, poor management of agricultural and industrial waste have contributed to increased water pollution (Koop *et al.*, 2017). Cases of elevated heavy metal concentrations in groundwater have been reported in various regions around the world, including Bangladesh (Petrusevski *et al.*, 2007), Thailand (Choprapawon *et al.*, 1997) China (Hu *et al.*, 2016) and Japan (Ekino *et al.*, 2007).

Metals with densities higher than 5 g cm^{-3} are defined as heavy metals (Flexner *et al.*, 1987). Heavy metals bioaccumulate in living organisms and are toxic to human health even at very low concentrations. The greatest risk to human health is caused by arsenic, cadmium, mercury, and lead. In addition, chromium, nickel, cobalt, iron and manganese are also known to cause harm to human health at elevated concentrations (Fernandez-Luqueno *et al.*, 2013). Humans are exposed to heavy metals through consumption of contaminated food, water and air. Children are most commonly exposed to heavy metals through ingestion, while industrial exposure is common in adults (Masindi *et al.*, 2018). Various agencies and organisations such as World Health Organisation (WHO) and Council of the European Union directive 98/83/EC (EC) have set drinking water guidelines for heavy metals in water (Table 1.1).

Table 1.1. Drinking water quality guidelines (μg L^{-1}) for heavy metals.

Heavy metal	Symbol	WHO[a]	EC[b]	US EPA[c]
Arsenic	As	10	10	10
Cadmium	Cd	3	5	5
Chromium	Cr	50	50	100
Copper	Cu	2000	2000	1300
Cobalt	Co	-	-	100
Iron	Fe	-	200	300
Lead	Pb	10	10	15
Manganese	Mn	100	50	50
Mercury	Hg	1	1	2
Nickel	Ni	70	20	-

a, World Health Organisation (WHO 2011); b, Council of the European Union directive 98/83/EC (EC, 1998); c, United Stated Environmental Protection Agency (US EPA 2011).

There is a great demand for regular water quality monitoring and assessment in order to identify and prevent heavy metal pollution in water. Sensitive and selective methods are required for effective heavy metal monitoring in both groundwater and surface water. To date water monitoring is largely based on manual sampling followed by laboratory analysis (Cleary *et al.*, 2013). A wide range of techniques have been employed for heavy metal detection in water, including atomic absorption spectrometry (AAS) (Bagheri *et al.,* 2012), electrothermal atomic absorption spectrometry (ETAAS) (Gomez *et al.*, 2007), flame atomic absorption spectrometry (FAAS) (Sohrabi *et al.*, 2013), energy dispersive X-ray fluorescence (EDXRF) (Obiajunwa *et*

al., 2002), inductively coupled plasma mass spectrometry (ICP-MS) (Djedjibegovic *et al.,* 2012) and inductively coupled plasma optical emission spectrometry (ICP-OES) (Faraji *et al.,* 2010). Although these methods are sensitive and highly accurate, there are several disadvantages associated with them.

Laboratory based equipment require regular maintenance and highly trained technicians in order to be used. Additionally, sample processing and maintenance costs are high for these detection instruments. Furthermore, sample collection and transportation adds additional costs which vary depending on the frequency of sampling required. Consequently, laboratory based methods are not suitable for routine high frequency sample analysis (Cui *et al.*,2015). Therefore, cost effective, sensitive and selective methods that are easy to use are required for heavy metal monitoring (Lin *et al.,* 2016).

Numerous researchers have moved to microfluidic detection in order to improve environmental analysis. Microfluidic detection systems are characterised by their ability to process small amounts of analyte using channels with dimensions ranging from ten to hundred micrometres (Whitesides *et al.*, 2006). Microfluidic detection systems can potentially incorporate important experimental steps such as sample preparation, reaction, separation and detection onto one device (Gai *et al.*, 2011). A typical microfluidic detection system requires a method for reagent and sample introduction, a method for transporting and mixing the sample and reagent within the system and a detection device (Whitesides *et al.*, 2006). Some microfluidic detection systems employ features such as membranes, pneumatic controls, monoliths and pillars which can improve the performance of the analysis (Nge *et al.*, 2013). For microfluidic devices based on optical detection a range of different components such as optical waveguides and microlenses can be utilised. This topic is outlined in more detail in reviews by Yang *et al.* (Yang *et al.*, 2018) and Gai *et al.* (Gai *et al.*, 2011).

Manz *et al.* was the first to introduce the idea of miniaturised analysis systems (Manz *et al.*, 1990). Since then rapid advances in optoelectronics have enabled miniaturisation of functional and detection components of microfluidic detection systems (Chiu *et al.*, 2017). Microfluidic detection systems have a wide range of applications, including medical diagnostics (Einav *et al.*, 2008), protein studies (Gerber *et al.*, 2009), drug screening (*Walsh et al.*, 2009), environmental monitoring (Dossi *et al.*, 2009) and food analysis (Llopis *et al.*, 2009). A variety of detection strategies, including optical detection, electrochemical and mass spectrometry, have been used for microfluidic detection. Different optical detection strategies have been outlined by Pol et al. (Pol *et al.*, 2017) and Ullah et al (Ullah *et al.*, 2018). In addition, the latest progress in electrochemical based microfluidic detection has been described by Liu et al. (Liu *et al.*, 2019), Waheed et al. (Waheed *et al.*, 2018) and Li et al. (Li *et al.*, 2018).

A range of studies have outlined the advantages of microfluidic detection systems over standard laboratory based methods (Herold *et al.*, 2009; Dong *et al.*, 2011). Firstly, the small dimensions of the detection channel enable lower reagent consumption and minimised waste production in comparison to conventional methods (Becker *et al.*, 2002; Manz *et al.*, 1992). Secondly, the high ratio between surface area and volume along with the short diffusion distance enables fast reaction times (Liang *et al.*, 2016). Thirdly, miniaturised onsite analysis of samples also reduces contamination risk during sample handling and transportation.

This review is focused on recent developments in heavy metal monitoring using microfluidic detection systems and the different detection strategies with an emphasis on optical and electrochemical based detection methods. Other metal detection strategies along with heavy metal such as arsenic, cadmium, lead and mercury are outlined in this review. Although metals such as cobalt, nickel, copper, iron, manganese, and chromium are not classified as heavy

metals, high concentrations of these metals can lead to water quality deterioration and negative effect on human health (Mohod *et al.*,2013).

1.3 Properties of heavy metals

1.3.1 Arsenic

Arsenic (As) is a highly toxic element that is widespread in the environment. Arsenic is widely distributed in Earth's crust mostly in form of arsenic sulphide, arsenides, or arsenates (Gomez-Caminero *et al.,* 2001). Arsenic is used in pharmaceuticals, wood preservation, metallurgy and semiconductor manufacturing. In the past it has also been extensively used in pesticide production. Arsenic is introduced into the environment mainly through mining and burning of fossil fuels (WHO 2000). Arsenic concentration in surface waters typically ranges between 0.1-0.8 mg L^{-1}, whereas arsenic concentrations in groundwater are generally below 10 mg L^{-1} (Smedley *et al.,* 2002). Dissolution of iron and mangansese oxides is considered to be the main cause of arsenic release in water from sediments (Gou *et al.,* 2011). Reductive dissolution of iron and manganese oxides occurs in reducing conditions near pH 7 (Smedley *et al.,* 2002).

The oxidation state determines the toxicity and mobility of arsenic. Arsenic exists in the environment in several oxidation states- -III, 0, III and V. As III is the most mobile and also the most toxic of As species in water (Dzombak *et al.,* 1990). It is estimated that arsenite is hundred times more toxic than arsenate. The ratio between As III and As V in groundwaters can differ depending on the diffusion of oxygen from the atmosphere, microbial activity and presence of organic carbon. As III is most commonly found in waters with reducing conditions in presence of organic carbon, iron and sulfate and low dissolved oxygen concentrations (Tuzen *et al.,* 2010, Seyler *et al.,* 1990). Arsenic becomes mobile at pH values typical to groundwaters (pH 6.5-8.5). In anoxic waters with pH below 9.2 H_3AsO_3 is the dominant species (Smedley *et al.,* 2002).

Unlike arsenite, arsenate is stable in oxygen rich environments and, therefore, is the dominant species in surface waters (Fischel *et al.,* 2015, Seyler *et al.,* 1990). The most commonly found As V species are monovalent H_2AsO and divalent $HAsO_2$. At pH below 6.9 and oxidising conditions H_2AsO_4 is the dominant form of arsenic, whereas at higher pH conditions $HAsO_2$ Is more commonly found (Smedley *et al.,* 2002).

Arsenite can oxidise to arsenate during water sampling process, transportation or storage. Therefore, accurate on site determination of arsenite is important in toxicity studies (Bissen *et al.,* 2003).

Chronic exposure to high concentrations of arsenic through drinking water can result in a condition known as arsenicosis (Argos *et al.,* 2010). The various symptoms of arsenicosis include skin damage, circulatory system damage, renal system failure and development of various cancers (Mandal *et al.,* 2002; Kapaj *et al.,* 2006).

Arsenic can be introduced in the environment through mining activity and combustion of fossil fuels. In mining areas arsenic concentrations can reach $\mu g\ L^{-1}$ level. One of the worst arsenic contamination cases that arose as a result of mining activity has been documented in Ron Phibun district, Thailand. Arsenic concentrations as high as 5000 $\mu g\ L^{-1}$ were found in the groundwaters near the mining site (Choprapawon and Rodcline, 1997).

High concentrations of inorganic arsenic occur naturally in the groundwater of Bangladesh. The maximum allowable concentration of arsenic in Bangladesh is 50 $\mu g\ L^{-1}$. Arsenic concentrations as high as 2500 $\mu g\ L^{-1}$ have been recorded in numerous groundwater samples obtained from the region's wells (Petrusevski *et al.,* 2007).

Additionally, elevated arsenic concentrations have been reported in Vietnam's rural groundwater. Millions of people are exposed to groundwater exceeding arsenic concentration of 3050 µg L^{-1} which greatly exceeds the WHO limit of 10 µg L^{-1} (Berg *et al.*, 2001).

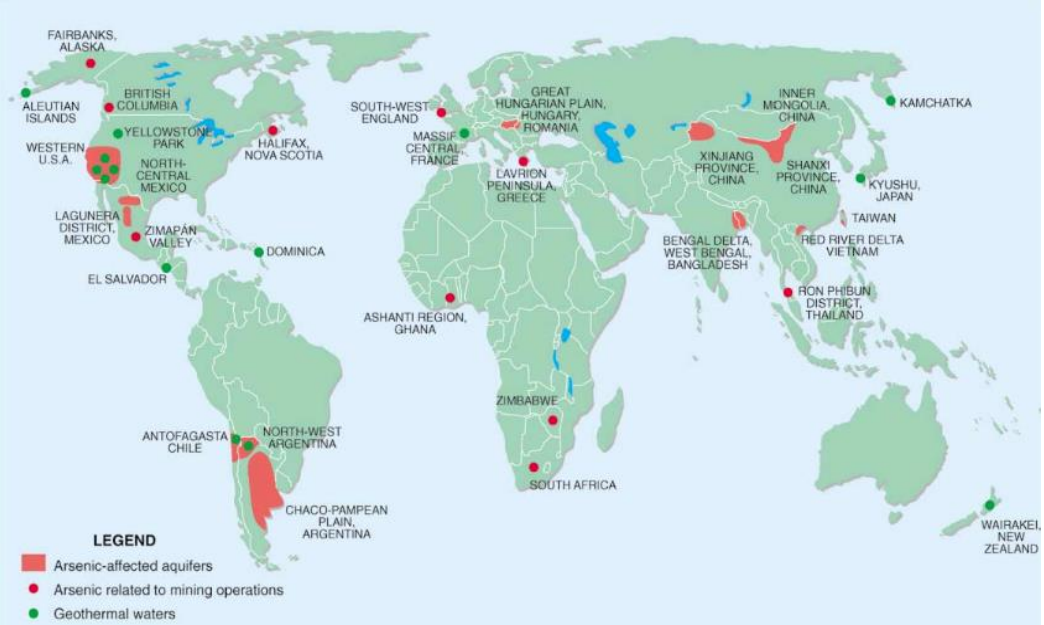

Figure 1.1. Areas with high arsenic concentrations in groundwater and surface water sources. The figure is reproduced from Yogorajah *et al.*, 2015 with permission from Elsevier.

1.3.2 Lead

Lead (Pb) is a naturally occurring metal which can be found in rocks and soil, water and air (Tchounwou *et al.*, 2012). Lead occurs in natural waters at very low concentrations as lead salts are poorly soluble in water. Typically, lead concentrations in surface water and groundwater ranges between 0.2-200 µg L^{-1} (Env. Disposal of lead 2017). Lead is widely used in battery production, paints and electroplating (Sharma *et al.*, 2009). Lead is usually introduced into the environment through industrial effluents and mining activity. Use of lead pipes, solders, and fittings in plumbing systems can result in lead transfer into tap water (Quinn *et al.*, 1990).

Lead can exist in a wide range of oxidation states in the environment, such as I, II, II and IV with Pb (II) being the most toxic form of lead (Abadin *et al.,* 2007). Pb II is the dominant species of lead in the environment at pH values near 7. In waters where dissolved organic matter is not present Pb forms hydroxo species such as Pb OH. In most natural waters with pH range between 6.5-9.5 lead carbonate compounds are more abundant than lead hydroxo species. In polluted waters with high dissolved sulfate concentrations free lead Pb II ion is the dominant species of lead. In waters with high chloride concentrations and alkaline pH lead can be found in lead carbonate compound form such as $PbCO_3$ and $Pb(CO_3)_2$ (Powell *et al.,* 2009).

Lead is toxic to human health even at very low concentrations and can be easily absorbed through the gastrointestinal tract (Karve *et al.,* 2007). Due to the chemical similarity between lead and calcium, lead can be readily accumulated in bones (Parveen *et al.,* 2011). Exposure to lead can cause nausea, vomiting, nervous system impairment and mental health issues. In addition, lead can affect brain and liver cell permeability and cause damage (Vilar *et al.,* 2007, Asgharipour *et al.,* 2012). Lead is also known to cause haematological impairment by enzyme inhibition (Majolagbe *et al.,* 2007). Importantly, lead can be particularly damaging to children affecting their mental health and brain development (Needleman 2004).

Lead contamination of surface and groundwater has been found in Chennai, India. As a result of industrial and domestic waste dumping lead concentrations as high as 0.5 mg L^{-1} were reported (Sridhar *et al.,* 2017). In Madagascar lead concentrations obtained from groundwater pumps were found to exceed the WHO limit of 0.01 mg L^{-1} (WHO 2008; Akers *et al.,* 2015). Additionally, lead concentrations as high as 0.423 mg L^{-1} were reported in groundwater of Esfahan province, Iran. The naturally occurring high lead concentrations in this region were caused by silicate rock weathering (Pazand *et al.,* 2018).

1.3.3 Cadmium

Cadmium naturally occurs in the earth's crust at concentrations between 0.1–0.5 mg L^{-1} (Morrow 2010). Cadmium can enter groundwater through rock erosion, especially in acidic conditions (Ryan *et al.,* 2000). Cadmium is used in battery production, pigment, coating and electronic device manufacturing and plastic production (USGS 2008). Industrial practices such as mining, smelting and fossil fuel combustion have lead to an increase in cadmium levels in the environment (Chaney 1999).

Cadmium concentrations in groundwater are generally below 1 µg L^{-1}(Friberg *et al.,* 1986). Cadmium easily binds to organic substances and minerals that contain iron hydroxide (Kabata-Pendias and Pendias, 2000; Lai *et al.,* 2002). In natural waters cadmium the most commonly found oxidation states of cadmium are I and II. Cd II is the most toxic form of cadmium and is the dominant form of cadmium species in surface waters with pH below 8.5 (Moore *et al.,* 1984). In natural waters cadmium can be most commonly found as Cd II ion, $Cd(OH)_2$ and $CaCO_3$ (McComish and Ong 1988). $CaCO_3$ and $Cd(OH)_2$ are poorly soluble in water, however, interaction with oxygen and light can increase their solubility (IARC 1993). Dissolved forms of cadmium in water include Cd II, CdOH, CdCl and $CdCO_3$. Cd II occurs at pH below 8, whereas at higher pH conditions CdOH is found (Naniesnik *et al.,* 2010).

Cadmium has a tendency to bioaccumulate in living organisms and is considered a priority pollutant due to its high toxicity (Khairy *et al.,* 2014). Exposure to cadmium can result in renal damage, osteoporosis, cardiovascular problems and different types of cancers, including lung and prostate cancer (Rahimzadeh *et al.,* 2017). The WHO limit for cadmium in drinking water is 3 µg L^{-1} (WHO 2004).

Elevated cadmium concentrations have been reported in various regions in the world. In Utter Praddesh, India, cadmium concentration was found to exceed 0.05 mg L^{-1} in the groundwater

collected from wells and bores (Idrees *et al.,* 2018). In Winder, Pakistan, cadmium concentration of 30 μg L^{-1} was reported in the groundwater (Burke *et al.,* 2016).

In addition, widespread cadmium pollution of surface and groundwater has occurred in China as a result of rapid industrial development and lack of environmental protection (Hu *et al.,* 2016). It is estimated that 13 million hectares of land in China has been contaminated by cadmium (Yu *et al.,* 2006). Zhao *et al.*found cadmium concentrations as high as 45 μg L^{-1} in Liujiang River, China (Zhao *et al.,* 2018). Cadmium is easily absorbed by roots of rice plants and can accumulate to dangerous concentrations. Moreover, rice is the most widely consumed cereal in the world, therefore, cadmium pollution of rice paddies in China is a critical global concern (Hu *et al.,*2016).

1.3.4 Mercury

Mercury exists in nature primarily as elemental mercury or as a sulfide and is found in the earth's crust at approximately 0.5 mg L^{-1} (Boylan, Cain 2003). Mercury is widely used in the industry. It has an important role in lamp, laboratory and industrial instrument production. Mercury compounds are also used in pharmaceutical product manufacturing (IPCS, 2003).
In groundwater and surface waters mercury can be found at very low concentrations, usually less than 0.5 μg L^{-1}. In nature most common oxidation form of mercury is II. The solubility of mercury compounds is variable. Mercury chloride (II) is the most soluble form, whereas mercury (I) chloride and mercury sulphide have low solubility (II) (WHO/SDE/WSH/05.08/10).

Among all heavy metals, mercury is considered to be the most dangerous because of its strong affinity to sulphur containing ligands that result in the blocking of sulphydryl(-SH) groups in

proteins and enzymes (Rurack *et al.,* 2002). Methylmercury is the most toxic form of mercury and can bioaccumulate in the aquatic food chain posing a great risk to populations with high seafood intake (Clarkson 1993). Exposure to mercury can result in broad range of health defects, including gingivitis, stomatitis, renal failure, neurological disorders, ataxia and pulmonary system failure (Satoh *et al.,* 2000; Risher *et al.,* 2005). The WHO limit for mercury in drinking water is 1 μg L^{-1} (WHO 2003).

Mercury can be introduced into the environment through mining, fossil fuel emissions, volcanic activity, industrial and medical waste (Clifton 2007). One of the most infamous cases of mass mercury poisoning occurred in Minamata village, Japan, where an acetaldehyde plant released mercury waste into the sea resulting in mercury accumulation in fish and shellfish (Ekino *et al.,* 2007). It is estimated that 27 tonnes of mercury were dumped in the sea (McCurry *et al.,* 2006).

In addition, China is known to release the largest amount of mercury in the world. One of the largest mercury pollution sites in China was the Songhua River, where 113. 2 tonnes of total mercury and 5.4 tonnes of methyl mercury was discharged directly into the river (Feng *et al.,* 2005). Elevated mercury concentrations in water due to intense mining activity have been reported in numerous regions in Africa (Donkor *et al.,* 2005). For example, in Senegal mercury levels were found to exceed the standard limit ten fold in surface waters near mining sites (Gerson *et al.,* 2018). In Nagodi region, Ghana, average mercury concentration in drinking water was found to be 0.038 mg L^{-1} with concentrations as high as 0.259 mg L^{-1} reported (Cobbina *et al.,* 2015).

1.3.5 Chromium

Chromium has a major role in the industry and is used in metal plating, leather tanning, chemical manufacturing, textile production, pigment and paint manufacturing and corrosion

control. Therefore, chromium can be introduced into the environment through industrial waste disposal (Kimbrough *et al.*,1999). Chromium naturally occurs in earth's crust and can be found in rocks, soil and water (Dernbach, 2008). Chromium is found in nature in combination with other elements such as iron. Chromite ($FeCr_2O_4$) is the most commonly found chromium containing mineral (Nriagu 1988). In surface waters chromium concentrations typically range between 0.5-2 μg L^{-1}, whereas in groundwater chromium concentrations are generally below 2 μg L^{-1} (Rakhunde *et al.*,2012).

Chromium has several oxidation states, including II, III and VI, I, IV and V. Cr III and Cr VI are the most commonly found chromium forms in the water (Jin *et al.*, 2014). Cr III is the most stable Cr oxidation form and is found in surface waters where pH values range from pH 5-7 (Swietlik 1998). Cr VI is most commonly found in oxidising conditions, whereas Cr III predominates in reducing conditions (Guertin *et al.*, 2005). Cr VI is more mobile than Cr III. Cr VI mobility in groundwater is increased when pH values are above 8 (Jacks 2017). In presence of manganese oxides Cr III is oxidised to Cr VI (Jacks 2017). Cr VI is the dominant Cr species in waste water from metallurgical industry (Rakhunde *et al.*,2012).

Unlike Cr III, Cr VI is toxic and can cause ulcers, teeth abnormalities, kidney failure, intestinal bleeding, diarrhoea and different types of cancer (Katz and Salem 1993, Vinutha *et al.*, 2007, Achmad *et al.*, 2017). The WHO limit for maximum allowable chromium concentration in groundwater is 0.05 mg L^{-1} (WHO 2003).

Chromium contamination of groundwater is a big issue in Bangalore region in India, where the metal has been introduced in the environment from waste of tanneries and leather factories (Shankar *et al.*,2009). Chromium concentrations as high as 1.41 mg L^{-1} was found in the water samples from the Bangalore area. In addition, the average chromium concentration from the thirty water samples that were collected was 0.173 mg L^{-1}.

In 1987 elevated chromium concentrations were found in the groundwater of Liaoning Province in China. The mortality rates for stomach and lung cancer were significantly higher in the villages located in the region compared to other regions. Waste water containing hexavalent chromium was being released in the river from a ferrochromium factory. Additionally, chromium was released in the groundwater through faulty equipment. Furthermore, with chromium concentrations exceeding 0.5 mg L^{-1} the water in the wells had turned yellow (Beaumont *et al.,* 2008).

1.3.6 Iron

Iron is one of the most commonly found metals of Earth's crust. Iron oxides have an important role in pharmaceutical and cosmetic industry, paint production and ink manufacturing (Egirani *et al.,* 2018). In natural waters iron occurs in several oxidation forms: I,II and III (Chaturvedi *et al.,* 2012). In oxygen rich waters ferric iron (Fe II) is stable and in conditions with neutral pH forms insoluble hydroxides. Ferrous iron (Fe III) is stable in anoxic waters and in presence of high carbonate, sulphide and orthophosphate concentrations forms insoluble salts (Xing *et al.,*2011).

Generally, iron concentrations in groundwater are below 0.3 mg L^{-1}. In surface water iron concentrations typically range between 0.5-10 mg L^{-1} (National Research Council 1979).

High iron concentrations in water are known to result in numerous issues, including corrosion of water pipes, coloration of water and undesired taste (Mehta *et al.,*2012). Additionally, iron can enable bacterial growth in water supply systems which results in biofilm formation on pipes (Department of National Health and Welfare 1990). High iron consumption can have a negative impact on human heath causing heamochromatosis, gastrointestinal irritation and cardiovascular issues (Rao *et al.,* 2008, Agrawal *et al.,* 2017). Iron is introduced into the surface water and groundwater through waste disposal, mining activity and corrosion of iron

pipes (Sarkar *et al.,* 2013; Ghosh *et al.,* 2008). Due to extensive agriculture in the Upper Yamuna basin, India, the iron levels in region's groundwater have reached 4 mg L^{-1} (Sarkar *et al.,* 2018). Iron concentrations below 2 mg L^{-1} do not pose risk to human health, however, discolouration of the water might be present (EPA 2014). Therefore, EC has set a standard limit of 200 µg L^{-1} for iron in drinking water (EC 1998).

1.3.7 Manganese

Manganese is naturally found in surface and groundwater, however, anthropogenic activity can lead to excessive manganese concentrations. Manganese is widely used for the manufacturing of iron and steel alloys (IPCS, 1999). Manganese can enter the groundwater through weathering of manganese containing minerals (Groschen *et al.*,2009). Manganese is found in a wide range of geological systems and it naturally occurs in three oxidation states: II, III and IV (Post *et al.,* 1999). Mn II is highly mobile in surface and groundwater especially in acidic conditions (Crerar 1980). Manganese is considered an essential nutrient in human diet, however, excessive consumption can have an adverse effect on the nervous system. A study by Bouchard et al. showed that chronic exposure to drinking water containing manganese has a negative effect on children (Bouchard *et al.,* 2010). Similar findings have been reported by He *et al.* , Zhang *et al.* and Wasserman *et al.* (He *et al.,* 1994; Zhang *et al.,* 1995; Wasserman *et al.*,2006).

The WHO limit for manganese was 0.4 mg L^{-1}, however, in 2011 this limit was discontinued as it was considered too high (Frisbie *et al.,* 2012).

1.3.8 Cobalt

In nature cobalt is most commonly found in form of arsenides and sulphides. Cobalt can be found in a wide range of different oxidations states: -I, I, II, III and V. Co II is the most common oxidation form. In oxidising environmental conditions Co II oxidised to Co III which is higly mobile (Barałkiewicz *et al.*, 1999). Cobalt naturally is found at concentrations below 5 μg L^{-1} in groundwater and surface waters. It can be introduced into the environment through natural processes such as weathering, erosion of rocks and volcanic activity (Barceloux *et al.*,1999). Additionally, cobalt can enter into the environmental water through mining and smelting processes (Smith *et al.*, 1981). Exposure to high concentrations of cobalt can result in cardiovascular and pulmonary defects (Sheikh *et al.*, 2016).

1.3.9 Copper

In the environment copper can be found in three oxidation states: 0, I and II (National Research Council. 2000). In surface water copper concentration can range between 0.5 to 1000 μg L^{-1}. The average copper concentration in groundwater is 5 μg L^{-1} (ATSDR 2004). Incineration and mining are the main sources of copper pollution. Additionally, copper can be enter the water through industrial discharge and antifouling paints (IPCS 1998). Copper can leach into drinking water trough copper containing water pipes especially at low pH and high temperature (National Research Council. 2000).

Copper is considered an essential nutrient in the human diet, however, at elevated concentrations it can result in gastro intestinal problems and liver damage (Delves *et al.*, 1980, Fitch *et al.*, 1993). The WHO limit for copper is 2000 μg L^{-1} (WHO 2004). Elevated copper concentrations have been reported in the United Kingdom, where copper levels in private water supply were found to be as high as 26 mg L^{-1} (Fewtrell *et al.*, 1996). High copper concentrations

were also found in water samples collected from households in Berlin, Germany, with maximum copper concentration of 4.2 mg L^{-1} reported (Zeitz *et al.*, 2003).

1.3.10 Nickel

Nickel is naturally found in earth's crust. In nature nickel can be found in various mineral forms. Nickel occurs in several oxidation states: -I, I, II, III and IV. In the environment Ni II is the most commonly found oxidation state (Cempel *et al.*, 2005). Generally, nickel occurs at very small concentrations in surface waters and groundwater with concentrations ranging from 1-3 μg L^{-1} (Barałkiewicz *et al.*, 1999). Nickel concentration in surface waters ranges between and sea water is typically around 0.3 μg L^{-1} (Barceloux *et al.*, 1999).

Prolonged exposure to nickel can lead to dermatitis, cardiovascular and kidney diseases (Kitaura *et al.* 2003; Cavani 2005). Furthermore, most nickel compounds are toxic to human health. Nickel is introduced into the environment through industrial activity and mining. It is also used for stainless steel production, electroplating and electronic equipment manufacture (Denkhaus *et al.*, 2002; Cempel *et al.*, 2006). The WHO limit for nickel in water is 0.07 mg L^{-1}(WHO 2003). The EC has set a standard limit of 20 μg L^{-1} for nickel in drinking water (EC 1998).

1.4. Microfluidic detection strategies

1.4.1 Absorbance based detection

UV-vis spectroscopy is a commonly used detection method due to its sensitivity and ease of use. In a microfluidic chip optical path length through the sample is very small compared to conventional analysis which leads to decreased sensitivity of the measurements (Marle *et al.*, 2005). However, there are various strategies have been developed to address this issue. For example, optical length can be enlarged by using different channel geometries (Lu *et al.*, 2006),

use of mirrors at the end of microchannels (Billot *et al.*, 2008) and embedding waveguide optics into the microfluidic channel (Petersen *et al.,* 2002; Llobera *et al.,* 2004, Gustafsson *et al.,* 2008).

Absorbance based detection also requires a light source. A wide range of light emitting diodes (LEDs) coupled to fibre optics have been used in microfluidic detection systems. LEDs emit a relatively narrow band of wavelength, therefore, LED based sensors do not require optical couplers or monochromators (Yeh *et al.*, 2016). In addition, LEDs are robust and can withstand adverse conditions such as high humidity and mechanical vibrations (Novak *et al.,* 2007).

Milani *et al.,* developed an autonomous microfluidic detection device based on colorimetric detection for iron Fe (II) and manganese determination in water. The analytical device consisted of a polymethyl metha acrylate (PMMA) microfluidic chip, custom designed syringe pumps, LEDs, lithium battery and a microcontroller encased in a cylindrical housing. The authors used the ferrozine (3-(2-pyridyl)-5,6- diphenyl-1,2,4-triazine) method for iron determination and PAN (1-(2-pyridylazo)-2-naphthol) method for manganese determination. The ferrozine molecule upon reaction with iron formed a purple colour species with maximum absorbance wavelength (λ_{max}) of 562 nm, whereas the PAN molecule generated a red colour complex once reacted with manganese with λ_{max} at 560 nm. The limits of detection (LOD) for iron and manganese were 5.6 μg L^{-1} and 1.56 μg L^{-1}, respectively. The linear range for iron was reported to be 0.006-0.1 mg L^{-1}, and the linear range for manganese was found to be 0.002-0.329 mg L^{-1}. Five minutes were required for one iron sample analysis, and ten minutes were needed for a manganese sample measurement. Moreover, the method was applied for sea water sample analysis and was not affected by high salt concentration (Milani *et al.,* 2015).

Du *et al.,* used a microfluidic detection based flow injection analysis for iron detection in water. The method utilised liquid core waveguide spectrometric detection. Flow injection and sample

introduction were carried out linearly moving an array with sample vials. Sample and carried solution were passed onto microfluidic chip by gravity and phenantroline was used as a colour reagent. Very high sample throughput was obtained with this method as the method was able to analyse 300 samples in an hour. Linear response was reported to be between 0.06-5.58 mg L^{-1} and LOD was 0.055 mg L^{-1} (Du *et al.*, 2005).

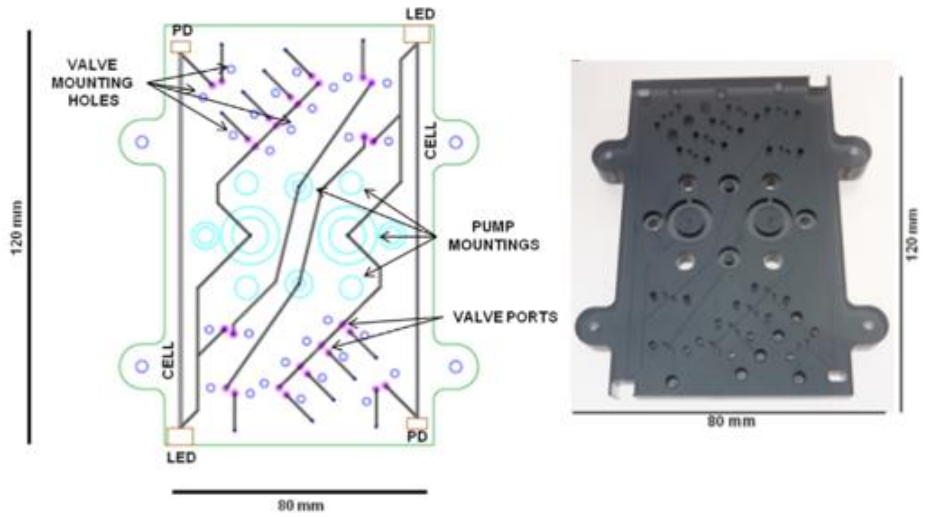

Figure 1.2. (Left) Diagram of the microfluidic chip; (right) photograph of the tinted PMMA chip (Du et al 2005). Figure reprinted from with permission from Elsevier.

Nuriman *et al.*, developed a method for mercury detection in water using optical fiber. Absorbance was measured within the microfluidic chip that contained a chromoionophore PVC film. Tris[2-(4-phenyldiazenyl)phenylamino)ethoxy]-cyclotriveratrylene was used as chromophore, and λ_{max} was found to be 495 nm. The detection system was able to measure fifteen samples in one hour. The linear range was obtained from 0.2-50.14 mg L^{-1}, and LOD was reported to be 0.1 mg L^{-1}. Furthermore, good agreement between the developed method and cold vapour atomic absorption spectrometry was obtained. The method was applied to river water sample analysis with over 90 % recovery reported. However, copper, nickel, lead, and

cadmium were found to interfere with the method at small concentrations (Nuriman *et al.*, 2011).

Microfluidic paper-based analytical devices (μPADs) have numerous properties that make them suitable for use in microfluidic detection. They are cost effective, biodegradable, portable, and can be easily produced and patterned. Additionally, no additional power sources are required for liquid transportation within the device as the liquid within the μPADs is driven by capillary force (Busa *et al.*, 2016). Satarpai *et al.*, used μPADs based on colorimetric detection for lead detection in water samples. Sodium rhodizonate in tartrate buffer was used a colour reagent which formed a pink colour upon reaction with lead. The total analysis time was less than 15 min, and the results were recorded using a digital camera. LOD was reported to be 10 μg L^{-1}, and the linear range was observed between 10 μg L^{-1} and 100 μg L^{-1}. In addition, the method was used for tap water and surface water sample analysis. Moreover, a good agreement was obtained between the novel method and graphite furnace atomic absorption spectrometry (GF-AAS) (Satarpai *et al.*, 2006).

Chauhan *et al.*, reported a method for arsenic detection in water using iron oxide nanoparticles. Arsenic was reduced to arsine by cysteine capped iron oxide nanoparticles and reacted with silver nitrate embedded onto μPAD resulting in a formation of a dark red colour complex. Ten minutes were required for complete colour formation. The LOD was reported to be 0.01 mg L^{-1}, and linear range was observed between 0.001-0.9 mg L^{-1}. The method was applied for river water analysis and showed good correlation with measurements obtained from AAS (Chauhan *et al.*, 2018).

Cai *et al.*, developed a method a distance based detection method for mercury using μPADs, where dithiozone in NaOH solution was loaded onto paper channels. Insoluble colour precipitate was formed by reaction between dithiozone and mercury. Because of the linear

relationship between the length of the precipitate and the concentration of mercury, the concentration of mercury was determined by simple measurements with a ruler. Therefore, the method did not require instrumentation making it portable and easy to use. Authors reported that cobalt, zinc, nickel and silver at concentration higher than 5 mg L^{-1} interfered with the determination of mercury. LOD was found to be 0.93 mg L^{-1}, linear range was obeyed between 1-30 mg L^{-1} (Cai *et al.,* 2017).

Chowdury *et al.,* used paper based microfluidic device with gold nanosensor functionalised with α-lipophilic acid and thioguanine for arsenic detection in well water. In presence of arsenic the nanosensor changed from red to black colour. Desktop scanner was used to analyse the results obtained from μPADs. The linear range was observed between 1- 50 μg L^{-1}. Fe III was found to interfere with the determination of arsenic. However, the interference was overcome by adjusting the pH of the water samples to 12.1. In addition, good correlation between the method's performance and ICP-OES measurements was obtained (Chowdury *et al.,* 2017).

Devadhasan *et al.,* developed chemically functionalised μPADs for nickel, Cr VI and mercury detection in water. Silane compounds terminating at amine, carboxyl and thiol groups were embedded on a chromatography paper through condensation reactions. Chromogenic reagents were coupled to the functional groups. Dimethylglyoxime was used for nickel determination which formed a pink colour upon reaction with the metal. Cr VI was reacted with 1,5 diphenylcarbazide which produced a purple colour upon reaction. Finally, Michler's thioketone was used for mercury detection which formed a brown colour upon reaction. The LOD for nickel, Cr VI and mercury was found to be 0.24 mg L^{-1}, 0.18 mg L^{-1} and 0.19 mg L^{-1}, respectively. In addition, various lake water samples were analysed using the method and the results were compared to ICP-MS measurements showing good correlation (Devadhasan *et al.,* 2018).

Gold nanoparticle application in microfluidic detection provides reduced complexity and enhanced sensitivity. In addition, gold nanoparticles are stable and show visible colour change upon aggregation (Sun *et al.,* 2014). Li *et al.,* developed a mercury detection method using a microfluidic detection with the ability to synthesise gold nanoparticles. Helium plasma was used to reduce gold ions and create nanoparticles. Gold nanoparticles were functionalised with 3-mercaptopropionic acid. The functionalised nanoparticles aggregated and changed colour from red to blue in the presence of mercury. The concentration of mercury was determined by UV-vis spectroscopy, and LOD was found to be 0.2 mg L^{-1} (Li *et al.,* 2017).

1.4.2 Fluorescence detection

Fluorescence detection is widely used due to its high selectivity and sensitivity (Reyes *et al.,* 2002, Hata *et al.,,* 2003). Some of the most commonly used excitation sources for fluorescence based detection include light emitting diodes (LEDs), laser, mercury and xenon arc lamp (Gai *et al.,* 2011). LEDs have a broad commercially available spectral range making them suitable for use as light sources (Zukauskas *et al.,* 2002; Kovac *et al.,* 2003). LEDs are competent for integration into microfluidic chips as they are very efficient at producing light and require low power current (Miyaki *et al.,* 2005).

Laser induced fluorescence (LIF) is a very sensitive method and is commonly used in combination with point detectors used as photomultiplier tubes. Laser induced fluorescence is applicable to small sample volumes and, therefore, it is suitable for use in microfluidic chips (Auroux *et al.,* 2002; Gao *et al.,* 2004; Lee *et al.,* 2005). High pressure vapour discharge lamps are commonly used in fluorescence microscopy as they have broad spectrum and wide range of wavelengths. Borodiazaindacene (BODIPY) dyes are characterised by sharp emission and absorption peaks, chemical stability and simple chemical alteration (Rezende *et al.,*2015). Bell *et al.* developed a droplet based microfluidic sensor for mercury detection in water. Gated

mesophorous nanoparticles were combined with a fluorescent BODIPY dye. Microfluidic detection system consisted of transparent perfluoroalkoxyalkane (PFA) tubing which enabled direct fluorescence measurements. LEDs were used as excitation source while the signal was obtained using optical fiber bundles. Response time was found to be 10 min, and the method yielded the optimum response at pH 7.3. Additionally, no significant interferences from other meals were reported. The LOD was 0.02 μg L^{-1}. The linear range was obtained between 0.02-200 μg L^{-1} (Bell *et al.*, 2016).

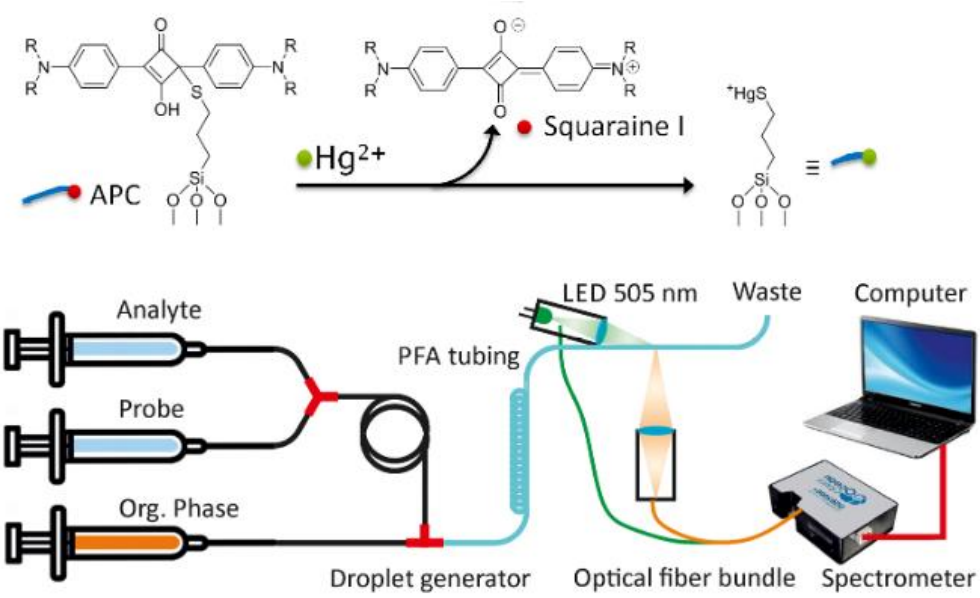

Figure 1.3. Diagram illustrating the uncapping reaction between 2,4-bis(4-dialkylaminophenyl)-3-hydroxy-4-alkylsulfanylcyclobut-2-enone (APC) and Hg (top) and the microfluidic detection system setup (bottom) (Bell *et al.*, 2016). Copyright (2016) American Chemical Society.

Kou *et al.* developed a microfluidic detection system for lead, cadmium and mercury detection in water. Inverted microscope was used for obtaining images from the detection system. Boradiazaindacene (BODIPY) was used as a fluorophore for cadmium detection with λ_{max} of

597 nm. For lead sensing a fluorescent sensor consisting of four Bis(2-pyridylmethyl)amine groups was used which showed maximum fluorescence intensity at 560 nm upon reaction with lead. Rhodamine derivative was used for mercury detection with λ_{max} of 575 nm. Mercury lamp was used for fluorescence excitation. LOD for Cd was found to be 5.62 mg L^{-1}. In addition, similar results were obtained for mercury and lead ions. Linear range for cadmium was observed between 5.62-112.41 mg L^{-1} (Kou *et al.,* 2009).

Calixarene derivatives have been widely used as building blocks and neutral molecule receptors in fluorescent reagent design (Morakot *et al.,* 2005). Faye *et al.* synthesised fluorescent sensor Calix-DANS3-OH consisting of three dansyl groups and alkyl chain for lead determination in water. The sensor was embedded in the wall of a polydimethylsiloxane (PDMS) microfluidic detection chip. LOD was reported to be 42 μg L^{-1}, and λ_{max} was found to be 496 nm. The measurements in the microfluidic detection system were carried out at pH 3 with total analysis time of 3 min. No significant interference from other metals was reported (Faye *et al.,* 2012).

Zhao *et al.* used a microfluidic detection system for lead determination water using Calix-DANS4 as a fluorimetric sensor. Y shaped microchannels were designed with optical fibre detection on a PDMS microfluidic detection chip, and the concentration of lead ions were quantified using ASV. LOD was found to be 5 μg L^{-1}. Additionally, the method was applied for surface water analysis, with calcium found to cause interference (Zhao *et al.,* 2009).

Wu *et al.* used a microfluidic detection device capable of detecting fluorescence *in situ* for lead determination in water. The microfluidic device was combined with microcolumn absorption based on a microcapillary filled with aminopropyl silica. Calix- DANS4 was used as a fluorescent sensor for lead determination in water. Emission spectra was acquired using a spectrofluorimeter. Concentration of lead was calculated by ASV. In total twenty five minutes

were required for complete analysis, and no significant interferences from other metals were reported. The linear range for lead was found to be between 2.07-16.5 μg L^{-1}, and LOD was 2 μg L^{-1}. Furthermore, the method was compared to AAS with good agreement between the measurements obtained (Wu *et al.,* 2012).

Rhodamine chromophores have been widely used for fluorescent labelling because of their unique properties, such as long wavelengths of excitation (greater than 550 nm) and emission (590 nm), good bioavailability, large absorption coefficients, and high fluorescent quantum yields (Xiang *et al.,* 2006; Lu *et al.,* 2011; Saha *et al.,* 2012; Xu *et al.,* 2012;). Kim *et al.* synthesised ethylenediamine derivative of a rhodamine 6G silica particle (RSSP) and embedded it onto a PDMS microfluidic chip for iron sensing in water samples. Aluminium and mercury were found to interfere with iron determination. However, the chemosensor was capable of detecting iron at a wide pH range. The linear range was obtained between 2-8 μg L^{-1}, and λ_{max} was found to be 552 nm (Kim *et al.,* 2016).

Zhang *et al.* used a microfluidic device based on fluorimetric detection for cadmium detection in water. Rhod-5N was used as a fluorescent sensor in a PDMS microfluidic chip with Y type mixer. The method yielded an optimum response at pH 7. LOD was 0.45 μg L^{-1}, and the linear range was found to be between 1.12-22.4 μg L^{-1}. Lead was found to interfere with the determination of cadmium, however, this issue was solved by using solid phase adsorption on aminopropyl silica (Zhang *et al.,* 2013).

Peng *et al.* developed a microfluidic detection based method for mercury determination in water using a rhodamine derivative. PDMS microfluidic chip coupled with LIF detection was used for measurements. Strong fluorescence signal in the presence of mercury was obtained at 579 nm. Copper, zinc and iron were found to cause interference with the mercury detection. Authors reported a detection limit of 0.006 mg L^{-1}. The linear range for mercury was observed

between 6.21-14.05 mg L^{-1}. In addition, the method was applied for environmental water sample analysis. The recoveries obtained for mercury from the environmental sample analysis ranged from 85-103 % (Peng *et al.,* 2017).

Flourescence signal can be enhanced with aid of metal nanoparticles (Kang *et al.,* 2011). Lafleur *et al.* used a gold nanoparticle based microfluidic sensor for mercury detection in water using PDMS microfluidic chip. Gold nanoparticles were functionalised with rhodamine 6 G. Fluorescence measurements were carried out using an inverted microscope. The LOD was found to be 0.6 μg L^{-1}, and the linear range was obeyed between 0.6-60 μg L^{-1}. The method was applied to groundwater sample analysis, where LOD was found to be 16 μg L^{-1} due to interferences in the matrix. Additionally, cadmium was found to cause interference (Lafleur *et al.,* 2012).

Digital microfluidics (DMF) use surface tension modulation induced by an electric field to manipulate sample as individual droplets. This allows to eliminate blockages, decreases the reaction time and improves sensitivity and selectivity of the method (Jebrail *et al.,* 2010). Zhang *et al.* developed a method for mercury detection in coastal water using DMF with rhodamine based fluorescent agent (1-Rhodamine B hydrazide-3-phenylthiourea). Upon reaction with mercury pink colour formation was observed. The detection system consisted of a DMF chip, controller unit and a voltage amplifier. Fluorescence spectrometer was used for measurements. Less than 20 s were required for the analysis. Linear range was obeyed between 0-10 μg L^{-1}, and the LOD was 0.7 μg L^{-1}. The method's performance was not affected by highly saline conditions. Moreover, the results obtained from the method were in good agreement with atomic fluorescence measurements (Zhang *et al.,* 2019).

1.4.3 Chemiluminescence

Chemiluminescnce based detection methods are highly sensitive and require simple instrumentation in comparison to other optical detection methods (Lee *et al.,* 2005). Additionally, chemiluminescence based detection does not require an external light source. This in turn eliminates interferences from the microfluidic substrate and background emission and makes the analysis system more cost effective (Schwarz *et al.,* 2001). However, chemiluminescence is limited to reagents such as luminol (Esch *et al.,* 2001), peroxyalata and oxalate (Broyles *et al.,* 2003) and ruthenium complexes (Bromber *et al.,* 2003). Additionally, it is affected by several factors such as temperature, pH and solution composition. Consequently, this can result in poor reproducibility (Barnett *et al.,* 2005).

Nogami *et al.* used a microfluidic detection device based on chemiluminescence for iron, copper and cobalt detection in water. 1,10 phenanthroline was reacted with hydrogen peroxide in presence of metals which served as catalysts. From the reaction dioxetane compound was obtained and transformed to excited state of 3,39-diformyl-2,29-dipyridyl. Once the compound returned to the ground state, chemiluminescence signal was emitted. The LOD for copper, cobalt and iron was found to be 0.47, 35.35 and 55.84 mg L^{-1}, respectively. Copper had a linear range between 0.47-6.73 mg L^{-1} (Nogami *et al.,* 2009).

Sun *et al.*,used a paper based microfluidic detection device for lead detection. The analysis involved incubation of the sample, followed by mixing. The detection device was made from aluminium and PMMA, and the optical signal was detected by a smartphone. Unlike conventional μPAD methods, this method used wetting and gravity as a driving force. G-quadruplex based luminescence was used for measuring lead ions. Lead ions enhance single stranded DNAs to generate a G-quadruplex which in turn enhances the luminescence of iridium probe. Linear range for lead was observed from 2-20 μg L^{-1}. The method was applied for

environmental water sample testing, however, the waste water and sea water samples required a pretreatment step. Good agreement was obtained between measurements carried out by the method and AAS and fluorescence spectrophotometry (Sun *et al.*, 2018).

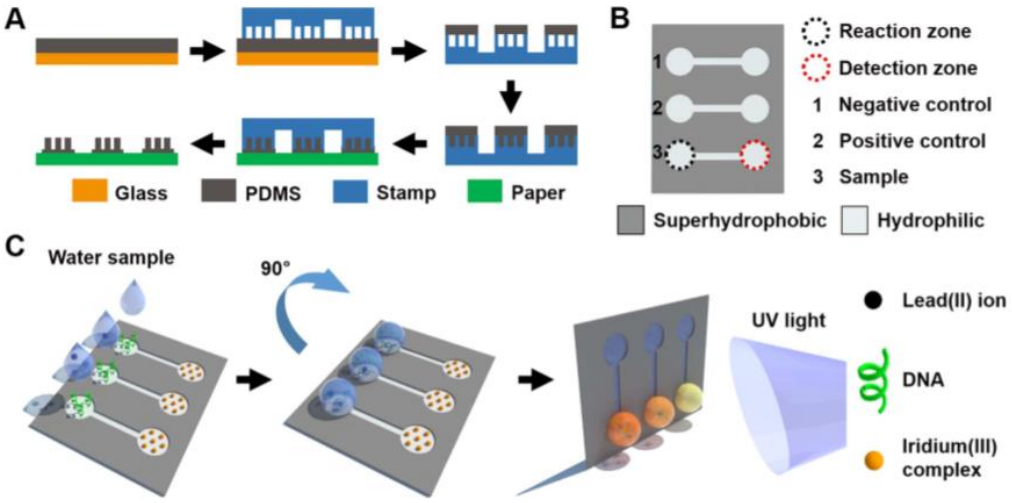

Figure 1.4. A diagram of the fabrication process of SD-µPADs by Sun *et al.*, 2018. (A) The manufacturing process of superhydrophobic coating on the paper substrate. A negative-relief Teflon stamp was placed onto a PDMS-coated glass slide and then removed to obtain a thin liquid PDMS coating. Following this, the stamp was pressed onto paper and heated at 90 °C for 15 min. The teflon stamp was peeled off, making a paper chip with superhydrophobic patterns. (B) The configuration of the paper-based chip. The zones and channels are hydrophilic, while the rest regions are superhydrophobic. (C) Diagram of lead (II) detection on the chip. The water samples were added to the reaction zone. After three minutes, the chip was turned by 90°, which enabled the droplet to travel to the detection zone and react with the iridium (III) complex. Figure reprinted with *permission from Elsevier.*

Som-aum *et al.* used a microfluidic detection device for arsenic detection in water samples based on chemiluminescence detection. Chemiluminescence was detected on chip using luminol with hetropoly acid complex. In the the presence of arsenic vanadomolybdoarsenate heteropoly acid complex was formed which is highly selective, and therefore, the luminol chemiluminescence measurements were not affected by interfering metals such as iron, cobalt and copper, however, chromate and phosphate were found to interfere with the analysis. The linear range was observed from 7.49-3.74 mg L^{-1}, and the LOD was 6.6 ng L^{-1}. Five minutes were required for complete analysis. The method was applied to arsenic determination in tap water samples and mineral water (Som-aum *et al.,* 2008).

Luminol (5-amino-2,3-dihydro-1,4-phthalazinedione) is one of the most widely used chemiluminescent compounds because of its availability and low cost (Khan *et al.,* 2014). Som-aum *et al.* developed a method for total chromium determination in water using chemiluminescence based microfluidic detection device. The chemiluminescence reaction was based on luminol oxidation by hydrogen peroxide with chromium acting as a catalyst. Sodium hydrogen sulphite was used to reduce Cr VI to Cr III. Glass microfluidic chip with a T mixer and negative pressure pumping system was used. Interference from iron, aluminium, nickel and zinc was reported. The LOD was found to be 0.31×10^{-4} ng L^{-1}, and the linear range for chromium was between 0.05×10^{-3} ng L^{-1}. The total analysis time was under one minute. Additionally, the method was applied for seawater sample analysis with good recovery obtained (Som-aum *et al.,* 2007).

Lv *et al.* used a microfluidic chip coupled with chemiluminescence for iron determination in water. Air stream sampling was used for the analysis which reduced background interference and air bubble formation, and luminol was immobilised on an exchange resin in the microfluidic chip. In total three minutes were required for each sample analysis. The linear

range was obeyed between 0.06-2.79 mg L^{-1}, and LOD was found to be 0.017 mg L^{-1}. Furthermore, good agreement was obtained between the novel method and spectrophotometry (Lv *et al.,* 2004).

Chen *et al.* developed a method for cobalt detection in water using microfluidic detection based on chemiluminescence. The reaction was based on luminol oxidation by hydrogen peroxide which took place in a PDMS chip with a serpentine mixing channel. Less than two minutes were required for the analysis. The linear range for cobalt was found to be between 0.05-1.0 mg L^{-1}, and LOD was 0.2 mg L^{-1} (Chen *et al.,* 2015).

Microfluidic paper based analytical devices are useful for chemiluminescence detection as no excitation source or optical filters are needed. Chemiluminescence based method combination with μPADs allows for low cost, simple and easily disposable detection system development (Ge *et al.,* 2014). Alahmad *et al.* developed a microfluidic paper based analytical device based on chemiluminescence detection for chromium detection in water. The μPAD was fabricated using wax printing, and optical fibers were used to capture the chemiluminescence signal. Cr III catalysed the oxidation reaction of luminol by hydrogen peroxidase with less than one minute was required for the analysis. The method did not require a separation and preconcentration step. The linear range was observed from 0.05 to 1 mg L^{-1}, and the LOD was 0.02 mg L^{-1}. Furthermore, the method was applied for water sample analysis. Good agreement was found between the method and ICP-OES (Alahmad *et al.,* 2016).

Bhandari *et al.* introduced the lab on a cloth concept (Bhandari *et al.,* 2011). Microchannels can be easily built into cloth using wax screen printing. Lab on cloths are simple and cost effective while combining the properties of conventional lab on a chip detection systems (Li *et al.,* 2017). Liu *et al.* used flow chemiluminescence for chromium detection in water using a lab on cloth device. The gravity and capillary force drove the liquid in the lab on the cloth that was

fabricated using wax screen printing. Luminol was oxidised by hydrogen peroxide with Cr III acting as a catalyst and the resulting signal was measured by charge-coupled device camera. The method had a linear range between 0.01-100 mg L^{-1}, and the LOD was found to be 6.2 µg L^{-1}. Various water samples were measured with recoveries ranging between 100 and 110 %. In addition, less than 30 s were required for sample analysis (Liu *et al.*, 2016).

1.4.4 Surface plasmon resonance

Surface plasmon resonance (SPR) can considerably enhance the sensitivity and accuracy of chemical detection and accurately detect various molecular reactions (Wang *et al.*, 2017). In this technique plasmonic waves are generated between a metal layer and a dielectric medium (Kim *et al.*, 2012). Additionally, SPR has been widely used for detection of various analytes because of characteristics such as simple design, high sensitivity and low cost (Olaru *et al.*, 2015, Tabassum *et al.*, 2016). Motalbizadeh *et al.* used a smartphone based microfluidic detection system for arsenic and mercury detection using surface plasmon resonance (SPR) of gold nanoparticles. Colour change was obtained from nanoparticle aggregate formation as gold nanoparticles reacted with dithiothreitol-10,12 pentacosadiynoic acid and lysine in presence of mercury and arsenic. The linear range for mercury and arsenic was between 710 to 1278 µg L^{-1}. The LOD for mercury and arsenic was 10.77 to 53.86 µg L^{-1}, respectively (Motalbizadeh *et al.*, 2018).

Gomez-de Pedro *et al.* developed a microfluidic detection system for mercury monitoring using modified gold nanoparticles. The mercury ions were detected by synthesised thiourea ionophores which were attached to the nanoparticles. Upon reaction with mercury ions a change of the gold SPR band was obtained. The microfluidic device set up consisted of a flow in injection analysis system. Optimum results were obtained with a flowrate of 1.6 ml min^{-1}, with 3.3 min required for one sample analysis. The LOD was found to be 11 µg L^{-1}, and the

linear range was observed between 11 -100 µg L^{-1}. No significant interference was reported (Gomez-de Pedro *et al.,* 2013).

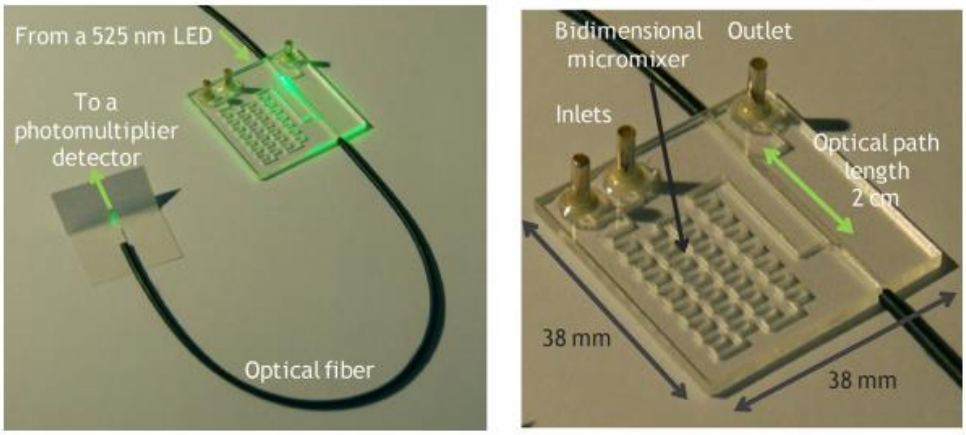

Figure 1.5. Images of a microfluidic platform for the continuous monitoring of Hg (II) (Gomez-de Pedro *et al.,* 2013). The figure is reproduced with permission from Elsevier.

Apilux *et al.* developed a µPADs for mercury detection in water using silver nanoparticles. Interaction between mercury ions and silver nanoparticles was examined by scanning electron microscope. Silver nanoparticles were oxidised by mercury ions resulting in particle fragmentation, and consequently, change of SPR band. In addition, the method was precise, with maximum RSD of 8.6 % reported. The linear range was obeyed between 5-75 mg L^{-1}, and LOD was 12 mg L^{-1}. Moreover, the method was applied for mercury detection in spiked drinking and tap water samples with high recoveries obtained (Apilux *et al.*, 2012).

Although silver and gold nanoparticles are widely used for SPR based analysis they are reportedly toxic (Johnston *et al.*, 2010, Lapresta-Fernandez *et al.*, 2012). In contrast, curcumin nanoparticles are nontoxic and it can readily chelate a range of different metals. Pourreza *et al.* developed a chemosensor for mercury detection in water using curcumin nanoparticles integrated into a paper based analytical device. With preconcentration the linear range was observed between 0.01-0.4 mg L^{-1}, and LOD was 0.003 mg L^{-1}. The method was precise, with RSD of 4.47 % reported. No interference was reported. The method was applied for various

environmental water sample analysis, with good agreement found between the measurements carried out by cold vapour generation atomic absorption spectrometry (Pourreza *et al.,* 2016).

Molecularly imprinted nanoparticles are the polymeric nanoparticles with binding sites that are the same size and shape of the target molecule (Wackerlig *et al.,* 2015). Advantages associated with molecularly imprinted nanoparticles include high stability, simple synthesis process, robustness and sensitivity (Chen *et al.,* 2011). The changes in optical properties of nanoparticles that are caused by target molecule interaction can be measured using SPR (Shrivastav *et al.,*2017). Shristav *et al.* developed a method for simultaneous lead and copper detection in water samples using SPR. Molecularly imprinted nanoparticles were synthesised and coated over sensor's optical fiber and a probe was attached to a flow cell. Response time for the method was 15 s. Additionally, no significant interference was reported. The linear range for copper and lead was reported to be between 4.06-1000 µg L^{-1}. LOD for copper and lead was 8.18×10^{-4} and 4.06×10^{-6} µg L^{-1}, respectively (Shristav *et al.,* 2018).

1.4.5 Electrochemical detection

Electrochemical detection is characterised by target analyte interaction with electrodes or probes. As a result, various electrical signals are obtained which enable quantitative analysis of the analytes (Wongkaew *et al.,* 2013). Electrodes can be easily integrated into microfluidic detection systems resulting in simple, low powered and cost effective detection with high sensitivity (Wang *et al.,* 2002). Additionally, minimal loss of sensitivity is observed through electrochemical method miniaturisation (Dong *et al.,* 2007). One of the disadvantages, however, associated with electrochemical detection is the short shelf life of electrodes. Because of high sensitivity, fast response and easy integration into a microfluidic chip electrochemical methods are widely used in heavy metal detection (Gencoglu *et al.,* 2014).

Hong *et al.* developed a 3 D printed microfluidic device for cadmium and lead determination in water using microporous screen printed electrode (SPE) modified with Mn_2O_3. Metal organic framework is a multifunctional material that is used for pourous material preparation with specific surface area (Morozan *et al.,* 2012). Mn_2O_3 obtained from manganese metal organic frameworks is a nanomaterial with distinctive mechanical, electronical and thermal characteristics (Li *et al.,* 2013; Yang *et al.,* 2014). The detection system was created by integrating metal organic framework derived Mn_2O_3 modified SPE into a 3D microfluidic cell. The sensor was connected to a USB which transmitted the data to a computer allowing for real time detection of heavy metals. Linear range for cadmium was found to be between 0.5-8 µg L^{-1}, and the LOD was 0.5 µg L^{-1}. The linear range for lead was observed between 10 to 100 µg L^{-1}, and the LOD was 0.2 µg L^{-1} (Hong *et al.*,2016).

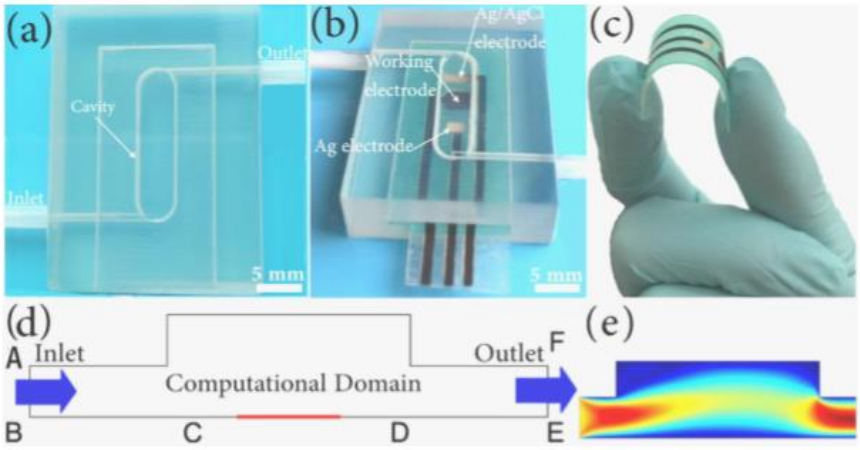

Figure 1.6. (a, b) Photographic images of the devices without and with the screen printed electrodes (SPE); (c) photograph of SPE; (d) the computational domain of microfluidic chip combined with work electrode; (e) the velocity outline of microfluidic cell. Figure adapted from Hong *et al.,* 2016. Copyright (2016) American Chemical Society.

Le *et al.* developed a microelectrodialyser for lead detection in water. Microsystem was fabricated using ion exchange membranes. The lead was analysed by square wave anodic

stripping voltammetry (SWASV) using a boron doped electrode. Peristaltic pumps were used to move the liquid through the system. Miniaturised platinum conductivity electrodes were used to measure the concentration of lead in samples in a PDMS microchannel. Linear range for lead was obtained between 20-100 μg L^{-1}, and LOD was found to be 4 μg L^{-1}. Furthermore, the method showed good reproducibility with relative standard deviation (RSD) of 0.35 % was reported (Le *et al.,* 2012).

Polyaniline (PANi) is a polymer modifier characterised by low cost, easy deposition on films, environmental stability and high conductivity (Li *et al.,* 2018). Nguyen *et al.* used a microfluidic detection chip based on sodium dodecyl sulfate-doped polyaniline (PANi-SDS) modified electrode for mercury detection in water. The electrode was integrated into a PDMS microfluidic detection chip. The lead samples were measured using SWASV. The linear range was observed between 1.20-7.02 μg L^{-1}, and LOD was 0.48 μg L^{-1}. The method was used for mercury analysis in water samples with high recovery rates obtained. Moreover, good reproducibility was obtained with RSD of 4.6 % (Nguyen *et al.,* 2017).

Paper is an excellent material for sensing device manufacturing as it is cost effective and biodegradable. Moreover, the porous composition of paper allows for effective chromatographic separation (Martinez *et al.,*2008; Martinez *et al.,* 2010). Electrochemical detection based μPADs also referred to as electrochemical paper based analytical devices (ePADs) have numerous advantages as they enable low cost monitoring with high selectivity and sensitivity (Adkins *et al.,*2015). Additionally, they are simple to use, do not require additional instrumentation and are easily disposable (Nie *et al.,* 2009). Screen printed technology can be easily utilised for the production of low cost disposable sensors. Shi *et al.* used paper based microfluidic devices for cadmium and lead determination using electrochemical detection. The authors combined paper strips with screen printed carbon

electrodes (SPCE). The SPE were constructed onto a PMMA platform. No pretreatment was needed for the water sample analysis, and the samples were measured using SWASV. The linear range for lead was between 0 to 100 μg L^{-1}. The LOD for lead and cadmium was 2 μg L^{-1} and 2.3 μg L^{-1}, respectively. In addition, the method was successfully applied for lead determination in salty water and groundwater analysis (Shi *et al.*, 2012).

Shen *et al.* developed a portable microfluidic detection device for cadmium and lead determination in water using a carbon based sensor. Carbon based materials can be used directly for heavy metal detection and are not toxic, unlike mercury based electrodes. Working and counter electrodes were embedded into a microfluidic paper channel. The microfluidic detection channel delivered the analyte to detection sites. The microfluidic detection system was based on graphite foil and paper making it cost effective. SWASV was used for sample measurements. Optimum results were obtained at pH 4.6 with 15 minutes required for one sample analysis. The LOD for cadmium and lead was found to be 1.2 μg L^{-1} and 1.8 μg L^{-1}, respectively. Both metals could be simultaneously detected in concentration range between 20 and 100 μg L^{-1}. However, copper was found to interfere with the detection method (Shen *et al.*, 2017).

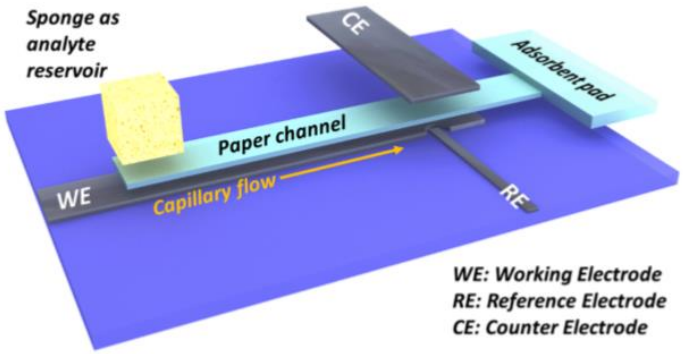

Figure 1.7. Diagram of the microfluidic detection device developed on paper (blue) and graphite foil (black) by Shen *et al.,* 2017 (https://pubs.acs.org/doi/10.1021/acsomega.7b00611). The figure is reproduced with permission from American Chemistry Society. Further permissions related to the material excerpted should be directed to American Chemistry Society.

Bismuth based electrodes are less toxic than those based on mercury making them more appealing for environmental monitoring purposes. Additionally, they are characterised by wide linear dynamic range and good resolution (Hutton *et al.,* 2004; Rehacek *et al.,* 2007). Zou *et al.,* 2008 developed a lab on a chip with a bismuth electrode. The author used microfabrication and screen printing techniques for device production. The sensor had a working bismuth sensor. The detection of lead and cadmium was carried out by anodic stripping voltammetry (ASV) inside the microchannels. The LOD for cadmium and lead determined to be 9.3 µg L^{-1} and 8 µg L^{-1}. The linear range for cadmium was found to be between 28-280 µg L^{-1}. The linear range for lead was observed between 25-400 µg L^{-1}. Additionally, the measurements were reproducible with RSD of less than 15 % reported (Zou *et al.,* 2008).

Nantaphol *et al.* developed a microfluidic paper based device for determination for lead and cadmium using boron doped diamond paste electrodes (BDDPEs). BDDPEs are characterised by low background current, robustness, stability in acidic and alkaline conditions and high sensitivity (Compton *et al.,* 2003; Luong *et al.,* 2009). The authors used flow through design

coupled with square wave anodic voltammetry. For standard analysis 0.1 M acetate buffer was used with pH 4.5. The linear range for lead was reported to be between 1 to 200 μg L^{-1}. The linear range for cadmium was between 25 and 200 μg L^{-1}. The LOD for lead and cadmium was found to be 1 μg L^{-1} and 25 μg L^{-1}, respectively. Additionally, the method was used for drinking water analysis. Moreover, good agreement was found between the reported method and ICP-OES (Nantaphol *et al.,* 2017).

Pungjunun *et al.*developed a μPAD based method using gold nanoparticles for total arsenic detection in water. Gold nanoparticles were modified on the boron doped electrode surface which was used as a working electrode. Thiosulfate solution was used to reduce the As (V) to As (III) which was deposited on boron doped diamond electrode. Arsenic was further measured using SWASV. The LOD was found to be 20 μg L^{-1}, and the linear range was between from 0.1-1.5 mg L^{-1}. Although copper was found to interfere with the detection of arsenic, ferricyanide was used as a complexing agent of copper to overcome the interference (Pungjunun *et al.,* 2018).

1.4.6 Quartz crystal microbalance

Quartz crystal microbalance (QCM) is a sensitive detection technique based on the piezoelectric effect, where the resonant frequency of the quartz crystal oscillation linearly decreases with mass loading on the crystal's surface (Jarup 2003). QCM is a sensitive, durable and cost effective sensing technique with the ability to take continuous *in situ* measurements (Sartore *et al.,* 2011). Furthermore, the substrates used for QCM sensing can be easily modified which enables versatility of this sensing method (Qiao *et al.,* 2016).

Dendrimers are branched polymers which are characterised by distinct sizes and geometries (Ghaedi *et al.,* 2007). Dendrimer ability to coordinate metal ions in their interior and exterior branches allows for highly selective sensor development (Grabchev *et al.,* 2011). Shen *et al.*

developed a method for copper ion determination using quartz crystal microbalance (QCM) sensor by combining phosphate modified dendrimer and ionophore. QCM sensor based on ion selective membrane was created and attached to a flow cell. Syringe pumps were used for sample introduction into the cell. The method was selective for copper in the presence of nickel, zinc and calcium ions. Linear range was observed between 0.006-6.355 mg L^{-1}. Additionally, the response time was 40 s with optimum results obtained at pH 5.7 (Shen *et al.*, 2016).

Wang *et al.* developed a QCM sensor based on phosphate modified dendrimer for copper detection in water. QCM sensor was integrated within a flow cell designed with a temperature controller which maintained 21°C throughout the analysis. A microinjector was used to introduce samples into the cell. The method was precise with maximum RSD of 2.9 % reported. Linear range was obeyed between 0.006-60 µg L^{-1}, and LOD was 0.006 µg L^{-1}. In addition, the response time was reported to be less than 40 s (Wang *et al.*, 2016).

Aptamers are nucleic acid based affinity probes which coordinate interaction between mercury ions and thymine (Miyake *et al.*, 2006; Clever *et al.*, 2007, Shen *et al.*, 2011). Dong *et al.* developed a method for mercury detection using QCM aptasensor using gold nanoparticles. The authors combined QCM based sensor with a flow system for mercury detection utilising mercury specific aptamer with gold nanoparticles. Short thiolated mercury specific aptamers were set on the surface of QCM as capture probes, whereas the mercury specific aptamers attached to gold nanoparticles served as linking probes. In presence of mercury ions, change in the resonance frequency was obtained. The LOD was 0.048 µg L^{-1}. Furthermore, the method was applied for spiked tap and waste water analysis with recoveries ranging from 96.8 to 101.6 % (Dong *et al.*, 2012).

DNAzyme based sensors are sensitive and have been used in various signal transduction mechanisms for metal ion detection (Li *et al.*,2000, Ono *et al.*,2004). Teh *et al.*developed a

DNAzyme based QCM method with dissipation monitoring for lead determination in water. Gold nanoparticles were used for signal amplification. Lead specific DNAzymes were immobilised on QCM surface allowing them to bind with gold nanoparticles, and GR-5 DNAzyme was used as a recognition probe. In the presence of lead ions, the gold nanoparticles were removed from the sensor surface causing a dissipation change. Linear range for lead was observed from 0.013-0.062 mg L^{-1}, and the LOD was 0.041 mg L^{-1}. Additionally, the method was used for spiked tap water sample analysis with good recovery obtained. Moreover, the results were in a good agreement with ICP-MS measurements (Teh *et al.,* 2014).

Can *et al.* 2016 developed a method for cadmium determination in water using a QCM sensor coupled with (2,3,7,8,12,13,17,18-Octakis(4-tert-butylbenzylthio)-porphyrazinato)Mg(II) (MgPz). QCM sensor was placed in a flow cell attached to a peristaltic pump. Optimum flow rate was found to be 0.3 µl min^{-1}. Experiments were carried out at 25 °C temperature, and no significant interference was reported. Double deionised water was passed through the detection system after each measurement. LOD of 10 mg L^{-1} was reported (Can *et al.*, 2016).

1.4.7 Other methods

Gammoudi *et al.* used a hybrid *in situ* monitoring system for cadmium using bacteria based Love wave transducer. PDMS microfluidic chip was used for controlling the flow movement. *Escherichia coli* were used as bioreceptor. The sensitive biofilm was embedded onto polyelectrolyte multilayer which was measure using acoustic wave phase velocity. The method was validated using atomic force microscopy and LOD for cadmium was found to be 2.1 µg L^{-1} (Gammoudi *et al.,* 2014).

Epitaxial graphene on silicon carbide is a complex structure with distinctive structural and electronic properties (de Heer 2011). Santangelo *et al.*used epitaxial graphene integrated microfluidic detection device for lead determination in water. The microfluidic chip design

enabled sample interaction with graphene sensing surface. Conductivity change between lead samples and graphene surface was measured. The analytical performance was evaluated using density functional theory calculations. Linear range for lead was observed from 0.026 to 103.6 mg L^{-1}, and LOD was 0.0196 mg L^{-1} (Santangelo *et al.*, 2018).

Multiple analytes can be analysed using a target responsive aptamer crosslinked hydrogel which can control fluid flow. Aptamers are single stranded DNA molecules that can recognise a wide range of target ions, including metals, proteins, cells and viruses (Famulok *et al.*, 2007). Wei *et al.* developed a microfluidic paper based detection device for lead determination using a target responsive hydrogel. Aptamers modified with gold nanoparticles were bound in hydrogel. In the absence of target analyte hydrogel was generated in the flow channel preventing reaction with a colour dye, whereas in presence of lead no hydrogel was formed. In total six minutes were required for the analysis, and LOD for was found to be 0.041 mg L^{-1} (Wei *et al.*,2015).

Table 1.2. Summary of various microfluidic detection methods for heavy metals.

Detection principle	Mechanism	Target analyte	LOD	Linear range	Interference*	Ref.
Abs.	Cell diffusing mixing technology with PAN and ferrozine	Fe (II), Mn (II)	Mn 1.56 µg L^{-1}, Fe 5.60 µg L^{-1}	Fe 5.6-100 µg L^{-1}, Mn 1.5-329 µg L^{-1}	-	Milani *et al.*, 2015
Abs.	Flow injection analysis using phenanthroline	Fe (II)	0.055 mg L^{-1}	0.055-5.580 mg L^{-1}	-	Du *et al.*, 2005
Abs.	Chromoionophore PVC film	Hg (II)	0.1 mg L^{-1}	0.2-50.14 mg L^{-1}	Cu, Ni, Pb, Cd	Nuriman 2011
Abs.	µPADs using sodium rhodizonate	Pb (II)	10 µg L^{-1}	10-100 µg L^{-1}	Fe II	Satarapi 2016
Abs.	Iron oxide nanoparticles and µPADs	As (III)	0.01 mg L^{-1}	0.01-0.90 mg L^{-1}	-	Chauhan 2018
Abs.	Distance based detection using µPADs	Hg (II)	0.93 mg L^{-1}	1-30 mg L^{-1}	Co, Zn, Ni, Au	Cai *et al.*, 2017
Abs.	µPADs and gold nanoparticles	As (III)	-	1- 50 µg L^{-1}	Fe III	Chowdury *et al.*, 2018
Abs.	Chemically patterned µPADs	Hg (II), Ni (II), Cr (VI)	Ni 0.24 mg L^{-1}, Cr 0.18 mg L^{-1}, Hg 0.19 mg L^{-1}	-	_	Devadhasan *et al.*, 2018
Abs.	Droplet-based AuNP synthesis with dielectric barrier discharge plasma	Hg (II)	0.2 mg L^{-1}	-	-	Li *et al.*, 2017

SPR	Gold nanoparticles	Hg (II), As (III)	-	Hg 0.710-1.278 mg L^{-1}, As 0.011-0.054 mg L^{-1}	-	Motalbizadeh *et al.*, 2018
SPR	Gold nanoparticles	Hg (II)	11 µg L^{-1}	11 -100 µg L^{-1}	-	Gomez-de Pedro *et al.*, 2013
SPR	Curcumin nanoparticles	Hg (II)	0.003 mg L^{-1}	0.01-0.4 mg L^{-}	-	Pourreza *et al.*, 2016
SPR	µPADs with silver nanoparticles	Hg (II)	0.12 mg L^{-1}	5-75 mg L^{-1}	Cu	Apilux *et al.*, 2012
SPR	Molecularly imprinted nanoparticles	Cu (II), Pb (II)	Cu 8.18×10^{-4}, Pb 4.06×10^{-6}	4.06-1000 µg L^{-1}	-	Shristav *et al.*, 2018
Fl.	Droplet based sensor using nanoparticles	Hg (II)	0.02 µg L^{-1}	0.02 µg L^{-1}-200 µg L^{-1}	-	Bell *et al.*, 2015
Fl.	BODIPY and nanoparticles	Cd (II)	5.62 mg L L^{-1}	5.62-112.41 mg L^{-1}	-	Kou *et al.*, 2009
Fl.	Calix-DANS3-OH	Pb (II)	42 µg L^{-1}	-	Mn, Co, Hg	Faye *et al.*, 2012
Fl.	Calix-DANS3-OH	Pb (II)	5 µg L^{-1}	-	Ca	Zhao *et al.*, 2009
Fl.	Precolumn adsorbtion and flourimetric detection using Calix-DANS4	Pb (II)	2 µg L^{-1}	2.07-16.5 µg L^{-1}	Cu, Ca, Hg, Zn, Cr III	Wu *et al.*, 2012
Fl.	Rhodamine 6G silica particle embedded onto mesopourous silica	Fe (III)	-	2-8 µg L^{-1}	K, Li, Al, Hg	Kim *et al.*, 2016

Fl.	Flow injection detection	Cd (II)	0.45 μg L^{-1}	1.12-22.40 μg L^{-1}	Pb	Zhang *et al.*, 2012
Fl.	On line fluorescnet derivitazation	Hg (II)	0.006 mg L^{-1}	6.21-14.041 mg L^{-1}	Cu, Zn, Fe	Peng *et al.*,2018
Fl.	Gold nanoparticles	Hg (II)	0.6 μg L^{-1}	0.6-60 μg L^{-1}	Cd	Lafleur *et al.*, 2012
Fl.	Digital microfluidics (DMF)	Hg (II)	0.7 μg L^{-1}	0.7-10 μg L^{-1}	Cd, Ni, Fe II, Mn, Fe III, Cu, Mg, Pb	Zhang *et al.*, 2019
C.L.	1,10 phenanthroline based	Cu (II), Co (II), Fe (II)	Cu 0.47 mg L^{-1}, Co 35.35 mg L^{-1}, Fe 55.84 mg L^{-1}	Cu 0.47-6.73 mg L^{-1}	-	Nogami *et al.*, 2009
C.L.	G-quadruplex based luminescence	Pb (II)	-	2-200 μg L^{-1}	-	Sun *et al.*, 2018
C.L.	Luminol with hetropoly acid complex	As (V)	6.6 μg L^{-1}	0.075 - 3.74 mg L^{-1}	PO_4, CrO_4	Som-aum *et al.*, 2008
C.L.	Luminol oxidation reaction	Cr (III), Cr (VI)	0.312×10^{-4} ng L^{-1}	0.052×10^{-3}-0.052×10^{-1} ng L^{-1}	Fe II, Al, Zn, Ni	Som-aum *et al.*, 2007
C.L.	Microchip with air sampling	Fe (II)	0.017 mg L^{-1}	0.06 - 2.79 mg L^{-1}	-	Lv *et al.*, 2004
C.L.	μPADs	Cr (III)	0.2 mg L^{-1}	0.05 -1 mg L^{-1}	-	Alahmad *et al.*, 2016
C.L.	Lab on a cloth	Cr (III)	0.006 mg L^{-1}	0.01-100 mg L^{-1}	-	Liu *et al.*, 2018
C.L.	Luminol oxidation reaction	Co (II)	2 ng L^{-1}	5.89-5.89×10^{7} ng L^{-1}	-	Chen *et al.*, 2013

E.C.	Microporous SPE modified with Mn2O3	Cd (II), Pb (II)	Cd 0.5 µg L^{-1}, Pb 0.2 µg L^{-1}	Cd 0.5 to 8 µg L^{-1}, Pb 10-100 µg L^{-1}	-	Hong *et al.*, 2016
E.C.	Microelectrodialyser combined with boron doped diamond electrode	Pb (II)	4 µg L^{-1}	20-100 µg L^{-1}	-	Le *et al.*, 2012
E.C.	SPE coupled with PANi-SDS	Hg (II)	0.481 µg L^{-1}	1.203-7.021 µg L^{-1}	-	Nguyen *et al.*, 2016
E.C.	SPCE combined with	Cd (II), Pb (II)	Pb 2 µg L^{-1}, Cd 2.3 µg L^{-1}	2- 100 µg L^{-1}	-	Shi *et al.*, 2012
E.C.	µPADs with carbon based sensor on µPADs	Cd (II), Pb (II)	Cd 1.2 µg L^{-1}, Pb 1.8 µg L^{-1}	20-100 µg L^{-1}	Cu	Shen *et al.*, 2017
E.C.	µPADs with boron doped diamond paste electrodes (BDDPEs)	Cd (II), Pb (II)	Pb 1 µg L-1, Cd 25 µg L^{-1}	Cd 25 - 200 µg L^{-1}, Pb 1-200 µg L^{-1}	-	Nantaphol *et al.*, 2017
E.C.	SPE based on bismuth electrode detection	Cd (II),Pb (II)	Cd 9.3 µg L^{-1}, Pb 8 µg L^{-1}	25-400 µg L^{-1}	-	Zou *et al.*, 2008
E.C.	µPADs with gold nanoparticles	As (III), As (V)	0.02 mg L^{-1}	0.1-1.5mg L^{-1}	Cu	Pungjunun *et al.*, 2018
QCM	Phosphate modified dendrimers	Cu (II)	-	0.006-6.355 µg L^{-1}	-	Shen *et al.*, 2016
QCM	Aptasensor with gold nanoparticles	Hg (II)	0.048 mg L^{-1}	-	Au	Dong *et al.*, 2012
QCM	DNAzymes and gold nanoparticles	Pb (II)	0.013 mg L^{-1}	0.013-0.062 mg L^{-1}	Zn, Ba	Teh *et al.*, 2014
QCM	Phosphate modified dendrimers	Cu (II)	0.006 µg L^{-1}	0.006-60 µg L^{-1}	-	Wang *et al.*, 2016

QCM	Magnesium porphyrazine	Cd (II)	10 mg L^{-1}	-	-	Can *et al.*, 2016	*
Acoustic	Biosensor based on E.coli	Cd (II)	2.1 µg L^{-1}	-	-	Gammoudi *et al.*, 2014	
Conductivity based	Epitaxial graphene sensor	Pb (II)	0.0196 mg L^{-1}	0.026 - 103.6 mg L^{-1}	-	Santangelo *et al.*, 2018	
Aptamer based	DNA hydrogel mediated sensor	Pb (II)	0.041 mg L^{-1}	-	-	Wei *et al.*, 2015	

*Substances identified in cited studies as interfering with the detection method.

Tolerance limits not included in the table due to inconsistent reporting.

1.5 Discussion and future outlook

Numerous research groups have developed microfluidic detection systems for heavy metal monitoring in order to create portable and cost effective alternative to costly laboratory based detection methods. Microfluidic detection system performance depends on the effectiveness of the detection method used for the analysis (Baker *et al.*, 2009). Further research in optical and electrochemical detection methods is needed to allow microfluidic sensor development. Additionally, improvements in microfabrication and new material development for microfluidic detection systems are required (Wu *et al.*, 2011). Future developments would also be concentrated on microfluidic detection system application Challenges such as analysis of complex water matrices and variable environmental conditions with minimum power consumption will need to be addressed.

At present *in situ* monitoring for microfluidic detection systems is limited due to various issues. Biofouling is a serious concern, especially for sea water measurements. Biofilms can drastically reduce the width of the channels, therefore, affecting the flow rate and in some cases even stopping it (Drescher *et al.*, 2013). Additionally, biofilms can alter the composition of metal compounds in water leading to unreliable measurements (van Hullebusch *et al.*, 2003). Another major issue is the formation of air bubbles which can significantly affect the flow rate within the microfluidic channels. Irregular flow rate can also be caused by variation in pressure in the syringe pumps (Zeng *et al.*, 2015). In addition, syringe pumps can cause oscillations in the flow due to the frictional forces between the syringe piston and the syringe wall (Atencia *et al.*, 2006). The stability of the materials is another

restriction that can shorten the life time of a detection system. In addition, once the microfluidic detection system is deployed in the field, the electronics within the microfluidic detection system are subjected to oxidation reactions which in turn affect the readings (Pol *et al.,* 2017). Moreover, deployable microfluidic detection systems should be able to operate for long periods of time. However, achieving this requirement without elevating the manufacturing cost is a serious challenge (Niessner 2010).

Many research groups have developed microfluidic detection systems with high sensitivity. For example, Bell *et al.* developed a method for mercury determination with LOD of 0.2 μg L^{-1} using fluorescence based microfluidic detection system (Bell *et al.,* 2016). Hong *et al.,* developed an electrochemical based method for cadmium and lead analysis, with LOD of 0.2 and 0.5 μg L^{-1}, respectively (Hong *et al.,* 2016). Exceptionally low detection limits have been achieved using chemiluminescence based methods. Chen *et al.,* described a method for cobalt determination in water with LOD of 2 ng L^{-1} (Chen *et al.*,2013). Som-aum *et al.* reported a LOD of 3.12×10^{-4} ng L^{-1} for chromium using luminol (Som-aum *et al.*, 2007).

Microfluidic detection methods that have been applied for water sample analysis with various matrices have been reported by numerous research groups. In environmental water sample analysis complex water matrices lead to interferences which affect the analysis of target analyte and decrease the life time of the detection system. This issue can be resolved by using highly selective molecules. Additionally, envrionmental samples also contain colloidal particles which can

affect optical and electrochemical based detection methods. This issue could be mitigated by introducing filtration systems in microfluidic detection devices (Pol *et al.,* 2017). Numerous strategies for solving interference related issues have been developed by researchers. Zhang *et al.* used solid phase absorption to overcome interference (Zhang *et al.,* 2012). Chowdury *et al.,* adjusted pH in order to prevent iron interference on arsenic determination (Chowdury *et al.,* 2018). Punjunum *et al.,* used ferricyanide for copper interference elimination (Punjunum *et al.,* 2018). In general, however, more extensive research is needed to assess microfluidic detection method capability to produce reliable and reproducible measurements in a wide range of complex environmental water matrices.

A small number of microfluidic detection methods have been developed into fully integrated autonomous detection devices. In future a lot of research would be focused on transforming microfluidic detection systems into autonomous, fully integrated detection devices that would be readily used in the field. Ideally, autonomous detection system should be able to operate for long time periods such as several weeks or even months. The supply of power is limited for autonomous *in situ* microfluidic detection system operation in the field. This issue can be overcome by using efficient batteries or reducing energy consumption. Ultra low power electronic and optoelectronic components have already been developed and reported (Capitan-Vallvey *et al.,* 2011).

Numerous researchers have achieved good agreement between the microfluidic detection methods and standard laboratory based methods such as ICP-OES, AAS, ICP-MS and GFAAS. However, more extensive validation of microfluidic

detection methods is needed in order for them to become competitive with standard laboratory based methods.

Microfluidic technology is currently used mainly for small scale analysis. Mass production of microfluidic detection systems is limited due to high manufacturing costs. Therefore, more cost effective and standardised fabrication of microfluidic detection systems is needed. Potentially 3-D printing could be used to produce integrated microfluidic detection systems using a wide range of materials (Bohr *et al.*, 2019). This would enable engineers to set up fabrication protocols that could be carried out by researchers with limited access to sepcialised facilities and confined knowledge in manufacturing (Convery *et al.*, 2019).

In summary, microfluidic detection systems have been shown to be effective for heavy metal detection in water with the ability to analyse small volumes of sample and with high sensitivity towards target analytes. With further detection method development and miniaturisation, as well as microfluidic technology advancement, it is expected that microfluidic detection devices would have an important role in environmental monitoring in the near future.

1.6 Conclusion

In recent years microfluidic technology has undergone rapid development which in turn has widened their application to environmental monitoring. Numerous microfluidic detection devices based on optical and electrochemical detection principles have been developed by various research groups around the world. Many of these methods have reached high sensitivity and showed good agreement with standard laboratory based detection methods such as ICP-MS. Microfluidic detection technology, however, has not been developed enough for routine water monitoring. However, the full potential of microfluidic detection system applications has not been achieved yet.

A small number of microfluidic detection systems have been fully automated and transformed into autonomous devices with the ability to take measurements in the field for long time period. Improvements in wireless connectivity would be important to overcome challenges associated with autonomous monitoring. In future collaboration between scientists from different fields would be needed to allow for highly specific and efficient microfluidic detection system design. Moreover, this would aid large scale production protocol development.

Mass production of microfluidic detection systems is limited due to high costs and complicated set up. 3-D printing could potentially improve the manufacturing of microfluidic detection systems in the future making the production more cost effective and accessible to researchers with limited knowledge in fabrication.

Overall, it is expected that microfluidic detection systems will have an important role in environmental monitoring in the near future and potentially serve as a cost effective alternative to laboratory based detection methods.

Chapter 2

Assessment of variamine blue and molybdenum blue method potential application for arsenic monitoring in water using microfluidic detection systems

Authors: Annija Lace, David Ryan, and John Cleary

2.1 Abstract

Drinking water contamination with arsenic has become a major global concern. Consequently, it is important to effectively monitor arsenic in water. The most commonly used methods for arsenic monitoring are atomic absorption spectrometry and inductively coupled plasma mass spectrometry. Although these analytical techniques are highly selective and sensitive, they require sophisticated instrumentation, expensive maintenance, and highly trained technicians. Therefore, cost effective, fast, and reliable alternative detection methods are required for arsenic monitoring in the environment. This study aims to evaluate variamine blue and molybdenum blue method suitability for arsenic monitoring via microfluidic detection systems. Both methods' suitability was assessed using 1 mm quartz cuvettes, assessing method reproducibility and colour stability. Additionally, for each method optimum parameters such as acid concentration, temperature and pH were investigated.

Keywords: *heavy metals; arsenic; variamine blue; molybdenum blue; colorimetric methods*

2.2 Introduction

Arsenic (As) is a highly toxic element that has wide industrial applications (Loebenstein, 1994; Hsueh 2013). It is used in processing of glass, pigments, textiles, metal adhesives, wood preservatives, and ammunition (Pillai 1999; Mahzuz *et al.,* 2009). Arsenic compounds are used as alloying agents in transistor, laser, and semiconductor manufacturing. To a limited extent arsenic compounds are used as pesticides, feed additives, and pharmaceuticals (Gomez-Caminero *et al.,* 2001).

Arsenic can be introduced in the environment through mining activity and combustion of fossil fuels. In mining areas, arsenic concentrations can reach µg L^{-1} level (Smedley and Kinniburgh 2001). One of the worst arsenic contamination cases due to mining has been documented in Thailand in Ron Phibun district. Arsenic concentrations as high as 5000 µg L^{-1} were found in the ground waters near the mining site (Choprapawon and Rodcline, 1997). Mining related arsenic contamination has also been recorded in Lavrion region in Greece, Ashanti region in Ghana, Zimapan Valley in Mexico, and different regions in the United States (Wilson and Hawkins 1978; Welch *et al.,* 1988; Del Razo *et al.,* 1990; Smedley and Edmunds 1996, Nimick *et al.,* 1998).

The most common arsenic oxidation states in water are III and V (Panagiotaras 2015). Arsenate (As V) is the dominant species in oxic conditions, whereas arsenite (As III) predominates in reducing coniditons such as those commonly found in deep well waters (IARC 2012). Redox potential and pH have an important role in controlling As speciation. The ratio between As Ii and As V in groundwaters can differ depending on the diffusion of oxygen from the atmosphere, microbial activity

and presence of organic carbon. In reducing conditions where sulfates and Fe III are present, As III is the dominant species (Smedley 2002).

Chronic exposure to high concentrations of arsenic through drinking water can result in a condition known as arsenicosis (Saha 2003). The various symptoms of arsenicosis include skin damage, circulatory system damage and development of various cancers (Cullen *et al.*,1989). In populations consuming arsenic contaminated water, disorders like peripheral vascular disease, skin, bladder, and lung cancers have been recorded (Cebrian *et al.*,1983).

Because of the serious risks associated with arsenic exposure the World Health Organization (WHO) as well as EU directive EC/98/83 have set a standard limit of 10 µg L^{-1} for arsenic in drinking water (EU directive EC/98/83). Arsenic concentrations exceeding the standard limit have been reported in numerous regions around the world, including Bangladesh, Taiwan, Vietnam, Mexico and Ireland (Hsu *et al.*, 1997; Berg *et al.*, 2001; Petrusevski *et al.*, 2007; Armienta *et al.*, 2008; McGrory and Ellen 2017).

A range of different methods are used for arsenic detection and analysis. Some of the established laboratory methods used for arsenic detection include atomic absorption spectrometry(AAS), atomic fluorescene spectrometry (AFS), neutron activation analysis, X-ray fluorescence, induced couple plasma atomic emission spectrometry (ICP-MS), and hydrate generation atomic absorption spectrometry (HG-AAS) (Huang *et al.*, 2004). These laboratory methods are highly sensitive and selective, however, there are numerous disadvantages associated with them. These

methods require regular maintenance and highly trained technicians in order to be used. The cost of running a sample, as well as maintenance and repairing costs are high. Because of these issues these methods are not suitable for routine high frequency sample analysis (Moore *et al.,* 2009).

Consequently, a range of different portable detection methods have been developed (Dagupta *et al.,* 2002; Kundu *et al.,* 2002; Nath *et al.,* 2014). Field kits based on the Gutzeit reaction have been applied for arsenic detection in water. In this reaction arsenic is firstly reduced to arsine gas and then reacted with mercuric bromide that is embedded in the paper. Colour change occurs in the presence of arsenic and a yellow colour is obtained which varies in intensity depending on the amount of arsenic in the sample (Kinniburgh *et al.,* 2004). Although these kits are easily portable and cheap to produce, there have been numerous drawbacks reported. For example, high number of false positive and false negative results have been associated with these kits (Rahman *et al.,* 2002). In addition, it has been found that most of the arsine gas produced in the Gutzeit reaction escapes into the environment which presents a risk to the researcher (Arora *et al.,* 2009).

Electrochemical methods have been used for portable arsenic detection sensor development (Li *et al.,* 1996; Huan and Dasgupta 1999; Mays *et al.,* 2009). Concentration of the analyte in the solution can be accurately measured regardless of the sample size making them suitable for miniaturization (Matysik 2003). However, there are some disadvantages associated with electrochemical methods. The cost of electrode fabrication is high and the electrodes are not robust, thus not

suitable for long term use in the field (Chailapakul *et al.,* 2008). Metal interference is another issue with copper, zinc, and mercury being the most commonly reported interferants with the electrochemical analysis (Luong *et al.,* 2014).

Colorimetric detection is suitable for development of portable arsenic detection system as colorimetric methods can be easily integrated into detection system. A change in colour can be easily observed by naked eye or detected using spectroscopical methods such as ultra violet visible spectroscopy (UV-vis) (Tsai and Yogorajah 2015). Colorimetric methods have numerous advantages such as low cost, simple detection, and good sensitivity and selectivity (Lobnik *et al.*, 2006). Colorimetric methods have been integrated into microfluidic detection systems and used for phosphate (Floquet *et al.,* 2011), nitrate (Cogan *et al.,* 2015), and ammonia (Daridon *et al.,* 2001) detection in water. However, to date very few commercially available microfluidic detection systems for heavy metals exist.

A range of different colorimetric methods for arsenic detection in water have been described in the literature. Dhar *et al.* have reported a method for arsenic detection in groundwater in the presence of phosphate using molybdate based dye. The method was based on previous work of Johnson and Pilson *et al.* (Johnson and Pilson 1972). The colour reagent was prepared by combining 10.8 % ascorbic acid with 3 % ammonium molybdate, 0.56 % antimony potassium tartrate, and 13.98 % sulphuric acid in the volumetric ratio of 2:2:1:5 (Dhar *et al.*,.2004).

The molybdenum blue reaction has several stages. Firstly, potassium iodate is used to oxidise arsenite to arsenate. Secondly, arsenate and molybdenum blue in acidic

conditions form a heteropoly acid. Secondly, the heteropoly acid is reduced by ascorbic acid forming a blue coloured species (Nagul *et al.*, 2015). The resulting colour is very stable with λ_{max} of 880 nm (Matsunaga *et al.*, 2005). The reaction mechanism for molybdenum blue is outlined in Figure 2.1.

$$12\ MoO_4^{2-} + AsO_4^{3-} + 24\ H^+ \longrightarrow [AsMo_{12}O_{12}]^{3-} + 12\ H_2O \quad (1)$$

$$[AsMo_{12}O_{40}]^{3-} \xrightarrow[\text{Ascorbic acid}]{} [AsMo_{12}O_{40}]^{7-} \quad (2)$$

Figure 2.1. Reaction mechamism for molybdenum blue method.

Narayana *et al.* developed a method for arsenic detection in environmental water and biological samples using variamine blue. In this method potassium iodate was reacted with arsenic in presence in acidic media to liberate iodine. The iodine in presence of sodium acetate oxidized variamine blue forming a violet colour with λ_{max} of 556 nm (Narayana *et al.*, 2006). The reaction mechanism for varimine blue method is shown in Figure 2.2.

$$2AsO_2 + 2IO_3 + 2H \longrightarrow I_2 + 2AsO_3 + 4H_2O \quad (1)$$

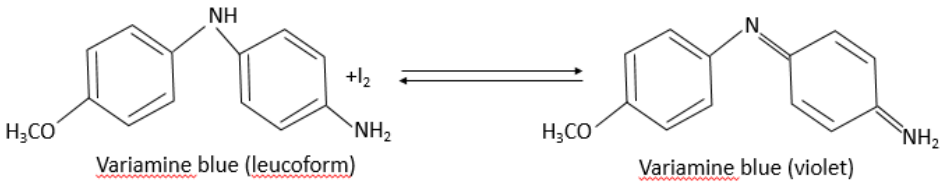

(2)

Figure 2.1. Reaction mechanism for variamine blue method.

Different parameters such as pH, colour stability, temperature and effect of acid concentration were evaluated for both methods. pH has an important role in colour formation and stability (Kumar *et al.*, 2007). Therefore, the optimum pH conditions for both methods were assessed. Likewise, temperature is an important factor in colour formation and reaction time. A range of various incubation temperatures were used in the analysis. Colour change occurs upon protonation, therefore acid concentration has an important role in colorimetric analysis. Numerous methods require strongly concentrated acids (Nagul *et al.*, 2015). Therefore, a range of different acid concentrations were assessed for both methods. Additionally, one of the greatest limitations with optochemical method integration within microfluidic detection systems is the reduced path length which can greatly limit method's sensitivity. Therefore, 1 mm path length cuvettes were used for sample measurements and the results were compared to 10 mm path length cuvette measurements.

This work aims to compare variamine blue and molybdenum blue methods and assess their suitability for arsenic detection in water using microfluidic detection systems.

2.3 Materials and methods

2.3.1 Apparatus

For both variamine blue and molybdenum blue methods Shimadzu 1800 UV-vis spectrometer was used with 10 mm and 1 mm Hellma quartz cuvettes for the absorbance measurements. Hanna pH 20 meter was used for measuring pH.

2.3.2 Reagents

All chemicals were of analytical grade and purchased from Sigma-Aldrich (Vale Road, Arklow, Co. Wicklow, Ireland) unless otherwise stated. Sodium meta-arsenite ($NaAsO_2$), was used to prepare stock solution at concentration 1000 µg mL^{-1} in double deionised water (HPLC grade). Arsenic working standards were prepared by serial dilutions. Acetic acid (99.8%) (Sharlab S.L., Barcelona, Spain) was used to adjust the pH. Sodium acetate ($C_2H_3O_2Na$), antimony potassium tartrate ($C_8H_4K_2O_{12}Sb_2 \cdot 3H_2O$) ascorbic acid ($C_6H_8O_6$) (Applichem Pancreac, Germany), potassium iodate (KIO_3), variamine blue RT base salt ($C_6H_5NHC_6H_4NH_2$), ammonium molybdate ($(NH_4)_6Mo_7O_{24} \cdot 4H_2O$) were prepared by weighing out an appropriate amount and dissolving it in double deionised water. Hydrochloric acid (HCl) (38%) (Sharlab S.L.) was used to prepare hydrochloric acid solutions with various concentrations in double deionised water. Sulfuric acid (H_2SO_4) (97%) was used to prepare sulfuric acid solutions with various concentrations. Double deionized water was used for dilution of reagents and samples.

2.3.3 Sample preparation

For variamine blue method 1.25 ml of arsenic sample was transferred to a plastic cuvette. Potassium iodide (2 %, 0.25ml), then hydrochloric acid (1 M, 0.25 ml) were added to the cuvette. The cuvette was gently shaken. Variamine blue dye (0.05 %, 0.25 ml) was added, followed by sodium triacetate buffer (0.05 %, 0.5ml). The mixture was gently shaken and left for 5 min. The absorbance was measured at 550 nm against reagent blank.

For molybdenum blue method 5 ml of arsenic sample was transferred to a glass vial. Potassium iodate (0.04 %, 0.5 ml), then hydrochloric acid (2 %, 0.5 ml) were

added to the cuvette. The cuvette was gently shaken. Molybdenum blue dye mix was prepared by transferring ascorbic acid (10.8 %, 1 ml), to a volumetric flask followed by ammonium molybdate (3 %, 1 ml) and antimony potassium tatrate (0.56 %, 0.5 ml), and sulfuric acid (13.98 %, 2.5 ml). The dye mix (0.5 ml) was added to the arsenic sample and the solution was gently mixed. The mixture was gently shaken and left to incubate for 15 min. The absorbance was measured at 890 nm against reagent blank.

2.3.4 Path length

Effect of cuvette light path on absorbance was investigated. The variamine blue and molybdenum blue methods were carried out in standard 10 mm quartz cuvettes and micro cuvettes with 1 mm light path for 1–10 mg L^{-1} arsenic concentration range. Each measurement was carried out in triplicate. The average absorbance standard deviation and relative standard deviation were calculated. Calibration curves were plotted and compared.

2.3.5 Effect of acid

The effect of hydrochloric acid's concentration on variamine blue method was assessed using a range of various hydrochloric acid concentrations (0.2, 0.4, 0.6 and 1 M) for arsenic analysis.

2.3.6 Effect of potassium iodate concentration

The effect of potassium iodate concentration on molybdenum blue method was investigated by using a range of different potassium iodate concentrations (0.04,

0.05, 0.1, 0.15 and 0.2 %) for arsenic sample analysis. The procedure was carried out in triplicate.

2.3.7 Temperature

To investigate the effect of incubation temperature on variamine blue and molybdenum blue method various incubation temperatures ranging from 25-70 °C were used for the analysis. Each measurement was carried out in triplicate.

2.3.8 pH

For variamine blue and molybdenum blue methods the effect of pH was investigated by carrying out the analysis at various pH conditions ranging from 2.5-5.5. The measurements were carried out in triplicate.

2.3.9 Time

The stability of the coloured species for variamine blue method was tested over time. 1 mg L^{-1} arsenic sample was measured using UV-vis spectroscopy against reagent blank at 550 nm. Absorbance values were taken every 60 seconds immediately after the addition of the variamine blue colour reagent.

For molybdenum blue method 2 mg L^{-1} arsenic standard was analysed at 890 nm against reagent blank for 3 hour (180 minutes) time period after the addition of molybdenum blue dye. Absorbance was read every 60 seconds.

2.4 Results and discussion

2.4.1 Analytical data

Absorption spectra of 3 mg L^{-1} arsenic sample analysed in 10 mm and 1 mm path length cuvettes against reagent blank using variamine blue method are shown in Figure 2.3. For the variamine blue method Beer's law was obeyed in the range 1-10 mg L^{-1}. The limit of detection (LOD) (3 se m^{-1}) and limit of quantification (LOQ) (10 se m^{-1}) (where se is the standard deviation of the reagent blank, and m is the slope of the calibration curve) were found to be 0.011 mg L^{-1} and 0.038 mg L^{-1} respectively.

Absorption spectra of 1 mg L^{-1} arsenic sample analysed in 10 mm and 1 mm quartz cuvettes against reagent blank using molybdenum blue method are shown in Figure 2.4. For the molybdenum blue method Beer's law was obeyed in the range 0.1-10 mg L^{-1}. The limit of detection (3 se m^{-1}) and limit of quantification (10 se m^{-1}) were found to be 0.015 mg L^{-1} and 0.05 mg L^{-1} respectively.

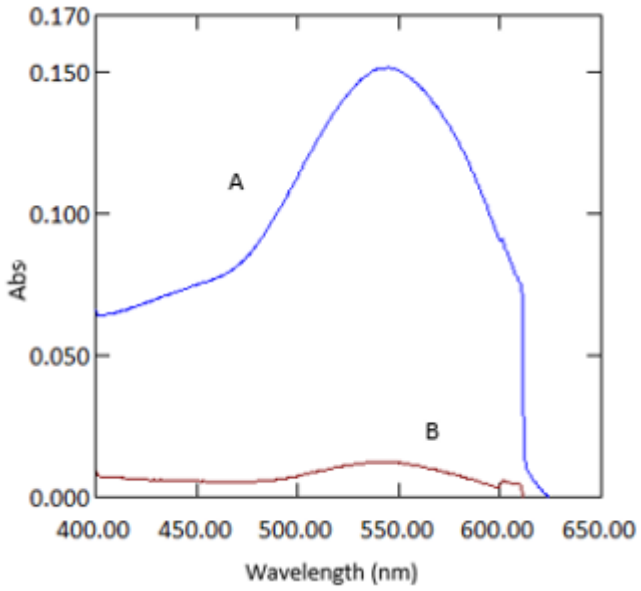

Figure 2.3. Absorption spectra of a sample containing 3 mg L^{-1} arsenic with variamine blue reagents measured in 10 mm cuvettes (A) and 1 mm quartz cuvettes (B) against reagent blank measured at 556 nm.

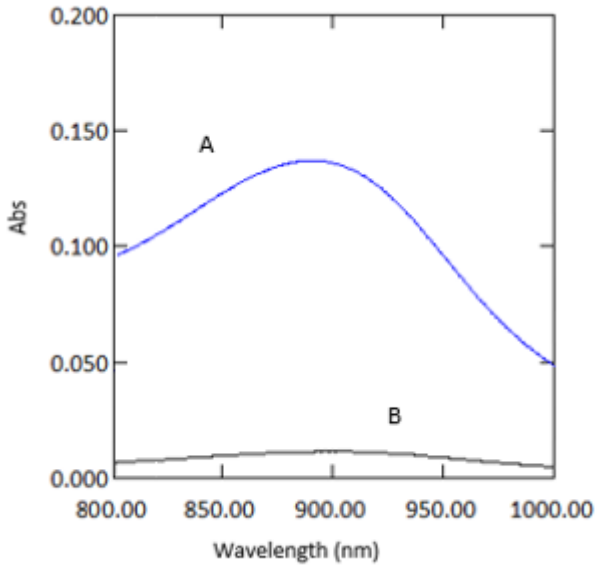

Figure 2.4. Absorption spectra of a sample containing 1 mg L^{-1} arsenic with molybdenum blue reagents measured in 10 mm cuvettes (A) and 1 mm quartz cuvettes (B) against reagent blank measured at 880 nm.

2.4.2 Path length and precision

Small sample volumes in microfluidic sensing can pose great challenges for analyte detection and reduce the sensitivity of the analytical method (Pires *et al.*, 2014). Therefore, only colorimetric methods with strong analytical response should be considered for applications in microfluidic detection. 1 mm quartz cuvettes were used to simulate the small scale and dimensions of microfluidic detection systems. The variamine blue method's sensitivity for arsenic samples measured in 1 mm path length quartz cuvettes was approximately ten times lower than for samples measured in 10 mm quartz cuvettes which could be explained by the ten fold path length difference (Table 2.1). However, linearity for both 10 mm and 1mm quartz cuvettes was very similar (Figure 2.5). Additionally, the samples measured in 1 mm microcuvettes showed good linearity. Despite the strong analytical signal obtained from 1 mm cuvette measurements the reproducibility of the method was poor.

The highest % RSD was found for 1 mg L^{-1} measurement using standard cuvette and 1 mg L^{-1} microcuvette measurements. Lowest % RSD for standard 10 mm cuvette measurements was detected for 3 mg L^{-1} arsenic sample. Preferably, the candidate method should yield reproducible results and, therefore, show a higher degree of precision than the one obtained from variamine blue method.

Table 2.1. Average absorbance values for arsenic samples (1–10 mg L^{-1}) analysed with variamine blue method and measured in two different types of cuvettes. All measurements were carried out in triplicate (n = 3).

	10 mm			**1 mm**		
Conc (mg L^{-1})	**10 mm**	**SD**	**% RSD**	**1 mm**	**SD**	**% RSD**
1	0.093	0.008	8.322	0.006	0.002	33.333
3	0.153	0.008	4.981	0.01	0.003	26.458
5	0.223	0.020	8.861	0.017	0.002	9.165
7	0.280	0.008	2.868	0.029	0.004	13.207
10	0.329	0.006	1.824	0.036	0.003	9.013

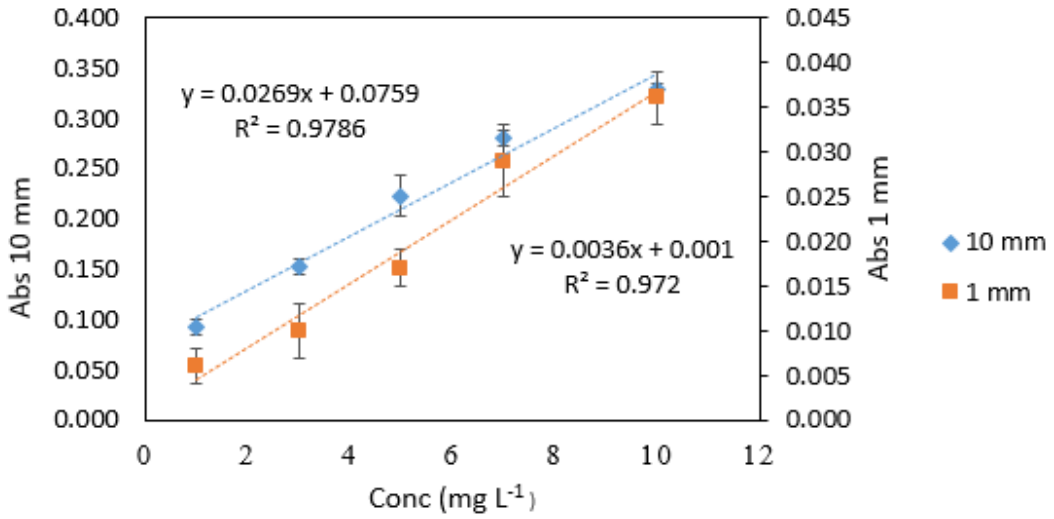

Figure 2.5. Comparison of arsenic standards (1–10 mg L^{-1}) analysed with variamine blue method and measured in quartz cuvettes with 10 mm and 1mm path lengths. Left vertical axes represent the absorbance of standards analysed in 10 mm quartz cuvettes. Right vertical axes represents the absorbance of standards analysed in 1mm quartz microcuvettes. All measurements were carried out in triplicate. Error bars represent standard deviations.

Similar results were obtained for molybdenum blue method. The absorbance values for arsenic samples analysed using molybdenum blue method and measured in 1 mm quartz cuvettes were ten times lower than measurements carried out in standard 10 mm cuvettes, as expected (Table 2.2). As it can be seen from the calibration graphs (Figure 2.6) the analytical response was strong for samples measured in microcuvettes. The lowest % RSD was reported for 10 mg L^{-1}using 10 mm quartz cuvettes which indicates that the method would not be reliable enough to be considered for integration into microfluidic detection systems.

Table 2.2. Average absorbance values for arsenic samples (1–10 mg L^{-1}) analysed with molybdenum blue method and measured in two different types of cuvettes. Abs 1, SD 1 and % RSD 1 show the data for measurements carried out with 10 mm quartz cuvettes. Abs 2, SD 2 and % RSD 2 show the data for measurements in 1 mm quartz cuvettes. All measurements were carried out in triplicate (n = 3).

	10 mm			1 mm		
Conc (mg L^{-1})	**Abs**	**SD**	**% RSD**	**Abs**	**SD**	**% RSD**
1	0.090	0.014	15.627	0.014	0.003	18.414
2	0.146	0.012	7.957	0.016	0.005	28.641
4	0.179	0.014	7.813	0.019	0.004	18.977
6	0.229	0.012	5.069	0.021	0.004	17.169
10	0.304	0.014	4.557	0.03	0.004	14.53

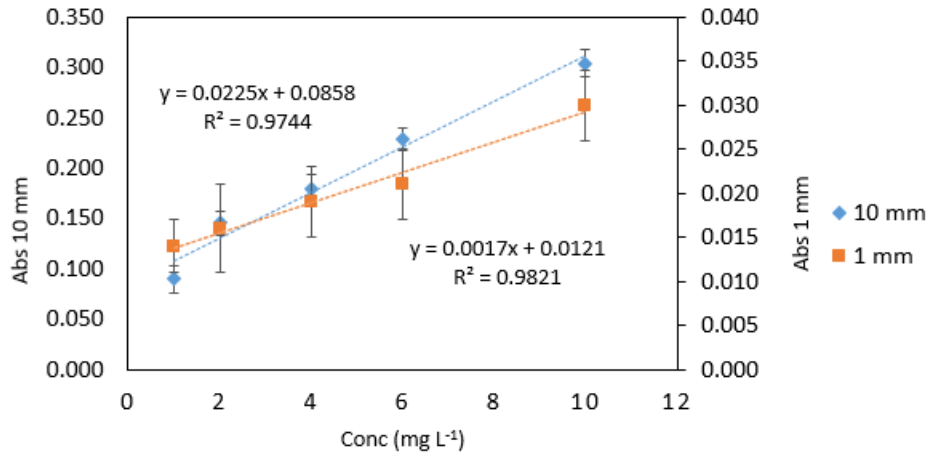

Figure 2.6. Comparison of arsenic standards (1–10 mg L^{-1}) analysed with molybdenum blue method and measured in quartz cuvettes with 10 mm and 1 mm path lengths. Left vertical axes represent the absorbance of standards analysed in 10 mm quartz cuvettes. Right vertical axes represents the absorbance of standards analysed in 1mm quartz microcuvettes. All measurements were carried out in triplicate. Error bars represent standard deviations of the measurements.

2.4.3 Effect of acid

The highest absorbance values for variamine blue method were obtained with 0.2 M hydrochloric acid (Table 2.3). The analytical signal obtained from 0.2 M hydrochloric acid was significantly stronger compared to other hydrochloric acid concentration evaluated. (Figure 2.7). The recommended acid concentration according to Narayana and Pasha *et al.*, was 0.4 M. Although 0.4 M hydrochloric acid concentration yielded linear results and strong analytical response, the linear response obtained from 0.2 M hydrochloric acid was stronger. Therefore, 0.2 M hydrochloric acid was used in subsequent experiments.

Table 2.3. Average absorbance values of arsenic samples (1–10 mg L^{-1}) analysed with various hydrochloric acid concentrations (0.2, 0.4, 0.6 and 1 M). All measurements were carried out in triplicate (n =3).

Conc (mg L^{-1})	**0.2 M**	**0.4 M**	**0.6 M**	**1 M**
1	0.066	0.040	0.109	0.185
SD	0.021	0.012	0.025	0.025
2	0.137	0.075	0.194	0.287
SD	0.028	0.011	0.032	0.034
4	0.227	0.192	0.257	0.394
SD	0.041	0.041	0.029	0.036
6	0.384	0.256	0.321	0.457
SD	0.056	0.056	0.022	0.020
10	0.772	0.338	0.390	0.555
SD	0.051	0.051	0.030	0.052
Slope	0.008	0.003	0.003	0.004
R^2	0.981	0.954	0.927	0.926

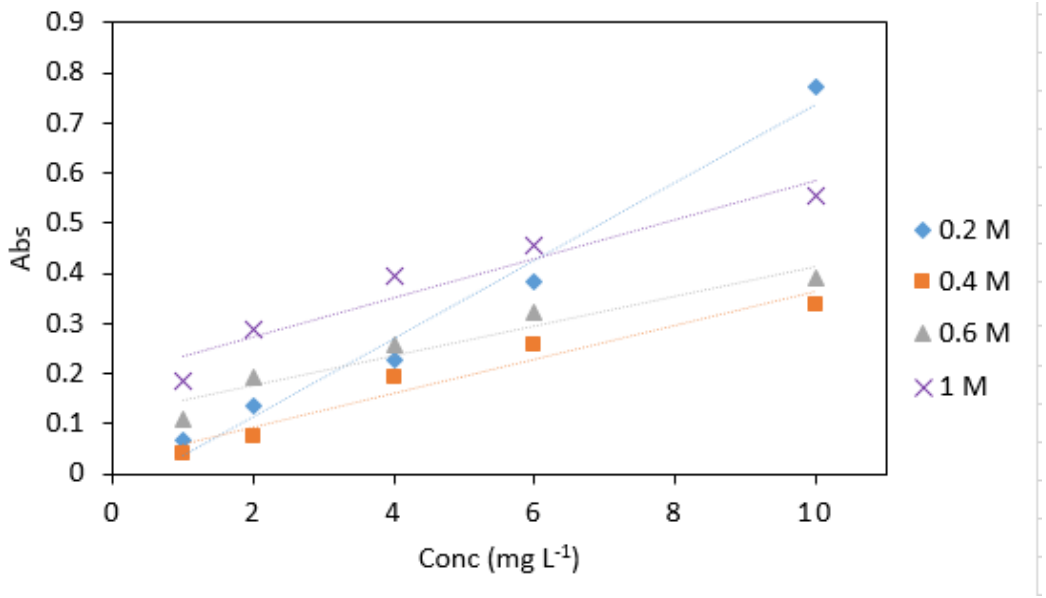

Figure 2.7. A comparison of average absorbance values of arsenic samples (1–10 mg L^{-1}) analysed with various hydrochloric acid concentrations (0.2, 0.4, 0.6 and 1 M). All measurements were carried out in triplicate (n = 3).

2.4.4 Effect of potassium iodate

The highest absorbance values were obtained using 0.15 % potassium iodate concentration (Table 2.4). The linear response obtained using 0.15 % potassium iodate for arsenic samples analysis was significantly higher than the response obtained from other potassium iodate concentrations (Figure 2.8). 0.15 % potassium iodate was used in subsequent arsenic analysis with molybdenum blue method.

Table 2.4. Average absorbance values of arsenic samples (1–6 mg L^{-1}) analysed with various potassium iodate concentrations (0.04, 0.05, 0.1, 0.15 and 0.2 %). All measurements were carried out in triplicate (n = 3).

Conc (mg L^{-1})	**0.04%**	**0.05%**	**0.10%**	**0.15%**	**0.20%**
1	0.098	0.108	0.157	0.221	0.146
SD	0.004	0.005	0.005	0.006	0.005
4	0.148	0.162	0.210	0.417	0.211
SD	0.006	0.004	0.008	0.004	0.004
6	0.192	0.231	0.233	0.516	0.236
SD	0.004	0.004	0.006	0.003	0.003
Slope	0.018	0.020	0.049	0.107	0.092
R^2	0.993	0.996	0.837	0.898	0.787

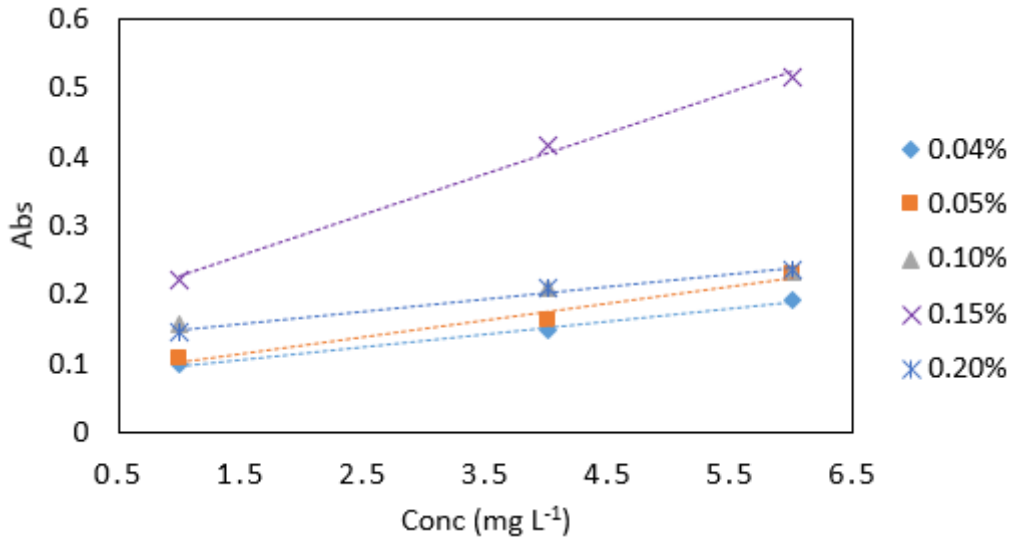

Figure 2.8. A comparison of average absorbance values for arsenic samples (1–6 mg L^{-1}) analysed with various potassium iodate concentrations (0.04, 0.05, 0.1, 0.15 and 0.2 %). All measurements were carried out in triplicate (n = 3).

2.4.5 Effect of pH

The highest absorbance values for variamine blue method were obtained using pH 3 buffer (Table 2.5). The analytical signal obtained from pH 3 buffer was significantly stronger compared to other pH buffers used in the analysis (Figure 2.9). The recommended pH according to Narayana and Pasha *et al.* was pH 4. Although using sodium acetate buffer with pH 4 resulted in linear results and strong analytical response, the pH 3 sodium buffer increased the sensitivity of the colorimetric method approximately two fold. Therefore, pH 3 buffer was found to be the optimum pH for the procedure and used in subsequent experiments.

Table 2.5. Average absorbance values of arsenic samples (1–10 mg L^{-1}) analysed at various pH conditions (3, 3.5, 4, 4.5, 5, 5.5) using variamine blue method. All measurements were carried out in triplicate (n = 3).

Conc (mg L^{-1})	**pH 3**	**pH 3.5**	**pH 4**	**pH 4.5**	**pH 5**	**pH 5.5**
1	0.135	0.118	0.093	0.163	0.086	0.087
SD	0.005	0.015	0.007	0.012	0.008	0.009
2	0.218	0.143	0.148	0.187	0.150	0.139
SD	0.007	0.011	0.013	0.007	0.005	0.008
4	0.338	0.242	0.176	0.227	0.190	0.184
SD	0.004	0.009	0.007	0.004	0.002	0.007
6	0.404	0.281	0.262	0.276	0.243	0.260
SD	0.007	0.014	0.005	0.007	0.012	0.006
10	0.537	0.362	0.333	0.307	0.333	0.343
SD	0.004	0.010	0.009	0.008	0.004	0.010
Slope	0.004	0.003	0.003	0.002	0.003	0.003
R^2	0.966	0.959	0.968	0.949	0.976	0.981

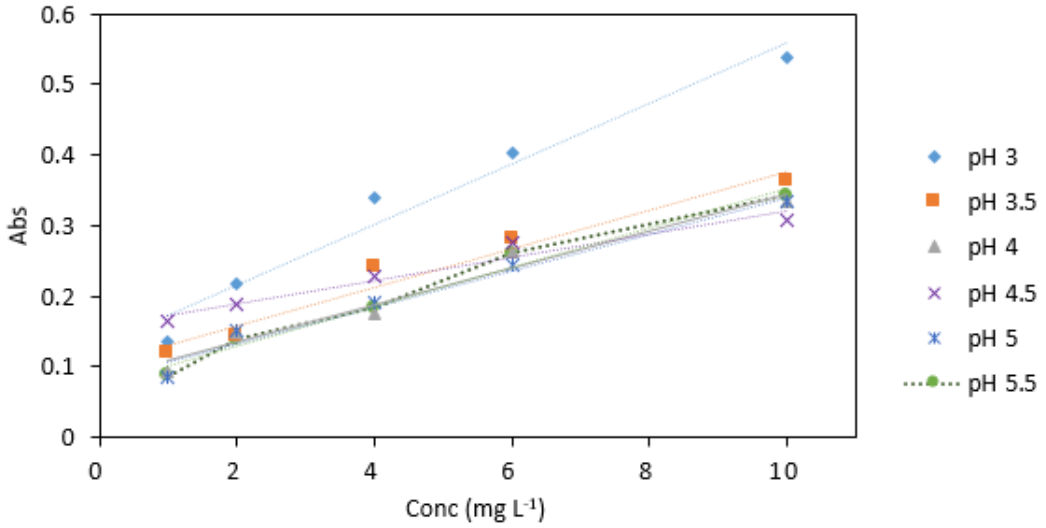

Figure 2.9. A comparison of arsenic samples (1–10 mg L^{-1}) analysed with variamine blue method at various pH conditions (3, 3.5, 4, 4.5, 5 and 5.5). All measurements were carried out in triplicate (n = 3).

For molybdenum blue method pH 5 buffer yielded the the strongest analytical signal with slope of 0.06 (Table 2.6). The pH 3 and 2.5 buffers showed the weakest analytical signal compared to the other pH buffers analysed (Figure 2.10). pH 5 buffer was found to be the optimum buffer for the procedure and used in subsequent measurements.

Table 2.6. Average absorbance values of arsenic samples (1–10 mg L^{-1}) analysed at various pH conditions (2.5, 3, 3.5, 4, 4.5, 5, 5.5) using molybdenum blue method. All measurements were carried out in triplicate (n = 3).

Conc (mg L^{-1})	**pH 2.5**	**pH 3**	**pH 3.5**	**pH 4**	**pH 4.5**	**pH 5**	**pH 5.5**
1	0.012	0.026	0.020	0.036	0.114	0.004	0.036
SD	0.005	0.006	0.002	0.004	0.005	0.004	0.007
3	0.027	0.035	0.060	0.116	0.249	0.149	0.130
SD	0.002	0.006	0.002	0.005	0.010	0.006	0.006
5	0.058	0.049	0.142	0.205	0.357	0.303	0.296
SD	0.014	0.011	0.009	0.007	0.005	0.008	0.012
7	0.099	0.072	0.200	0.244	0.413	0.416	0.377
SD	0.016	0.004	0.005	0.005	0.010	0.024	0.022
10	0.154	0.122	0.397	0.320	0.522	0.539	0.440
SD	0.012	0.005	0.014	0.006	0.009	0.004	0.020
Slope	0.016	0.011	0.041	0.031	0.044	0.060	0.047
R^2	0.980	0.938	0.955	0.975	0.971	0.981	0.011

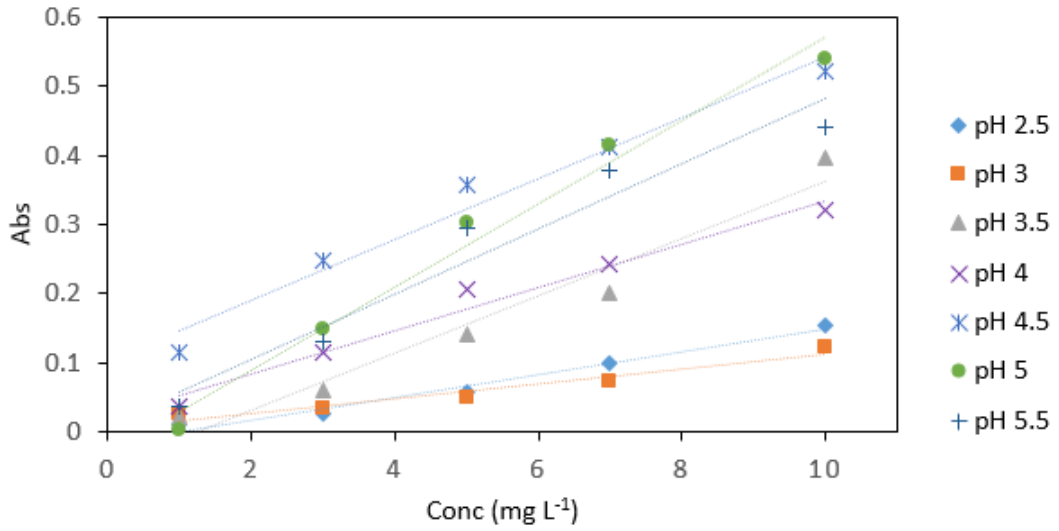

Figure 2.10. A comparison of arsenic samples (1–10 mg L^{-1}) analysed with molybdenum blue method at various pH conditions (2.5, 3, 3.5, 4, 4.5, 5 and 5.5). All measurements were carried out in triplicate (n = 3).

2.4.6 Effect of temperature

The variamine blue method performed best at 30 °C (Table 2.7). In contrast, 18 °C yielded the weakest analytical signal (Figure 2.11).

Table 2.7. Average absorbance values of arsenic samples (1–10 mg L^{-1}) analysed using various incubation temperatures (18, 30, 50, 60 and 70°C) using variamine blue method. All measurements were carried out in triplicate (*n* =3).

Conc (mg L^{-1})	**18°C**	**30°C**	**50°C**	**60°C**	**70°C**
1	0.093	0.101	0.272	0.126	0.139
SD	0.033	0.005	0.008	0.030	0.008
3	0.153	0.288	0.336	0.282	0.292
SD	0.018	0.015	0.013	0.010	0.010
5	0.227	0.450	0.407	0.394	0.365
SD	0.034	0.005	0.030	0.024	0.016
7	0.272	0.570	0.464	0.453	0.467
SD	0.053	0.003	0.026	0.008	0.084
10	0.325	0.685	0.532	0.562	0.557
SD	0.048	0.034	0.010	0.116	0.017
Slope	0.026	0.065	0.029	0.047	0.053
R^2	0.976	0.965	0.991	0.961	0.977

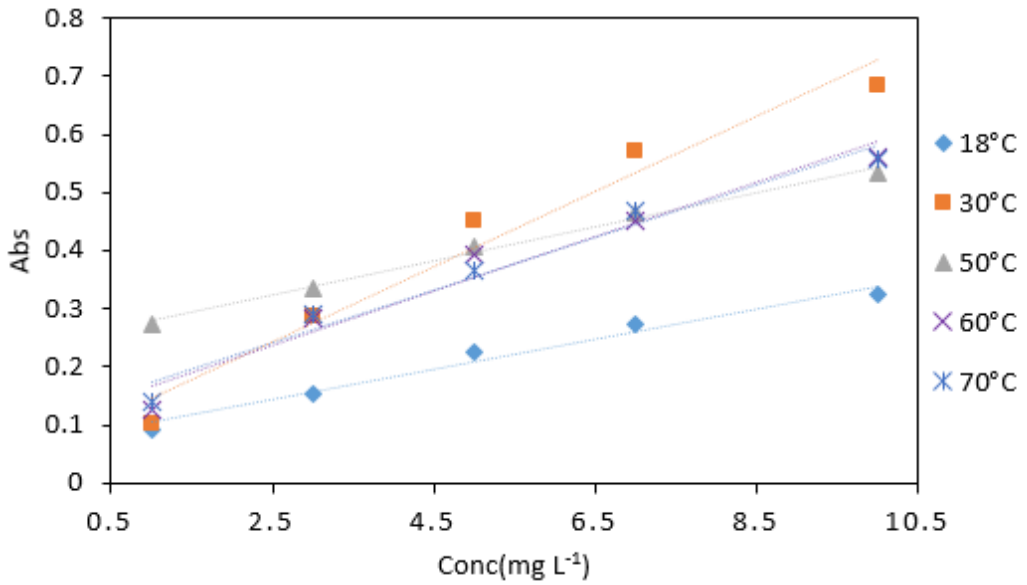

Figure 2.11. A comparison of arsenic samples (1–10 mg L^{-1}) analysed with variamine blue method at various incubation temperatures (18, 30, 50, 60 and 70°C). All measurements were carried out in triplicate (*n* =3).

The highest absorbance values for arsenic analysis using molybdenum blue method were obtained using 50º C incubation temperature (Table 2.8). However, the linearity for this incubation temperature was poor compared to the other incubation temperatures (Figure 2.12). For practical applications the ideal candidate method should be able to yield reliable results at low temperatures such as 18º C as this would both reduce the power consumption and the complexity of the detection system. Addition of heating unit for the detection method would result in additional costs and control requirements and therefore would not be desirable. In addition, the slope values obtained from both methods at low temperature analysis indicate limited sensitivity to arsenic.

Table 2.8. Average absorbance values of arsenic samples (1–10 mg L^{-1}) analysed using various incubation temperatures (18, 25, 30, 40 and 50°C) using molybdenum blue method. All measurements were carried out in triplicate (n = 3).

Conc (mg L^{-1})	**18 °C**	**25 °C**	**30 °C**	**40 °C**	**50 °C**
1	0.096	0.167	0.174	0.032	0.259
SD	0.031	0.031	0.012	0.005	0.021
2	0.135	0.170	0.313	0.062	0.288
SD	0.061	0.032	0.013	0.006	0.019
4	0.147	0.194	0.398	0.219	0.299
SD	0.045	0.012	0.020	0.017	0.071
6	0.180	0.198	0.479	0.250	0.383
SD	0.054	0.027	0.009	0.014	0.065
10	0.269	0.245	0.552	0.446	0.603
SD	0.056	0.040	0.010	0.027	0.014
Slope	0.018	0.009	0.060	0.046	0.034
R^2	0.971	0.967	0.978	0.976	0.776

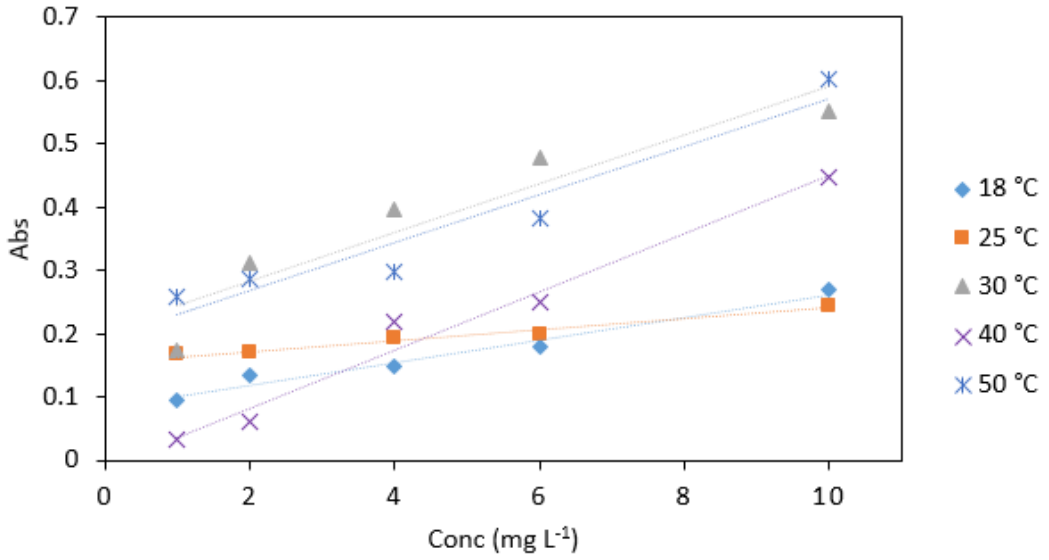

Figure 2.12. A comparison of arsenic samples (1–10 mg L^{-1}) analysed with molybdenum blue method at various incubation temperatures (18, 25, 30, 40 and 50 °C). All measurements were carried out in triplicate (n = 3).

2.4.7 Time

The colour formation after addition of the variamine blue dye was instant and the absorbance remained unchanged for 30 min (Figure 2.13). After this a slow decrease in absorbance was observed. After an hour 1.4 % decrease in absorbance was observed (relative to the absorbance obtained at 15 min after addition of the dye). For *in situ* microfluidic detection applications, more stable colour formation would be desirable than that demonstrated by variamine blue method.

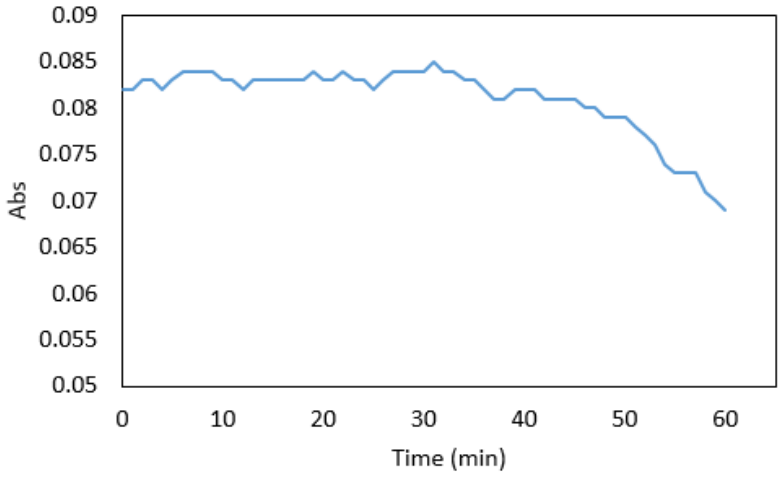

Figure 2.13. Absorbance of 1 mg L^{-1} arsenic sample premixed with varimine blue reagents over 60 min.

The colour formation after addition of the molybdenum blue dye occurred rapidly. The most rapid increase in absorbance was observed from the time in the first 26 minutes after the addition of the dye with a slow increase in absorbance observed afterwards (Figure 2.14).

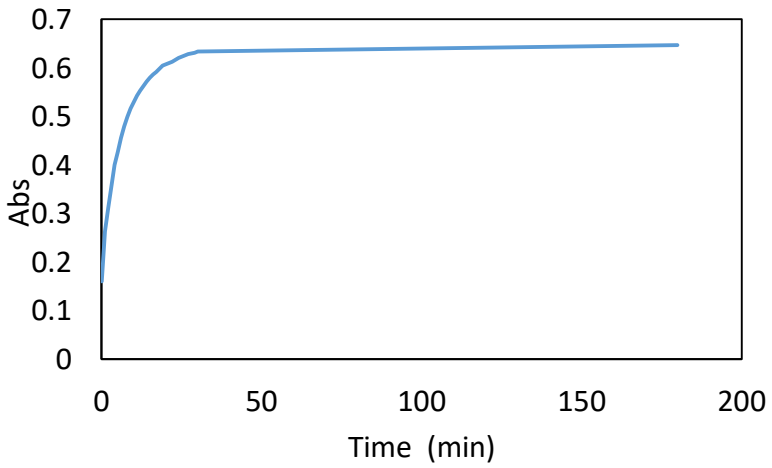

Figure 2.14. Absorbance of 2 mg L^{-1} arsenic sample premixed with molybdenum blue reagents over 180 min.

2.5 Discussion

Potassium iodate acts as an oxidising agent turning arsenite to arsenate in acidic conditions. For molybdenum blue method 0.15 % potassium iodate concentration was found to be the optimum, however, there was no obvious explanation for this. The colour reagent for molybdenum blue method was not stable and required daily preparation. Reagent stability is an important parameter for method application for environmental monitoring as analysis over long periods of time are required. Therefore, molybdenum blue method was not considered for further evaluation and optimisation.

Colour formation and stability is influenced by pH. For variamine blue method pH 3 was found to be the optimum. Narayana *et al*. reported pH 4 to be optimum for the arsenic determination method. This discrepancy was not investigated further due to the selection of the leucomalachite green method for further development. The optimum pH for molybdenum blue method was found to be pH 5 as it yielded the strongest analytical signal compared to other pH measurements with slope of 0.06. Based on these parameters both methods would be suitable for use in microfluidic detection systems as they do not require strongly alkaline or acidic conditions which would significantly limit the lifetime of a polymeric detection chip.

The linear range for molybdenum blue method was observed between 0.1 and 10 mg L^{-1} which was broader than the linear range for variamine blue method which was between 1-10 mg L^{-1}. Even though the linear range for molybdenum blue method was relatively broad, it was not able to measure low arsenic concentrations in comparison to other methods described. For example, Pillai *et al.* reported an

arsenic detection method using rhodamine –b dye with linear range between 0.04-0.4 mg L^{-1} (Pillai *et al.,* 1999). In addition, Revanasiddappa *et al.* reported an arsenic detection method using leucomalachite green with linear range between 0.09–0.9 mg L^{-1} (Revanasiddappa *et al.,* 2007). For applications in surface water monitoring ability to detect low arsenic concentrations would be desirable.

The stability of colour complex depends on the extent of reduction and the availability of excess reductant which prevents re oxidation by dissolved oxygen (Nagul *et al.,* 2015). Colour formed during variamine blue analysis was stable for at least 30 min after which a slow decrease in absorbance was noted. Narayana *et al.* reported that the formed colour species was stable for 8 hours. Colour complex formed during molybdenum blue analysis was stable for at least three hours with no decrease in absorbance detected.

Optimum incubation temperatures for variamine blue and molybdenum blue methods were 30º C and 50º C, respectively. In order to achieve these temperatures heating units can be integrated within microfluidic detection systems in order to achieve the desired experimental conditions. For example, microheaters can be applied for fast heating with even thermal distribution (Wu *et al.,* 2009). However, this would make the analysis less cost effective significant power supply in comparison to systems that do not require an incubation step such as the leucomalachite green method.

Overall, the based on these results and the positive findings from assessment of leucomalachite green method, the lecuomalachite green method was selected for further assessment and incorporation into microfluidic detection system.

2.6 Conclusion

The potential for variamine blue and molybdenum blue method application for arsenic determination in water using microfluidic detection systems was assessed. Strong analytical signal was obtained from measurements using 1 mm path length cuvettes for both methods. Strong colour development and stability for as observed for molybdenum blue method, whereas, the colour stability was poor for variamine blue method. The variamine blue method had a relatively small number of reagents in comparison to molybdenum blue method. In addition, the colour regent for molybdenum blue method had to be prepared before analysis which would not be desirable for microfluidic detection use as it would require a less cost effective and more complicated system design. Additionally, a large number of reagents were required for this method. In contrast, an ideal candidate colorimetric method would require minimal sample preparation and small number of reagents. Constant colour reagent preparation would also reduce the precision and reliability of the method. Both methods showed significantly lower sensitivity at room temperature to higher incubation temperatures such as 30º C and 50º C. Ideally, the candidate method should be able to yield reliable results at low temperatures as this would eliminate the need to incorporate heating device into microfluidic detection system which would add additional costs to the system design and power consumption. Lastly, the ideal candidate colorimetric method should demonstrate high precision and accuracy. These criteria were not met by either of the methods. Despite some of the advantages demonstrated by both of the methods such the performance in 1 mm path length cuvettes, there were a number of disadvantages detected with both methods. Overall, the study showed that variamine blue and molybdenum blue

methods would not be suitable for further optimisation and assessment for use in microfluidic detection systems.

Chapter 3

Arsenic Monitoring in Water by Colorimetry Using an Optimized Leucomalachite Green Method

This chapter was based on the following article published in the Journal: Molecules

ARSENIC MONITORING IN WATER BY COLORIMETRY USING AN OPTIMIZED LEUCOMALACHITE GREEN METHOD

DOI: 10.3390/molecules24020339

Authors: Annija Lace, David Ryan, Mark Bowkett and John Cleary

3.1 Abstract

Arsenic contamination of drinking water is a global concern. Standard laboratory methods that are commonly used for arsenic detection in water, such as atomic absorption spectrometry and mass spectrometry, are not suitable for mass monitoring purposes. Autonomous microfluidic detection systems combined with a suitable colorimetric reagent could provide an alternative to standard methods. Moreover, microfluidic detection systems would enable rapid and cost efficient *in situ* monitoring of water sources without the requirement of laborious sampling. The aim of this study is to optimize a colorimetric method based on leucomalachite green dye for integration into a microfluidic detection system. The colorimetric method is based on the reaction of arsenic (III) with potassium iodate in acid medium to liberate iodine, which oxidizes leucomalachite green to malachite green. Rapid colour development was observed after the addition of the dye. Beer's law was obeyed in the range between 0.07–3 mg L^{-1}. The detection limit and quantitation limit were found to be 0.065 and 0.21 mg L^{-1}, respectively.

Keywords: *arsenic; colorimetric methods; environmental monitoring; leucomalachite green; microfluidics*

3.2 Introduction

Arsenic contamination of groundwater and surface water is a major issue in certain regions of the world (Zhu *et al.,* 2008). Arsenic and its compounds are toxic and can cause serious health effects (Karim 2000). Human exposure to arsenic arises through consumption of arsenic contaminated food and water. Chronic exposure to high concentrations of arsenic can cause severe health implications, collectively known as arsenicosis (Argos *et al.,* 2010). Some of the symptoms of arsenicosis include skin lesions, nervous system disorders, gastrointestinal problems and various types of cancers (Mandal *et al.,* 2002; Kapaj *et al.,* 2006).

Inorganic arsenic is naturally present at high levels in the groundwater of several countries, including India (Mazumder *et al.,* 1998; Chowdhury *et al.,* 2000). Pakistan (Farooqi *et al.,* 2007), China (Rodriguez-Lado *et al.,* 2013), Vietnam (Ber *et al.,* 2001) and several parts of the United States (Korte 1991; Welch *et al.,*1998; Steinmaus *et al.,* 2003). Arsenic contamination of ground water in Bangladesh is one of the most serious examples of chronic arsenic exposure (Kinniburgh *et al.,* 2000). Arsenic concentrations in drinking water in Bangladesh far exceed the World Health Organization's (WHO) maximum permissible limit of 10 μg L^{-1} (Gomez-Caminero *et al.,* 2001). In some tube wells arsenic concentrations as high as 2500 μg L^{-1} have been detected (UNICEF 2008).

In order to improve and monitor the environmental quality of water, reliable and good quality information is needed. Analytical methods capable of detecting arsenic at low concentrations are usually based on sophisticated laboratory instrumentation (Hu *et al.,* 2012). Atomic absorption spectrometry (AAS), induced coupled plasma atomic emission spectrometry (ICP-AES), X-ray fluorescence, and atomic

fluorescence spectrometry are examples of sensitive and selective methods used for arsenic detection and analysis (Pillai *et al.,* 2000). While high quality data is obtained from these methods, the cost of analyzing water samples is significant due to the manpower and instrumentation requirements and the overall cost of analysis. Therefore, these powerful laboratory methods are not suitable for routine, high frequency arsenic monitoring (Moore *et al.,* 2009).

Given the challenges associated with rapid and affordable arsenic detection, much research has been carried out for alternative method development (Dasgupta *et al.,* 2002; Kundu *et al.,* 2002; Khairy *et al.,* 2010; Sanllorente-Mendez *et al.,* 2010; Nath *et al.,* 2014). Because of their small size microfluidic detection systems have many advantages over traditional laboratory-based analytical techniques (Whitesides 2006). The small size enables development of compact and portable sensing systems, sometimes referred to as point of need or point of care systems that can be directly applied at a sampling site without the need for sample collection, transport, or storage (Nguyen *et al.,* 2018). The micro scale enables fast reaction time which in turn results in high sample throughput. As small sample size is required when working on the microscale, reagent consumption and waste generation are minimized. These properties of microfluidic detection systems make them suitable for development of autonomous *in situ* water monitoring sensors (Cleary *et al.,* 2013).

Microfluidic detection systems have been developed for phosphate (Floquet *et al.,* 2011), nitrate (Gardolisnki *et al.,* 2002), ammonia (Daridon *et al.,* 2001) and pH (Patey *et al.,* 2008) monitoring in water. Nevertheless, very few commercially available microfluidic detection systems have been developed for heavy metal

monitoring in water. The low limit of detection for arsenic and other heavy metals poses a key challenge for development of microfluidic sensing systems for drinking water applications. Interfering substances, turbidity, sample colour, and limited selectivity pose additional issues in such applications (Niessner 2010).

Electrochemical sensors have been implemented for different heavy metal monitoring. Normally, electrochemical detection methods are very sensitive. Nonetheless, long term monitoring using these methods is challenging because of limitations such as sensor drift, high maintenance cost, biofouling, and difficulty in analyzing complex matrices (Chailapakul *et al.,* 2008).

Analysis using optical detection systems minimizes fouling effects by avoiding the need for direct contact between sample and sensor. Colorimetric methods allow simple detection systems, therefore, making them suitable for portable heavy metal monitoring (Yogorajah *et al.,* 2015).

In the literature a wide range of different chromophoric dyes for heavy metal detection in water have been described (Ranyuk *et al.,* 2009; Want *et al.,* 2011; Wu *et al.,* 2011; Abalos *et al.,* 2012; Xie *et al.,* 2012). Leucomalachite green (LMG) dye has been used for arsenic detection in environmental samples. In the procedure described by Revanasiddappa *et al.* arsenic is reacted with potassium iodate in order to liberate iodine. The liberated iodine in turn oxidises LMG to malachite green (MG) which in the presence of sodium acetate buffer forms a strong green colour. The intensity of the formed colour depends on the concentration of arsenic in the sample (Revanasiddappa *et al.,* 2007). The reaction mechanism of LMG method is outlined in Figure 3.1. To date the LMG method has not been incorporated into a microfluidic detection system.

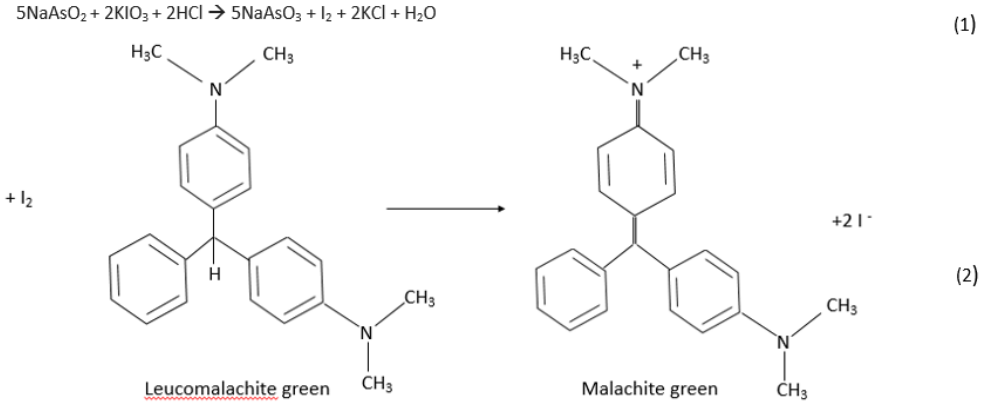

Figure 3.1. Reaction mechanism of leucomalachite green method.

A range of different parameters such as pH, temperature, reagent ratio and reagent stability were evaluated. Both pH and temperature have a significant role in colour formation rate. Microfluidic monitoring devices ideally should be able to yield reproducible and reliable results for long periods of time once deployed in the field. Consequently, reagent stability can be a major limitation for method's use in deployable detection systems (Cleary *et al.*,. 2013). Therefore, reagent stability was assessed for the leucomalachite green method. Ideal microfluidic detection sytem should be cost effective (Tsai *et al.*, 2015). Reducing the complexity and number of separate reagents used in colorimetric methods has been shown to simplify microfluidic systm design without compromising analytical performance (Cogan *et al.*, 2013, Cogan *et al.*,2014). Leucomalachite green method's performance using various regant ratio was assessed. Finally, environmental water analysis poses a great challange for most of analytical detection methods. Complicated water matrices can contain high quantities of interfering which can affect the accuracy of the measurements (Pol *et al.*, 2017). Therefore, a range of samples with various water matrices such as river water, groundwater and lake water were analysed.

Additonally, leucomalachite green method's performance was compared to those of ICP-MS, which is a widely used instrument for quantitative analysis of heavy metals water.

Accordingly, this study aims to optimize a LMG method for cost effective and simple integration into a microfluidic detection system. LMG was selected due to the intense colour development in the visible region at 617 nm. Performance of the optimized method was evaluated in the laboratory on macro- and microscale.

3.3 Materials and methods

3.3.1 Apparatus

A 1800 UV-visible spectrometer (Shimadzu, Canby, USA) was used with Hellma (Mullheim, Germany) 10 mm and 1 mm quartz cuvettes for the absorbance measurements. A pH 20 pH meter (Hanna, Nusfalau, Romania) was used for pH measurements.

3.3.2 Reagents

All chemicals were of analytical grade and purchased from Sigma-Aldrich (Vale Road, Arklow, Co. Wicklow, Ireland) unless otherwise stated. Sodium meta-arsenite ($NaAsO_2$), iron sulphate heptahydrate ($FeSO_4 \cdot 7H_2O$**)** (Fisher Scientific, Leicestershire, UK), magnesium sulphate ($MgSO_4$) (Fisher Scientific), potassium dihydrogen phosphate (KH_2PO_4), manganese sulphate monohydrate ($MnSO4 \cdot H_2O$), and sodium nitrate ($NaNO_3$)were used to prepare stock solutions at concentration 1000 mg L^{-1} in double deionised water (HPLC grade). Working standards were prepared by serial dilutions. Acetic acid (99.8%) (Sharlab S.L., Barcelona, Spain) was used to adjust the pH. Trimethanolamine ($(HOCH_2CH_2)_3N$),

citric acid, ($HOC(COOH)(CH_2COOH)_2$) ascorbic acid (C6H8O6), potassium iodate (KIO_3), leucomalachite green dye ($C_6H_5CH[C_6H_4N(CH_3)_2]_2$), sodium triacetate trihydrate ($C_2H_3NaO_2 \cdot 3H_2O$) were prepared by weighing out an appropriate amount and dissolving it in double deionised water. Hydrochloric acid (38%) (Sharlab S.L.) was used to prepare hydrochloric acid solutions with various concentrations in double deionised water. Double deionized water was used for dilution of reagents and samples.

3.3.3 Sample preparation

Arsenic (As) sample (6 mL) was transferred to a glass vial. Potassium iodate (1%, 1 mL) and hydrochloric acid (1 M, 0.5 mL) were added, and the mixture was gently shaken and left for 2 min. Leucomalachite green dye was added (0.05%, 0.5 mL), followed by sodium triacetate buffer (13.6%, 2 mL). The mixture was gently shaken and left for 5 min. The absorbance was measured at 617 nm against reagent blank.

3.3.4 Path length

Effect of cuvette light path on absorbance was investigated. The procedure was carried out in standard 10 mm quartz cuvettes and micro cuvettes with 1 mm light path for 1–10 mg L^{-1} arsenic concentration range. The experiment was carried out in triplicate. The average absorbance was calculated and showed in the result tables and calibration curves were plotted.

3.3.6 Interference

The effect of various foreign species at mg L^{-1} level on the determination of arsenic was examined. Various foreign ions with concentrations ranging from 100 to 200

mg L^{-1} were introduced to 1 mg L^{-1} arsenic sample. Tolerance limits of interfering agents were established at concentrations that do not cause more than 5% error in the absorbance values of arsenic at 1 mg L^{-1}.

3.3.5 Time

The stability of the colour of the sample was tested over time. One mg L^{-1} arsenic sample was analyzed for a time period of 600 min. The absorbance measurement was started after the addition of the dye. The procedure was carried out in triplicate.

3.3.7 Optimisation of parameters

3.3.7.1 Temperature

A range of different incubation temperatures (4–60 °C) were analyzed. Low temperatures were used in order to determine the viability of the method in low-temperature environments.

3.3.7.2 pH

The effect of sodium triacetate buffer pH was studied using a range of different pH (3.7–7.3). Also, one-way analysis of variance (ANOVA, Single Factor) was applied to analyze the results.

3.3.7.3 Reagent ratio

The effect of combining different reagents and changing the reagent ratio was studied. The original ratio of the method was: 6 (As): 1(KIO_3): 0.5 (1 M HCl): 0.5: (LMG): 2 (sodium triacetate buffer) (A). Firstly, the dye and the buffer were combined to give a reagent ratio: 6 (As): 2.5 (KIO_3): 2.5 (0.2 M HCl): 2.5: (LMG

and buffer) (B). Secondly, 1% KIO_3 and HCl were combined to give reagent ratio of: 6 (As): 2.5 (KIO_3 and 0.4 M HCl): 2.5 (LMG and buffer) (C). Thirdly, reagent ratio tested was: 2 (As): 2 (1% KIO_3 and 0.4 M HCl): 2 (LMG and sodium triacetate buffer) (D). Fourthly, reagent the ratio assessed was: 2 (As): 1(1% KIO_3 and 0.4 M HCl): 1 (LMG and sodium triacetate buffer) (E). Additionally, one-way analysis of variance (ANOVA, Single Factor) was used to analyze the results obtained from the different reagent ratios.

3.3.8 Reagent stability

The effect of reagent stability on the arsenic determination was investigated. 1% KIO_3 and 0.4 M HCl reagent mixture was prepared and used for arsenic determination over a 5 day time period. Over the course of the experiment fresh arsenic standards and dye and buffer reagent mixture was prepared daily.

The sodium triacetate buffer and LMG dye mixture was prepared and used for arsenic analysis over a 4 day time period. During this fresh arsenic standards and KIO_3 and 0.4 M HCl mixture was prepared daily.

3.3.9 Environmental samples

Water samples were collected from Bog Lake, Co. Laois (pH 8.39), Killeshin water reservoir, Co. Laois (pH 7. 93), groundwater well Co. Laois (pH 7.4), St. Mullins, Co. Carlow (Barrow 1) (pH 7.31) and the River Barrow Carlow (Barrow 2) (pH 7. 27). All water samples were analyzed in triplicate. The sample matrices were analyzed using the leucomalachite green method in order to determine whether or not arsenic was present in concentrations detectable by the method. The different water matrices were then spiked with arsenic (0.03–20 mg L^{-1}) and appropriate

dilutions were made. Prior to the analysis the water samples were filtered firstly using Whatman grade 1 filter paper and secondly with sterile 0.2 μm syringe filters. The pH of the water samples was adjusted to 5.5. The absorbances between different water matrices were compared. In addition, one-way analysis of variance (ANOVA, Single Factor) was used to analyze the results for the different water matrices.

3.3.10 Comparison between optimised LMG method and ICP-MS

The optimised LMG method was compared to accredited ICP-MS which is the gold standard method for heavy metal analysis in water. A calibration curve in a range of 0.2-3 mg L^{-1} was obtained using the optimised LMG method. 1 mg L^{-1} sample was analysed as unknown. The concentration of the sample was calculated from the calibration curve ($y = 0.1028x - 0.0106$). 1 mg L^{-1} environmental water samples were analysed using ICP-MS. The concentration for 1 mg L^{-1} water samples obtained from optimised LMG method and the ICP-MS were compared. Percentage difference was calculated using formula: (Conc. ICP MS –Conc. LMG method) × 100/Conc. ICP MS. All measurements were carried out in triplicate.

3.4 Results and discussion

3.4.1 Analytical data

Absorption spectra of 1 mg L^{-1} arsenic sample against reagent blank and reagent blank against double deionized water are shown in Figure 3.2. Beer's law was obeyed in the range of 0.07–3 mg L^{-1}. The molar absorptivity coefficient was found to be 1.5×10^4 L mol^{-1} cm^{-1}. Sandell's sensitivity was found to be 0.2×10^{-2} µg cm^{-1}. The limit of detection (LOD = 3 sd b m^{-1}) and the limit of quantification (LOQ = 10 sd b m^{-1}), where sd b is the standard deviation of blank and m is the slope of the calibration curve) were found to be 0.065 and 0.22 mg L^{-1}, respectively. In comparison, Narayana *et al.* described a colorimetric arsenic detection method with a LOD of 0.022 mg L^{-1} and linear range between 0.2 and 14 mg L^{-1} (Narayana *et al.*,2005). Chakraborty *et al.* described an arsenic detection method with a LOD of 0.4 mg L^{-1} and linear range between 0.4 and 12 mg L^{-1} (Chakraborty *et al.*, 2012). Alternatively, electrochemical methods have been utilized which have shown lower detection limits with broader linear ranges. For example, Lin *et al.* developed an arsenic detection assay based on G-quadropole complex with LOD of 4.5 µg L^{-1} and linear range of 0.74–14.98 mg L^{-1} (Lin *et al.,* 2017). Dai and Compton used electrodes coated with gold nanoparticles for determination of arsenic and achieved LOD of 5 µg L^{-1} and a linear range of 1–180 µg L^{-1} (Dai *et al.*,2006).

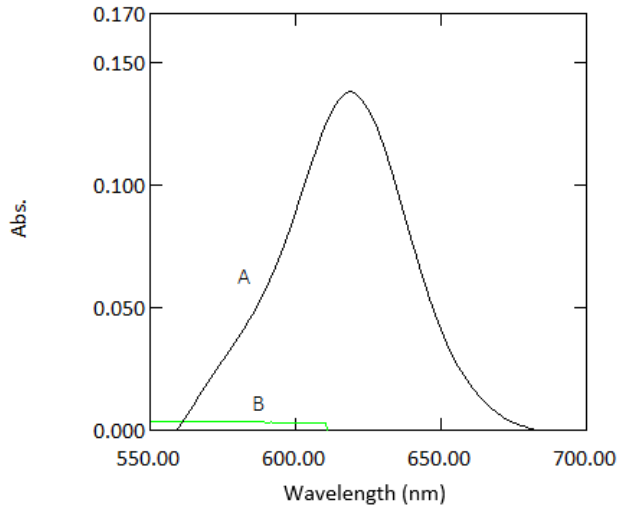

Figure 3.2. Absorption spectra of coloured species (1 mg mL^{-1} arsenic) versus reagent blank (A) and reagent blank versus double deionized water (B) measured at 617 nm.

However, colorimetric methods should be considered for arsenic monitoring purposes as they have several advantages over electrochemical methods in terms of cost effectiveness, portability, and lower susceptibility to fouling.

3.4.2 Path length

The absorbance values for 1 mm quartz cuvette measurements was 10 times lower than for standard cuvette measurements, as expected (Table 3.1 and Figure 3.3). As it can be seen from the calibration graphs (Figure 3.4) the analytical response was strong for samples measured in microcuvettes. The linearity compared to standard quartz cuvette measurements was good. The response signal and linearity obtained from the microcuvettes was strong which indicates that the leucomalachite green method is suitable for use in microfluidic detection systems.

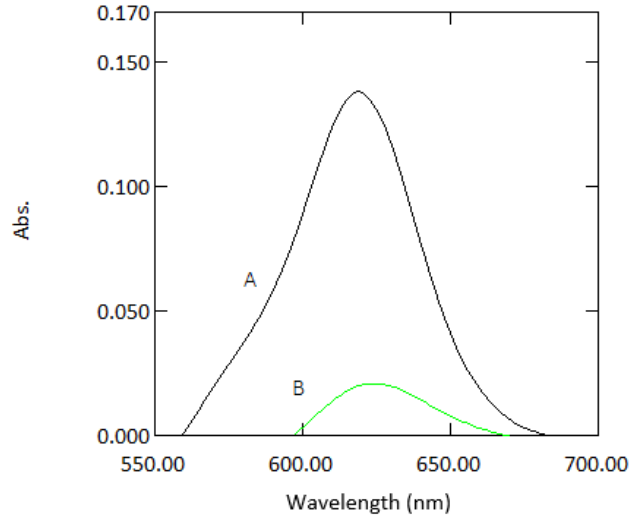

Figure 3.3. Absorption spectra of a sample containing 1 mg L^{-1} arsenic with reagents measured in 10 mm cuvettes (A) and 1 mm quartz cuvettes (B) against reagent blank measured at 617 nm.

Table 3.1. Average absorbance values for arsenic samples (0.2–1 mg L^{-1}) analyzed in two different types of cuvettes. All measurements were carried out in triplicate (n = 3).

	10 mm			**1 mm**		
Conc (mg L^{-1})	**Abs**	**SD**	**% RSD**	**Abs**	**SD**	**% RSD**
0.1	0.025	0.002	6.030	0.039	0.001	0.058
0.3	0.066	0.001	0.115	0.121	0.007	0.681
0.5	0.132	0.006	0.624	0.199	0.006	0.569
0.7	0.192	0.003	0.252	0.285	0.008	0.802
1	0.254	0.004	0.416	0.389	0.006	0.643

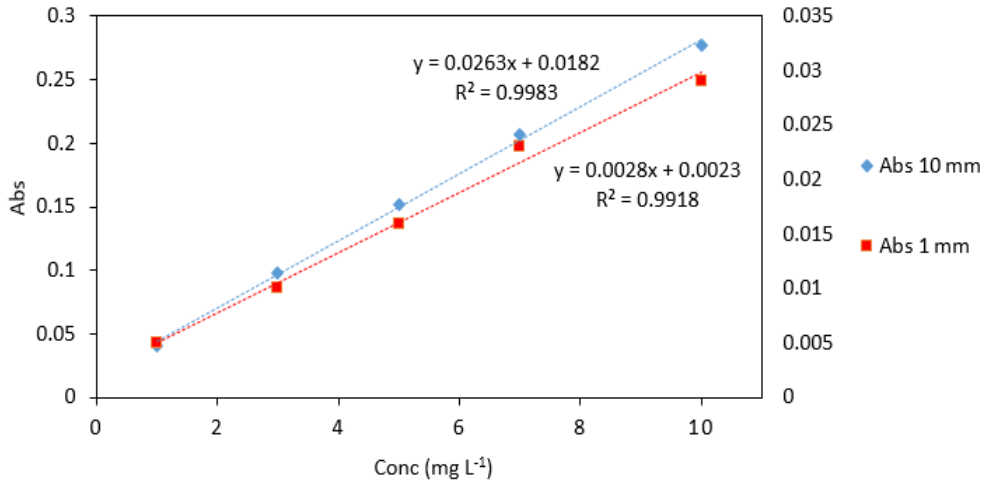

Figure 3.4. Comparison of arsenic standards (1–10 mg L^{-1}) measured in quartz cuvettes with 10 mm and 1 mm path lengths. Left vertical axes represent the absorbance of standards analyzed in 10 mm quartz cuvettes (blue markers). Right vertical axes represent the absorbance of standards analyzed in 1 mm quartz microcuvettes (red markers). All measurements were carried out in triplicate. Error bars represent standard deviations of the measurements.

3.4.3 Time

The maximum absorbance was reached 73 min after the addition of the dye, however, the absorbance reached 95% of the maximum value within approximately 5 min. At this time the absorbance was sufficiently stable to allow a measurement to be taken, and a 5 min reaction time was used in subsequent experiments. After the maximum absorbance was observed, there was a gradual decrease in absorbance up to a time of 600 min (Figure 3.5). Overall, the colour stability was good and suitable for measurements in a microfluidic detection system.

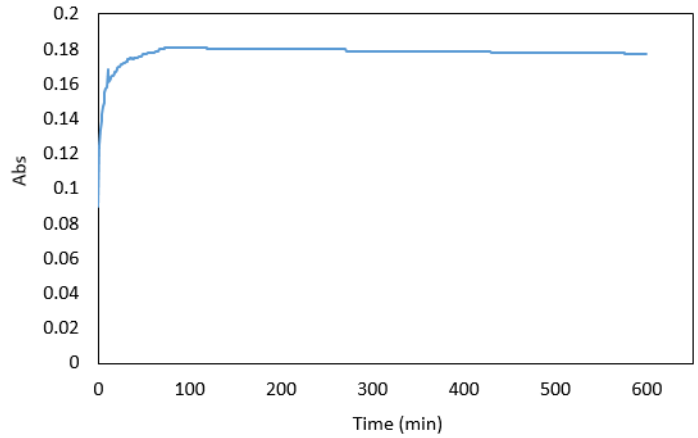

Figure 3.5. Absorbance of 1 mg L^{-1} arsenic sample premixed with the reagents over 600 min.

3.4.4 Interference

Among the different species investigated, Fe (II) interfered with the leucomalachite green method (Table 3.2). Typical surface waters can contain a range of different ions, including iron, nitrate, magnesium, manganese, phosphates and nitrates. Therefore, the interference of these ions was assessed.

Masking agents such as EDTA, citric acid, ascorbic acid and trimethylethanolamine were tested to overcome the interference, but it was found, that EDTA trimethylethanolamine, and citric acid themselves interfered with the leucomalachite green method. Iron interference was therefore masked by 1% ascorbic acid.

Table 3.2. Effect of foreign species on the determination of arsenic (III) (1 mg L^{-1}).

Interferents	Tolerance Limit (mg L^{-1})
Mn, Mg, PO_4, NO_3	100
Fe (II)	0.1
EDTA	3,800
Citric acid	100,000
Trimethylethanolamine	450

3.4.5 Optimisation of Parameters

3.4.5.1 Temperature

The method performed best at 50 °C (Figure 3.6). For practical applications, carrying out the method at high temperatures would add to the cost and overall complexity of the method. The slope and linearity of 4 °C incubation temperature was low compared to the other temperatures (Table 3.3). It can, however, be concluded that the method has the potential to be applied in low temperature environments, and further examination of the kinetics of the reaction at low temperatures will be carried out.

Table 3.3. Average absorbance values of arsenic samples (0.2–1 mg L^{-1}) analyzed at various incubation temperatures (4, 10, 18, 30, 40, 50 and 60 °C). All measurements were carried out in triplicate (*n* =3).

Conc (mg L^{-1})	**4 °C**	**10 °C**	**18 °C**	**30 °C**	**40 °C**	**50 °C**	**60 °C**
0.2	0.024	0.021	0.030	0.051	0.056	0.063	0.044
SD	0.005	0.002	0.001	0.005	0.001	0.003	0.003
0.4	0.034	0.069	0.073	0.107	0.106	0.113	0.099
SD	0.004	0.007	0.001	0.003	0.000	0.001	0.001
0.6	0.049	0.106	0.104	0.157	0.159	0.169	0.157
SD	0.005	0.018	0.002	0.004	0.001	0.002	0.003
0.8	0.072	0.133	0.135	0.191	0.204	0.217	0.220
SD	0.004	0.023	0.002	0.003	0.001	0.002	0.002
1	0.093	0.197	0.167	0.246	0.254	0.279	0.261
SD	0.010	0.005	0.001	0.001	0.001	0.001	0.002
Slope	0.088	0.208	0.168	0.2429	0.2526	0.2733	0.2701
R^2	0.9774	0.9832	0.9953	0.9961	0.9991	0.9987	0.9968

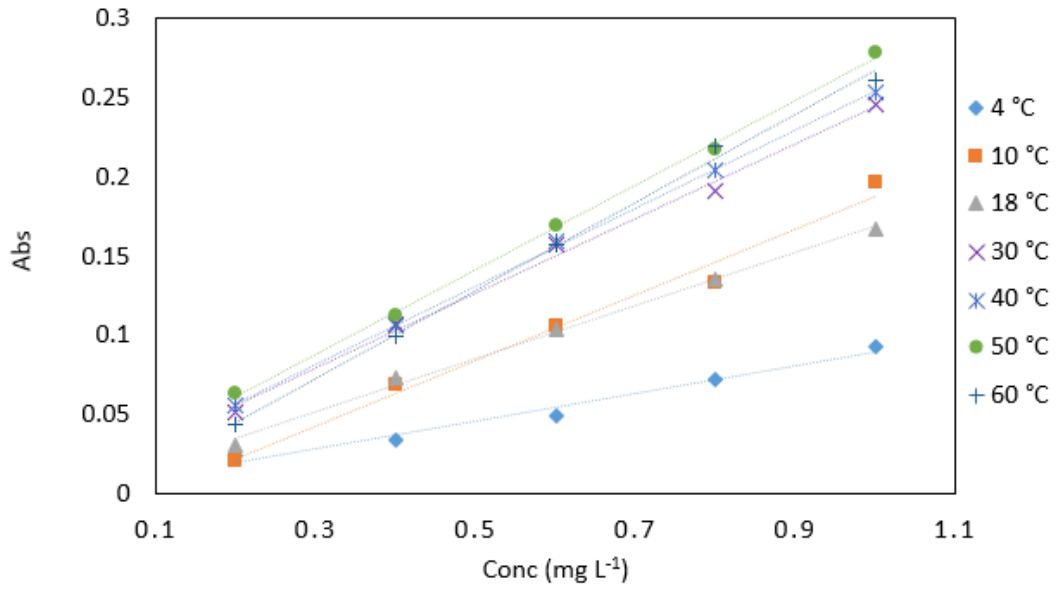

Figure 3.6. A comparison of arsenic samples (0.2–1 mg L^{-1}) analyzed at various incubation temperatures (4, 10, 18, 30, 40, 50 and 60 °C). All measurements were carried out in triplicate (n = 3).

3.4.5.2 pH

Table 3.4 shows the results obtained when arsenic samples were analyzed using different buffer pH values. The highest absorbance values were obtained when using pH 5.5 buffer (Table 3.4). Because of the analytical response buffer pH of 5.5 was found to be the optimum pH for the procedure (Figure 3.7) and used in subsequent experiments. Using ANOVA analysis, a significant difference was found between the absorbances at different buffer pH ($p < 0.05$).

Table 3.4. Average absorbance of arsenic samples (0.2–1 mg L^{-1}) analyzed with various sodium triacetate buffer pH. All measurements were carried out in triplicate (n = 3).

Conc (mg L^{-1})	**pH 3.5**	**pH 3.9**	**pH 4**	**pH 4.7**	**pH 5**	**pH 5.5**	**pH 5.8**	**pH 6**
0.2	0.037	0.039	0.057	0.048	0.048	0.057	0.048	0.038
SD	0.003	0.002	0.011	0.003	0.002	0.003	0.003	0.003
0.4	0.068	0.074	0.088	0.108	0.097	0.106	0.083	0.084
SD	0.002	0.002	0.002	0.002	0.004	0.001	0.006	0.004
0.6	0.085	0.102	0.120	0.130	0.138	0.161	0.125	0.116
SD	0.003	0.001	0.003	0.003	0.005	0.001	0.003	0.006
0.8	0.109	0.127	0.149	0.154	0.168	0.205	0.155	0.156
SD	0.003	0.002	0.004	0.003	0.002	0.002	0.005	0.004
1	0.129	0.157	0.174	0.196	0.201	0.254	0.190	0.185
SD	0.001	0.002	0.004	0.002	0.001	0.004	0.005	0.002
Slope	0.126	0.081	0.168	0.171	0.200	0.253	0.188	0.188
R^2	0.983	0.989	0.979	0.968	0.990	0.999	0.995	0.997

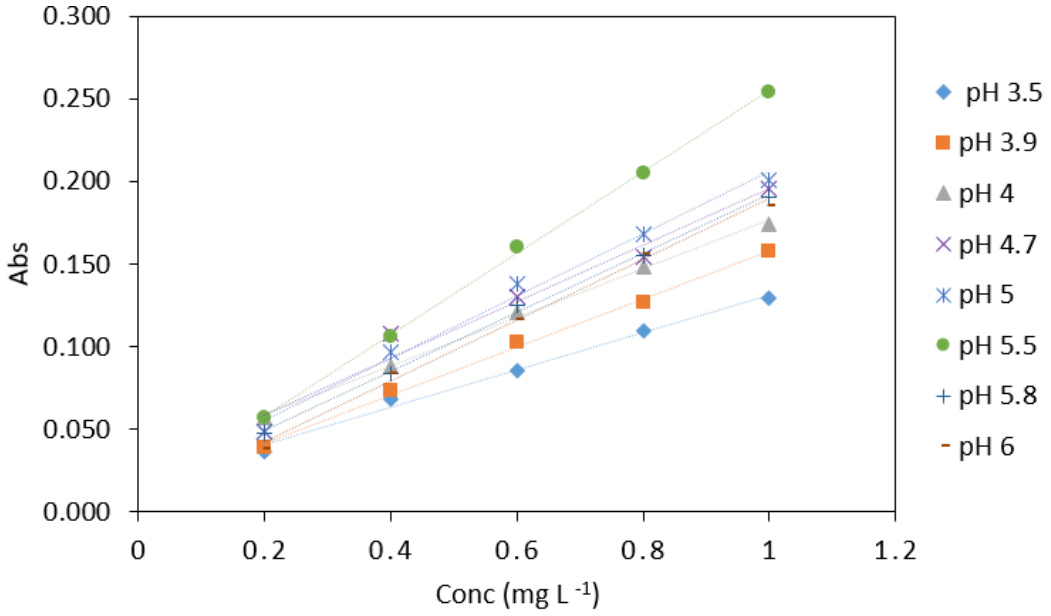

Figure 3.7. Comparison of arsenic samples (0.2–1 mg L^{-1}) analyzed using various sodium triacetate buffers (pH 3.5, 3.9, 4, 4.7, 5, 5.5, 5.8, 6). All measurements were carried out in triplicate (n = 3).

3.4.5.3 Reagent ratio

The order in which reagents interact with one another is important in LMG rmethod. Arsenic reacts firstly with potassium iodate to liberate iodine in acidic medium achieved by addition of hydrochloric acid. Once this reaction has occurred leucomalachite green dye is introduced resulting in oxidation of the dye and colour formation in presence of sodium actetate buffer at pH values around 4.5 (Kamaya *et al.*, 2015). The statistical analysis showed that there was a significant difference between the absorbances obtained using different reagent ratios ($p < 0.05$). Reagent ratio A gave the best response as it had the highest slope (Figure 3.8) from all the reagent ratios tested and also the highest absorbance values (Table 3.5). However, for microfluidic detection system use reagent ratio D was chosen as it has the simplest reagent ratio. Small number of reagents is desirable for colorimetric

method's incorporation into microfluidic chip, as this reduces the fabrication costs. Therefore, this would simplify the design of the microfluidic detection system and the overall device.

Table 3.5. Average absorbance of arsenic samples (0.2–1 mg L^{-1}) analyzed using various reagent ratios: A), 6 (As): 1(KIO_3): 0.5 (1 M HCl): 0.5: (LMG): 2 (sodium triacetate buffer), (B), 6 (As): 2.5 (KIO_3): 2.5 (0.2 M HCl): 2.5: (LMG and buffer), (C), 6 (As): 2.5 (KIO_3 and 0.4 M HCl): 2.5 (LMG and buffer), (D), 2 (As): 2 (1% KIO_3 and 0.4 M HCl): 2 (LMG and sodium triacetate buffer) and (E) 2 (As): 1(1% KIO_3 and 0.4 M HCl): 1 (LMG and sodium triacetate buffer). All measurements were carried out in triplicate (n = 3).

	Reagent Ratio				
Conc (mg L^{-1})	**A**	**B**	**C**	**D**	**E**
0.2	0.053	0.052	0.045	0.043	0.056
SD	0.004	0.004	0.008	0.009	0.01
0.4	0.094	0.101	0.081	0.071	0.089
SD	0.007	0.006	0.004	0.021	0.008
0.6	0.148	0.113	0.132	0.104	0.126
SD	0.006	0.01	0.009	0.024	0.008
0.8	0.179	0.137	0.168	0.114	0.162
SD	0.006	0.006	0.01	0.008	0.007
1	0.24	0.171	0.201	0.135	0.186
SD	0.006	0.006	0.003	0.018	0.016
Slope	0.232	0.16	0.203	0.114	0.167
R^2	0.996	0.957	0.996	0.971	0.996

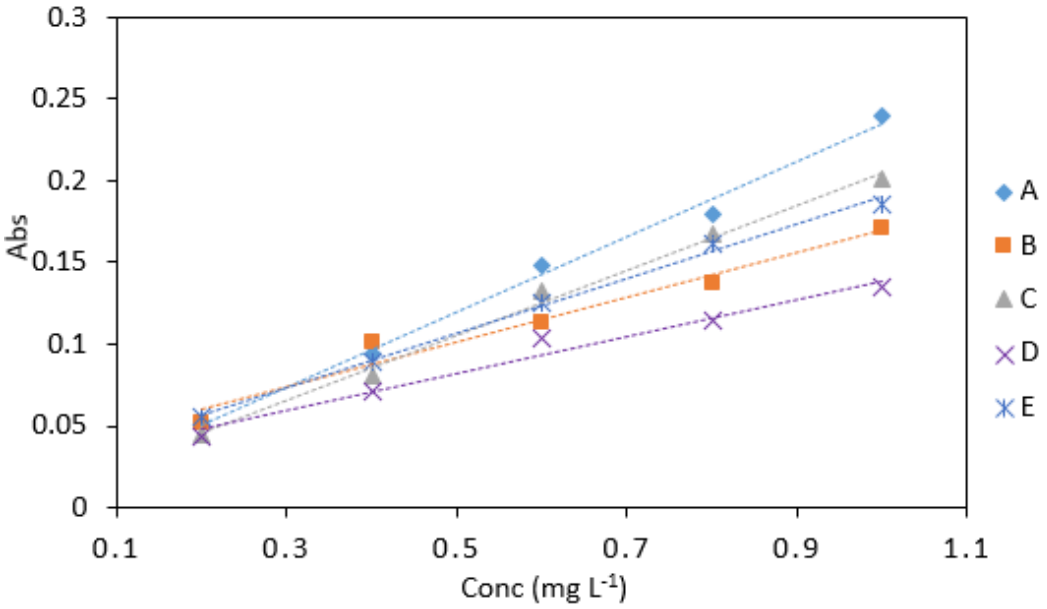

Figure 3.8. A comparison of arsenic samples (0.2–1 mg L^{-1}) analyzed using several reagent ratios: (A), 6 (As): 1(KIO_3): 0.5 (1 M HCl): 0.5: (LMG): 2 (sodium triacetate buffer), (B), 6 (As): 2.5 (KIO_3): 2.5 (0.2 M HCl): 2.5: (LMG and buffer), (C), 6 (As): 2.5 (KIO_3 and 0.4 M HCl): 2.5 (LMG and buffer), (D), 2 (As): 2 (1% KIO_3 and 0.4 M HCl): 2 (LMG and sodium triacetate buffer) and (E) 2 (As): 1(1% KIO_3 and 0.4 M HCl): 1 (LMG and sodium triacetate buffer).

3.4.5.4 Reagent stability

Decreasing absorbance values over time were noted for KIO_3 and 0.4 M HCl mixture (Table 3.6 and Figure 3.9), however, the slope of the calibration line was relatively consistent in each case. The method yielded analytically useful calibration data over the time period studied and for implementation in a microfluidic device, the change in absolute absorbance values can be corrected for using a regular calibration protocol.

Table 3.6. Average absorbance values for arsenic samples (0.2–1 mg L^{-1}) analyzed periodically on day 0, 1, 2, 3, 4 and 5 under the same conditions with the same potassium iodate and hydrochloric acid mix. All measurements were carried out in triplicate (n = 3).

	Time (Days)				
Conc (mg L^{-1})	**0**	**1**	**2**	**3**	**5**
0.2	0.055	0.051	0.059	0.039	0.044
SD	0.004	0.004	0.001	0.003	0.003
0.4	0.104	0.098	0.094	0.081	0.075
SD	0.003	0.004	0.007	0.007	0.003
0.6	0.151	0.137	0.136	0.118	0.115
SD	0.005	0.003	0.006	0.005	0.004
0.8	0.188	0.173	0.168	0.149	0.138
SD	0.007	0.005	0.006	0.005	0.005
1	0.221	0.204	0.200	0.170	0.174
SD	0.005	0.008	0.003	0.007	0.003
Slope	0.208	0.139	0.134	0.174	0.170
R^2	0.993	0.991	0.988	0.990	0.994

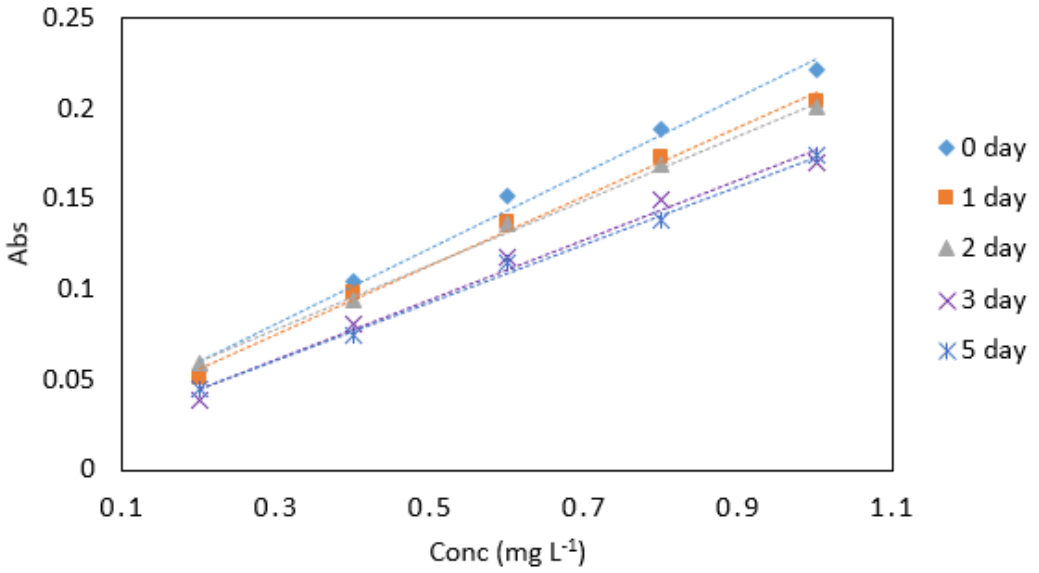

Figure 3.9. Stability of potassium iodate and hydrochloric acid mix in arsenic samples (0.2–1 mg L^{-1}) analyzed periodically over day 0, 1, 2, 3, 4, and 5. All measurements were carried out in triplicate (n =3).

A decrease in absorbance for sodium triacetate buffer and LMG dye mix was observed over a five day period (Table 3.7 and Figure 3.10), however, the slope of the calibration line was relatively consistent in each case.

Table 3.7. Average absorbance for arsenic samples (0.2–1 mg L^{-1}) analyzed periodically on day 0, 1, 2, 3, 4 and 5 under the same conditions with the same dye and buffer mix. All measurements were carried out in triplicate (n = 3).

	Time (Days)					
Conc (mg L^{-1})	**0**	**1**	**2**	**3**	**4**	**5**
0.2	0.089	0.053	0.055	0.053	0.051	0.036
SD	0.003	0.003	0.003	0.003	0.004	0.003
0.4	0.145	0.106	0.104	0.094	0.105	0.062
SD	0.003	0.003	0.003	0.004	0.004	0.003
0.6	0.184	0.147	0.151	0.148	0.142	0.098
SD	0.002	0.004	0.003	0.003	0.004	0.004
0.8	0.220	0.187	0.188	0.179	0.175	0.132
SD	0.003	0.003	0.003	0.004	0.001	0.004
1	0.244	0.228	0.221	0.240	0.218	0.196
SD	0.005	0.003	0.003	0.003	0.004	0.002
Slope	0.193	0.216	0.208	0.233	0.202	0.186
R^2	0.978	0.997	0.993	0.995	0.993	0.978

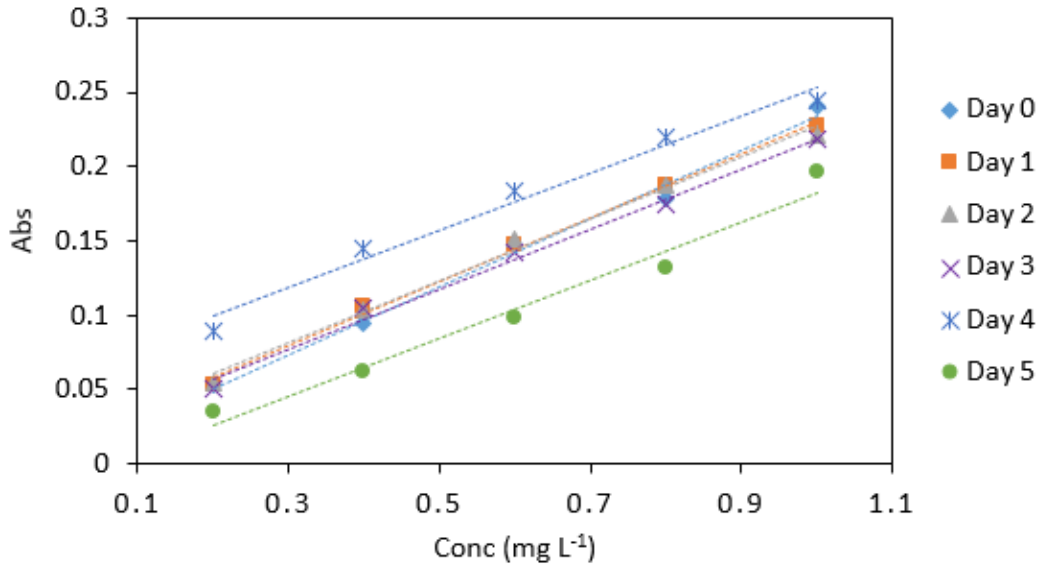

Figure 3.10. Comparison of arsenic samples (0.2–1 mg L^{-1}) analyzed periodically on day 0, 1, 2, 3 and 5 under the same conditions with the leucomalachite green dye and in sodium triacetate buffer (pH 5.5). All measurements were carried out in triplicate (n = 3).

3.4.5.5 Environmental samples

The highest absorbance values were observed in samples collected from the St Mullins site. The lowest absorbance was obtained from Bog Lake samples (Table 3.8). Water samples collected and analyzed from Killeshin reservoir and the River Barrow Carlow site had a similar response to control samples (Figure 3.11).

Table 3.8. The average absorbance of arsenic samples (0.1–1 mg L^{-1}) analyzed in different water matrices. The measurements were carried out in triplicate (n = 3).

Conc (mg L^{-1})	**Control**	**Ground**	**Killeshin Res.**	**Bog Lake**	**Barrow 1**	**Barrow 2**
0.1	0.014	0.013	0.027	0.001	0.006	0.027
SD	0.000	0.001	0.002	0.002	0.001	0.002
0.3	0.024	0.037	0.042	0.003	0.027	0.068
SD	0.001	0.003	0.002	0.002	0.001	0.006
0.5	0.050	0.066	0.061	0.009	0.042	0.094
SD	0.002	0.002	0.006	0.003	0.005	0.002
0.7	0.075	0.077	0.087	0.024	0.061	0.135
SD	0.007	0.002	0.002	0.001	0.004	0.005
1	0.122	0.139	0.131	0.050	0.121	0.163
SD	0.007	0.005	0.005	0.004	0.010	0.007
Slope	0.114	0.135	0.104	0.072	0.123	0.09
R^2	0.996	0.978	0.996	0.996	0.955	0.999

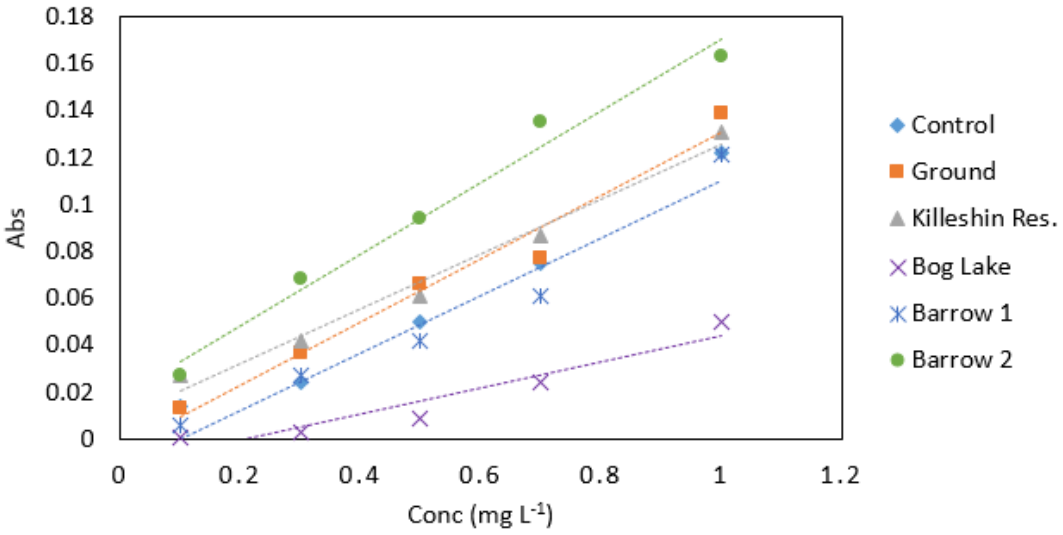

Figure 3.11. Comparison of arsenic samples (0.1–1 mg L^{-1}) analyzed in several water matrices. All measurements were carried out in triplicate (n = 3).

This would indicate that these water samples matrices did not contain high amounts of interfering substances. Statistical analysis revealed a significant difference between Bog Lake and all the other water samples ($p < 0.05$). Also, significant difference was found between Barrow 2 and the other water sample matrices, except for control. The difference in absorbance values could be explained by factors such as sample colour and chemical composition. The Bog Lake sample was strongly coloured due to the presence of humic substances. From this it can be concluded that different water matrices have the potential to affect the result of the leucomalachite green method and this should be taken into account when designing the calibration protocol in any future analytical device.

3.4.5.6 Comparison between optimised LMG method and ICP-MS

Evaluation of arsenic concentrations determined for samples using ICP –MS and the microfluidic detection system showed that the arsenic concentrations were comparable. The results are shown in the Table. The smallest percentage difference (0.12%) was found for double deionised water sample, whereas the greatest percentage difference was observed for lake water sample (13.19%). This could be explained by the strong colour present in the river sample and also by the different factors affecting the microfluidic detection system such as air bubbles and interference from other samples in microfluidic detection channels. Overall, the microfluidic detection systems comparison to ICP-MS emphasizes the effectiveness of microfluidic detection system for arsenic determination in various water matrices. In future studies a wider range of various sample matrices would need to be assessed including waste water.

Table 3.9. A comparison between arsenic concentrations determined using the optimised LMG method and measurements obtained from an accredited ICP-MS.

Sample	ICP-MS Unspiked sample (mg L^{-1})	ICP-MS (mg L^{-1})	LMG method (mg L^{-1})	Percentage difference (%)
Control	0.002	0.97	0.97	0.12
Gound	0.00	0.97	1.02	5.64
Killeshin	0.004	1.08	1.06	2.18
St Mullins	0.00	1.03	1.07	3.51
Bog	0.001	1.06	0.92	13.19
Barrow	0.002	0.97	1.00	2.89

3.5 Discussion

Leucomalachite green method showed great potential for applications via microfluidic detection systems due to the fast reaction time, colour stability and simplicity of method. The strong analytical signal obtained by combining reagents enables simple microfluidic chip design which is desirable for microfluidic detection analysis. Leucomalachite green method had an LOD of 0.065 mg L^{-1}. The leucomalachite green method was more sensitive than method reported by Gulstrom *et al.* which uses ammonium molybdate and was reported to have a dynamic range between 1- 30 mg L^{-1} (Gulstrom *et al.*, 1953). Pillai *et al.* reported an arsenic detection method using rhodamine-b with linear range between 0.04-4 mg L^{-1} (Pillai *et al.*, 1999). In comparison to these methods leucmalachite green method had a relatively broad linear range between 0.07 and 3 mg L^{-1}.

Leucomalachite green method was capable to yield strong analytical response at ambient incubation temperatures which would eliminate the need to use external heating source for microfluidic detection system and, therefore, minimise the power requirement making the analysis more cost effective. Leucomalachite green method was found to yield optimum results at pH 5.5 which would be compatible with microfluidic detection chips made of polymeric materials such as PMMA.

In addition, the method was capable to analyse arsenic in a range of environmental samples. Method's performance was compared to ICP- MS, showing small percentage difference between the measurements. These results highlight method's effectiveness for applications in surface water analysis. Iron was found to interfere with the arsenic measurements, however, the interference could be masked by addition of ascorbic acid. In future, a broader range of interferents and their effect

on arsenic determination should be assessed, including zinc, nickel, bismuth and copper which have been reported to interfere with arsenic determination in other studies (Gullstrom *et al.*,1953, Das *et al.*, 2013, Yogorajah *et al.*,2015).

3.6 Conclusion

The leucomalachite green method proved to be a good candidate for deployment in microfluidic detection systems and arsenic detection in water. The method was optimized for integration into small scale detection systems. The optimum reaction conditions and other analytical parameters were evaluated. The method was found to be simple, fast and robust. The reagent mixtures yielded the optimum results on the day of their preparation, with a gradual decrease in absorbance noted over five days which is an implication for deployable lifetime of system based on this method. Strong analytical response was obtained from 1 mm light path cuvettes indicating that the method would be suitable for use in small dimension microfluidic detection system. The optimized method was also cost effective as only a small number of reagents were required. The method yielded good results with simple 1 to 1 sample to reagent ratio which would be ideal for microfluidic detection applications. Following an investigation of method's performance in different water samples, it was shown that the method is capable to determine arsenic in various water matrices. There is a potential for method's application in waste water monitoring as well as arsenic detection in areas with particularly high arsenic levels.

Chapter 4

Chromium monitoring in water by colorimetry using optimised 1,5-diphenylcarbazide method

This chapter was based on the following article published in the journal:

International Journal of Environmental Research and Public Health

CHROMIUM MONITORING IN WATER BY COLORIMETRY USING OPTIMISED 1,5-DIPHENYLCARBAZIDE METHOD

(EISSN 1660-4601, DOI:10.3390/ijerph16101803)

Authors: Annija Lace, David Ryan, Mark Bowkett and John Cleary

4.1 Abstract

Chromium contamination of drinking water has become a global problem due to its extensive use in industry. The most commonly used methods for chromium detection in water are laboratory-based methods, such as atomic absorption spectrometry and mass spectrometry. Although these methods are both highly selective and sensitive, they require expensive maintenance and highly trained staff. Therefore, there is a growing demand for cost effective and portable detection methods that would meet the demand for mass monitoring. Microfluidic detection systems based on optical detection have great potential for onsite monitoring applications. Furthermore, their small size enables rapid sample throughput and minimises both reagent consumption and waste generation. In contrast to standard laboratory methods, there is also no requirement for sample transport and storage. The aim of this study is to optimise a colorimetric method based on 1,5-diphenylcarbazide dye for incorporation into a microfluidic detection system. Rapid colour development was observed after the addition of the dye and samples were measured at 543 nm. Beer's law was obeyed in the range between 0.03–3 mg L^{-1}. The detection limit and quantitation limit were found to be 0.023 and 0.076 mg L^{-1}, respectively.

Keywords: *chromium; colorimetric methods; environmental monitoring; 1,5-diphenylcarbazide; microfluidics*

4.2 Introduction

Environmental contamination of chromium has become a global concern because of its major role in the industry (Sloof 1990; Quantin *et al.,* 2008, Ashraf *et al.,* 2017). Chromium is widely used in leather tanning, electroplating, paint manufacture, wood treatment, metallurgy, and mining (Kimbrough *et al.,* 1990, Richard *et al.,* 1991, Chen *et al.,* 2012; Butera *et al.,* 2015). Significant amounts of chromium are introduced into the environment through poorly regulated disposal of chromium containing waste (Gao *et al.,* 2011). As a result, chromium concentrations in surface and drinking water can exceed the World Health Organization's maximum allowable concentration of 0.05 mg L^{-1} (Sharma *et al.,* 1993; WHO 1996).

Chromium can exist in several oxidation states: I, II, III, IV, V and VI. In water, chromium can be most commonly found in two oxidation states—hexavalent (Cr VI) and trivalent (Cr III) (Jin *et al.,* 2014). Redox and pH conditions determine chromium speciation in water. Generally, Cr VI is more abundant oxygen rich waters, while Cr III dominates under anaerobic conditions (Guertin *et al.,* 2005, McNeill *et al.,* 2012). Genrally, in waters where pH ranges between 5-7 Cr III is the dominant species (Swietlik, 1998). In water Cr III can be found in several different forms such as $Cr(OH)_2$, $Cr(OH)_3$, Cr(OH), Cr(SO4) and Cr (OH)Cl (Rakhunde 2012). Cr VI is most commonly found as a chromate ion CrO_2, however it can also exist in form of chromate, dichromate, chromic acid and hydrogen chromate (Comber and Gardner, 2003).

Cr III, at appropriate levels, is beneficial for human health and is involved in lipid and glucose metabolism, whereas Cr VI is toxic (Cespón-Romero *et al.,* 1996; Owlad *et al.,* 2008). Health problems associated with Cr VI exposure include skin rashes, kidney and liver damage, internal haemorrhage, teeth abnormalities, and respiratory ailments, including lung cancer (Martone *et al.*, 2013; Achmad *et al.,* 2017; Shahid *et al.,* 2017; Kim *et al.*, 2018).

High Cr VI concentrations have been reported in numerous groundwater sources around the world (Fantoni *et al.,* 2002; Becquer *et al.,* 2003; Gray *et al.*, 2003; Beaumont *et al.,* 2008,). One of the most infamous cases of Cr VI pollution took place in Hinkley, California, where concentrations as high as 0.580 mg L^{-1} were reported in groundwater samples (Pellerin *et al.,* 2000). In Kanpur, India, due to poor waste disposal practices, Cr VI concentration had reached 16.3 mg L^{-1} (Singh *et al.,* 2009). In Leon Valley, Mexico, Cr VI concentrations were found to have reached 50 mg L^{-1} due to industrial runoff (Armienta *et al.,* 2006).

Due to the high toxicity of Cr VI and its presence in the environment, effective and reliable monitoring of the species is required. The most commonly used methods for Cr VI detection are atomic absorption spectrophotometry (AAS) and inductively coupled plasma-mass spectrometry (ICP-MS) (Ressalan *et al.,* 1997, Parks *et al.,* 2004). Although these are powerful and sensitive methods that can detect Cr VI even at trace levels, they are also expensive and require skilled analysts and laborious sampling. Different oxidation states of Cr VI in groundwater can be unstable

when exposed to air, temperature fluctuations, and change in pH (Izbicki *et al.,* 2009). Because of this, Cr VI should ideally be detected on site, and therefore, simple, portable, sensitive, and cost-effective methods would be greatly beneficial (Dong *et al.,* 2016).

In recent years, application of microfluidic detection systems for environmental monitoring has gained great interest (Li *et al.,* 2008, Liu *et al.,* 2013, Provin *et al.,* 2013; Cogan *et al.,* 2015, Milani *et al.,* 2015). Microfluidic detection systems are characterised by their small size, which offers the potential for portable sensing system development of portable sensing systems, which has with the ability to analyse samples on a sub-millilitre scale (Nie *et al.,* 2010). There are numerous advantages associated with miniaturisation, including reduced sample volume, fast reaction time, and minimised waste production (Nguyen *et al.,* 2018). Additionally, microfluidic detection systems facilitate the development of portable and/or autonomous devices, which can be used on site without the requirement of sample collection and transportation (Cleary *et al.,,* 2013).

Electrochemical sensors have been used for heavy metal monitoring in water, including Cr VI (Xing *et al.,* 2011; Ravishankar *et al.,* 2015; Khanfar *et al.,* 2017; Sari *et al.,* 2018; Tu *et al.,* 2018). Methods based on electrochemical detection can achieve very low detection limits and high selectivity (Li *et al.,* 2011). There are, however, numerous limitations associated with electrochemical detection methods that make them difficult to implement for

long-term monitoring, such as inability to analyse complex water matrices, sensor drift, high maintenance cost, and biofouling (Chailapakul *et al.,* 2008).

Biofouling is significantly minimised in optical detection systems as they do not require direct contact between the sensor and the sample. Optical detection methods are widely used in the microfluidic analysis (Yu *et al.*, 2006; Baker *et al.,* 2009; Abi Kaed Bey *et al.,* 2011; Chen *et al.,* 2016). Colorimetric methods can be implemented using simple and low-cost detection systems based on light emitting diodes (LEDs) as light source and photodiode detectors, making them suitable for use in portable microfluidic detection systems (Yogarajah*et al.,* 2015).

In recent years, paper based microfluidic analytical devices (μPADs) have been used for environmental monitoring (Martinez *et al.,* 2007). μPADs use capillary forces instead of pumps and have low manufacturing costs (Lin *et al.,* 2016). Asano *et al.* used μPADs based on 1,5-diphenyl-carbazide for Cr VI detection in water and obtained a LOD of 30 mg L^{-1} with a linear range between 40–400 mg L^{-1} (Asano *et al.,* 2015). Idros *et al.* utilised μPADs for Cr VI detection in water using colorimetric detection with LOD of 0.019 mg L^{-1} and linear range between 0.019–1.4 mg L^{-1} (Idros *et al.,* 2018). In 2018, Sun *et al.* developed a Cr VI detection method using a μPADs-based rotational device with linear range between 0.5–10 mg L^{-1} and LOD of 0.18 mg L^{-1} (Sun *et al.*,2018).

The use of different chromophoric dyes for spectrometric Cr VI detection in water has been described in the literature (Revanasiddappa *et al.,* 2001; Li *et*

al., 2008; Sreevani *et al.,* 2013; Sunil *et al.,* 2015). Onocke and Sasu developed a method for Cr VI detection in groundwater and industrial waste samples (Onchoke *et al.,* 2016). In this method, Cr VI was reacted with 1,5-diphenylcarbazide (DPC) dye, which, in acidic conditions, forms a purple-coloured species. As a result of a redox reaction, Cr VI is reduced to Cr III, and DPC is oxidised to 1,5-diphenylcarbazone (DPCA). Cr III and DPCA form a purple-coloured species with λ_{max} of 540 nm (Wurster *et al.,* 2012). To date, DPC method has not been implemented into an autonomous detection system. The reaction mechanism of DPC method is outlined in figure.

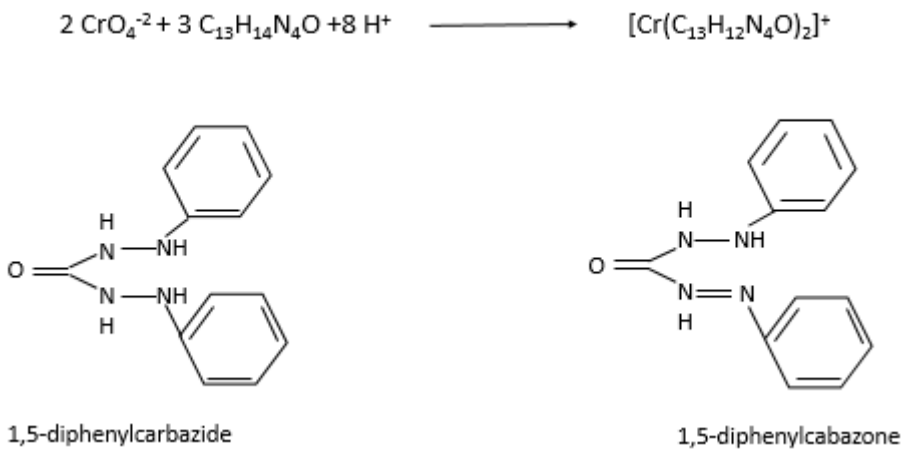

Figure 4.1. Reaction mechanism of DPC method.

Similarly to chapter 3 different parameters such as pH, reagent stability, reagent ratio and effect of acid concentrations were evaluated for the DPC method. Additonally, cleaning validation of sample cells was carried out to assess if DPC method could be used in microfluidic detection systems without the need of extensive cleaning steps or highly concentrated cleaning solutions which could damage the polymeric microfluidic chip.

The aim of this study is to optimise a DPC method for low-cost and simple incorporation into a microfluidic detection system (Figure 4.1). The DPC method was chosen because of the intense colour development at 543 nm region. The method's performance was evaluated in the laboratory on both macro and micro scale.

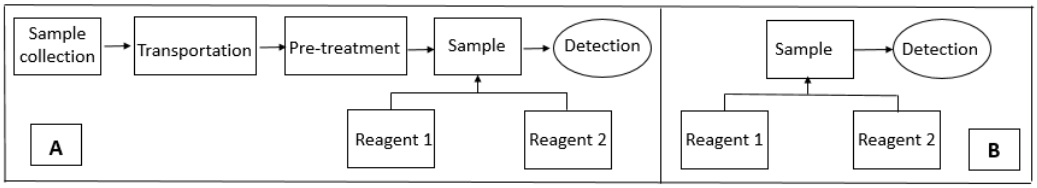

Figure 4.2. (A) Conventional method analysis incorporating multiple steps for Cr VI analysis, (B) microfluidic detection-based analysis using modified 1,5-diphenylcarbazide method for Cr VI detection.

4.3 Materials and Methods

4.3.1 Apparatus

Shimadzu 1800 UV- visible spectrometer was used with Hellma 10 mm and 1 mm quartz cuvettes for the absorbance measurements. Hanna 20 pH meter was used for pH measurements. Varian 820-MS ion coupled plasma mass spectrometer (ICP-MS) was used to determine Cr VI concentration in the water samples (Table 4.1).

Table 4.1. ICP-MS settings.

Instrumental parameters	Scanning parameters
Plasma flow: 15 L min^{-1}	Scanning mode: Peak hopping
Auxillary flow: 1.55 L min^{-1}	Number of replicates: 3
Nebuliser flow: 0.9 L min^{-1}	Pump rate: 9 rpm
Sheath gas flow: 0.2 L min^{-1}	Rinse time: 40 s
Sampling depth: 6.5 mm	Sample uptake delay: 50 s
Power: 1.4 kW	Internal standards: Li^{6}, Sc^{45}, Y^{89}, Tb^{159}, Ho^{165}, Th^{232}

4.3.2 Reagents

All chemicals were of analytical grade and purchased from Sigma-Aldrich (Arklow, Ireland) unless otherwise stated. Potassium dichromate ($K_2Cr_2O_7$), iron chloride 6-hydrate ($FeCl_3 \cdot 6H_2O$) (Fisher Scientific, Leicestershire, UK), magnesium sulphate ($MgSO_4$) (Fisher Scientific, Leicestershire, UK), potassium dihydrogen phosphate (KH_2PO_4), manganese sulphate1-hydrate ($MnSO_4 \cdot H_2O$), sodium nitrate ($NaNO_3$)

and chromium chloride hexahydrate ($CrCl_3 \cdot 6H_2O$) were used to prepare stock solutions at concentration 1000 mg L^{-1} in double deionised water. Working standards were prepared by serial dilution. Methanol (CH_3OH), Tween 20 ($C_{58}H_{114}O_{26}$), acetonitrile (CH_3CN) (Lennox, Dublin), hydrochloric acid (HCl) and nitric acid (HNO_3) (SciChem, Bilston, UK) were used for sample cell cleaning validation. Ascorbic acid ($C_6H_8O_6$), 1,5-diphenylcarbazide ($C_6H_5NHNHCONHNHC_6H_5$) and sodium hydroxide (NaOH) (Sharlab S.L., Barcelona, Spain) were prepared by weighing out an appropriate amount and dissolving it in double deionised water. Sulfuric acid (H_2SO_4) (97%) was used to prepare sulfuric acid solutions with various concentrations in double deionised water. Double deionised water was used for dilution of reagents and samples.

4.3.3 Sample preparation

Cr VI sample (2 mL) was transferred to a glass vial. Sulfuric acid (0.2 M, 1 mL) and 1,5-diphenylcarbazide (0.5 % w/v, 1 mL) were added, and the mixture was gently shaken and left for five minutes. The absorbance the at 543 nm against reagent blank.

4.3.4 Path length

Effect of optical path length on absorbance was investigated in order to simulate the conditions in a microfluidic detection system. The procedure was carried out in standard 10 mm quartz cuvettes and microcuvettes with 1 mm light path for Cr VI solutions with concentrations of 0.1- 1.0 mg L^{-1}. The experiment was carried out in triplicate. The average absorbance was calculated and calibration curves were plotted.

4.3.5 Sample cell cleaning validation

10 mm quartz cuvettes were filled with a solution containing Cr VI and reagents and left to stand for one hour. Double deionised water, 1 % hydrochloric acid, 1 % nitric acid, methanol, acetonitrile, acetone, Tween 20 and 1 % sulfuric acid were used to rinse the cuvettes. The absorbance of cuvettes was measured at 543 nm. The absorbance obtained from different solvents was compared to clean quartz cuvettes (control). All measurements were carried out in triplicate.

4.3.6 Optimisation of parameters

4.3.6.1 pH

The effect of pH on the method was studied. Sulfuric acid and sodium hydroxide were used to adjust the pH of the double deionised water in which the chromium samples (Cr VI) were prepared.

4.3.6.2 Sample/reagent ratio

The effect on absorbance of combining the different reagents into a single reagent solution was studied in order to simplify the detection process which would in turn enable cost effective and uncomplicated microfluidic chip design and fabrication. Sulfuric acid and the DPC dye were mixed together in a 1:1 ratio to form a combined reagent which was then used for the analysis of Cr VI samples. 2 mL of sample was placed into a glass vial to which 2 mL of combined reagent was added (sample/reagent ratio B). After five minutes, measurements were taken at 543 nm using quartz cuvettes. The absorbance was compared to the original sample/reagent

ratio: 1 (sample): 1(0.4 M sulfuric acid):1(DPC), described as sample/reagent ratio A in the results section.

4.3.6.3 Reagent stability

The effect of reagent stability on the Cr VI determination was investigated. Firstly, 0.5 % DPC dye was used for Cr VI determination over 28 days with fresh 0.4 M sulfuric acid prepared every week. Secondly, 0.5 % DPC and 0.4 M sulfuric acid reagent mixture was prepared and used for Cr VI determination over 28 days. Absorbance was measured every week and compared.

4.3.7 Effect of different acid concentrations

The effect of varying sulphuric acid concentration was studied. Cr VI ranging from 0.1 to 1 mg L^{-1} were analysed. One-way analysis of variance (ANOVA, single factor) was used to analyse the results obtained.

4.3.8 Colour stability

1 mg L^{-1} Cr VI was analysed using Shimadzu UV-vis time scan option, the measurements were taken every 60 seconds for 600 min at 543 nm straight after addition of the reagents. The absorbance was plotted against time (min).

4.3.9 Interference

Fe (III), Cr (III), NO_3, PO_4, Mg and Mn were introduced to 1 mg L^{-1} Cr VI prepared in double deionised water prior to analysis. These interfering ions were chosen as they can typically be found in both surface and groundwater. Tolerance limits of

interfering agents were established at those concentrations that do not cause more than 5 % error in the absorbance values of Cr VI at 1 mg L^{-1}.

4.3.10 Environmental samples

Water samples were collected from Killeshin water reservoir, Killeshin, Co. Laois, groundwater well, Co. Laois, and River Barrow at Carlow (Barrow 1) and St. Mullins, Co. Carlow (Barrow 2). All water samples were analysed in triplicate. The sample matrices were analysed using the DPC method in order to determine whether or not Cr VI was present in concentrations detectable by the method. The different water matrices were then spiked with Cr VI (0.1-1 mg L^{-1}) and appropriate dilutions were made. Prior to the analysis the water samples were filtered firstly using Whatman grade 1 filter paper and secondly with sterile 0.2 μm syringe filters. The pH of the water samples was adjusted to 2.2.

4.3.11 Comparison between optimised DPC method and ICP-MS

The optimised DPC method was compared to accredited ICP-MS which is the gold standard method for heavy metal analysis in water. A calibration curve in a range of 0.2-3 mg L^{-1} was obtained using the optimised DPC method. 1 mg L^{-1} sample was analysed as unknown. The concentration of the sample was calculated from the calibration curve ($y = 0.2962x - 0.0287$). 1 mg L^{-1} environmental water samples were analysed using ICP-MS. The concentration for 1 mg L^{-1} water samples obtained from optimised DPC method and the ICP-MS were compared. Percentage difference was calculated using formula: (Conc. ICP MS –Conc. DPC method) × 100/Conc. ICP MS.

4.4 Results

4.4.1 Analytical data

Beer's law was obeyed in the range between 0.03–3 mg L^{-1} (Figure 4.3). The molar absorptivity coefficient was found to be 2.021×10^4 $mol^{-1}cm^{-1}$. Sandell's sensitivity was found to be 2.574×10^{-3} µg cm^{-2}. The limit of detection (3 sd b m^{-1}) and the limit of quantification (10 se m^{-1}) (where *sd b* is the standard deviation of the reagent blank, and *m* is the slope of the calibration curve) were found to be 0.023 and 0.076 mg L^{-1}, respectively. Absorption spectra of 1 mg L^{-1} Cr VI against reagent blank and reagent blank against double deionised water are shown in Figure 4.4.

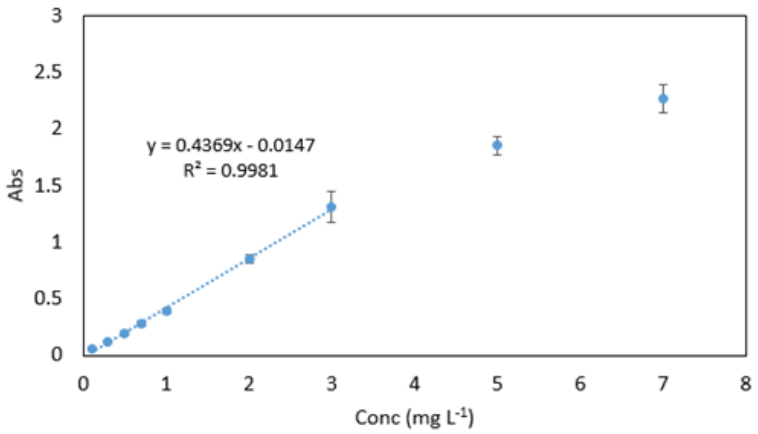

Figure 4.3. Calibration curve for Cr VI ranging between 0.03–7 mg L^{-1}. All measurements were carried out in triplicate (n = 3). Error bars represent standard deviations of the measurements.

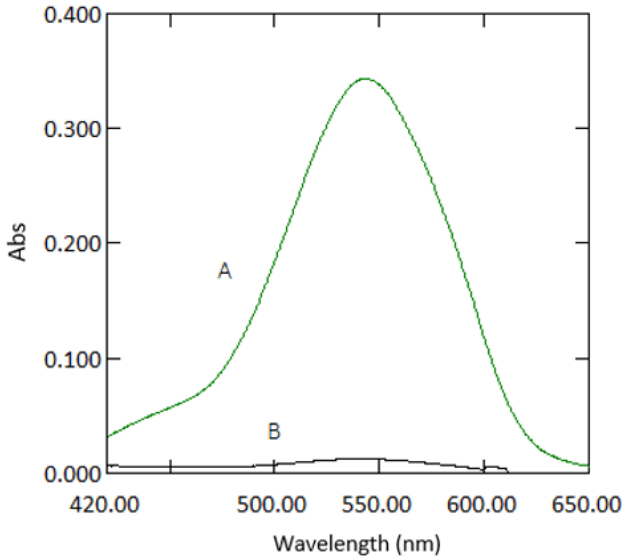

Figure 4.4. Absorption spectra of coloured species (1 mg L^{-1} chromium) versus reagent blank (A) and reagent blank versus double deionised water (B) measured at 543 nm.

4.4.2 Path length

As expected, the absorbance values and the slope for 1 mm quartz cuvette measurements were 10 times lower than those obtained from 10 mm standard cuvette measurements (Figure 4.5). The analytical response was strong for samples measured in microcuvettes, as can be seen from the calibration graphs (Figure 4.6) and Table 4.2. The good response signal and the linearity obtained from microcuvette measurements strongly indicate that the DPC method is applicable for use in microfluidic detection systems.

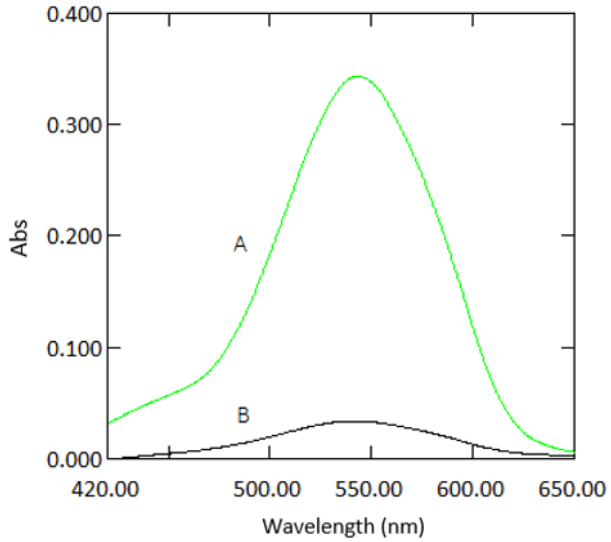

Figure 4.5. Absorption spectra of a sample containing 1 mg L^{-1} Cr VI with reagents measured in 10 mm cuvettes (A) and 1 mm quartz cuvettes (B) against reagent blank measured at 543 nm.

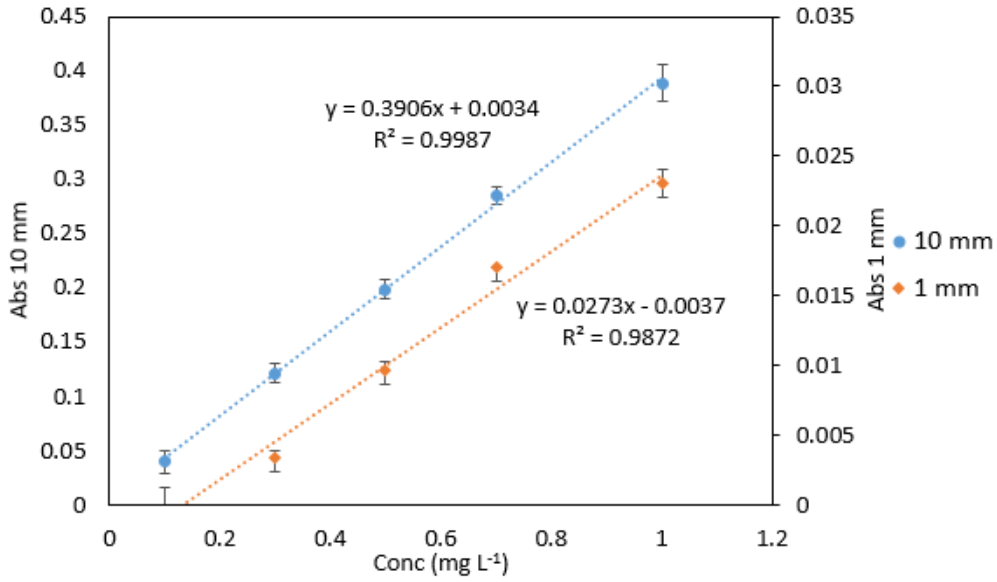

Figure 4.6. Comparison of Cr VI standards (0.1–1 mg L^{-1}) measured in quartz cuvettes with 10 mm and 1mm path lengths. All measurements were carried out in triplicate (n = 3). Error bars represent standard deviations of the measurements.

Table 4.2. Measurements of Cr VI standards (0.1–1 mg L^{-1}) measured in quartz cuvettes with 10 mm and 1mm path lengths. All measurements were carried out in triplicate (n = 3).

	10 mm			1 mm		
Conc (mg L^{-1})	**Average**	**SD**	**% RSD**	**Average**	**SD**	**% RSD**
0.1	0.039	0.010	24.812	0.000	0.002	0.153
0.3	0.128	0.009	16.433	0.003	0.001	0.058
0.5	0.166	0.009	18.387	0.010	0.001	0.058
0.7	0.254	0.009	21.169	0.017	0.000	0.000
1	0.402	0.017	11.678	0.023	0.001	0.100

4.4.3 Sample cell cleaning validation

Sample cell cleaning is important for residue removal from previous analysis that can otherwise cause low sensitivity and lack of precision. Ideally, the cleaning method should be time efficient and simple. 1 % nitric acid proved to be the most effective solvent for quartz cuvette rinsing as it removed all the stains caused by the DPC method's colour reaction, whereas methanol was found to be the least effective (Table 4.3). 1 % nitric acid could be applied for rinsing sample cells in microfluidic detection systems.

Table 4.3. A comparison between absorbance values of quartz cuvettes rinsed with different solvents.

Solvent	Abs	Abs	Abs	Average	SD	% RSD
Water	0.012	0.018	0.014	0.015	0.003	20.830
1 % HCl	0.041	0.017	0.081	0.046	0.032	69.780
1 % HNO_3	0.004	0.003	0.001	0.003	0.002	57.282
Methanol	0.088	0.101	0.105	0.098	0.009	9.070
Acetonitrile	0.021	0.022	0.033	0.025	0.007	26.283
Acetone	0.085	0.081	0.086	0.084	0.003	3.150
Tween 20	0.013	0.012	0.007	0.011	0.003	30.136
1 % H_2SO_4	0.006	0.005	0.006	0.006	0.001	10.189
Control	0.002	0.001	0.002	0.002	0.001	34.641

4.4.4 Optimisation of parameters

4.4.5 pH

The highest absorbance values were obtained at pH 2.2 (Figure 4.7 and Table 4.4). The analytical response pH 2.2 was found to be the optimum pH for the procedure and used in subsequent experiments.

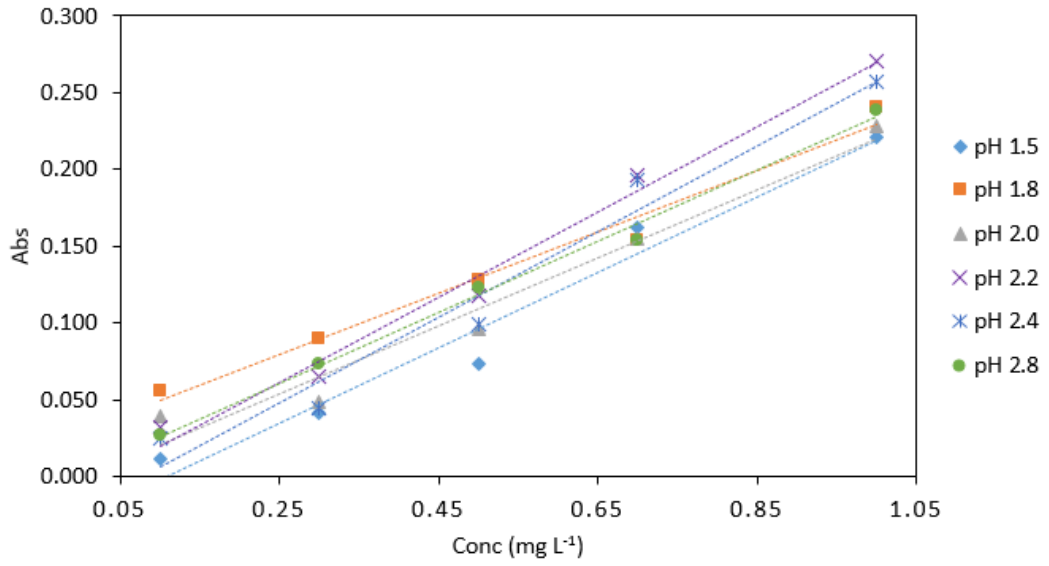

Figure 4.7. Comparison of Cr VI (0.1–1 mg L^{-1}) analysed at various pH conditions (pH 1.5, 1.8, 2.0, 2.2, 2.4, 2.8). All measurements were carried out in triplicate (*n* = 3).

Table 4.4. Measurements of Cr VI (0.1–1 mg L^{-1}) analysed at various pH conditions (pH 1.5, 1.8, 2.0, 2.2, 2.4, 2.8). All measurements were carried out in triplicate (n = 3).

Conc (mg L^{-1})	**pH 1.5**	**pH 1.8**	**pH 2.0**	**pH 2.2**	**pH 2.4**	**pH 2.8**
0.1	0.011	0.056	0.040	0.032	0.025	0.027
SD	0.001	0.003	0.044	0.001	0.006	0.001
0.3	0.041	0.090	0.049	0.066	0.044	0.073
SD	0.002	0.003	0.012	0.001	0.007	0.002
0.5	0.073	0.128	0.096	0.118	0.099	0.123
SD	0.002	0.003	0.010	0.008	0.005	0.010
0.7	0.162	0.154	0.155	0.196	0.193	0.154
SD	0.000	0.002	0.010	0.017	0.003	0.012
1	0.221	0.241	0.228	0.271	0.257	0.239
SD	0.002	0.003	0.012	0.005	0.008	0.013
Slope	0.245	0.199	0.221	0.278	0.277	0.231
R^2	0.966	0.978	0.965	0.965	0.986	0.994

4.4.5 Sample/reagent ratio

Sample/reagent ratio B gave the best response with higher absorbance values than sample/reagent ratio A (Figure 4.8 and Table 4.5). The slope obtained from ratio B was also higher than that of ratio A. Therefore, ratio B was chosen for use in microfluidic detection systems. Furthermore, ratio B requires a small number of separate reagents, which allows for cost efficient fabrication and simple microfluidic design.

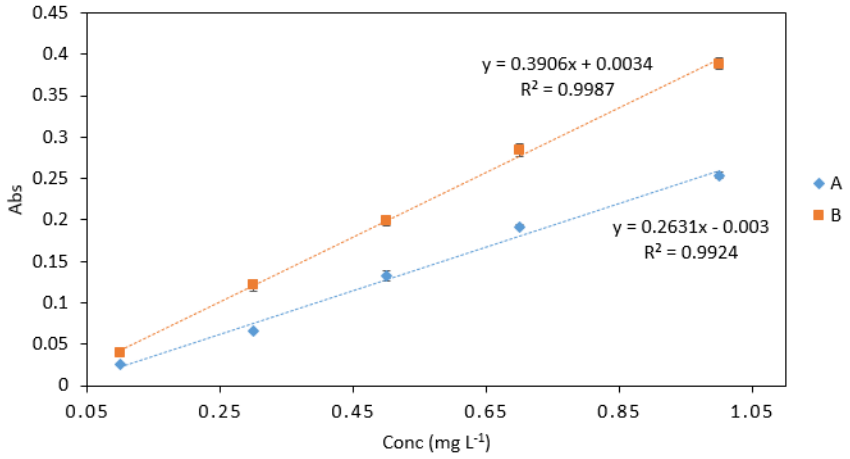

Figure 4.8. A comparison of Cr VI (0.1–1 mg L^{-1}) analysed using two sample/reagent ratios: (A), 2 (Cr): 2 (0.4 M sulphuric acid): 2 (DPC) and (B), 2 (Cr): 2 (0.4 M sulphuric acid and DPC mix). All measurements were carried out in triplicate (n = 3). Error bars represent standard deviations of the measurements.

Table 4.5. A comparison of Cr VI (0.1–1 mg L^{-1}) analysed using two sample/reagent ratios: (A), 2 (Cr): 2 (0.4 M sulphuric acid): 2 (DPC) and (B), 2 (Cr): 2 (0.4 M sulphuric acid and DPC mix). All measurements were carried out in triplicate (n = 3).

	A			B		
Conc (mg L^{-1})	**Abs**	**SD**	**% RSD**	**Abs**	**SD**	**% RSD**
0.1	0.025	0.002	6.030	0.039	0.001	0.058
0.3	0.066	0.001	0.115	0.121	0.007	0.681
0.5	0.132	0.006	0.624	0.199	0.006	0.569
0.7	0.192	0.003	0.252	0.285	0.008	0.802
1	0.254	0.004	0.416	0.389	0.006	0.643

4.4.6 Reagent stability

For the DPC dye stability experiment, an increase in absorbance was noted after seven days. After that, decreasing absorbance values over time were noted (Figure 4.9). A similar trend was observed for DPC dye and sulphuric acid reagent mixture's stability experiment. The absorbance increased after seven to 14 days and then decreased over time (Figure 4.6). Furthermore, the method yielded analytically useful calibration data over the time period studied and showed good potential for application in a microfluidic analysis system. Regular calibration protocol should be implemented for correcting the change in absolute absorbance values.

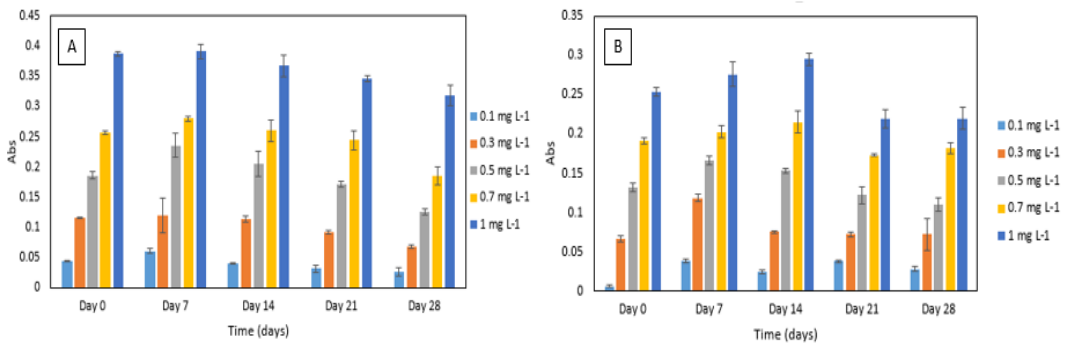

Figure 4.9. (A) Stability of 1,5-diphenylcarbazide (DPC) dye in Cr VI (0.1–1 mg L^{-1}) analysed periodically over day 0, 7, 14, 21 and 28. All measurements were carried out in triplicate (n = 3); (B) stability of sulphuric acid and DPC dye mixture in Cr VI (0.1–1 mg L^{-1}) analysed periodically over day 1, 7, 14, 21 and 28. All measurements were carried out in triplicate (n = 3).

4.4.7 Effect of different acid concentrations

0.4 M sulphuric acid yielded the highest absorbance values and the highest slope in comparison to other acid concentrations analysed (Figure 4.10 and Table 4.6). The statistical analysis showed that there was a significant difference between the different acid concentrations ($p < 0.05$). No significant difference was found between 0.4, 0.6, and 0.8 M acid concentrations. The 0.4 M sulphuric acid was used in subsequent experiments.

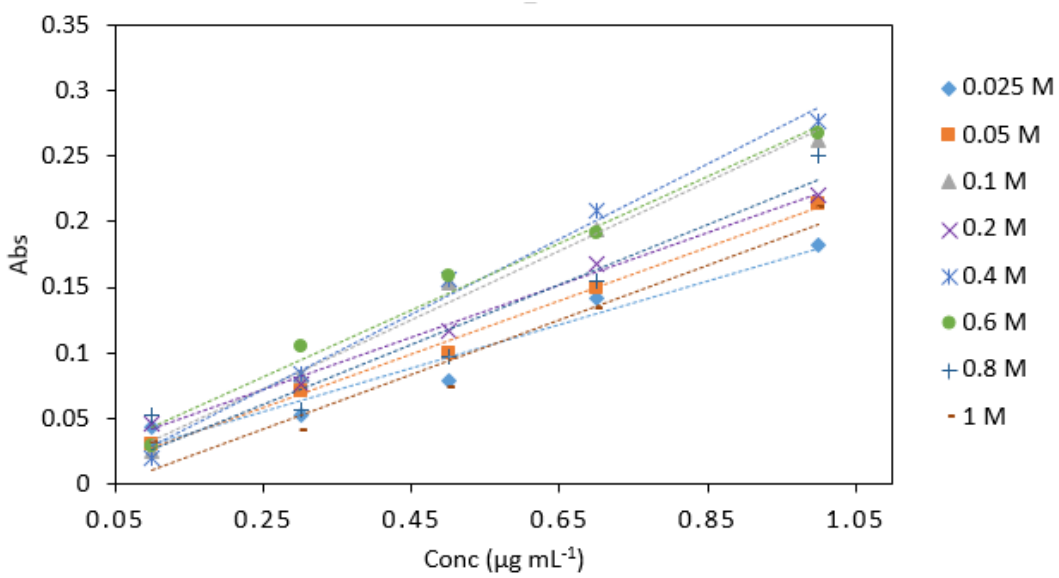

Figure 4.10. A comparison of Cr VI (0.1–1 mg L^{-1}) analysed with various sulphuric acid concentrations (0.025, 0.05, 0.1, 0.2, 0.4, 0.6, 0.8 and 1 M). All measurements were carried out in triplicate ($n = 3$).

Table 4.6. The average measurements of Cr VI (0.1–1 mg L^{-1}) analysed with various sulphuric acid concentrations (0.025, 0.05, 0.1, 0.2, 0.4, 0.6, 0.8 and 1 M). All measurements were carried out in triplicate (n = 3).

Conc (mg L^{-1})	**0.025 M**	**0.05 M**	**0.1 M**	**0.2 M**	**0.4 M**	**0.6 M**	**0.8 M**	**1 M**
0.1	0.044	0.030	0.025	0.046	0.020	0.029	0.053	0.032
SD	0.010	0.009	0.030	0.008	0.011	0.013	0.042	0.040
0.3	0.052	0.071	0.083	0.076	0.084	0.105	0.057	0.041
SD	0.004	0.010	0.018	0.024	0.021	0.019	0.004	0.009
0.5	0.079	0.100	0.153	0.117	0.156	0.158	0.097	0.073
SD	0.006	0.025	0.006	0.009	0.004	0.015	0.004	0.012
0.7	0.141	0.150	0.194	0.168	0.209	0.191	0.155	0.134
SD	0.002	0.004	0.002	0.012	0.025	0.024	0.018	0.010
1	0.182	0.214	0.262	0.220	0.276	0.268	0.251	0.211
SD	0.005	0.004	0.013	0.024	0.009	0.011	0.004	0.032
Slope	0.166	0.204	0.264	0.199	0.287	0.255	0.229	0.208
R^2	0.947	0.995	0.989	0.994	0.989	0.990	0.934	0.947

4.4.8 Colour stability

Maximum absorbance was reached five minutes after the addition of the dye (Figure 4.11). At this time the absorbance was sufficiently stable for measurements, and five-minute reaction time was used in subsequent experiments. After 600 min, a 24% decrease in absorbance was observed. Overall, the colour stability was good and suitable for measurements in a microfluidic detection system.

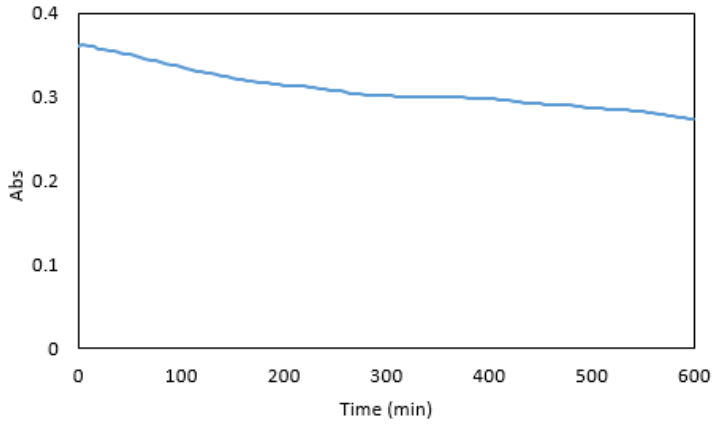

Figure 4.11. Absorbance of 1 mg L^{-1} chromium sample premixed with the reagents over 600 min.

4.4.9 Interference

From the different species investigated, Fe (III) interfered most strongly with the DPC method (Table 4.7). Iron interference was masked by 1% ascorbic acid. Slight interference was observed from Cr (III), Mn, Mg, and NO_3. In general, Cr (III) and Mn concentrations in surface water would be expected to occur below the tolerance limit and would not pose any interference with the optimised DPC method (Revanasiddappa *et al.,* 2001). However, the method's effectiveness would be affected in surface waters with high magnesium and nitrate levels and should be taken into account when designing calibration protocols for detection devices (Sreevani *et al.,* 2013).

Table 4.7. Effect of foreign species on the determination of chromium (VI) (1 mg L^{-1}).

Interferents	Tolerance limit (mg L^{-1})
Fe (III)	1
Cr (III), Mn, Mg, NO_3	10
PO_4	100

4.4.10 Environmental water samples

Groundwater samples had a similar response to the control samples (Figure 4.12 and Table 4.8). This would indicate that groundwater samples did not contain a high amount of interfering substances. The highest absorbance values were observed in samples collected from Bog Lake. The lowest absorbance was obtained from Killeshin reservoir. The difference in absorbance values could be explained by factors such as sample colour and chemical composition. Overall, different water matrices have the potential to affect the result of the DPC method. Despite the robust results shown in Table 4.4, this should be considered for calibration protocol development in microfluidic detection devices.

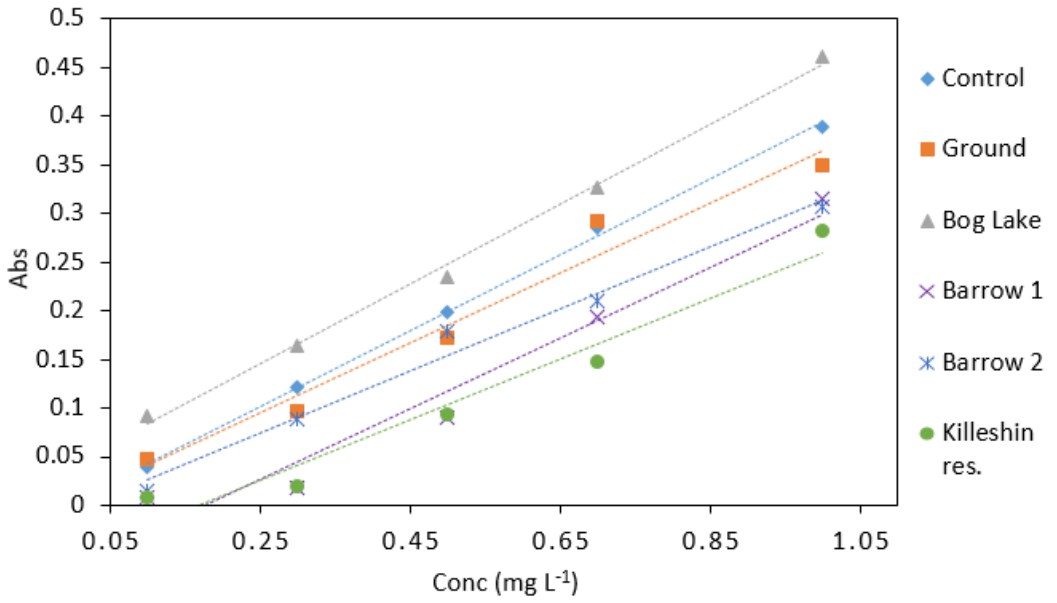

Figure 4.12. Comparison of Cr VI (0.1–1 mg L^{-1}) analysed in several water matrices. All measurements were carried out in triplicate (n = 3).

Table 4.8. Average measurements of Cr VI (0.1–1 mg L^{-1}) analysed in several water matrices. All measurements were carried out in triplicate (n = 3).

Conc (mg L^{-1})	Control	Ground	Bog Lake	Barrow 1	Barrow 2	Killeshin res.
0.1	0.039	0.048	0.092	0.008	0.015	0.008
SD	0.001	0.003	0.002	0.000	0.002	0.004
0.3	0.121	0.097	0.164	0.018	0.088	0.019
SD	0.007	0.001	0.002	0.002	0.021	0.002
0.5	0.199	0.173	0.234	0.090	0.179	0.093
SD	0.006	0.007	0.002	0.012	0.004	0.008
0.7	0.285	0.292	0.327	0.194	0.210	0.147
SD	0.008	0.006	0.011	0.028	0.008	0.019
1	0.389	0.349	0.461	0.315	0.307	0.282
SD	0.010	0.021	0.012	0.013	0.011	0.009
Slope	0.367	0.358	0.41	0.367	0.319	0.311
R^2	0.992	0.969	0.998	0.954	0.983	0.953

4.4.11 Comparison between optimised DPC method and ICP-MS

Evaluation of Cr VI in different water samples using ICP-MS and the optimised colorimetric DPC method showed that the Cr VI concentrations are comparable (Table 4.9). The largest percentage difference between ICP-MS and the optimised method was observed for the control sample as 14.6%, whereas the smallest percentage difference was found for the groundwater sample as difference of 7.5% was obtained. Therefore, it can be concluded that the optimised DPC method is effective in terms of Cr VI determination in various water matrices.

Table 4.9. A comparison between Cr VI concentrations determined using the optimised DPC method and measurements obtained from an accredited ICP-MS.

Sample	ICP-MS Unspiked Sample (mg L^{-1})	ICP-MS (mg L^{-1})	DPC Method (mg L^{-1})	Percentage Difference (%)
Control	0.000	0.883	1.012	14.607
Ground	0.002	0.930	1.000	7.544
Killeshin res.	0.002	0.959	1.063	10.805
St Mullins	0.001	0.987	1.101	11.595
Bog Lake	0.001	1.060	0.960	9.467
Barrow	0.002	0.907	1.024	13.249

4.5 Discussion

The results showed the optimised DPC method was more sensitive than some of the previous studies (Wurster *et al.,* 2012; Asano *et al.,* 2015; Sun *et al.,* 2018) (Table 4.10). Although the Cr VI determination method proposed by Amin *et al.* yielded very low detection limit (Amin *et al.,* 2015), the ADTP reagent had to be synthesised in the laboratory prior to the analysis. One of the advantages associated with the optimised DPC method is that the reagents are commercially available. Wang *et al.* used gold nanoparticles to develop a method for Cr III and Cr VI determination in water with a detection limit of 0.001 mg L^{-1} for Cr VI (Wang *et al.,*2015). However, there are several drawbacks associated with gold nanoparticle synthesis and cost (Eustis *et al.,* 2006). The simplicity of the method and the relatively wide linear range indicates that the proposed method is suitable for use in autonomous microfluidic detection systems and Cr VI determination in chromium-containing effluents and environmental waters.

From the different interfering ions analysed, iron was found to have the strongest effect on analysis, however, interference was masked using 1 % ascorbic acid. For future investigations effect of other ions should be investigated, including copper, vanadium, mercury and molybdenum which are known to interfere with chromium determination using diphenylcarabzide method (Standard methods 1989).

The method yielded optimum results at pH 2.2. Hue *et al.* reported that optimum reaction conditions for DPC method were achieved at pH 2 (Hue *et al.,* 2009). Method 7196A recommends using pH of 2 ± 0.5 (USEPA 1992) .In acidic conditions achieved by addition of sulfuric acid Cr VI reacts with

diphenylcarbazide which results in oxidation of the colour reagent to diphenylcarbazode and simultaneous reduction of Cr VI to Cr III. Complexation of Cr III with diphenylcarbazode results in intense colour formation (Pflaum *et al.*, 1956).

Table 4.10. Comparison of spectrophotometric methods of the Cr VI determination.

Detection Principle	**λ_{max} (nm)**	**LOD (mg L^{-1})**	**Linear Range (mg L^{-1})**	**Reference**
µPDAs	453	0.041	0.041–0.072	Idros *et al.,* 2018
µPDAs	530	30.000	40.000–400.000	Asano *et al.,* 2015
Rotational µPDAs	445	0.180	0.500–10.000	Sun *et al.*, 2018
Gold nanoparticles	520	0.001	0.010–0.130	Wang *et al.,* 2015
Spectrophotometric	503	0.030	0.010–0.400	Amin *et al.,* 2015
Spectrophotometric	385	0.014	0.260–26.000	Sreevani *et al.,* 2013
Spectrophotometric	543	0.023	0.030–3.000	This study

4.6 Conclusion

The DPC method showed great potential for use in autonomous microfluidic detection systems for Cr VI detection in water. The method was optimised for incorporation into micro scale detection systems. The method proved to be simple, fast, and robust. Strong analytical response was obtained from 1 mm light path cuvettes, demonstrating that the method would be effective in a small-scale detection system. Furthermore, the optimised method required a small number of reagents, resulting in cost effective analysis. Strong analytical response was obtained from a simple 1:1 sample/reagent ratio. The reagent mixtures were stable for two weeks, with a gradual decrease in absorbance observed after that. Investigation of the method's performance in different water samples and the good agreement obtained with ICP-MS measurements revealed that the method is suitable for the determination of Cr VI in various water matrices.

Chapter 5

Arsenic detection in water using microfluidic detection systems based on leucomalachite green method

This chapter was based on the following article submitted to the Journal:

Analytical methods

ARSENIC DETECTION IN WATER USING MICROFLUIDIC DETECTION SYSTEMS BASED ON LEUCOMALACHITE GREEN METHOD

Authors: Annija Lace, David Ryan, and John Cleary

5.1. Abstract

This work describes a novel system for arsenic detection in water using leucomalachite green dye in a microfluidic platform. A simplified leucomalachite green method was integrated into a microfluidic detection system. In acidic medium arsenic is reacted with potassium iodate to liberate iodine, which in turn oxidises leucomalachite green to malachite green forming a green colour associated with an absorbance band in the visible region (λ_{max}=617 nm). 1:1 v/v sample to reagent ratio was used for the analysis. Syringe pumps were used to introduce and transport reagents and samples into a PMMA microfluidic detection chip. The optical detection system consisted of a LED light source with a photodiode detector. The modified method can determine arsenic over the linear range of 0.3 -2 mg L^{-1} with a limit of detection of 0.32 mg L^{-1}. The average % RSD and recovery was 21.1% and 93. 7 %, respectively. The sample run time was optimised to 25 minutes. A range of environmental water samples were analysed using the modified method.

Keywords: *arsenic; microfluidics; leucomalachite green; environmental monitoring; water.*

5.2. Introduction

Arsenic contamination of drinking water is a major concern (Zhu *et al.*, 2008). Arsenic is toxic and has the ability to bioaccumulate in living organisms (Williams *et al.*, 2006). Exposure to arsenic can cause various health defects, including hyperpigmentation, neuropathy, cardiovascular diseases, diabetes and various types of cancers (Mandal *et al.*, 2002; Kapaj *et al.*, 2006; Argos *et al.*, 2010). Due to its toxicity arsenic is listed as priority hazardous substance under the European Directive on Environmental Quality Standards (Directive 2008/105/FC). The maximum allowable concentration for arsenic in groundwater set by World Health Organisation is 10 μg L^{-1} (Gomez-Caminero *et al.*, 2001). However, arsenic concentrations exceeding the WHO limit have been reported in numerous regions around the world (Mazumder *et al.*, 1998; Chowdhury *et al.*, 2000; Farooqi *et al.*, 2007; Rodríguez-Lado *et al.*, 2013). Therefore, reliable and selective arsenic monitoring methods are needed.

Field kits have been widely used for arsenic determination in groundwater as the measurements can be conducted on site (Melamed *et al.*, 2005; Steinmaus *et al.*, 2006; Das *et al.*, 2013). Majority of the field kits are based on Gutzeit method where arsine gas is generated by reduction of arsenic using zinc and hydrochloric acid (Grosse *et al.*, 2017). Fields kits are cost effective, rapid and applicable for on-site analysis (Das *et al.*, 2013; Haque *et al.*, 2018). There are, however, numerous disadvantages associated with field kits such as poor reproducibility, inability to reach low detection limits and limited selectivity (Kinniburgh *et al.*, 2002; Morita *et al.*, 2006). Moreover, the field kit evaluations based on Gutzeit method are not

accurate as various people can interpret the same result differently (Rahmad *et al.*, 2002).

In recent years there has been a great interest in microfluidic detection system application to environmental monitoring (Gardolinski *et al.*, 2002; Floquet *et al.*, 2011; Yogorajah *et al.*, 2015). Microfluidic detection systems are characterised by the ability to analyse small volume of liquids, usually on the sub-millilitre scale (Azzaro *et al.*, 2006). The small size of the detection systems has numerous advantages over standard macro scale laboratory methods. Microfluidic detection systems have the potential to incorporate all experimental steps such as sample preparation, separation, mixing and detection onto one device (Patev *et al.*, 2008). Miniaturisation enables fast sample throughput, reduced reagent consumption, minimised waste production and portability which in turn reduces the manufacturing costs (Whitesides *et al.*, 2006; Prakash *et al.*, 2007). Therefore, microfluidic detection systems are suitable for autonomous *in situ* water monitoring. However, there are also some challenges associated with microfluidic detection. Formation of air bubbles within the microfluidic channels is a major issue. Additionally, mixing within a microfluidic detection system can be problematic due to laminar flow (Sung *et al.*, 2009).

Paper-based analytical devices (µPADs) are biodegradable, portable and cost effective which makes them suitable for microfluidic analysis (Busa *et al.*, 2016). However, the challenges associated with µPADs include fluid control and low sensitivity in comparison to standard laboratory methods (Fu *et al.*, 2017). Nath *et al.* developed a paper based colorimetric detection method for arsenic in water using europium coordinated gold nanoparticles. Limit of detection (LOD) for As^{3+} and

As $^{5+}$ was 10 and 1 µg L^{-1}, respectively. The method was applied to groundwater analysis with good agreement found between the results and AAS measurements (Nath *et al.,* 2018). Priyadarshni *et al.* developed a paper sensor for arsenic detection in water samples using functionalised gold nanorod with dimercaptosuccinic acid. LOD or both As^{3+} and As^{5+} was reported to be 1 µg L^{-1}. The method was used for arsenic detection in groundwater with strong correlation obtained between the results and AAS measurements (Priyadarshini *et al.,* 2018). Pena-Pereira *et al.* developed a silver nitrate embedded paper based sensor for arsenic detection in water. In this method inorganic arsenic was converted to arsine gas which in turn reacted with silver nitrate producing a colour complex. LOD was found to be 1.1 µg L^{-1}. The toxicity of the arsine gas produced, however, was one of the method's key limitations (Pena-Pereira *et al.,* 2018).

Microfluidic lab-on-chip (LOC) devices have the potential to integrate multiple analysis steps onto one platform (Samiei *et al.,* 2016). In optical detection based LOC devices colour change produced from analyte and reagent interaction is measured. LOC devices can be adapted to a wide range of analysis by customising the microfluidic chip channels (Pol *et al.,* 2017). Majority of microfluidic devices are made from polymeric materials such as polydimethylsiloxane (PDMS) and poly(methylmethacrylate) (PMMA) (Ren *et al.,* 2013).

Microfluidic detection systems based on colorimetric methods have been applied for ammonia (Lieberzeit *et al.,* 2007), nitrate (Daridon *et al.,* 2001), phosphate (Greenway *et al.,* 1999), iron (Doku *et al.,*1999) and manganese (Sieben *et al.,* 2010) monitoring in water. Additionally, Milani *et al.* developed an autonomous LOC detection device for iron and manganese detection in water. Ferrozine ((3-(2-

pyridyl)-5,6- diphenyl-1,2,4-triazine) and PAN (1-(2-pyridylazo)-2-naphthol) were used for iron and manganese detection. LOD for iron and manganese was 5.6 μg L^{-1} and 1.56 μg L^{-1}, respectively (Milani *et al.,* 2015). Clinton-Bailey *et al.* used phosphate blue assay with polyvinylpyrrolidone for phosphate detection in aqueous samples. The method was rapid, with 5 min required for a complete colour change. LOD of 3.8 μg L^{-1} was reported. In addition, the method was employed for phosphate analysis in river water with 4 % infield inaccuracy reported (Clinton-Bailey *et al.,* 2017).

However, only a small number of commercially available microfluidic detection systems have been developed for heavy metal monitoring. Some of the main challenges for microfluidic system application to heavy metal monitoring in drinking water monitoring include the low limits of detection set by WHO and European Union legislation. Additional challenges are posed by limited selectivity, interfering substances, turbidity and sample colour (Niessner *et al.,* 2010).

A wide range of laboratory based methods using various chromophoric dyes for heavy metal detection in water have been described in the literature (Ranyuk *et al.,* 2009; Wang *et al.,* 2011; Wu *et al.,* 2011; Abalos *et al.,* 2012; Xie *et al.,* 2012). Revanasiddappa *et al.,* used leuco malachite green (LMG) dye for arsenic determination in environmental water samples. In this method arsenic is reacted with potassium iodate to liberate iodine. The liberated iodine in the presence of sodium acetate buffer oxidises LMG to malachite green resulting in a green colour formation (Revanasiddappa *et al.,* 2007). To date LMG method has not been integrated into microfluidic detection system for arsenic determination.

The aim of this paper is to present an easy to use and robust arsenic (As^{3+}) detection system for water. LMG method was chosen because of the intense and rapid colour development in the visible region at 617 nm. Additionally, the formed colour complex was stable making it suitable for application in microfluidic analysis. PMMA three port microfluidic detection chip with serpentine channels was used for mixing and detection. The sensing was based on light emitting diode (LED) optical detection.

5.3 Experimental

5.3.1. Standards

All chemicals were of analytical grade and purchased from Sigma-Aldrich (Vale Road, Arklow, Co. Wicklow, Ireland) unless otherwise stated. Sodium meta-arsenite ($NaAsO_2$) and iron sulphate heptahydrate ($FeSO_4 \cdot 7H_2O$) (Fisher Scientific, Leicestershire, UK), were used to prepare stock solutions at concentration 1000 µg mL^{-1} in double deionised water (HPLC grade). Working standards were prepared every week from the stock solution by serial dilutions. Acetic acid (99.8%) (Sharlab S.L., Barcelona, Spain) was used to adjust the pH. Potassium iodate (KIO_3), leucomalachite green dye ($C_6H_5CH[C_6H_4N(CH_3)_2]_2$ and sodium acetate trihydrate ($C_2H_3NaO_2 \cdot 3H_2O$) were prepared by weighing out an appropriate amount and dissolving it in double deionised water. Hydrochloric acid (38%) (Sharlab S.L.) was used to prepare hydrochloric acid solutions with various concentrations in double deionised water. Double deionised water was used for dilution of reagents and samples.

5.3.2. Colorimetric reagents

Reagent 1 was prepared by mixing 15 ml of 1 % w/v potassium iodate with 15 ml of 0.4 M hydrochloric acid.

Reagent 2 was prepared by mixing 5 ml of 0.05 % w/v leucomalachite green dye with 20 ml of 13.6 % w/v sodium acetate trihydrate.

5.3.3. Calibration study and limit of detection

As^{3+} samples with concentrations ranging from 0.1-4 mg L^{-1} were analysed using the microfluidic detection system. Firstly, a blank solution was passed through the microfluidic detection system three times. Afterwards As^{3+} samples were passed through the chip and analysed starting from the lowest concentrations to the highest. Four minutes were required to fill the syringes with the reagent and sample. Fifteen minutes were required to pump and mix the reagents and the sample to the microfluidic chip with a flow rate of 0.2 ml min^{-1}. The flow was stopped and two minutes were allowed before taking the measurements. LED was switched on and the intensity of the light in the microfluidic detection channel was measured by photodiode. The voltage values obtained by photodiode were converted to absorbance using the blank solution as the reference sample. The results obtained from the microfluidic detection system were compared to the benchtop method. In bench top method arsenic sample (6 ml) was mixed with 1 % potassium iodate (1 ml) and 1 M hydrochloric acid (0.5 ml). Following this the mixture was gently shaken. After 2 min incubation period 0.05 % leucomalachite green dye (0.5 ml) was added, followed by 13.6 % sodium triacetate buffer (2 ml). The mixture was

gently shaken. After 5 min incubation period the solution was measured using 10 mm quartz cuvettes at 617 nm against reagent blank.

The repeatability of the method was assessed by running As^{3+} samples several times. Double deionised water was flushed through the system two times when switching from high concentration measurements to low.

Two point calibration was used using blank as the low concentration and 1 mg L^{-1} As^{3+} as the high concentration. Each sample concentration was measured two times and compared to the blank and 1 mg L^{-1} concentration.

The linear range, LOD and limit of quantification (LOQ) of the microfluidic detection method were determined. The set up for the microfluidic detection system is shown in Figure 5.1.

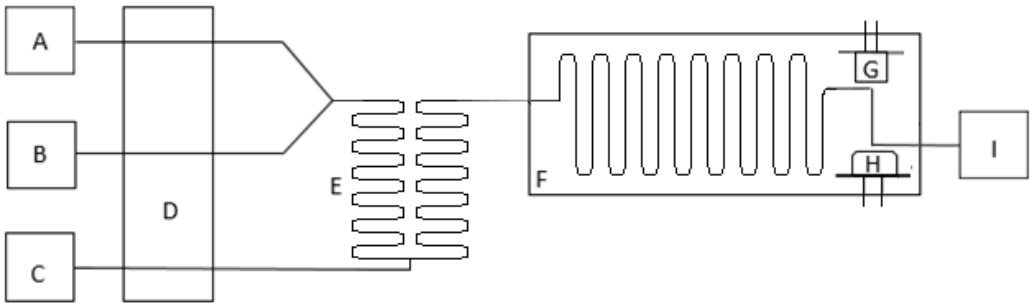

Figure 5.1. Schematic diagram of microfluidic detection system. (A) sample, (B) reagent 1, (C) reagent 2, (D) syringe pump, (E) mixing coil, (F) microfluidic chip, (G) LED, (H)photodiode, (I) waste container.

5.3.4. Validation and environmental water sample testing

The microfluidic detection system was used to determine As^{3+} concentration in water samples with various sample matrices. Water samples were collected from Bog Lake, Co. Laois, groundwater well Co. Laois and the River Barrow at Carlow, Co. Carlow. The different water matrices were then spiked with known concentrations of As^{3+} (0.5 and 1 mg L^{-1}). Additionally, As^{3+} standards prepared in double deionised water (0.5, 0.7 and 0.9 mg L^{-1}) were analysed using the microfluidic detection system. Prior to the analysis the water samples were filtered firstly using Whatman grade 1 filter paper and secondly with sterile 0.2 µm syringe filters. The samples were analysed in triplicate. For each sample % recovery, standard deviation and % relative standard deviation was obtained.

Two point calibration was applied. The concentration of water samples was obtained using the linear equation from the calibration curve.

5.3.5. Interference

In previous studies iron (Fe^{2+}) was found to interfere with As^{3+} determination by the leucomalachite green method (Lace *et al.,* 2019). It is important to study the effect of interference in order to achieve reliable results when analysing various water samples. The effect of Fe^{2+} interference was investigated by preparing dual standards of 0.7 mg L^{-1} As^{3+} with various concentrations of Fe^{2+} (0.1, 1 and 10 mg L^{-1}) and comparing results to a 0.7 mg L^{-1} As^{3+} standard. Voltage for each sample was obtained and converted to absorbance. Two point internal calibration used. The absorbance of the $As^{3+}$and Fe^{2+} samples was divided by the absorbance obtained

from 1 mg L^{-1} As^{3+} standard. All samples were measured in triplicate. Recovery (%), standard deviation and relative standard deviation were calculated for each sample.

5.3.6. Instrumentation design and measurement procedure

The mixing of the sample and reagents took place in mixing coil and the microfluidic chip. The PMMA microfluidic chip with dimensions 60 × 40 × 16 mm consisted of channels with a cross sectional area of 300 × 300 μm and 20 mm long detection channel (Figure 5.2). It had three inlets with M6 fittings. The microfluidic chip was manufactured in Laboratory for Analysis and Architecture of Systems, Toulouse, and bonded in TE Laboratories. Detection of the resulting complex took place within the microfluidic chip. A custom made syringe pump array was used to deliver the sample and reagents to the microfluidic chip.

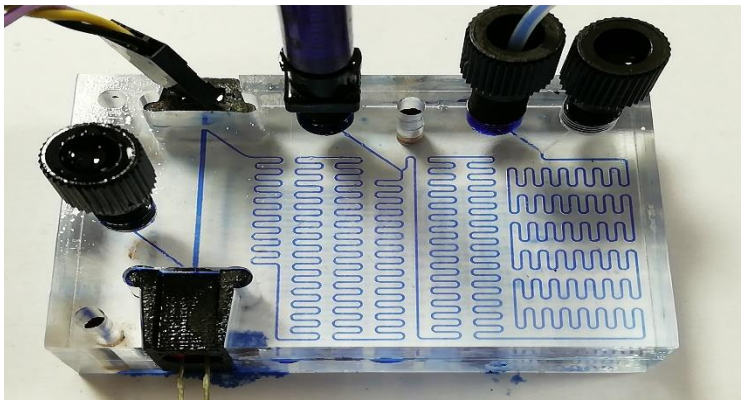

Figure 5.2. PMMA microfluidic chip with dimensions 60 × 40 × 16 mm consisted of serpentine channels with cross sectional area of 300 × 300 μm and 20 mm long detection channel.

The leucomalachite green method uses two reagents which are stable when stored separately. For each sample assay blank consisting of double deionised water,

reagent 1 and reagent 2 was measured initially. The sample, reagent 1 and reagent 2 were pumped into mixing coil using syringe pump through double check valves (Nordson) in 1:1 v/v ratio. The initial mixing of reagent 1 and the sample took place in a mixing coil designed using a Tygon tubing (Nordson). About 2 minutes later the reagent 2 was added to the reagent 1 and sample in the mixing coil and mixed. The resulting solution was then pumped into the microfluidic chip where detection took place. When the chip was filled the flow was stopped for 5 minutes to allow for further colour formation. Additionally, analysis using stopped flow minimises the consumption of reagents and minimises waste. The absorbance was measured by using the LED-photodioide set up. The photodiode and the optical detector were aligned on the opposite sides of the microfluidic chip's optical cuvette to measure absorbance of the leucomalachite green and As^{3+} complex. The reaction mechanism between arsenic and potassium iodate and leucomalachite green oxidation reaction is shown in Figure 5.3. The different reaction steps are outlined in Figure 5.4.

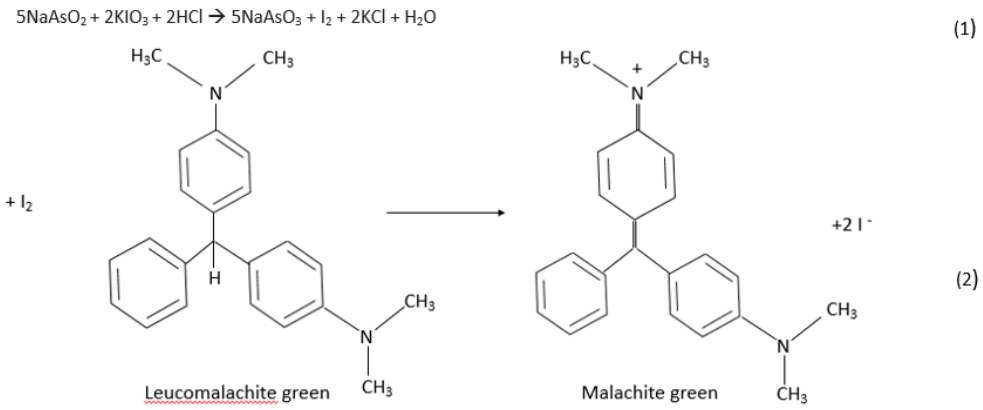

Figure 5.3. Arsenic and potassium iodate reaction (1) and leucomalachite green oxidation reaction to malachite green (2).

Two columns of data were outputted, the first showing the count of the time (seconds) and second- photodiode readings. This procedure was followed for all sample measurements. The data was analysed using Microsoft Excel.

Each measurement was compared to the blank. The sample concentration was estimated firstly by converting voltage to absorbance using equation 1, where asb is the absorbance of the sample, s.v. is the sample voltage and b.v. is the blank voltage. The results were plotted in a calibration curve Abs vs. conc.

$$\text{abs} = -\log_{10}\left(\frac{\text{s.v}}{\text{b.v}}\right) \qquad (1)$$

Equation 1. Equation for determining arsenic concentration in water samples.

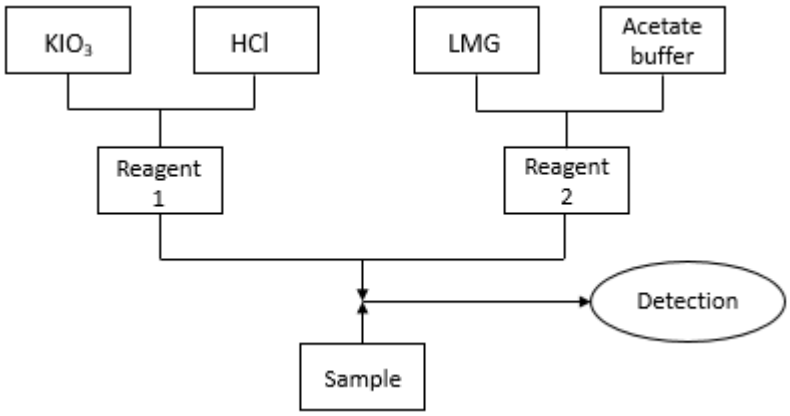

Figure 5.4. Reaction steps for the optimised leucomalachite green method.

5.4. Results and discussion

5.4.1. Optimisation of method parameters

Firstly, LED (Radionix, King Bright) and photodioide (TSL T47) were assessed by running premixed arsenic samples through a model chip. The samples were

manually injected in the chip using a plastic syringe and measured after 2 minutes incubation period. Voltage of samples was measured using a mutlimeter and converted into absorbance. The results were plotted on a calibration curve Abs vs conc. During the procedure the microfluidic chip was kept in a closed container to avoid straight light interfering with the readings. After reproducible results were obtained, a PMMA with dimensions 100×45×15 mm and 20 mm detection channel was used for reagent mixing and measurements. Custom made syringe pumps were integrated into the microfluidic detection system to introduce the sample into the cell.

However, the PMMA microfluidic chip did not show efficient mixing as the channels were not long enough. So three chips were used- two identical mixing chips with equal channel lengths and one detection chip. Mixing within the microfluidic chip was tested using different food colour dyes. Yellow and blue dye were used to simulate sample and reagent 1 mixing process. Green colour was obtained and could be easily viewed through the clear PMMA detection chip (Fig. 2). Red colour dye was used to simulate reagent 2 and was mixed with the resulting green coloured dye. However, throughout mixing was not observed. Additionally, significant fluid backflow was observed during the evaluation. Also, a fault in the detection channel's design prevented this microfluidic chip to be used in further studies. Subsequently, a new microfluidic chip was designed. The new microfluidic chip was manufactured in in Laboratory for Analysis and Architecture of Systems, Toulouse, and bonded in TE Laboratories. The PMMA chip with dimensions 60 × 40 × 16 mm consisted of serpentine channels with cross sectional area of 300 × 300 μm and 20 mm long detection channel width 600 μm depth (Fig. 3). It had three

inlets with M6 fittings. Different syringe pump speeds were tested, the mixing was assessed from measuring the waste effluent and the voltage of samples. A mixing coil consisting of Tygon tubing (Nordson) looped around several times was added to the microfluidic detection system to enhance reagent and sample mixing. Therefore, the microfluidic chip was used for detection of the leucomalachite green and As^{3+} complex.

5.4.2. Calibration study and the limit of detection

LOD, defined as the concentration equal to three times the standard deviation of the measurement above the background absorbance (McGraw *et al.*, 2007) was 0.032 mg L^{-1} (n=12). LOQ, defined as ten times the standard deviation of the measurement above the background absorbance, was 0.105 mg L^{-1}. The leucomalachite green method carried out in a microfluidic detection system yielded a linear response to As^{3+} concentrations ranging between 0.3- 2 mg L^{-1} (Figure 5.5). 0.3 mg L^{-1} As^{3+} sample showed the greatest RSD value (37.46 %) indicating that the method is less precise at lower As^{3+} concentrations (Table 5.1).

Table 5.1. Average absorbance values for As^{3+} samples (0.3–2 mg L^{-1}) analysed with microfluidic detection system. All measurements were carried out in duplicate (*n* =2).

Conc (mg L^{-1})	Abs 1	Abs 2	Average	SD	% RSD
0.3	0.02	0.03	0.02	0.01	37.46
0.5	0.04	0.04	0.04	0.00	7.75
0.7	0.06	0.08	0.07	0.01	16.47
1	0.10	0.11	0.10	0.01	6.48
2	0.21	0.17	0.19	0.03	14.14

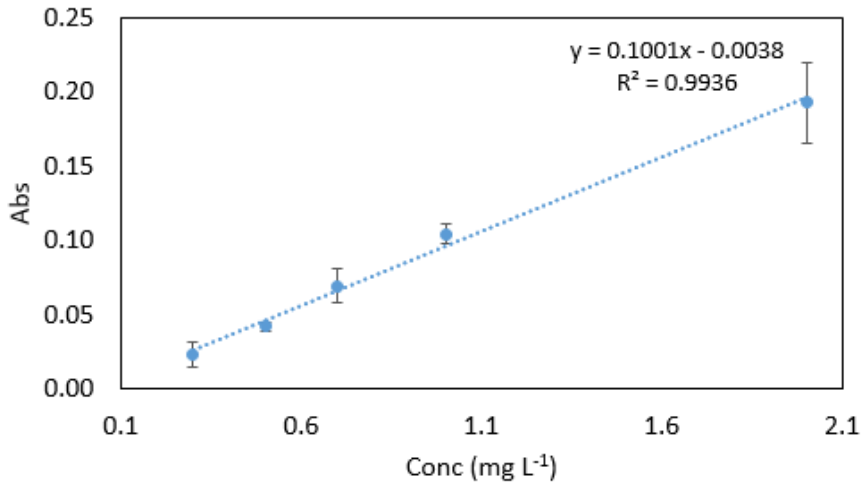

Figure 5.5. Leucomalachite green method calibration curve obtained from the microfluidic detection system using As^{3+} standards ranging from 0.3- 2 mg L^{-1}. The error bars represent standard deviations. The measurements were carried out in duplicate (*n*=2). Error bars represent standard deviations of the measurements.

5.4.3. Interference

Fe^{2+} concentrations of 10 mg L^{-1} and 1 mg L^{-1} had a significant impact on As^{3+} determination in water samples. 0.7 mg L^{-1} As^{3+} sample with 10 mg L^{-1} Fe^{2+} showed recovery of 38.57 %, whereas As^{3+} sample containing 0.1 mg L^{-1} Fe^{2+} was found to have 90 % recovery (Table 5.2). It can be concluded that Fe^{2+} at concentrations higher than 0.1 mg L^{-1} interferes with As^{3+} determination using the microfluidic detection system. This should be noted when deploying the system in surface water.

Table 5.2. A comparison between As^{3+} samples spiked with various Fe^{2+} concentrations obtained from the microfluidic detection system. (A) represents 0.7 mg L^{-1} As^{3+} sample, (B) represents 0.7 mg L^{-1} As^{3+} sample spiked with 0.1 mg L^{-1} Fe^{2+}, (C) represents 0.7 mg L^{-1} As^{3+} sample spiked with 1 mg L^{-1} Fe^{2+} and (D) represents 0.7 mg L^{-1} As^{3+} sample spiked with 10 mg L^{-1} Fe^{2+}.

Sample	Fe spiked (mg L^{-1})	As spiked (mg L^{-1})	As detected (mg L^{-1})	Recovery %	SD	RSD %
A	0	0.7	0.63	90.0	0.01	0.5
B	0.1	0.7	0.6	85.7	0.15	5.3
C	1	0.7	0.48	68.6	0.04	1.3
D	10	0.7	0.27	38.6	0.09	2.9

5.4.4. Comparison to colorimetric method

The performance of microfluidic detection system was compared to that of the benchtop colorimetric method. Various As^{3+} samples with concentration ranging between 0.3-2 mg L^{-1} were analysed. The effluent from different As^{3+} samples analysed with the microfluidic detection system was collected and measured using UV-vis spectrometer at 617 nm. 10 mm quartz cuvettes were used for all measurements. All measurements were carried out in triplicate.

The colour obtained from As^{3+} samples analysed using microfluidic detection system was slightly weaker than that of As^{3+} samples analysed using the benchtop method (Figure 5.6). There was a distinguishable colour difference between various concentration As^{3+} samples analysed both by benchtop and microfluidic detection system. Although a stronger colour was obtained from the benchtop method, the various As^{3+} samples analysed with the microfluidic detection system had visibly different colour intensities with a more intense colour observed in As^{3+} samples with high concentrations. Both linearity and analytical response were strong for samples measured with the microfluidic detection system and close to those of the benchtop method as it can be seen from the calibration curves in Figure 5.7. Therefore, it can be concluded that the microfluidic detection system with integrated leucomalachite green method is competent for As^{3+} determination in water.

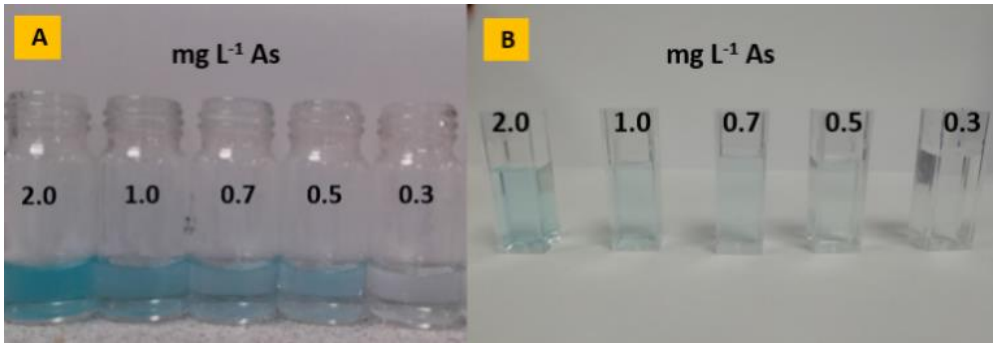

Figure 5.6. Comparison between As^{3+} samples ranging between 0.3- 2 mg L^{-1} analysed using benchtop and the microfluidic detection system. (A) shows As^{3+} samples analysed using the benchtop method, (B) represents the effluent collected from As^{3+} samples analysed using microfluidic detection system.

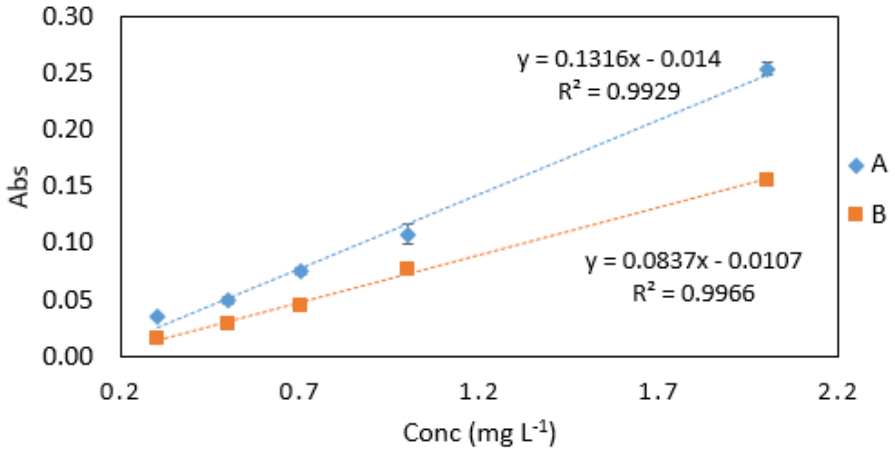

Figure 5.7. Comparison of As^{3+} standards (0.3–2 mg L−1) obtained from benchtop and microfluidic detection system. The effluent from samples ran through the microfluidic detection system was collected and measured using UV-vis spectrometer. (A) represents the absorbance of standards analysed using benchtop method (blue markers). (B) represents the absorbance of standards analysed using the microfluidic detection system. All measurements were carried out in triplicate (n=3). Standard deviations are represented by error bars.

Table 1. Comparison of As^{3+} standards (0.3–2 mg L^{-1}) obtained from benchtop and microfluidic detection system. The effluent from samples ran through the microfluidic detection system was collected and measured using UV-vis spectrometer. (A) represents the absorbance of standards analysed using benchtop method (blue markers). All measurements were carried out in triplicate (*n=3*).

Conc (mg L^{-1})	A	B	SD A	SD B	% RSD A	% RSD B
0.3	0.035	0.017	0.002	0.003	5.714	15.252
0.5	0.050	0.029	0.003	0.003	6.110	10.345
0.7	0.075	0.044	0.003	0.003	4.286	5.674
1	0.108	0.078	0.009	0.002	8.230	1.971
2	0.254	0.156	0.006	0.002	2.239	1.334

5.4.5. Validation of system and environmental sample testing

The smallest percentage recovery (85.71 %) was found for the 0.7 mg L^{-1} As^{3+} sample prepared in double deionised water, whereas the greatest percentage recovery was observed for the 1 mg L^{-1} river water sample (122.00 %) as it can be seen in Table 5.3. This could be explained by sample colour and the differences in sample matrices, as river water would have a range of potential interferants ions that could interfere with As^{3+} analysis in contrast to the double deionised water sample. Overall, water samples with the same water matrix showed similar percentage recovery with the exception of lake water samples. This could be due to different factors affecting the microfluidic detection system such as air bubbles and interference from other samples in microfluidic detection channels.

Overall, the results show that the microfluidic detection system is capable of determining As^{3+} in various water matrices. In future studies a wider range of various sample matrices would need to be assessed including waste water.

Table 5.3. Assessment of microfluidic detection system using As^{3+} samples with various concentrations and sample matrices. (A) represents river water, (B) represents lake water, (C) represents groundwater and (D) represents double deionised water. All measurements were carried out in duplicate (*n*=2).

Sample characteristics	**Spiked (mg L^{-1})**	**Detected (mg L^{-1})**	**Recovery %**	**SD**	**RSD %**
A	0.50	0.61	122.00	0.06	7.51
A	1.00	1.20	120.10	0.01	7.61
B	0.50	0.44	88.00	0.04	8.79
B	1.00	1.02	101.50	0.01	5.46
C	0.50	0.49	98.00	0.07	2.04
C	1.00	1.11	111.30	0.02	15.37
D	0.50	0.43	86.00	0.05	11.02
D	0.70	0.60	85.71	0.15	5.25
D	0.90	0.79	87.78	0.08	2.92

5.4.6. Limitations of the method

External mixing was required to enhance the mixing of reagents and samples. Fluid back flow and air bubble formation were noted in several occasions during the analysis, affecting the reagent and sample mixing and voltage readings. The air bubbles could have formed during the injection step or syringe filling process. Liquid pumping for prolonged time and short intervals of fast pumping speed eliminated the air bubbles from the system. Infrequent leaks also occurred in the microfluidic chips used, typically at the edges of the chip. This could be due to the air high pressure within the chip during analysis and weakening of the adhesive used for bonding the layers of the chip together.

The limit of detection for the optimised method was high in comparison to the As^{3+} limit in drinking water set by EU regulations and WHO. However, the detection system could be applied for surface water analysis with known high As^{3+} concentrations and waste water monitoring. Emission limit value for arsenic industrial waste water effluent within the EU is 0.15 mg L^{-1} (Directive 2010/75/EU) which could be detected using leucomalachite green method integrated within microfluidic chip as the LOQ for the method is 0.105 mg L^{-1}. In industrial effluent nitrate and phosphate concentrations are generally present below the tolerance leucomalachite green method's limit of 100 mg L^{-1}, however, interference of water colour could pose potential issues for arsenic monitoring.

One of the main limitations was the slow sample throughput. The throughput time for one sample was twenty five minutes. Ideally, a more rapid sample throughput would be desirable for environmental water monitoring *in situ*.

5.5 Conclusion

A simple analysis system was developed for direct As^{3+} detection in water using the leucomalachite green method. The leucomalachite green method was optimised for integration into the microfluidic detection system. The results presented here are the first for microfluidic As^{3+} determination using leucomalachite green method. The optimised microfluidic detection method was simple, robust and reproducible with a linear range between 0.3 and 2 mg L^{-1}. The results obtained from the microfluidic detection system had a good correlation with those of the benchtop method. Even though the method's linear range was too high to be considered for groundwater analysis, it has great potential for As^{3+} determination in surface waters with known high As^{3+} concentrations and waste water.

Further developments should focus on improving the sample throughput time and improving the mixing efficiency of the analytical system by incorporating mixing enhancing features into the microfluidic chip. Subsequently, the main focus should be on field deployments with modified approach for *in situ* environmental monitoring. Also, the main objectives would include issues related to environmental water sample analysis and development of microfluidic detection systems capable of autonomous operation over an extended period of time.

Ultimately, this system may provide a basis for As^{3+} monitoring in surface and waste waters *in situ* and become a simple and more cost effective alternative to standard methods.

Chapter 6

Synopsis and future perspectives

6.1. Discussion

Groundwater pollution has become a serious global problem. Approximately 1.6 million children die each year from consuming contaminated drinking water (Fernandez-n *et al.*, 2013). Although many of these deaths are due to microbiological contamination, and data on mortalities or illnesses caused by heavy metal contamination is not readily available. Heavy metals are considered as some of the most dangerous chemical pollutants due to their high toxicity. Heavy metals do not biodegrade, and therefore, they have the ability to bioaccumulate in living organisms causing a serious threat to ecological systems (Lin *et al.*, 2016). Therefore, large scale routine monitoring of heavy metals is very important.

A wide range of different laboratory based techniques have been developed for heavy metal determination in water, such as inductively coupled plasma mass spectrometry (ICP-MS), flame atomic absorption spectrometry (FAAS), electrochemical methods and atomic absorption spectrometry (AAS) (Bagheri *et al.*, 2012; Djedjibegovic *et al.*, 2012, Sohrabi *et al.*, 2013, Ma *et al.*, 2015). These methods are reliable, highly specific, and have the ability to detect heavy metals even at very low concentrations (Neves *et al.*, 2009). ICP-MS and AAS are some of the most commonly used techniques for heavy metal detection due to their high selectivity and sensitivity (Lin *et al.*, 2016). Despite the many advantages associated with the laboratory based methods, the complex instrumentation and requirement for highly trained technicians make these techniques unsuitable for high frequency routine monitoring (Cui *et al.*, 2015). Low cost portable detection methods that are easy to use are required for effective heavy metal monitoring, especially in countries with limited financial resources and professional expertise.

The increasing demand for autonomous and cost effective monitoring systems has resulted in rapid development of microfluidic detection systems (Pol *et al.,* 2017). Microfluidics is a relatively novel field which is concentrated on development of miniaturised, integrated lab on a chip analytical devices (Yogorajah *et al.,* 2015). Miniaturisation has many advantages such as low reagent consumption and waste production, fast analysis, and portability (Nge *et al.,* 2013, Stanley *et al.,* 2015). These properties make microfluidic detection systems suitable for environmental monitoring (Haswell *et al.,* 1997). Additionally, microfluidic detection systems can potentially incorporate a wide range of experimental processes such as sample preparation, mixing, and detection onto one platform. Optical detection methods are widely used in microfluidic analysis as they are simple, cost effective and versatile (Baker *et al.,* 2009; Jokerst *et al.,* 2012).

The main goal of the present work was to investigate the application of optical based detection based methods for heavy metal monitoring in water samples using microfluidic detection systems. In Chapter 2 various colorimetric methods for arsenic detection in water were assessed using UV-vis spectroscopy. Various parameters such as limit of detection (LOD), linear range, reproducibility and colour stability was determined. From extensive literature review variamine blue and molybdenum blue methods were chosen. The method performance in various pH conditions and incubation temperatures was investigated. As the dimensions in microfluidic detection systems are small, the path length is reduced. This in turn can decrease the sensitivity of the method, therefore, the chosen optical detection method has to be highly sensitive (Marle *et al.,* 2005). The method performance in microfluidic detection system was simulated using small scale 1 mm light path

quartz cuvettes. In comparison to measurements carried out in 10 mm standard quartz cuvettes, the expected ten fold decrease in absorbance was detected.

A strong analytical signal was obtained from 1 mm path length cuvette measurements for both methods. However, the molybdenum blue method required a number of separate reagents. The molybdenum blue dye had to be prepared on daily basis prior analysis as it is not commercially available. Ideally, a method for microfluidic detection applications should have a small number of reagents in order to reduce the cost and complexity of the analysis. Although the variamine blue method required a relatively small number of reagents, the colour stability was not as strong as that of molybdenum blue method. Additionally, the reproducibility of the methods was not adequate for further studies and application to microfluidic detection systems.

In chapter 3 the leucomalachite green (LMG) method was assessed for its potential application for arsenic detection in water using microfluidic detection systems. The method was chosen due to the intense colour formation with λ_{max} of 617 nm. A strong analytical response was obtained from measurements carried out in 1 mm quartz cuvettes indicating the method's suitability for microfluidic analysis. Additionally, only five minutes were required for a complete colour change. A range of spiked environmental water samples that were collected from river, lake and groundwater were analysed using the LMG method. The results revealed that the method is capable of determining arsenic in wide range of sample matrices. However, absorbance measurements were affected by strongly coloured environmental samples, such as the lake sample. In addition, iron was found to

interfere with the determination of arsenic. This should be noted in future calibration protocol design.

A small number of reagents were required for the LMG method. Moreover, the reagents could be combined by simplifying the analysis and the design of a microfluidic detection chip. Potassium iodate was combined with hydrochloric acid forming the first combined reagent, whereas leucomalachite green dye was mixed with sodium triacetate buffer creating the second combined reagent. Additionally, the small number of reagents would also improve mixing as usually in fast reactions where two or more reagents are used in separate streams, uniform mixing is very rare (deMello *et al.*, 2006). Good results were obtained using a simple 1 to 1 sample to reagent ratio. Overall, the method showed great potential for applications in microfluidic detection systems, and therefore, was further optimised and integrated into microfluidic detection system.

Chapter 4 was focused on the assessment of 1,5-diphenylcarbazide (DPC) method for chromium (VI) detection in water using microfluidic detection systems. The DPC method was selected due to its simplicity and the small number of reagents required. Only two reagents were required for this method. Moreover, these reagents could be combined resulting in a simplified analysis using 1 to 1 sample to reagent ratio, which would enable cost effective and simple microfluidic chip design. Additionally, the reagents were also stable, with decrease in absorbance detected after a fourteen day period. Reagent stability is an important factor when developing an autonomous microfluidic detection system as long deployable life times are desirable. Long life times are difficult to attain in microfluidic detection systems, and it remains one of the key challenges in their application to *in situ*

monitoring (Niessner *et al.,* 2010). Additionally, a strong analytical signal was obtained from measurements carried out in 1 mm quartz cuvettes. An intense purple colour was formed immediately after reacting spiked chromium water samples with the reagents with λ_{max} of 543 nm. Although the formed colour stained the surface of quartz cuvettes, the staining was removed by use of 1 % nitric acid solution. This cleaning process was rapid and simple which would be ideal for use in microfluidic detection systems.

The method has a broad linear range, between 0.03–3 mg L^{-1}. The method was also sensitive at low chromium concentrations, with LOD of 0.023 mg L^{-1}. Similarly to chapter 3, a range of water samples collected from different sources were analysed. Although, the determination of chromium was slightly affected by the different water matrices, overall, the DPC method proved to be robust in terms of chromium determination. This is very important for practical applications of environmental monitoring. Most importantly, the optimised DPC method showed good agreement with results obtained from ICP-MS which is one of the most commonly used methods for heavy metal detection in water samples. Therefore, it could be concluded that the DPC method is suitable for integration into microfluidic detection systems.

Nitrate concentrations exceeding 50 mg L^{-1} have been reported in several locations in Ireland (Toner *et al.,* 2005), therefore, it's interference on DPC method should be considered when applying the method for surface water monitoring *in situ* as it exceeds the method's tolerance limit for nitrate which is 10 mg L^{-1}. Additionally, iron concentrations in surface waters are likely to exceed the 1 mg L^{-1} tolerance limit. Further work to address this issue is required prior method's incorporation

and application for surface water monitoring. In addition, DPC method has a potential to be applied for waste water monitoring, for example, detection of chromium in industrial waste effluent from tanneries. Chromium concentrations in industrial effluent have been reported to range between 3.9-56 ppm (Hohenblum *et al.*, 2001). In Turkey hexavalent chromium concentration in tannery waste water have been reported to reach concentrations as high as 127 mg L^{-1} (Sungur *et al.*, 2017). Emission limit value for chromium in waste water within the EU is 0.5 mg L^{-1} which is within the linear range of DPC method (0.03-3 mg L^{-1}) (Directive 2010/75/EU). Nitrate concentrations in industrial waste water are likely to be present at concentrations exceeding 10 mg L^{-1} which limit DPC method's application for waste water analysis.

The work described in Chapter 5 was a continuation of work that is represented in Chapter 3. The optimised leucomalachite green method was integrated into a microfluidic detection system for arsenic analysis in water samples. A PMMA microfluidic chip was designed for the arsenic detection using leucomalachite green method. The design of the chip was relatively simple due to the small number of reagents required which was achieved by combining some of the reagents as described in chapter 3. The function of the microfluidic chip was to mix the reagents with the water samples and to detect the corresponding signal. Photodiode and LED which functioned as a light source and a photodiode which served as a detector were coupled to the microfluidic detection channel. Low flow rate and minimal pulsation is required for fluid movement within a microfluidic detection system (Marle *et al.*, 2005). Syringe pumps were chosen for introducing water samples and reagents into

microfluidic detection system as they are capable of delivering stable low volume flow with a relatively low power requirement (Nightingale *et al.*, 2015).

A simple and reproducible analysis system for arsenic was developed. Linear range was observed between 0.3 and 2 mg L^{-1}. LOD and limit of quantification (LOQ) were found to be 0.032 mg L^{-1} and 0.105 mg L^{-1}. Although the method's linear range was too high for applications in groundwater analysis, it could be applied for arsenic monitoring in surface waters with known high arsenic concentrations and waste water.

A range of water samples were analysed using the microfluidic detection system. Spiked lake, river and groundwater samples were passed through the microfluidic detection system. Overall, good recoveries were obtained for these samples which indicates that the method is robust enough to be considered for real water samples analysis. Similarly to results described in chapter 3, iron was found to interfere with the arsenic determination. Therefore, it is important to be able to measure the concentration of iron in environmental water when using the leucomalachite green method for arsenic detection in water. In natural waters phosphate and nitrate background concentrations are likely to be present below 100 mg L^{-1} which is the tolerance limit for LMG method. However, iron concentrations are likely to exceed 0.1 mg L^{-1} which is LMG method' tolerance limit for iron. Therefore, this limitation should be considered when deploying microfluidic detection systems in the environment. Additionally, routine microchannel cleaning should be carried out using low concentrated acid solution, for example, to avoid interference and biofilm formation within the microfluidic channels as use of microfilters might not prevent all microorganisms form entering the microfluidic detection system.

One of the greatest challenges associated with the leucomalachite green method's integration in a microfluidic chip was reagent and sample mixing. Because of the small dimensions of mixing channels, laminar flow was present which prevents adequate mixing of reagents and samples. As a result, microfluidic devices depend on diffusive mixing which is a much slower process than turbulent mixing which can be obtained in macro scale analysis systems (Ward *et al.*, 2015). Consequently, mixing in microfluidic devices is a slow process and requires a long channel to achieve adequate mixing (Lee *et al.*, 2011). The mixing of reagents and samples in the microfluidic chip was enhanced by elongating the mixing channel using an external mixing coil. The improvement in mixing was observed both visually and from the voltage readings.

Formation of air bubbles in microfluidic detection systems is a serious issue. Air bubbles in microfluidic channels can lead to unstable and irregular flow which in turn can affect both mixing and detection of the analyte (Nakayama *et al.*, 2006). Additionally, air bubbles are difficult to remove as they can easily stick to the inner surface of the channels (Sung *et al.*, 2009). Air bubbles were observed throughout the microfluidic analysis of arsenic causing numerous issues with reagent and sample mixing. Air bubbles' presence in detection cell leads to an inability to accurately measure arsenic concentration in the sample. This issue was mitigated by increasing the flow rate and carrying out flushes of the detection system using double deionised water. Additionally, all samples and reagents were filtered prior analysis.

Overall, the optimised leucomalachite green method was successfully integrated into microfluidic detection system and showed great potential for use in environmental water monitoring.

6.2. Future work

The chromium determination method using 1,5-diphenylcarbazide showed a great potential for applications in microfluidic detection systems. This method could be further integrated and optimised in a microfluidic detection system with a simple design microfluidic detection chip required.

Both the 1,5-diphenylcarbazide and leucomalachite green method demonstrated ability to determine target analytes in environmental samples. For further method development towards autonomous analyte detection *in situ*, a larger set of environmental samples should be investigated. Sample colour and presence of large number of interfering ions are known to negatively affect the microfluidic measurements. A wide range of environmental samples characterised by strong colour should be analysed in order to assess both method performance in highly complex water matrices. Additionally, both the capability of both methods to analyse waste water samples should be assessed.

The analysis time for one arsenic sample using the microfluidic detection system with leucomalachite green method was twenty five minutes. Ideally, faster reaction times should be obtained for successful application in environmental monitoring. Further optimisation for increasing the mixing capability of the leucomalachite green method within the microfluidic chip is required. Faster sample throughput

would result in larger number of samples analysed, and therefore, more reliable data.

Iron interference on arsenic determination using the leucomalachite green method is an issue. Therefore, the concentration of iron in the water source where sampling is carried out should be determined. This could be done by developing a separate microfluidic detection system for iron that would be used in parallel with arsenic determination. For iron monitoring, the 1,10 phenanthroline method could be used as it is one of the most established optical detection methods methods for iron determination in water.

The microfluidic detection system based on leucomalachite green method for arsenic could be developed further by integrating it into a completely autonomous detection system. Effective low cost power source would be required for function of microcontroller and syringe pumps. Additionally, automated filtering step should be added prior sample injection into microfluidic detection system. For autonomous operation a more effective pumping system should be developed as the current syringe pump set up is a subject to air bubble development and is affected by back pressure within the system. The integrated system should be as compact as possible and easily portable. Great focus of the future work would be on field deployments and assessment of microfluidic detection systems capability of operating over extended period of time. Additionally, the system's ability to endure various weather conditions should be evaluated.

Overall, the work carried out in this research can potentially serve as a base for cost effective alternative to standard methods for arsenic monitoring in surface waters.

Chapter 7

Dissemination of thesis

7.1 Peer reviewed journal publications

- Lace, A., Ryan, D., Bowkett, M., Cleary, J. (2019). Arsenic Monitoring in Water by Colorimetry Using an Optimized Leucomalachite Green Method. *Molecules*, *24*, 339.

- Lace, A., Ryan, D., Bowkett, M., Cleary, J. (2019). Chromium Monitoring in Water by Colorimetry Using Optimised 1,5-Diphenylcarbazide Method. *International Journal of Environmental Research and Public Health*, *16*, 1803.

- Lace, A., Ryan, D., Cleary, J. (2019). Arsenic detection in water using microfluidic detection systems based on leucomalachite green method. *Analytical methods* (in review).

- Lace, A., Ryan, D., Cleary, J. (2019). A review of microfluidic detection strategies for heavy metals in water. *Microchemical journal* (in review).

7.2 Conference oral presentations

- Lace, A., Ryan, D., Cleary, J. (2016). Optimization of colorimetric methods for arsenic detection in water, 15th workshop on Progress in trace metal speciation for environmental analytical chemistry, Gdansk, Poland, 4th- 7th September 2016.

- Lace, A., Ryan, D., Bowkett, M., Cleary, J. (2017). Candidate method identification for arsenite detection and quanitification in water using optochemical strategies, 27th Irish Environmental Researchers Colloquium, Athlone Institute of Technology, Athlone, Ireland, 10th – 12th April 2017.

- Lace, A., Ryan, D., Bowkett, M., Cleary, J. Candidate method identification for heavy metal detection and quantification in water using optochemical strategies, 15th International Conference on Environmental Science and Technology, Rhodes, Greece, 31st August – 2nd September 2017.

- Lace, A., Ryan, D., Bowkett, M., Cleary, J. (2019). Candidate method selection for heavy metal detection in water using optochemical strategies, 29th Irish Environmental Researchers Colloquium, Institute of Technology Carlow, Carlow, Ireland, 15th - 17th April 2019.

7.3 Conference poster presentations

- Lace, A., Ryan, D., Bowkett, M., Cleary, J. (2016). Candidate method selection for heavy metal detection in water using optochemical strategies, 26th Irish Environmental Researchers Colloquium, University of Limerick, Ireland, 22nd- 24th March 2016.
- Lace, A., Ryan, D., Bowkett, M., Cleary, J. (2018). Candidate method identification for lead and arsenic detection and quanitification in water using optochemical detection systems, 28th Irish Environmental Researchers Colloquium, Cork Institute of Technology, Cork, Ireland, 26nd- 28th March 2018.

Chapter 8

References

Abadin, H., Ashizawa, A., Stevens, Y. W., Llados, F., Diamond, G., Sage, G., and Swarts, S. G. (2007). Analytical Methods. In *Toxicological Profile for Lead*. Agency for Toxic Substances and Disease Registry (US).

Abalos, T., Moragues, M., Royo, S., Jimenez, D., Martinez-Manez, R., Soto, J., Sancenon, F., Gil, S., and Cano, J. (2012). *European Journal of Inorganic Chemistry*, 76–84, https://doi.org/10.1002/ejic.201100834.

Abi Kaed Bey, S.K., Connelly, D.P., Legiret, F.-E., Harris, A.J.K., and Mowlem, M.C. (2011). A high-resolution analyser for the measurement of ammonium in oligotrophic seawater. *Ocean Dynamics,* 61, 1555–1565, https://doi.org/10.1007/s10236-011-0469-5.

Achmad, R. T. and Ibrahim, E. (2017). Effects of chromium on human body. *Annual Research and Review in Biology*, 13 (2), ARRB-33462, https://doi.org/10.9734/ARRB/2017/33462.

Adkins, J., Boehle, K., and Henry, C. (2015). Electrochemical paper-based microfluidic devices. *Electrophoresis,* 36 (16), 1811-1824, https://doi.org/10.1002/elps.201500084.

Agency for Toxic Substances and Disease Registry (ATSDR) (2004). Toxicological profile for Copper. Department of Health and Human Services, Public Health Service: Atlanta, U.S

Agrawal, S., Berggren, K. L., Marks, E., and Fox, J. H. (2017). Impact of high iron intake on cognition and neurodegeneration in humans and in animal models: a systematic review. *Nutrition Reviews,* 75 (6), 456–470, https://doi.org/10.1093/nutrit/nux015.

Akers, D. B., MacCarthy, M. F., Cunningham, J. A., Annis, J., and Mihelcic, J. R. (2015). Lead (Pb) contamination of self-supply groundwater systems in coastal Madagascar and predictions of blood lead levels in exposed children. *Environmental Science & Technology*, 49 (5), 2685-2693, https://doi.org/10.1021/es504517r.

Alahmad, W., Uraisin, K., Nacapricha, D., and Kaneta, T. (2016). A miniaturized chemiluminescence detection system for a microfluidic paper-based analytical device and its application to the determination of chromium (III). *Analytical Methods*, 8 (27), 5414-5420, https://doi.org/10.1039/C6AY00954A.

Amin, A.S., El-Sheikh, R., and Shaltout, M.I. (2015). Utilization of 2-Amino-6-(1,3-thiazol-2yldiazenyl)phenol for Chromium speciation in environmental samples spectrophotometrically. *Canadian Chemical Transactions, 3*, 171–183, https://doi.org/10.13179/canchemtrans.2015.03.02.0182.

Apilux, A., Siangproh, W., Praphairaksit, N., and Chailapakul, O. (2012). Simple and rapid colorimetric detection of Hg (II) by a paper-based device using silver nanoplates. *Talanta*, 97, 388–394, https://doi.org/10.1016/j.talanta.2012.04.050.

Argos, M., Kalra, T., Rathouz, P. J., Chen, Y., Pierce, B., Parvez, F., Islam, T., Ahmed, A., Rakibuz-Zaman, M., Hasan, R., Slakovich, V., van Geen, A., Graziano, J., Ahsan, H., and Sarwar, G. (2010). Arsenic exposure from drinking water, and all-cause and chronic-disease mortalities in Bangladesh (HEALS): a prospective cohort study. *The Lancet*, *376*(9737), 252-258, https://doi.org/10.1016/S0140-6736(10)60481-3.

Argos, M., Kalra, T., Rathouz, P. J., Chen, Y., Pierce, B., Parvez, F., and Ahsan H. (2010). Arsenic exposure from drinking water, and all-cause and chronic-disease mortalities in Bangladesh (HEALS): a prospective cohort study. *The Lancet*, 376, 252–258, https://doi.org/10.1016/S0140-6736(10)60481-3.

Armienta, M. A., and Segovia, N. (2008). Arsenic and fluoride in the groundwater of Mexico. *Environmental Geochemistry and Health*, 30, 345–353, https://doi.org/10.1007/s10653-008-9167-8.

Armienta, M.A., Morton, O., Rodríguez, R., Cruz, O., Aguayo, A., and Ceniceros, N. (2001). Chromium in a Tannery Wastewater Irrigated Area, León Valley, Mexico. *Bulletin of Environmental Contamination and Toxicology, 66*, 189–195, https://doi.org/10.1007/s0012800224.

Asano, H., and Shiraishi, Y. (2015). Development of paper-based microfluidic analytical device for iron assay using photomask printed with 3D printer for fabrication of hydrophilic and hydrophobic zones on paper by photolithography. *Analytica Chimica Acta*, 883, 55–60, https://doi.org/10.1016/j.aca.2015.04.014.

Asgharipour, M. R., and Sirousmehr, A. R. (2012). Comparison of three techniques for estimating phytotoxicity in municipal solid waste compost. *Annals of Biological Research*, 3 (2), 1094-1101.

Ashraf, A., Bibi, I., Niazi, N.K., Ok, Y.S., Murtaza, G., Shahid, M., Kunhikrishnan, A., Li, D., and Mahmood, T. (2017). Chromium (VI) sorption efficiency of acid-activated banana peel over organo-montmorillonite in aqueous solutions. *International journal of phytoremediation, 19*, 605–613, https://doi.org/10.1080/15226514.2016.125637.

Atencia, J., and Beebe, D. J. (2006). Steady flow generation in microcirculatory systems. *Lab on a Chip*, 6 (4), 567, https://doi.org/10.1039/B514070F.

Auroux, P. A., Iossifidis, D., Reyes, D. R., and Manz, A. (2002). Micro total analysis systems. Analytical standard operations and applications. *Analytical chemistry*, 74 (12), 2637-2652, https://doi.org/10.1021/ac020239t.

Azzaro, F., and Galletta, M. (2006). Automatic colorimetric analyzer prototype for high frequency measurement of nutrients in seawater. *Marine chemistry*, 99 (1-4), 191-198, https://doi.org/10.1016/j.marchem.2005.07.006.

Bagheri, H., Afkhami, A., Saber-Tehrani, M., and Khoshsafar, H. (2012). Preparation and characterization of magnetic nanocomposite of Schiff base/silica/magnetite as a preconcentration phase for the trace determination of heavy metal ions in water, food and biological samples using atomic absorption spectrometry. *Talanta*, 97, 87-95, https://doi.org/10.1016/j.talanta.2012.03.066.

Baker, C. A., Duong, C. T., Grimley, A., and Roper, M. G. (2009). Recent advances in microfluidic detection systems. *Bioanalysis*, 1(5), 967-975, https://doi.org/10.4155/bio.09.86.

Barałkiewicz, D., and Siepak, J. (1999). Chromium, nickel and cobalt in environmental samples and existing legal norms. *Polish Journal of Environmental Studies*, *8*(4), 201-208.

Barceloux, D. G., and Barceloux, D. (1999). Cobalt. *Journal of Toxicology: Clinical Toxicology*, 37(2), 201-216, https://doi.org/10.1081/CLT-100102420.

Barnett, N.W., Francis, P.S. (2005). Chemiluminescence: Liquid-Phase, Encyclopedia of Analytical Science, 2nd ed., Elsevier Academic Press: London.

Beaumont, J.J., Sedman, R.M., Reynolds, S.D., Sherman, C.D., Li, L.H., Howd, R.A., Sandy, M.S., Zeise, L., and Alexeeff, G.V. (2008). Cancer mortality in a Chinese population exposed to hexavalent chromium in drinking water. *Epidemiology*, 19, 12–23, https://doi.org/10.1097/EDE.0b013e31815cea4c.

Becker, H., and Locascio, L. E. (2002). Polymer microfluidic devices. *Talanta*, 56 (2), 267-287, https://doi.org/10.1016/S0039-9140(01)00594-X.

Becquer, T., Quantin, C., Sicot, M., and Boudot, J. (2003). Chromium availability in ultramafic soils from New Caledonia. *Science of the Total Environment*, 301, 251–261, https://doi.org/10.1016/S0048-9697(02)00298-X.

Behari, J. R., and Prakash, R. (2006). Determination of total arsenic content in water by atomic absorption spectroscopy (AAS) using vapour generation assembly (VGA). *Chemosphere*, 63(1), 17-21, https://doi.org/10.1016/j.chemosphere.2005.07.073.

Bell, J., Climent, E., Hecht, M., Buurman, M., and Rurack, K. (2016). Combining a droplet-based microfluidic tubing system with gated indicator releasing nanoparticles for mercury trace detection. *ACS Sensors*, 1 (4), 334-338, https://doi.org/10.1021/acssensors.5b00303.

Berg, M., Tran, H.C., Nguyen, T.C., Pham, H.V., Schertenleib, R., and Giger, W. (2001). Arsenic contamination of groundwater and drinking water in Vietnam: a human health threat. *Environmental science and technology,* 35, 2621-2626, https://doi.org/10.1021/es010027y.

Bhandari, P., Narahari, T., and Dendukuri, D. (2011). 'Fab-Chips': a versatile, fabric-based platform for low-cost, rapid and multiplexed diagnostics. *Lab on a Chip*, 11 (15), 2493-2499, https://doi.org/10.1039/C1LC20373H.

Billot, L., Plecis, A., and Chen, Y. (2008). Multi-reflection based on chip label free molecules detection. *Microelectronic Engineering*, *85* (5-6), 1269-1271, https://doi.org/10.1016/j.mee.2008.01.099.

Bohr, A., Colombo, S., and Jensen, H. (2019). Future of Microfluidics in Research and in the Market. In *Microfluidics for Pharmaceutical Applications*, Santos, H.A, Liu, D., Zhang, H. (ed.), William Andrew Publishing: New York, 425-465.

Boylan, H. M., Cain, R. D., & Kingston, H. S. (2003). A new method to assess mercury emissions: a study of three coal-fired electric-generating power station configurations. *Journal of the Air & Waste Management Association*, *53*(11), 1318-1325.

Bouchard, M. F., Sauve, S., Barbeau, B., Legrand, M., Brodeur, M. E., Bouffard, T., Limoges, E., Bellinger, D. C., and Mergler, D. (2010). Intellectual impairment in school-age children exposed to manganese from drinking water. *Environmental health perspectives*, *119*(1), 138-143, https://doi.org/10.1289/ehp.1002321.

Bromberg, A., and Mathies, R. A. (2003). Homogeneous immunoassay for detection of TNT and its analogues on a microfabricated capillary electrophoresis chip. *Analytical chemistry*, 75 (5), 1188-1195, https://doi.org/10.1021/ac020599g.

Broyles, B. S., Jacobson, S. C., and Ramsey, J. M. (2003). Sample filtration, concentration, and separation integrated on microfluidic devices. *Analytical chemistry*, 75 (11), 2761-2767, https://doi.org/10.1021/ac025503x.

Burke, F., Hamza, S., Naseem, S., Nawaz-ul-Huda, S., Azam, M., and Khan, I. (2016). Impact of cadmium polluted groundwater on human health: winder, Balochistan. *Sage Open*, 6 (1), 2158244016634409.

Busa, L., Mohammadi, S., Maeki, M., Ishida, A., Tani, H., and Tokeshi, M. (2016). Advances in microfluidic paper-based analytical devices for food and water analysis. *Micromachines*, 7(5), 86, https://doi.org/10.3390/mi7050086.

Butera, S., Trapp, S., Astrup, T.F., and Christensen, T.H. (2015). Soil retention of hexavalent chromium released from construction and demolition waste in a road-base-application scenario. *Journal of Hazardous Materials*, 298, 361–367, https://doi.org/10.1080/15226514.2016.1256372.

Cai, L., Fang, Y., Mo, Y., Huang, Y., Xu, C., Zhang, Z., and Wang, M. (2017). Visual quantification of Hg on a microfluidic paper-based analytical device using distance-based detection technique. *AIP Advances*, 7 (8), 085214, https://doi.org/10.1063/1.4999784.

Can, N., Omur, B. C., and Altındal, A. (2016). Adsorption kinetics of Cd2+ ions onto MgPz thin film. *Anadolu Üniversitesi Bilim Ve Teknoloji Dergisi A-Uygulamalı Bilimler ve Mühendislik*, 17(4), 622-632, https://doi.org/10.18038/aubtda.266443.

Capitan-Vallvey, L. F., and Palma, A. J. (2011). Recent developments in handheld and portable optosensing—A review. *Analytica chimica acta*, 696 (1-2), 27-46, https://doi.org/10.1016/j.aca.2011.04.005.

Cavani, A. (2005). Breaking tolerance to nickel. *Toxicology*, 209 (2), 119-121, https://doi.org/10.1016/j.tox.2004.12.021.

Cempel, M., and Nikel, G. (2006). Nickel: A review of its sources and environmental toxicology. *Polish Journal of Environmental Studies*, 15 (3), 375-382.

Cespón-Romero, R.M., Yebra-Biurrun, M.C., and Bermejo-Barrera, M.P. (1996). Preconcentration and speciation of chromium by the determination of total chromium and chromium (III) in natural waters by flame atomic absorption spectrometry with a chelating ion-exchange flow injection system. *Analytica Chimica Acta*, 327, 37–45, https://doi.org/10.1016/0003-2670(96)00062-1.

Chailapakul, O., Korsrisakul, S., Siangproh, W., and Grudpan, K. (2008). Fast and simultaneous detection of heavy metals using a simple and reliable microchip-electrochemistry route: An alternative approach to food analysis. *Talanta*, 74, 683–689, https://doi.org/10.1016/j.talanta.2007.06.034.

Chakraborty, P., Babu, P.R., and Sarma, V.V. (2012). A new spectrofluorometric method for the determination of total arsenic in sediments and its application to kinetic speciation. *International. Journal of Environmental Analytical Chemistry*, 92, 133–147, doi:10.1080/03067319.2010.500058.

Chaney, R. L., Ryan, J. A., Li, Y. M., Brown, S. L., McLaughlin, M. J., and Singh, B. R. (1999). Cadmium in soils and plants. McLaughlin MJ, Singh BR, Kluwer (Ed.), Springer: Netherlands.

Chaturvedi, S., and Dave, P. N. (2012). Removal of iron for safe drinking water. *Desalination, 303*, 1–11, https://doi:10.1016/j.desal.2012.07.003.

Chauhan, S., and Upadhyay, L. S. B. (2018). An efficient protocol to use iron oxide nanoparticles in microfluidic paper device for arsenic detection. *MethodsX*, 5, 1528-1533, https://doi.org/10.1016/j.mex.2018.10.017.

Chen, G., Guo, Z., Zeng, G., and Tang, L. (2015). Fluorescent and colorimetric sensors for environmental mercury detection. *Analyst*, 140 (16), 5400-5443, https://doi.org/10.1039/C5AN00389J.

Chen, L., Xu, S., and Li, J. (2011). Recent advances in molecular imprinting technology: current status, challenges and highlighted applications. *Chemical Society Reviews*, 40 (5), 2922–2942, https://doi.org/10.1039/C0CS00084A.

Chen, T., Chang, Q., Liu, J., Clevers, J.G.P.W., and Kooistra, L.(2016). Identification of soil heavy metal sources and improvement in spatial mapping based on soil spectral information: A case study in northwest China. *Science of the Total Environment*, 565, 155–164, https://doi.org/10.1016/j.scitotenv.2016.04.163.

Chen, X., Liu, C., Xu, Z., Pan, Y., Liu, J., and Du, L. (2012). An effective PDMS microfluidic chip for chemiluminescence detection of cobalt (II) in water. *Microsystem technologies*, 19, 99–103, https://doi.org/10.1080/15226514.2016.1256372.

Chiu, D. T., deMello, A. J., Di Carlo, D., Doyle, P. S., Hansen, C., Maceiczyk, R. M., and Wootton, R. C. (2017). Small but perfectly formed? Successes, challenges, and opportunities for microfluidics in the chemical and biological sciences. *Chem*, *2* (2), 201-223, https://doi.org/10.1016/j.chempr.2017.01.009.

Choprapawon, C. and Rodcline, A. (1997). Chronic arsenic poisoning in Ronpibool Nakhon Sri Thammarat, the southern province of Thailand. In Arsenic (pp. 69-77). Springer, Dordrecht.

Chowdhury, U. K., Biswas, B. K., Chowdhury, T. R., Samanta, G., Mandal, B. K., Basu, G. C., Chanda, C.R., Lodh, D., Saha, K. C., Mukherjee , S. K., Roy, S., Kabir, S., Quamruzzaman , Q., and Chakraborti , D. (2000). Groundwater arsenic contamination in Bangladesh and West Bengal, India. *Environmental health perspectives*, *108*(5), 393-397, https://doi.org/10.1289/ehp.00108393.

Chowdury, M., Walji, N., Mahmud, M., and MacDonald, B. (2017). Paper based microfluidic device with a gold nanosensor to detect arsenic contamination of groundwater in Bangladesh. *Micromachines*, 8 (3), 71, https://doi.org/10.3390/mi8030071.

Clarkson, T. W. (1993). Mercury: major issues in environmental health. *Environmental Health Perspectives*, 100, 31-38, https://doi.org/10.1289/ehp.9310031.

Cleary, J., Maher, D., and Diamond, D. (2013). Development and Deployment of a Microfluidic Platform for Water Quality Monitoring. *Smart Sensors for Real-Time Water Quality Monitoring*, 4, 125–148, https://doi.org/10.1007/978-3-642-37006-9_6.

Clever, G. H., Kaul, C., and Carell, T. (2007). DNA–metal base pairs. *Angewandte Chemie International Edition*, 46 (33), 6226-6236, https://doi.org/10.1002/anie.200701185.

Clarkson, T. W. (1993). Mercury: major issues in environmental health. *Environmental Health Perspectives*, *100*, 31-38.

Clifton, J. C. (2007). Mercury exposure and public health. *Pediatric Clinics of North America*, 54 (2), 237-269, https://doi.org/10.1016/j.pcl.2007.02.005.

Clinton-Bailey, G. S., Grand, M. M., Beaton, A. D., Nightingale, A. M., Owsianka, D. R., Slavik, G. J., Connelly, D.P., Cardwell, C. L., and Mowlem, M. C. (2017). A lab-on-chip analyzer for *in situ* measurement of soluble reactive phosphate: improved phosphate blue assay and application to fluvial monitoring. *Environmental science & technology*, 51(17), 9989-9995, https://doi.org/10.1021/acs.est.7b01581.

Cobbina, S., Duwiejuah, A., Quansah, R., Obiri, S., and Bakobie, N. (2015). Comparative assessment of heavy metals in drinking water sources in two small-scale mining communities in northern Ghana. *International journal of environmental research and public health*, 12 (9), 10620-10634, https://doi.org/10.3390/ijerph120910620.

Cogan, D., Cleary, J., Phelan, T., McNamara, E., Bowkett, M., and Diamond, D. (2013). Integrated flow analysis platform for the direct detection of nitrate in water using a simplified chromotropic acid method. *Analytical Methods,* 5(18*),* 4798. https://doi.org/10.1039/c3ay41098f .

Cogan, D., Cleary, J., Fay, C., Rickard, A., Jankowski, K., Phelan, T., and Diamond, D. (2014). The development of an autonomous sensing platform for the monitoring of ammonia in water using a simplified Berthelot method. *Analytical Methods*, 6(19), 7606-7614.

Cogan, D., Fay, C., Boyle, D., Osborne, C., Kent, N., Cleary, J., and Diamond, D. (2015). Development of a low cost microfluidic sensor for the direct determination of nitrate using chromotropic acid in natural waters. *Analytical Methods*, 7, 5396–5405, https://doi.org/10.1039/C5AY01357G.

Comber, S., and Gardner, M. (2003). Chromium redox speciation in natural waters. *Journal of Environmental Monitoring*, 5, 410–413.

Compton, R. G., Foord, J. S., and Marken, F. (2003). Electroanalysis at diamond-like and doped-diamond electrodes. *Electroanalysis: An International Journal Devoted to Fundamental and Practical Aspects of Electroanalysis*, 15 (17), 1349-1363, https://doi.org/10.1002/elan.200302830.

Convery, N., and Gadegaard, N. (2019). 30 years of microfluidics. *Micro and Nano Engineering*, *2*, 76-91, https://doi.org/10.1016/j.mne.2019.01.003.

Crerar, D. A. ,Cormick, R.K., and Barnes, H.L. (1980). Geology and Geochemistry of Manganese, eds. Varentsov, I. M. and Grasselly, Gy. (E. Schweizerbart'sche Verlagsbuchhandlung, Stuttgart), Vol. 1, pp. 293–334.

Dai, X., and Compton, R.G. (2006). *Analytical Science*, 22, 567–570, https://doi.org/10.2116/analsci.22.567.

Daridon, A., Sequeira, M., Pennarun-Thomas, G., Dirac, H., Krog, J. P., Gravesen, P., Lichtenberg, J., Diamond, D., Verpoorte, E., and de Rooij, N. F. (2001). Chemical sensing using an integrated microfluidic system based on the Berthelot reaction. *Sensors and Actuators B: Chemical*, 76(1-3), 235-243, https://doi.org/10.1016/S0925-4005(01)00573-1.

Das, J., Sarkar, P., Panda, J., and Pal, P. (2014). Low-cost field test kits for arsenic detection in water. *Journal of Environmental Science and Health, Part A*, 49(1), 108-115, https://doi.org/10.1080/10934529.2013.824764.

Dasgupta, P.K., Huang, H., Zhang, G., and Cobb, G.P. (2002). Photometric measurement of trace As (III) and As (V) in drinking water. *Talanta*, 58, 153–164, https://doi.org/10.1016/s0039-9140(02)00264-3.

Department of National Health and Welfare (Canada) (1990). Nutrition recommendations. The report of the Scientific Review Committee: Ottawa, Canada.

De Heer, W. A., Berger, C., Wu, X., First, P. N., Conrad, E. H., Li, X., Li, T., Sprinkle, M., Hass, J., Sadowski, M.L., Martinez, G., and Potemski, M. (2007). Epitaxial graphene. *Solid State Communications*, 143 (1-2), 92-100, https://doi.org/10.1016/j.ssc.2007.04.023.

Delves, H.T. (1980). Dietary sources of copper. Excerpta Medica, Elsevier: USA. N

Denkhaus, E., and Salnikow, K. (2002). Nickel essentiality, toxicity, and carcinogenicity. *Critical reviews in oncology/hematology*, 42 (1), 35-56, https://doi.org/10.1016/S1040-8428(01)00214-1.

Dernbach, L. (2008). Staff report on background chromium study. *Hinkley, CA: Pacific Gas.*

Devadhasan, J. P., and Kim, J. (2018). A chemically functionalized paper-based microfluidic platform for multiplex heavy metal detection. *Sensors and Actuators B: Chemical*, 273, 18-24, https://doi.org/10.1016/j.snb.2018.06.005.

Directive 2008/105/EC. European Parliament and of the Council of 116th December, 2008. On environmental quality standards in the field of water policy, amending and subsequently repealing Council directives 82/176/EEC, 84/513/EEC, 84/491/EEC, 88/280/EEC and amending Directive 2000/60/EC of the European Parliament and of the Council. 38 (24.12.2008), 84-97.

Djedjibegovic, J., Larssen, T., Skrbo, A., Marjanovic, A., and Sober, M. (2012). Contents of cadmium, copper, mercury and lead in fish from the Neretva river (Bosnia and Herzegovina) determined by inductively coupled plasma mass spectrometry (ICP-MS). *Food Chemistry*, 131 (2), 469-476, https://doi.org/10.1039/C5DT04099J.

Doku, G. N., and Haswell, S. J. (1999). Further studies into the development of a micro-FIA (μFIA) system based on electroosmotic flow for the determination of phosphate as orthophosphate. *Analytica chimica acta*, 382(1-2), 1-13, https://doi.org/10.1016/S0003-2670(98)00830-7.

Dong, C., Wu, G., Wang, Z., Ren, W., Zhang, Y., Shen, Z., Li, T., and Wu, A. (2016). Selective colorimetric detection of Cr (III) and Cr (VI) using gallic acid capped gold nanoparticles. *Dalton Transactions***,** 45, 8347–8354, https://doi.org/10.1039/C5DT04099J.

Dong, H., Li, C. M., Zhang, Y. F., Cao, X. D., and Gan, Y. (2007). Screen-printed microfluidic device for electrochemical immuneoassay. *Lab on a Chip*, 7 (12), 1752-1758.

Dong, Z. M., and Zhao, G. C. (2012). Quartz crystal microbalance aptasensor for sensitive detection of mercury (II) based on signal amplification with gold nanoparticles. *Sensors*, 12 (6), 7080–7094.

Donkor, A. K., Bonzongo, J. C. J., Nartey, V. K., and Adotey, D. K. (2005). Heavy metals in sediments of the gold mining impacted Pra River Basin, Ghana, West Africa. *Soil & sediment contamination*, 14 (6), 479-503, https://doi.org/10.1080/15320380500263675.

Dossi, N., Susmel, S., Toniolo, R., Pizzariello, A., and Bontempelli, G. (2009). Application of microchip electrophoresis with electrochemical detection to environmental aldehyde monitoring. *Electrophoresis*, *30* (19), 3465-3471, https://doi.org/10.1002/elps.200900297.

Drescher, K., Shen, Y., Bassler, B. L., and Stone, H. A. (2013). Biofilm streamers cause catastrophic disruption of flow with consequences for environmental and medical systems. Proceedings of the National Academy of Sciences, 110 (11), 4345-4350, https://doi.org/10.1073/pnas.1300321110.

Du, W. B., Fang, Q., He, Q. H., and Fang, Z. L. (2005). High-throughput nanoliter sample introduction microfluidic chip-based flow injection analysis system with gravity-driven flows. *Analytical Chemistry*, 77 (5), 1330-1337, https://doi.org/10.1021/ac048675y.

Dzombak, D.A. and Morel, F.M.M., 1990. Surface Complexation Modelling-Hydrous Ferric Oxide, John Wiley: New York.

Egirani, D. E., Latif, M. T., Poyi, N. R., Wessey, N., and Acharjee, S. (2018). Genesis, uses and environment implications of iron oxides and ores. *Iron Ores and Iron Oxide Materials,* 23, https://doi:10.5772/intechopen.75776.

Einav, S., Gerber, D., Bryson, P. D., Sklan, E. H., Elazar, M., Maerkl, S. J., Glenn, J.S., and Quake, S. R. (2008). Discovery of a hepatitis C target and its pharmacological inhibitors by microfluidic affinity analysis. *Nature biotechnology*, *26* (9), 1019, https://doi.org/10.1038/nbt.1490.

Ekino, S., Susa, M., Ninomiya, T., Imamura, K., and Kitamura, T. (2007). Minamata disease revisited: an update on the acute and chronic manifestations of methyl mercury poisoning. *Journal of the neurological sciences*, 262 (1-2), 131-144, https://doi.org/10.1016/j.jns.2007.06.036.

EPA (2014). Drinking Water Parameters Microbiological, Chemical and Indicator Parameters in the 2014 Drinking Water Regulations 2014.

Esch, M. B., Locascio, L. E., Tarlov, M. J., and Durst, R. A. (2001). Detection of Viable Cryptosporidium Parvum Using DNA-Modified Liposomes in a Microfluidic Chip. *Analytical Chemistry*, 73 (13), 2952-2958.

European Commission. (1998). Council Directive 98/83/EC of 3 November 1998 on the quality of water intended for human consumption. *Official journal of the European communities*, *41*, 32-54.

European Parliament. (2010). Directive 2010/75/EU of the European Parliament and of the Council of 24 November 2010 on industrial emissions (integrated pollution prevention and control). *Official Journal of the European Union L*, 334, pp. 17-119.

Eustis, S., and El-Sayed, M.A. (2006). Why gold nanoparticles are more precious than pretty gold: Noble metal surface plasmon resonance and its enhancement of the radiative and nonradiative properties of nanocrystals of different shapes. *Chemical Society Reviews*, 35, 209–217, https://doi.org/10.1039/B514191E.

Famulok, M., Hartig, J. S., and Mayer, G. (2007). Functional aptamers and aptazymes in biotechnology, diagnostics, and therapy. *Chemical reviews*, 107 (9), 3715-3743, https://doi.org/10.1021/cr0306743.

Fantoni, D., Brozzo, G., Canepa, M., Cipolli, F., Marini, L., Ottonello, G., and Zuccolini, M. (2002). Natural hexavalent chromium in groundwaters interacting with ophiolitic rocks. *Environmental Geology*, 42, 871–882, https://doi.org/10.1007/s00254-002-0605-0.

Faraji, M., Yamini, Y., Saleh, A., Rezaee, M., Ghambarian, M., and Hassani, R. (2010). A nanoparticle-based solid-phase extraction procedure followed by flow injection inductively coupled plasma-optical emission spectrometry to determine some heavy metal ions in water samples. *Analytica chimica acta*, 659 (1-2), 172-177, https://doi.org/10.1016/j.aca.2009.11.053.

Farooqi, A., Masuda, H., and Firdous, N. (2007). Toxic fluoride and arsenic contaminated groundwater in the Lahore and Kasur districts, Punjab, Pakistan and possible contaminant sources. *Environmental Pollution*, 145(3), 839-849, https://doi.org/10.1016/j.envpol.2006.05.007.

Faye, D., Lefevre, J. P., Delaire, J. A., and Leray, I. (2012). A selective lead sensor based on a fluorescent molecular probe grafted on a PDMS microfluidic chip. *Journal of Photochemistry and Photobiology A: Chemistry*, 234, 115-122, https://doi.org/10.1016/j.jphotochem.2012.01.006.

Feng X. (2005). Mercury Pollution in China — An Overview. In: Pirrone N., Mahaffey K.R. (ed.) Dynamics of Mercury Pollution on Regional and Global Scales, Springer: Boston, pp. 657-678.

Fernandez-Luqueno, F., López-Valdez, F., Gamero-Melo, P., Luna-Suárez, S., Aguilera-González, E. N., Martínez, A. I., and Pérez-Velázquez, I. R. (2013). Heavy metal pollution in drinking water-a global risk for human health: A review. *African Journal of Environmental Science and Technology*, 7(7), 567-584.

Fewtrell, L., Kay, D., Jones, F., Baker, A., and Mowat, A. (1996). Copper in drinking water—an investigation into possible health effects. *Public Health*, 110 (3), 175-177, https://doi.org/10.1016/S0033-3506(96)80072-2.

Fiket, Z., Roje, V., Mikac, N., and Kniewald, G. (2007). Determination of arsenic and other trace elements in bottled waters by high resolution inductively coupled plasma mass spectrometry. *Croatica chemica acta*, 80(1), 91-100.

Fischel, M. H. H., Fischel, J. S., Lafferty, B. J., and Sparks, D. L. (2015). The influence of environmental conditions on kinetics of arsenite oxidation by manganese-oxides. *Geochemical Transactions*, 16(1), https://doi.org/10.1186/s12932-015-0030-4.

Fitch, M. W., Graham, D. W., Arnold, R. G., Agarwal, S. K., Phelps, P., Speitel, G. E., and Georgiou, G. (1993). Phenotypic characterization of copper-resistant mutants of Methylosinus trichosporium OB3b. *Applied and Environmental Microbiology*, 59 (9), 2771-2776.

Flexner, S. B. (1987). The Random House Dictionary of the English Language, 2nd ed., Random House: New York.

Floquet, C. F., Sieben, V. J., Milani, A., Joly, E. P., Ogilvie, I. R., Morgan, H., and Mowlem, M. C. (2011). Nanomolar detection with high sensitivity microfluidic absorption cells manufactured in tinted PMMA for chemical analysis. *Talanta*, 84(1), 235-239, https://doi.org/10.1016/j.talanta.2010.12.026.

Friberg, L. T., Elinder, G. G., Kjellstrom, T., & Nordberg, G. F. (Eds.). (2019). *Cadmium and Health: A Toxicological and Epidemiological Appraisal: Volume 2: Effects and Response* (Vol. 1). CRC press.

Frisbie, S. H., Mitchell, E. J., Dustin, H., Maynard, D. M., and Sarkar, B. (2012). World Health Organization discontinues its drinking-water guideline for manganese. *Environmental health perspectives*, 120 (6), 775-778, https://doi.org/10.1289/ehp.1104693.

Fu, E., and Downs, C. (2017). Progress in the development and integration of fluid flow control tools in paper microfluidics. *Lab on a Chip*, 17(4), 614-628, https://doi.org/10.1039/C6LC01451H.

Gammoudi, I., Raimbault, V., Tarbague, H., Moroté, F., Grauby-Heywang, C., Othmane, A., Kalfat, R., Moynet, D., Rebiere. D., Dejous, C., and Cohen-

Bouhacina, T. (2014). Enhanced bio-inspired microsensor based on microfluidic/bacteria/love wave hybrid structure for continuous control of heavy metals toxicity in liquid medium. *Sensors and Actuators B: Chemical*, 198, 278-284, https://doi.org/10.1016/j.snb.2014.01.104.

Gao, J., Yin, X. F., and Fang, Z. L. (2004). Integration of single cell injection, cell lysis, separation and detection of intracellular constituents on a microfluidic chip. *Lab on a Chip*, 4 (1), 47-52, https://doi.org/10.1039/B310552K.

Gao, Y., and Xia, J. (2011). Chromium contamination accident in China: Viewing environment policy of China. *Environmental Science and Technology*, 45, 8605–8606, https://doi.org/10.1080/15226514.2016.1256372.

Gardolinski, P.C., David, A.R., and Worsfold, P.J. (2002). Miniature flow injection analyser for laboratory, shipboard and *in situ* monitoring of nitrate in estuarine and coastal waters. *Talanta*, 58, 1015–1027, https://doi.org/10.1016/j.talanta.2010.12.026.

Ge, L., Yu, J., Ge, S., and Yan, M. (2014). Lab-on-paper-based devices using chemiluminescence and electrogenerated chemiluminescence detection. *Analytical and bioanalytical chemistry*, 406 (23), 5613-5630, https://doi.org/10.1007/s00216-014-7756-1.

Gencoglu, A., and Minerick, A. R. (2014). Electrochemical detection techniques in micro- and nanofluidic devices. *Microfluidics and Nanofluidics*, 17 (5), 781–807, https://doi.org/doi:10.1007/s10404-014-1385-z.

Gerber, D., Maerkl, S. J., and Quake, S. R. (2009). An in vitro microfluidic approach to generating protein-interaction networks. *Nature methods*, *6* (1), 71, https://doi.org/10.1038/nmeth.1289.

Gerson, J. R., Driscoll, C. T., Hsu-Kim, H., and Bernhardt, E. S. (2018). Senegalese artisanal gold mining leads to elevated total mercury and methylmercury concentrations in soils, sediments, and rivers. *Elementa Science of the Anthropocene*, 6 (1).

Ghaedi, M., Ahmadi, F., and Shokrollahi, A. (2007). Simultaneous preconcentration and determination of copper, nickel, cobalt and lead ions content by flame atomic absorption spectrometry. *Journal of Hazardous Materials*, 142, 272-278, https://doi.org/10.1016/j.jhazmat.2006.08.012.

Ghosh, D, Solanki, H., and Purkait, M. K. (2008). Removal of Fe (II) from tap water by electrocoagulation technique. *Journal of Hazardous Mater, 155*, 135-143, https://doi.org/10.1016/j.jhazmat.2007.11.042.

Gomez, M. R., Cerutti, S., Sombra, L. L., Silva, M. F., and Martínez, L. D. (2007). Determination of heavy metals for the quality control in argentinian herbal medicines by ETAAS and ICP-OES. *Food and Chemical Toxicology*, 45(6), 1060-1064, https://doi.org/10.1016/j.fct.2006.12.013.

Gómez-Ariza, J. L., Sánchez-Rodas, D., Giráldez, I., and Morales, E. (2000). A comparison between ICP-MS and AFS detection for arsenic speciation in environmental samples. *Talanta*, 51(2), 257-268, https://doi.org/10.1016/S0039-9140(99)00257-X.

Gomez-Caminero, A., Howe, P., Hughes, M., Kenyon, E., Lewis, D.R., Moore, M., Ng, J.C., Aitio, A., and Becking, G. *Arsenic and Arsenic Compounds*, 2nd ed., World Health Organization: Geneva, Switzerland, 2001, ISBN 92-4-157224-8.

Gómez-de Pedro, S., Lopes, D., Miltsov, S., Izquierdo, D., Alonso-Chamarro, J., and Puyol, M. (2014). Optical microfluidic system based on ionophore modified gold nanoparticles for the continuous monitoring of mercuric ion. *Sensors and Actuators B: Chemical*, 194, 19–26, https://doi.org/10.1016/j.snb.2013.12.076.

Grabchev, I., Staneva, D., Dumas, S., and Chovelon, J. M. (2011). Metal ions and protons sensing properties of new fluorescent 4-N-methylpiperazine-1, 8-naphthalimide terminated poly(propyleneamine) dendrimer. *Journal of Molecular Structure*, 999, 16-21, https://doi.org/10.1016/j.molstruc.2011.03.020.

Gray, D.J. (2003). Naturally occurring Cr^{6+} in shallow groundwaters of the Yilgarn Craton, Western Australia. *Geochemistry: Exploration, Environment, Analysis*, 3, 359–368, http://dx.doi.org/10.1144/1467-7873/03-012.

Greenway, G. M., Haswell, S. J., and Petsul, P. H. (1999). Characterisation of a micro-total analytical system for the determination of nitrite with spectrophotometric detection. *Analytica Chimica Acta*, 387(1), 1-10, https://doi.org/10.1016/S0003-2670(99)00047-1.

Groschen, G.E., Arnold, T.L., Morrow, W.S., and Warner, K.L. (2009). Occurrence and Distribution of Iron, Manganese, and Selected Trace Elements in Ground Water in the Glacial Aquifer System of the Northern United States. U.S. Geological Survey Scientific Investigations Report 2009-5006.

Grosse, R. (2017). Mobilizing chemistry expertise to solve humanitarian problems: Introduction. *Mobilizing Chemistry Expertise To Solve Humanitarian Problems Volume 1*, 1–9, https://doi.org/10.1021/bk-2017-1267.ch001.

Guertin, J., Jacobs, J.A., Avakian, C.P. (2005). *Chromium (VI) Handbook*, 1st ed., CRC Press: Boca Raton, USA.

Gullstrom, D. K., and Mellon, M. G. (1953). Spectrophotometric determination of arsenic and tungsten as mixed heteropoly acids. *Analytical Chemistry*, 25(12), 1809-1813.

Gustafsson, O., Mogensen, K. B., Ohlsson, P. D., Liu, Y., Jacobson, S. C., and Kutter, J. P. (2008). An electrochromatography chip with integrated waveguides for UV absorbance detection. *Journal of Micromechanics and Microengineering*, 18 (5).

Haque, E., Mailloux, B. J., de Wolff, D., Gilioli, S., Kelly, C., Ahmed, E., Small, C., Ahmed, K. M., van Geen, A., and Bostick, B. C. (2018). Quantitative drinking water arsenic concentrations in field environments using mobile phone photometry of field kits. *Science of the Total Environment*, 618, 579-585, https://doi.org/10.1016/j.scitotenv.2016.12.123.

Hata, K., Kichise, Y., Kaneta, T, and Imasaka, T. (2003). Hadamard transform microchip electrophoresis combined with diode laser fluorometry. *Analytical Chemistry*, 75 (7), 1765-1768, https://doi.org/10.1021/ac026330e.

He, P., Liu, D. H., and Zhang, G. Q. (1994). Effects of high-level-manganese sewage irrigation on children's neurobehavior. *Chinese journal of preventive medicine*, 28 (4), 216-218.

https://doi.org/10.1016/j.jtemb.2005.02.010.

Herold, K. E., and Rasooly, A. (Eds.). (2009). Lab on a Chip Technology: Fabrication and microfluidics (Vol. 1). Caister academic press: Norfolk, UK, pp. 12-13.

Hong, C. C., Murugesan, S., Kim, S., Beaucage, G., Choi, J. W., and Ahn, C. H. (2003). A functional on-chip pressure generator using solid chemical propellant for disposable lab-on-a-chip. *Lab on a Chip*, 3(4), 281-286, https://doi.org/10.1039/B306116G.

Hong, Y., Wu, M., Chen, G., Dai, Z., Zhang, Y., Chen, G., and Dong, X. (2016). 3D printed microfluidic device with microporous Mn_2O_3-modified screen printed electrode for real-time determination of heavy metal ions. *ACS applied materials and interfaces*, 8 (48), 32940-32947.

Hohenblum, P., Scharf, S., and Vogel, B. (2001). Investigations of sewage waters and groundwater bodies on selected components of washing and personal care products in Eastern Austria. *Vom wasser*, 97, 33-44.

Hu, S., Lu, J., and Jing, C. (2012). A novel colorimetric method for field arsenic speciation analysis. *Journal of Environmental Science*, 24, 1341–1346, https://doi.org/10.1016/s1001-0742(11)60922-4.

Hu, Y., Cheng, H., and Tao, S. (2016). The challenges and solutions for cadmium-contaminated rice in China: a critical review. *Environment international*, 92, 515-532, https://doi.org/10.1016/j.envint.2016.04.042.

Hutton, E. A., van Elteren, J. T., Ogorevc, B., and Smyth, M. R. (2004). Validation of bismuth film electrode for determination of cobalt and cadmium in soil extracts using ICP–MS. *Talanta*, 63 (4), 849-855, https://doi.org/10.1016/j.talanta.2003.12.038.

Idrees, N., Tabassum, B., Abd_Allah, E. F., Hashem, A., Sarah, R., and Hashim, M. (2018). Groundwater contamination with cadmium concentrations in some West UP Regions, India. *Saudi Journal of Biological Sciences*, 25 (7), 1365-1368, https://doi.org/10.1016/j.sjbs.2018.07.005.

Idros, N., and Chu, D. (2018). Triple-Indicator-Based Multidimensional Colorimetric Sensing Platform for Heavy Metal Ion Detections. *ACS Sensors, 3*, 1756–1764, https://doi.org/10.1021/acssensors.8b00490.

IPCS (1998) Copper. Environmental Health Criteria 200, Geneva, World Health Organization.

IPCS (1999) Manganese and its compounds. Geneva, World Health Organization, International Programme on Chemical Safety (Concise International Chemical Assessment Document 12.

Izbicki, J.A., Ball, J.W., Bullen, T.D., and Sutley, S.J. (2008). Chromium, chromium isotopes and selected trace elements, western Mojave Desert, USA. *Applied Geochemistry, 23*, 1325–1352, https://doi.org/10.1016/j.apgeochem.2007.11.015.

Jarup, L. (2003). Hazards of heavy metal contamination. *British medical bulletin*, 68 (1), 167-182, https://doi.org/10.1093/bmb/ldg032.

Jebrail, M. J., and Wheeler, A. R. (2010). Let's get digital: digitizing chemical biology with microfluidics. *Current opinion in chemical biology*, 14 (5), 574-581, https://doi.org/10.1016/j.cbpa.2010.06.187.

Jin, W., Huang, P., Wu, F., and Ma, L. H. (2015). Ultrasensitive colorimetric assay of cadmium ion based on silver nanoparticles functionalized with 5-sulfosalicylic acid for wide practical applications. *Analyst*, 140 (10), 3507-3513, https://doi.org/10.1039/C5AN00230C.

Jin, W., Wu, G., and Chen, A. (2014). Sensitive and selective electrochemical detection of chromium (vi) based on gold nanoparticle-decorated titanium nanotube arrays. *Analyst*, 139, 235–241, https://doi.org/10.1039/C3AN01614E.

Johnston, H. J., Hutchison, G., Christensen, F. M., Peters, S., Hankin, S., and Stone, V. (2010). A review of the in vivo and in vitro toxicity of silver and gold particulates: particle attributes and biological mechanisms responsible for the observed toxicity. *Critical reviews in toxicology*, 40 (4), 328-346, https://doi.org/10.3109/10408440903453074.

Jokerst, J. C., Emory, J. M., and Henry, C. S. (2012). Advances in microfluidics for environmental analysis. *Analyst*, 137 (1), 24-34, https://doi.org/10.1039/C1AN15368D.

Jothimuthu, P., Wilson, R. A., Herren, J., Haynes, E. N., Heineman, W. R., and Papautsky, I. (2011). Lab-on-a-chip sensor for detection of highly electronegative heavy metals by anodic stripping voltammetry. *Biomedical microdevices*, 13(4), 695-703, https://doi.org/10.1007/s10544-011-9539-1.

Kang, K. A., Wang, J., Jasinski, J. B., and Achilefu, S. (2011). Fluorescence manipulation by gold nanoparticles: from complete quenching to extensive enhancement. *Journal of nanobiotechnology*, 9 (1), 16, https://doi.org/10.1186/1477-3155-9-16.

Kapaj, S., Peterson, H., Liber, K., and Bhattacharya, P. (2006). Human health effects from chronic arsenic poisoning–a review. *Journal of Environmental Science and Health, Part A*, 41(10), 2399-2428, https://doi.org/10.1080/10934520600873571.

Karim, M.M. (2000). Arsenic in groundwater and health problems in Bangladesh.*Water Resources*, 34, 304–310, https://doi.org/ 10.1016/s0043-1354(99)00128-1.

Karve, M., and Rajgor, R. V. (2007). Solid phase extraction of lead on octadecyl bonded silica membrane disk modified with Cyanex302 and determination by flame atomic absorption spectrometry. *Journal of hazardous materials*, 141(3), 607-613, https://doi.org/10.1016/j.jhazmat.2006.07.013.

Katz, S.A., and Salem, H. (1993). The toxicology of chromium with respect to its chemical speciation: a review. *Journal of Applied Toxicology*, 13(3), 217-224, https://doi.org/10.1002/jat.2550130314.

Khairy, M., El-Safty, S. A., and Shenashen, M. A. (2014). Environmental remediation and monitoring of cadmium. *TrAC Trends in Analytical Chemistry*, 62, 56-68, https://doi.org/10.1016/j.trac.2014.06.013.

Khairy, M., Kampouris, D.K., Kadara, R.O., and Banks, C.E. (2010). Gold nanoparticle modified screen printed electrodes for the trace sensing of arsenic (III) in the presence of copper (II). *Electroanalysis*, 22, 2496–2501, https://doi.org/10.1002/elan.201000226.

Khan, P., Idrees, D., Moxley, M. A., Corbett, J. A., Ahmad, F., von Figura, G, Sly, W. S., Waheed, A., and Hassan, M. I. (2014). Luminol-based chemiluminescent signals: clinical and non-clinical application and future uses. *Applied biochemistry and biotechnology*, 173 (2), 333-355, https://doi.org/10.1007/s12010-014-0850-1.

Khanfar, M., Al-Faqheri, W., and Al-Halhouli, A. (2017). Low Cost Lab on Chip for the Colorimetric Detection of Nitrate in Mineral Water Products. *Sensors*, 17, 2345, https://doi.org/10.3390/s17102345.

Kim, E. J., Chung, B. H., and Lee, H. J. (2012). Parts per trillion detection of Ni (II) ions by nanoparticle-enhanced surface plasmon resonance. *Analytical chemistry*, 84 (22), 10091-10096, https://doi.org/10.1021/ac302584d.

Kim, H., Rao, B. A., Jeong, J., Angupillai, S., Choi, J. S., Nam, J. O., Lee, C. S., and Son, Y. A. (2016). A rhodamine scaffold immobilized onto mesoporous silica as a fluorescent probe for the detection of Fe (III) and applications in bio-imaging and microfluidic chips. *Sensors and Actuators B: Chemical*, 224, 404-412, https://doi.org/10.1016/j.snb.2015.10.058.

Kim, J., Seo, S., Kim, Y., and Kim, D.H. (2018). Review of carcinogenicity of hexavalent chrome and proposal of revising approval standards for an occupational cancers in Korea. *Annals of Occupational and Environmental Medicine*, 30, 7, http://dx.doi.org/10.1186/s40557-018-0215-2.

Kimbrough, D.E., Cohen, Y., Winer, A.M., Creelman, L., and Mabuni, C. A (1999). Critical Assessment of Chromium in the Environment. *International journal of phytoremediation,* 29, 1–46, https://doi.org/10.1080/15226514.2016.1256372.

Kinniburgh, D. G., and Kosmus, W. (2002). Arsenic contamination in groundwater: some analytical considerations. *Talanta,* 58(1), 165-180, https://doi.org/10.1016/S0039-9140(02)00265-5.

Kinniburgh, D.G., Smedley, P.L. (2000). *Arsenic Contamination of Groundwater in Bangladesh, Final Report Summary*, Bangladesh Department for Public Health Engineering, British Geological Survey: Keyworth, UK, 2000, Volume 2, pp. 1–12, ISBN 0852723849.

Kitaura, H., Nakao, N., Yoshida, N., and Yamada, T. (2003). Induced sensitization to nickel in guinea pigs immunized with mycobacteria by injection of purified protein derivative with nickel. *The new microbiologica*, 26 (1), 101-108.

Kondakis, X. G., Makris, N., Leotsinidis, M., Prinou, M., and Papapetropoulos, T. (1989). Possible health effects of high manganese concentration in drinking water. *Archives of Environmental Health: An International Journal*, 44 (3), 175-178, https://doi.org/10.1080/00039896.1989.9935883.

Koop, S.H.A., and van Leeuwen, C. J. (2017). The challenges of water, waste and climate change in cities. *Environment, development and sustainability*, 19, 385–418, https://doi.org/10.1007/s10668-016-9760-4.

Korte, N. (1991). *Environmental Geology and Water Sciences,*18, 137–141, https://doi.org/10.1007/BF01704667.

Kou, S., Nam, S. W., Shumi, W., Lee, M. H., Bae, S. W., Du, J., Kim, J. S., Hong, J. I., Peng, X., Yoon, J., and Park, S. S. (2009). Microfluidic detection of multiple heavy metal ions using fluorescent chemosensors. *Bulletin of the Korean Chemical Society*, 30 (5), 1173-1176.

Kovac, J., Peternai, L., and Lengyel, O. (2003). Advanced light emitting diodes structures for optoelectronic applications. *Thin Solid Films*, 433 (1-2), 22-26, https://doi.org/10.1016/S0040-6090(03)00314-6.

Kundu, S., Ghosh, S.K., Mandal, M., Pal, T., and Pal, A. (2002). Spectrophotometric determination of arsenic via arsine generation and in-situ colour bleaching of methylene blue (MB) in micellar medium. *Talanta***,** 58, 935–942, https://doi.org/10.1016/s0039-9140(02)00434-4.

Lace, A., Ryan, D., Bowkett, M., and Cleary, J. (2019). Arsenic monitoring in water by colorimetry using an optimized leucomalachite green method. *Molecules*, 24(2), 339, https://doi.org/10.3390/molecules24020339.

Lai, C. H., Chen, C. Y., Wei, B. L., and Yeh, S. H. (2002). Cadmium adsorption on goethite-coated sand in the presence of humic acid. *Water Research*, 36(20), 4943-4950.

Lafleur, J. P., Senkbeil, S., Jensen, T. G., and Kutter, J. P. (2012). Gold nanoparticle-based optical microfluidic sensors for analysis of environmental pollutants. *Lab on a Chip*, 12 (22), 4651-4656, https://doi.org/10.1039/C2LC40543A.

Lapresta-Fernández, A., Fernandez, A., and Blasco, J. (2012). Nanoecotoxicity effects of engineered silver and gold nanoparticles in aquatic organisms. *TrAC Trends in Analytical Chemistry*, 32, 40-59, https://doi.org/10.1016/j.trac.2011.09.007.

Le, T.S., Da Costa, P., Huguet, P., Sistat, P., Pichot, F., Silva, F., Renaud, L., and Cretin, M. (2012). Upstream microelectrodialysis for heavy metals detection on boron doped diamond. *Journal of Electroanalytical Chemistry*, 670, 50-55, https://doi.org/10.1016/j.jelechem.2012.02.015.

Lee, C. W., Park, H. S., Kim, J. G., Choi, B. K., Joo, S. W., and Gong, M. S. (2005). Polymeric humidity sensor using organic/inorganic hybrid polyelectrolytes. *Sensors and Actuators B: Chemical*, 109 (2), 315-322, https://doi.org/10.1016/j.snb.2004.12.063.

Li, H.F., and Lin, J.M. (2008). Applications of microfluidic systems in environmental analysis. *Analytical and Bioanalytical. Chemistry***,** 393, 555–567, https://doi.org/10.1007/s00216-008-2439-4.

Li, J., Wei, H., Guo, S., and Wang, E. (2008). Selective, peroxidase substrate based "signal-on" colorimetric assay for the detection of chromium (VI). *Analytica Chimica Acta*, 630, 181–185, https://doi.org/10.1016/j.aca.2008.10.004.

Li, Q., Yin, L., Li, Z., Wang, X., Qi, Y. and Ma, J. (2013). Copper doped hollow structured manganese oxide mesocrystals with controlled phase structure and morphology as anode materials for lithium ion battery with improved electrochemical performance. *ACS applied materials & interfaces*, 5 (21), 10975-10984, https://doi.org/10.1021/am403215j.

Li, S., Zhang, C., Wang, S., Liu, Q., Feng, H., Ma, X., and Guo, J. (2018). Electrochemical microfluidics techniques for heavy metal ion detection. *Analyst*, 143 (18), 4230-4246, https://doi.org/10.1039/C8AN01067F.

Li, Y., and Xue, H. (2001). Determination of Cr(III) and Cr(VI) species in natural waters by catalytic cathodic stripping voltammetry. *Analytica Chimica Acta*, 448, 121–134, https://doi.org/10.1016/S0003-2670(01)01314-9.

Li, Y., Liu, N., Liu, H., Wang, Y., Hao, Y., Ma, X., and Wang, C. (2017). A novel label-free fluorescence assay for one-step sensitive detection of Hg 2+ in environmental drinking water samples. *Scientific reports*, 7, 45974.

Liang, W., Lin, H., Chen, J., and Chen, C. (2016). Utilization of nanoparticles in microfluidic systems for optical detection. *Microsystem Technologies*, 22 (10), 2363-2370, https://doi.org/10.1007/s00542-016-2921-4.

Lieberzeit, P. A., and Dickert, F. L. (2007). Sensor technology and its application in environmental analysis. *Analytical and bioanalytical chemistry*, 387(1), 237-247, https://doi.org/10.1007/s00216-006-0926-z.

Lin, S., Wang, W., Hu, C., Yang, G., Ko, C. N., Ren, K., Leung, C. H., and Ma, D. L. (2017). The application of a G-quadruplex based assay with an iridium (iii) complex to arsenic ion detection and its utilization in a microfluidic chip. *Journal of Materials Chemistry B*, 5(3), 479-484, https://doi.org/10.1039/C6TB02656G.

Lin, Y., Gritsenko, D., Feng, S., Teh, Y.C., Lu, X., and Xu, J. (2016). Detection of heavy metal by paper-based microfluidics. *Biosensors and Bioelectronics*, 83, 256–266, https://doi.org/10.1016/j.bios.2016.04.061.

Liu, R., Zhang, P., Li, H., and Zhang, C. (2016). Lab-on-cloth integrated with gravity/capillary flow chemiluminescence (GCF-CL): towards simple, inexpensive, portable, flow system for measuring trivalent chromium in water. *Sensors and Actuators B: Chemical*, 236, 35-43, https://doi.org/10.1016/j.snb.2016.05.088.

Liu, Y., and Wang, X. (2013). Colorimetric speciation of Cr (III) and Cr (VI) with a gold nanoparticle probe. *Analytical Methods*, 5, 1442, https://doi.org/10.1039/C3AY00016H.

Llobera, A., Wilke, R., and Buttgenbach, S. (2004). Poly (dimethylsiloxane) hollow Abbe prism with microlenses for detection based on absorption and refractive index shift. *Lab on a Chip*, 4(1), 24-27, https://doi.org/10.1039/B310836H.

Llopis, X., Pumera, M., Alegret, S., and Merkoçi, A. (2009). Lab-on-a-chip for ultrasensitive detection of carbofuran by enzymatic inhibition with replacement of enzyme using magnetic beads. *Lab on a Chip, 9* (2), 213-218, https://doi.org/10.1039/B816643A.

Lu, H., Qi, S., Mack, J., Li, Z., Lei, J., Kobayashi, N., and Shen, Z. (2011). Facile Hg 2+ detection in water using fluorescent self-assembled monolayers of a rhodamine-based turn-on chemodosimeter formed via a “click” reaction. *Journal of Materials Chemistry*, 21 (29), 10878-10882, https://doi.org/10.1039/C1JM11319D.

Lu, L. T., Chang, I. C., Hsiao, T. Y., Yu, Y. H., and Ma, H. W. (2007). Identification of pollution source of cadmium in soil: application of material flow analysis and a case study in Taiwan. *Environmental science and pollution research international*, 14 (1), 49-59, https://doi.org/10.1065/espr2005.08.278.

Lu, Q., Copper, C. L., and Collins, G. E. (2006). Ultraviolet absorbance detection of colchicine and related alkaloids on a capillary electrophoresis microchip. *Analytica chimica acta*, 572 (2), 205-211, https://doi.org/10.1016/j.aca.2006.05.039.

Luong, J. H., Male, K. B., and Glennon, J. D. (2009). Boron-doped diamond electrode: synthesis, characterization, functionalization and analytical applications. *Analyst*, 134 (10), 1965-1979, https://doi.org/10.1039/B910206J.

Lv, J., and Zhang, Z. (2004). A microchip with air sampling and chemiluminescence detection for analyzing iron in nature water and in whole blood. *Analytical letters*, 37 (7), 1401-1410, https://doi.org/10.1081/AL-120035906.

Mahzuz, H. M. A., Alam, R., Alam, M. N., Basak, R., and Islam, M. S. (2009). Use of arsenic contaminated sludge in making ornamental bricks. *International Journal of Environment Science and Technology*, 6, 291-298.

Majolagbe, A. O., and Bamgbose, O. (2007). Levels of Heavy Metals in Lagos Dockyard Sediments. *Chemical and environmental research*, 16(1/2), 41.

Mandal, B. K., and Suzuki, K. T. (2002). Arsenic round the world: a review. *Talanta*, 58(1), 201-235, https://doi.org/10.1016/S0039-9140(02)00268-0.

Manz, A., Graber, N., and Widmer, H. A. (1990). Miniaturized total chemical analysis systems: a novel concept for chemical sensing. *Sensors and actuators B: Chemical*, 1(1-6), 244-248, https://doi.org/10.1016/0925-4005(90)80209-I.

Manz, A., Harrison, D. J., Verpoorte, E. M., Fettinger, J. C., Paulus, A., Ludi, H., and Widmer, H. M. (1992). Planar chips technology for miniaturization and integration of separation techniques into monitoring systems: capillary electrophoresis on a chip. *Journal of Chromatography A*, 593(1-2), 253-258, https://doi.org/10.1016/0021-9673(92)80293-4.

Marle, L., and Greenway, G. M. (2005). Microfluidic devices for environmental monitoring. *TrAC Trends in Analytical Chemistry*, 24 (9), 795-802, https://doi.org/10.1016/j.trac.2005.08.003.

Martinez, A. W., Phillips, S. T., Carrilho, E., Thomas III, S. W., Sindi, H., and Whitesides, G. M. (2008). Simple telemedicine for developing regions: camera phones and paper-based microfluidic devices for real-time, off-site diagnosis. *Analytical chemistry*, 80 (10), 3699-3707, https://doi.org/10.1021/ac800112r.

Martinez, A. W., Phillips, S. T., Nie, Z., Cheng, C. M., Carrilho, E., Wiley, B. J., and Whitesides, G. M. (2010). Programmable diagnostic devices made from paper and tape. *Lab on a Chip*, 10 (19), 2499-2504, https://doi.org/10.1039/C0LC00021C.

Martinez, A.W., Phillips, S.T., Butte, M.J., and Whitesides, G.M. (2007). Patterned paper as a platform for inexpensive, low-volume, portable bioassays. *Angewandte. Chemie International Edition*, 46, 1318–1320, https://doi.org/10.1002/anie.200603817.

Martone, N., Rahman, G.M.M., Pamuku, M., and Kingston, H.M.S. (2013). Determination of Chromium Species in Dietary Supplements Using Speciated Isotope Dilution Mass Spectrometry with Mass Balance. *Journal of agricultural and food chemistry,* 61, 9966–9976, https://doi.org/10.1021/jf403067c.

Masindi, V. and Muedi, K. L. (2018). Environmental Contamination by Heavy Metals. In *Heavy Metals*, Saleh, H. E. D. M, and Aglan, R. (ed.), IntechOpen: London, 115-128.

Masindi, V. and Muedi, K. L. (2018). Environmental Contamination by Heavy Metals. In *Heavy Metals*, Saleh, H. E. D. M, and Aglan, R. (ed.), IntechOpen: London, 115-128.

Matsunaga, H., Kanno, C., and Suzuki, T. (2005). Naked-eye detection of trace arsenic(V) in aqueous media using molybdenum-loaded chelating resin having β-hydroxypropyl-di(β-hydroxyethyl)amino moiety. *Talanta, 66(5),* 1287–1293, https://doi:10.1016/j.talanta.2005.01.057 .

Matysik, F. M. (2003). Miniaturization of electroanalytical systems. *Analytical and bioanalytical chemistry*, 375 (1), 33-35, https://doi.org/10.1007/s00216-002-1635-x.

Mays, D. E., and Hussam, A. (2009). Voltammetric methods for determination and speciation of inorganic arsenic in the environment—a review. *Analytica chimica acta,* 646 (1-2), 6-16, https://doi.org/10.1016/j.aca.2009.05.006.

Mazumder, D. N. G., Haque, R., Ghosh, N., De, B. K., Santra, A., Chakraborty, D., and Smith, A. H. (1998). Arsenic levels in drinking water and the prevalence of skin lesions in West Bengal, India. *International journal of epidemiology*, 27(5), 871-877, https://doi.org/10.1093/ije/27.5.871.

McCurry, J. (2006). Japan remembers minamata. *The Lancet,* 367 (9505), 99-100, https://doi.org/10.1016/S0140-6736(06)67944-0.

McGraw, C. M., Stitzel, S. E., Cleary, J., Slater, C., and Diamond, D. (2007). Autonomous microfluidic system for phosphate detection. *Talanta*, 71(3), 1180-1185, https://doi.org/10.1016/j.talanta.2006.06.011.

McNeill, L.S., McLean, J.E., Parks, J.L., and Edwards, M.A. (2012). Hexavalent chromium review, part 2: Chemistry, occurrence, and treatment. *Journal-American Water Works Association,* 104, E395–E405, https://doi.org/10.5942/jawwa.2012.104.0092.

Mehta, B. C., and Srivastava, K. K. (2012). Iron in groundwater in India and its geochemistry. *Memoir, Indian society of applied geochemists*, (1), 209-225.

Melamed, D. (2005). Monitoring arsenic in the environment: a review of science and technologies with the potential for field measurements. *Analytica Chimica Acta*, 532(1), 1-13, https://doi.org/10.1016/j.aca.2004.10.047.

Milani, A., Statham, P.J., Mowlem, M.C., and Connelly, D.P. (2015). Development and application of a microfluidic in-situ analyzer for dissolved Fe and Mn in natural waters. *Talanta,* 136, 15–22, https://doi.org/10.1016/j.talanta.2014.12.045.

Miyake, Y., Togashi, H., Tashiro, M., Yamaguchi, H., Oda, S., Kudo, M. Tanaka, Y., Kondo, Y., Sawa, R., Fujimoto, T., Machinami, T., and Ono, A. (2006). MercuryII-mediated formation of thymine-HgII-thymine base pairs in DNA duplexes. *Journal of the American Chemical Society*, 128 (7), 2172-2173, https://doi.org/10.1021/ja056354d.

Miyaki, K., Guo, Y., Shimosaka, T., Nakagama, T., Nakajima, H., and Uchiyama, K. (2005). Fabrication of an integrated PDMS microchip incorporating an LED-induced fluorescence device. *Analytical and bioanalytical chemistry*, 382 (3), 810-816, https://doi.org/10.1007/s00216-004-3015-1.

Mogensen, K. B., Klank, H., and Kutter, J. P. (2004). Recent developments in detection for microfluidic systems. *Electrophoresis*, 25(21-22), 3498-3512, https://doi.org/10.1002/elps.200406108.

Mohod, C. V., and Dhote, J. (2013). Review of heavy metals in drinking water and their effect on human health. *International Journal of Innovative Research in Science, Engineering and Technology*, 2 (7), 2992-2996.

Moore, J.W., and Ramamoorthy, S. (1984). Cadmium. In *Heavy metals in natural waters: Applied monitoring and impact assessment*, Springer: Verlag, Berlin, 28–57.

Moore, T. S., Mullaugh, K. M., Holyoke, R. R., Madison, A. S., Yücel, M., and Luther III, G. W. (2009). Marine chemical technology and sensors for marine waters: potentials and limits. *Annual review of marine science*, 1, 91-115, https://doi.org/10.1146/annurev.marine.010908.163817.

Morakot, N., Tomapatanaget, B., Ngeon-Tae, W., Aeungmaitrepirom, W., and Tuntulani, T. (2005). Synthesis and fluorescence sensing properties of calix [4] arenes containing fluorophores. *Supramolecular Chemistry*, 17 (8), 655-659, https://doi.org/10.1080/10610270500142484.

Morita, K., and Kaneko, E. (2006). Spectrophotometric determination of arsenic in water samples based on micro particle formation of ethyl violet-molybdoarsenate. *Analytical sciences*, 22(8), 1085-1089, https://doi.org/10.2116/analsci.22.1085.

Morozan, A., and Jaouen, F. (2012). Metal organic frameworks for electrochemical applications. *Energy and environmental science*, 5 (11), 9269-9290, https://doi.org/10.1039/C2EE22989G.

Morrow, H. (2010). Cadmium and Cadmium Alloys. Kirk-Othmer Encyclopedia of Chemical Technology.

Motalebizadeh, A., Bagheri, H., Asiaei, S., Fekrat, N., and Afkhami, A. (2018). New portable smartphone-based PDMS microfluidic kit for the simultaneous colorimetric detection of arsenic and mercury. *RSC Advances*, 8 (48), 27091-27100, https://doi.org/10.1039/C8RA04006K .

Nagpal, N. K. (2004). *Technical report, water quality guidelines for cobalt*. Water Protection Section, Water, Air and Climate Change Branch, Ministry of Water, Land and Air Protection.

Nagul, E. A., McKelvie, I. D., Worsfold, P., and Kolev, S. D. (2015). The molybdenum blue reaction for the determination of orthophosphate revisited: opening the black box. *Analytica Chimica Acta*, *890*, 60-82.

Nantaphol, S., Channon, R. B., Kondo, T., Siangproh, W., Chailapakul, O., and Henry, C. S. (2017). Boron doped diamond paste electrodes for microfluidic paper-based analytical devices. *Analytical chemistry*, 89(7), 4100-4107, https://doi.org/10.1021/acs.analchem.6b05042.

Narayana, B., Cherian, T., Mathew, M., and Pasha, C. (2005). *Analytical Letters*, 38, 2207–2216, https://doi.org/10.1080/00032710500260555.

Nath, P., Arun, R.K., and Chanda, N. (2014). A paper based microfluidic device for the detection of arsenic using a gold nanosensor. *RSC Advances,* 4, 59558–59561, https://doi.org/10.1039/c4ra12946f.

Nath, P., Priyadarshni, N., and Chanda, N. (2017). Europium-coordinated gold nanoparticles on paper for the colorimetric detection of arsenic (III, V) in aqueous solution. *ACS Applied Nano Materials*, 1(1), 73-81, https://doi.org/10.1021/acsanm.7b00038.

National Research Council (1979). Iron. University Park Press: Baltimore, MD.

National Research Council (2000). *Copper in Drinking Water*. The National Academies Press Washington, DC: Washington, DC, https://doi.org/10.17226/9782.

Needleman, Herbert. (2004). Lead poisoning. *Annual. Review of Medicine,* 55, 209-222, https://doi.org/10.1146/annurev.med.55.091902.103653.

Nge, P. N., Rogers, C. I., and Woolley, A. T. (2013). Advances in microfluidic materials, functions, integration, and applications. *Chemical reviews, 113* (4), 2550-2583, https://doi.org/10.1021/cr300337x.

Nguyen, H. L., Cao, H. H., Nguyen, D. T., and Nguyen, V. A. (2017). Sodium dodecyl sulfate doped polyaniline for enhancing the electrochemical sensitivity of mercury ions. *Electroanalysis*, 29 (2), 595-601, https://doi.org/10.1002/elan.201600438.

Nguyen, N.L.T., Kim, E.J., Chang, S.K., and Park, T.J. (2016). Sensitive detection of lead ions using sodium thiosulfate and surfactant-capped gold nanoparticles. *BioChip Journal*, 10 (1), 65-73, https://doi.org/10.1007/s13206-016-0109-8.

Nguyen, T., Zoëga Andreasen, S., Wolff, A., and Duong Bang, D. (2018). From Lab on a Chip to Point of Care Devices: The Role of Open Source Microcontrollers. *Micromachines*, 9, 403, https://doi.org/10.3390/mi9080403.

Nie, Z., Nijhuis, C.A., Gong, J., Chen, X., Kumachev, A., Martinez, A.W., Narovlyansky, M., and Whitesides, G.M. (2010). Electrochemical sensing in paper-based microfluidic devices. *Lab Chip*, 10, 477–483, https://doi.org/10.1039/B917150A.

Niessner, R. (2010). Measuring the invisible. *Analytical Chemistry*, 82, 7863–7863, https://doi.org/10.1021/ac1023217.

Nogami, T., Hashimoto, M., and Tsukagoshi, K. (2009). Metal ion analysis using microchip CE with chemiluminescence detection based on 1, 10-phenanthroline–hydrogen peroxide reaction. *Journal of separation science*, 32 (3), 408-412, https://doi.org/10.1002/jssc.200800448.

Nordstrom, D. K. (2002). Public health: Enhanced: Worldwide Occurrences of Arsenic in Ground Water. *Science*, 296 (5576), 2143–2145, https://doi.org/10.1126/science.1072375.

Novak, L., Neuzil, P., Pipper, J., Zhang, Y., and Lee, S. (2007). An integrated fluorescence detection system for lab-on-a-chip applications. *Lab on a Chip*, 7(1), 27-29, https://doi.org/10.1039/B611745G.

Nuriman, Kuswandi, B., and Verboom, W. (2011). Optical fiber chemical sensing of Hg(II) ions in aqueous samples using a microfluidic device containing a selective tripodal chromoionophore-PVC film. *Sensors and Actuators B: Chemical,* 157 (2), 438–443, https://doi.org/10.1016/j.snb.2011.04.084.

Obiajunwa, E. I., Pelemo, D. A., Owolabi, S. A., Fasasi, M. K., and Johnson-Fatokun, F. O. (2002). Characterisation of heavy metal pollutants of soils and sediments around a crude-oil production terminal using EDXRF. *Nuclear Instruments and Methods in Physics Research Section B: Beam Interactions with Materials and Atoms*, 194 (1), 61-64, https://doi.org/10.1016/S0168-583X(02)00499-8.

Olaru, A., Bala, C., Jaffrezic-Renault, N., and Aboul-Enein, H.Y. (2015). Surface plasmon resonance (SPR) biosensors in pharmaceutical analysis. *Critical reviews in analytical chemistry,* 45 (2), 97-105, https://doi.org/10.1080/10408347.2014.881250.

Onchoke, K.K., and Sasu, S.A. (2016). Determination of Hexavalent Chromium (Cr(VI)) Concentrations via Ion Chromatography and UV-Vis Spectrophotometry in Samples Collected from Nacogdoches Wastewater Treatment Plant, East Texas (USA). *Advances in Environmental Chemistry,* 3468635, http://dx.doi.org/10.1155/2016/3468635.

Ono, A. and Togashi, H. (2004). Highly selective oligonucleotide-based sensor for mercury (II) in aqueous solutions. *Angewandte Chemie International Edition,* 43 (33), 4300-4302.

Owlad, M., Aroua, M.K., Daud, W.A.W., and Baroutian, S. (2008). Removal of Hexavalent Chromium-Contaminated Water and Wastewater: A Review. *Water, Air and Soil Pollution*, 200, 59–77, https://doi.org/10.1007/s11270-008-9893-7.

Parks, J.L., McNeill, L., Frey, M., Eaton, A.D., Haghani, A., Ramirez, L., and Edwards, M. (2004). Determination of total chromium in environmental water samples. *Water Research*, 38, 2827–2838, https://doi.org/10.1016/j.watres.2004.04.024.

Patey, M. D., Rijkenberg, M. J., Statham, P. J., Stinchcombe, M. C., Achterberg, E. P., and Mowlem, M. (2008). Determination of nitrate and phosphate in seawater at nanomolar concentrations. *TrAC Trends in Analytical Chemistry*, 27(2), 169-182, https://doi.org/10.1016/j.trac.2007.12.006.

Pazand, K., Khosravi, D., Ghaderi, M. R., and Rezvanianzadeh, M. R. (2018). Identification of the hydrogeochemical processes and assessment of groundwater in a semi-arid region using major ion chemistry: A case study of Ardestan basin in Central Iran. *Groundwater for Sustainable Development*, 6, 245-254, https://doi.org/10.1016/j.gsd.2018.01.008.

Pellerin, C., Booker, S.M. (2000). Reflections on hexavalent chromium: Health hazards of an industrial heavyweight. *Environmental Health Perspectives*, 108, 402–407, https://doi.org/10.1289/ehp.108-a402.

Pena-Pereira, F., Villar-Blanco, L., Lavilla, I., and Bendicho, C. (2018). Test for arsenic speciation in waters based on a paper-based analytical device with scanometric detection. *Analytica chimica acta*, 1011, 1-10, https://doi.org/10.1016/j.aca.2018.01.007.

Peng, G., Chen, Y., Deng, R., He, Q., Liu, D., Lu, Y., and Lin, J.-M. (2018). Highly sensitive and selective determination of Hg(II) based on microfluidic chip with on-line fluorescent derivatization. Spectrochimica Acta Part A: Molecular and Biomolecular Spectroscopy, 204, 1–6. doi:10.1016/j.saa.2018.06.006.

Petersen, N. J., Mogensen, K. B., and Kutter, J. P. (2002). Performance of an in-plane detection cell with integrated waveguides for UV/Vis absorbance measurements on microfluidic separation devices. *Electrophoresis,* 23(20), 3528-3536, https://doi.org/10.1002/1522-2683(200210)23:20<3528::AID-ELPS3528>3.0.CO;2-5.

Petrusevski, B., Sharma, S., Schippers, J. C., and Shordt, K. (2007). Arsenic in drinking water. *Delft: IRC International Water and Sanitation Centre,* 17(1), 36-44.

Pillai, A., Sunita, G., and Gupta, V.K. (2000). A new system for the spectrophotometric determination of arsenic in environmental and biological samples. *Analytica Chimica Acta*, 408, 111–115, https://doi.org/10.1016/s0003-2670(99)00832-6.

Pires, N., Dong, T., Hanke, U., and Hoivik, N. (2014). Recent developments in optical detection technologies in lab-on-a-chip devices for biosensing applications. *Sensors*, 14(8), 15458-15479, https://doi.org/10.3390/s140815458.

Pol, R., Céspedes, F., Gabriel, D., and Baeza, M. (2017). Microfluidic lab-on-a-chip platforms for environmental monitoring. *TrAC Trends in Analytical Chemistry*, 95, 62-68, https://doi.org/10.1016/j.trac.2017.08.001.

Post, J. E. (1999). Manganese oxide minerals: Crystal structures and economic and environmental significance. *Proceedings of the National Academy of Sciences, 96(7), 3447–3454*, https://doi.org/10.1073/pnas.96.7.3447.

Pourreza, N., Golmohammadi, H., and Rastegarzadeh, S. (2016). Highly selective and portable chemosensor for mercury determination in water samples using curcumin nanoparticles in a paper based analytical device. *RSC Advances*, 6 (73), 69060–69066, https://doi.org/10.1039/C6RA08879A.

Powell, K.J., P.L. Brown, R.H. Byrne, T. Gajda, G. Hefter, A.K. Leuz, S. Sjoberg and H. Wanne. (2009). Chemical speciation of environmentally significant metals with inorganic ligands, Part 3. The Pb2+ + OH-, Cl-, CO32-, SO42-, and PO43-– systems. *Pure Applied Chemistry*, 81(12), 2425-2476.

Prakash, M., and Gershenfeld, N. (2007). Microfluidic bubble logic. *Science*, 315(5813), 832-835, https://doi.org/10.1126/science.1136907.

Priyadarshni, N., Nath, P., Nagahanumaiah, and Chanda, N. (2018). DMSA-functionalized gold Nanorod on paper for colorimetric detection and estimation of arsenic (III and V) contamination in groundwater. *ACS Sustainable Chemistry & Engineering*, 6(5), 6264-6272, https://doi.org/10.1021/acssuschemeng.8b00068.

Provin, C., Fukuba, T., Okamura, K., Fujii, T. (2013). An integrated microfluidic system for manganese anomaly detection based on chemiluminescence: Description and practical use to discover hydrothermal plumes near the Okinawa Trough. *IEEE Journal of Oceanic Engineering*, 38, 178–185, https://doi.org/10.1109/JOE.2012.2208849.

Pungjunun, K., Chaiyo, S., Jantrahong, I., Nantaphol, S., Siangproh, W., and Chailapakul, O. (2018). Anodic stripping voltammetric determination of total arsenic using a gold nanoparticle-modified boron-doped diamond electrode on a paper-based device. *Microchimica Acta*, 185 (7), 324, https://doi.org/10.1007/s00604-018-2821-7.

Qiao, X., Zhang, X., Tian, Y., and Meng, Y. (2016). Progresses on the theory and application of quartz crystal microbalance. *Applied Physics Reviews*, 3 (3), 031106, https://doi.org/10.1063/1.4963312.

Quantin, C., Ettler, V., Garnier, J., and Sebek, O. (2008). Sources and extractibility of chromium and nickel in soil profiles developed on Czech serpentinites. *Comptes Rendus Geoscience*, 340, 872–882, https://doi.org/10.1016/j.crte.2008.07.013.

Quinn, M.J., Sherlock, J. C. (1990). The correspondence between U.K. 'action levels' for lead in blood and in water. *Food additives andcontaminants*, 7, 387-424, https://doi.org/10.1080/02652039009373904.

Rahimzadeh, M. R., Rahimzadeh, M. R., Kazemi, S., and Moghadamnia, A. A. (2017). Cadmium toxicity and treatment: An update. *Caspian journal of internal medicine*, 8 (3), 135, https://doi.org/10.22088/cjim.8.3.135.

Rahman, M. M., Mukherjee, D., Sengupta, M. K., Chowdhury, U. K., Lodh, D., Chanda, C. R., Roy, S., Selim, M., Quamruzzaman, Q., Milton, A. H., Shahidullah, S. M., Rahman, M. T., and Chakraboti, D.(2002). Effectiveness and reliability of arsenic field testing kits: are the million dollar screening projects effective or not? *Environmental science & technology*, 36 (24), 5385-5394, https://doi.org/10.1021/es020591o.

Rakhunde, R., Deshpande, L., and Juneja, H. D. (2012). Chemical speciation of chromium in water: a review. *Critical reviews in environmental science and technology*, 42(7), 776-810, https://doi.org/10.1080/10643389.2010.534029.

Ranyuk, E., Douaihy, C. M., Bessmertnykh, A., Denat, F., Averin, A., Beletskaya, I., and Guilard, R. (2009). Diaminoanthraquinone-linked polyazamacrocycles: efficient and simple colorimetric sensor for lead ion in aqueous solution. *Organic letters*, 11(4), 987-990, https://doi.org/10.1021/ol802926m.

Rao, N. S. (2008). Iron content in groundwaters of Visakhapatnam environs, Andhra Pradesh, India. *Environmental monitoring and assessment*, 136 (1-3), 437-447, https://doi.org/10.1007/s10661-007-9698-y.

Ravishankar, T.N., Muralikrishna, S., Suresh kumar, K., Nagaraju, G., and Ramakrishnappa, T. (2015). Electrochemical detection and photochemical detoxification of hexavalent chromium (Cr(vi)) by Ag doped TiO_2 nanoparticles. *Analytical Methods*, 7, 3493–3499, https://doi.org/10.1039/C5AY00096C.

Rehacek, V., Hotovy, I., and Vojs, M. (2007). Bismuth-coated diamond-like carbon microelectrodes for heavy metals determination. *Sensors and Actuators B: Chemical*, 127 (1), 193-197, https://doi.org/10.1016/j.snb.2007.07.031.

Ren, K., Zhou, J., and Wu, H. (2013). Materials for microfluidic chip fabrication. *Accounts of chemical research*, 46(11), 2396-2406, https://doi.org/10.1021/ar300314s.

Ressalan, S., Chauhan, R.S., Goswami, A.K., and Purohit, D.N. (1997). Review of Spectrophotometric Methods for Determination of Chromium. *Reviews in Analytical Chemistry*, 16, 69–171, https://doi.org/10.1515/REVAC.1997.16.2.69.

Revanasiddappa, H. D., Dayananda, B. P., and Kumar, T. N. K. (2007). A sensitive spectrophotometric method for the determination of arsenic in environmental samples. *Environmental Chemistry Letters*, 5(3), 151-155, https://doi.org/10.1007/s10311-007-0097-y.

Revanasiddappa, H.D., and Kumar, T.N.K. (2001). Spectrophotometric determination of trace amounts of chromium with citrazinic acid. *Journal of Analytical Chemistry*, 56, 1084–1088, https://doi.org/10.1023/A:1012928731437.

Reyes, D. R., Iossifidis, D., Auroux, P. A., and Manz, A. (2002). Micro total analysis systems. Introduction, theory, and technology. *Analytical chemistry*, 74 (12), 2623-2636, https://doi.org/10.1021/ac0202435.

Rezende, L. C., and Emery, F. S. (2015). Fluorescence quenching of two meso-substituted tetramethyl BODIPY dyes by Fe (III) cation. *Journal of the Brazilian Chemical Society*, 26 (5), 1048-1053, http://dx.doi.org/10.5935/0103-5053.20150054.

Richard, F.C., and Bourg, A.C.M. (1991). Aqueous geochemistry of chromium: A review. *Water Research*, 25, 807–816, https://doi.org/10.1080/15226514.2016.1256372.

Risher, J. F., and Amler, S. N. (2005). Mercury exposure: evaluation and intervention: the inappropriate use of chelating agents in the diagnosis and treatment of putative mercury poisoning. *Neurotoxicology*, 26 (4), 691-699, https://doi.org/10.1016/j.neuro.2005.05.004.

Rodríguez-Lado, L., Sun, G., Berg, M., Zhang, Q., Xue, H., Zheng, Q., and Johnson, C. A. (2013). Groundwater arsenic contamination throughout China. *Science*, 341(6148), 866-868, https://doi.org/10.1016/j.envpol.2006.05.007.

Rowe, A. A., Bonham, A. J., White, R. J., Zimmer, M. P., Yadgar, R. J., Hobza, T. M., Honea, J. W., Benyaacov, K. W., and Plaxco, K. W. (2011). CheapStat: an open-source,"Do-It-Yourself" potentiostat for analytical and educational applications. *PloS one*, *6*(9), e23783, https://doi.org/10.1371/journal.pone.0023783.

Ruecha, N., Rodthongkum, N., Cate, D. M., Volckens, J., Chailapakul, O., and Henry, C. S. (2015). Sensitive electrochemical sensor using a graphene–polyaniline nanocomposite for simultaneous detection of Zn (II), Cd (II), and Pb (II). *Analytica chimica acta*, 874, 40-48, https://doi.org/10.1016/j.aca.2015.02.064.

Rurack, K., Hoffmann, K., Al-Soufi, W., and Resch-Genger, U. (2002). 2, 2'-bipyridyl-3, 3'-diol incorporated into AlPO4-5 crystals and its spectroscopic properties as related to aqueous liquid media. *The Journal of Physical Chemistry B*, 106 (38), 9744-9752.

Ryan, P. B., Huet, N., and MacIntosh, D. L. (2000). Longitudinal investigation of exposure to arsenic, cadmium, and lead in drinking water. *Environmental health perspectives*, 108 (8), 731-735, https://doi.org/10.1289/ehp.00108731.

Saha, K. C. (2003). Diagnosis of Arsenicosis. *Journal of Environmental Science and Health, Part A*, 38 (1), 255–272, https://doi.org/10.1081/ese-120016893.

Saha, S., Mahato, P., Baidya, M., Ghosh, S. K., and Das, A. (2012). An interrupted PET coupled TBET process for the design of a specific receptor for Hg 2+ and its intracellular detection in MCF7 cells. *Chemical Communications*, 48 (74), 9293-9295, https://doi.org/10.1039/C2CC34490D.

Samiei, E., Tabrizian, M., and Hoorfar, M. (2016). A review of digital microfluidics as portable platforms for lab-on a-chip applications. *Lab on a Chip*, 16(13), 2376-2396, https://doi.org/10.1039/C6LC00387G.

Sanllorente-Méndez, S., Domínguez-Renedo, O., and Arcos-Martínez, M.J. (2010). Immobilization of acetylcholinesterase on screen-printed electrodes. Application to the determination of arsenic (III). *Sensors*, 10, 2119–2128, https://doi.org/10.3390/s100302119.

Santangelo, M. F., Shtepliuk, I., Filippini, D., Ivanov, I. G., Yakimova, R., and Eriksson, J. (2019). Real-time sensing of lead with epitaxial graphene-integrated microfluidic devices. *Sensors and Actuators B: Chemical*, 288, 425-431, https://doi.org/10.1016/j.snb.2019.03.021.

Sari, T.K., Takahashi, F., Jin, J., Zein, R., and Munaf, E. (2018). Electrochemical determination of chromium(VI) in river water with gold nanoparticles–graphene nanocomposites modified electrodes. *Analytical Science*, 34, 155–160, https://doi.org/10.2116/analsci.34.155.

Sarkar, A., and Shekhar, S. (2018). Iron contamination in the waters of Upper Yamuna basin. *Groundwater for Sustainable Development*, 7, 421-429, https://doi.org/10.1016/j.gsd.2017.12.011.

Sarkar, A., and Shekhar, S. (2013). Memoir 1: Applied Geochemistry: Ground water Quality Evaluation and Control. *Episodes*, 36 (4), 305-306, https://doi.org/10.1007/s12594-013-0031-9.

Sartore, L., Barbaglio, M., Borgese, L., and Bontempi, E. (2011). Polymer-grafted QCM chemical sensor and application to heavy metal ions real time detection. *Sensors and Actuators B: Chemical*, 155 (2), 538-544, https://doi.org/10.1016/j.snb.2011.01.003.

Satarpai, T., Shiowatana, J., and Siripinyanond, A. (2016). Paper based analytical device for sampling, on-site preconcentration and detection of ppb lead in water. *Talanta*, 154, 504-510, https://doi.org/10.1016/j.talanta.2016.04.017.

Satoh, H. (2000). Occupational and environmental toxicology of mercury and its compounds. *Industrial health*, 38 (2), 153-164, https://doi.org/10.2486/indhealth.38.153.

Schwarz, M. A., and Hauser, P. C. (2001). Recent developments in detection methods for microfabricated analytical devices. *Lab on a Chip*, 1*(1)*, 1, https://doi.org/10.1039/B103795C.

Seyler, P., Martin, J.M. (1990). Distribution of arsenite and total dissolved arsenic in major French estuaries: dependence on biogeochemical processes and anthropogenic inputs. *Marine Chemistry*,29, 277–294.

Shahid, M., Shamshad, S., Rafiq, M., Khalid, S., Bibi, S.I., Niazi, S.N.K., Dumat, C., and Rashid, M.I. (2017). Chromium speciation, bioavailability, uptake, toxicity and detoxification in soil-plant system: A review. *Chemosphere*, 178, 513–533, https://doi.org/10.1016/j.chemosphere.2017.03.074.

Shankar, B. (2009). Chromium pollution in the groundwaters of an industrial area in Bangalore, India. *Environmental Engineering Science*, 26(2), 305-310, https://doi.org/10.1089/ees.2008.0043.

Sharma, D.C., and Forster, C.F. (1993). Removal of hexavalent chromium using sphagnum moss peat. *Water Research,* 27, 1201–1208, https://doi.org/10.1016/0043-1354(93)90012-7.

Sharma, R. K., Agrawal, M., and Marshall, F. M. (2009). Heavy metals in vegetables collected from production and market sites of a tropical urban area of India. *Food and chemical toxicology*, 47 (3), 583-591, https://doi.org/10.1016/j.fct.2008.12.016.

Sheikh, T. A., Arshad, M. N., Rahman, M. M., Asiri, A. M., and Alamry, K. A. (2016). Development of highly efficient Co 2+ ions sensor based on N, N′-(ethane-1, 2-diyl) bis (2, 5-dimethoxybenzenesulfonamide)(EBDMBS) fabricated glassy carbon electrode. *Journal of Organometallic Chemistry*, 822, 53-61, https://doi.org/10.1016/j.jorganchem.2016.08.010.

Shen, C.Y., Yeh, R., Chung, M.H., and Hwang, R.C. (2016). Analytical Performance and Characterization of a Quartz Crystal Microbalance for the Detection of Cu (II) Ions in Water. *Journal of Electrical and ElectronicEngineering*, 4 (5), 103-108, https://doi.org/10.11648/j.jeee.20160405.13.

Shen, L. L., Zhang, G. R., Li, W., Biesalski, M., and Etzold, B. J. (2017). Modifier-free microfluidic electrochemical sensor for heavy-metal detection. *ACS omega*, 2 (8), 4593-4603, https://doi.org/10.1021/acsomega.7b00611.

Sheng, Z.H., Han, J.H., Zhang, J.P., Zhao, H., Jiang, L. (2011). Method for detection of Hg2+ based on the specific thymine-Hg2+-thymine interaction in the DNA hybridization on the surface of quartz crystal microbalance. *Colloids and Surfaces B: Biointerfaces*, 87(2), 289–292, https://doi.org/10.1016/j.colsurfb.2011.05.031.

Shi, J., Tang, F., Xing, H., Zheng, H., Lianhua, B., and Wei, W. (2012). Electrochemical detection of Pb and Cd in paper-based microfluidic devices. *Journal of the Brazilian Chemical Society*, 23(6), 1124-1130, http://dx.doi.org/10.1590/S0103-50532012000600018.

Shrivastav, A. M., Usha, S. P., and Gupta, B. D. (2017). Highly sensitive and selective erythromycin nanosensor employing fiber optic SPR/ERY imprinted nanostructure: application in milk and honey. *Biosensors and Bioelectronics*, 90, 516–524, https://doi.org/10.1016/j.bios.2016.10.041.

Shrivastav, A.M., and Gupta, B.D. (2018). Ion-imprinted nanoparticles for the concurrent estimation of Pb (II) and Cu (II) ions over a two channel surface plasmon resonance-based fiber optic platform. *Journal of biomedical optics*, 23 (1), 017001, https://doi.org/10.1117/1.JBO.23.1.017001.

Sieben, V. J., Floquet, C. F., Ogilvie, I. R., Mowlem, M. C., and Morgan, H. (2010). Microfluidic colourimetric chemical analysis system: Application to nitrite detection. *Analytical Methods*, 2(5), 484-491, https://doi.org/10.1039/C002672G .

Singh, R.K., Sengupta, B., Bali, R., Shukla, B.P., Gurunadharao, V.V.S., and Srivatstava, R. (2009). Identification and mapping of chromium (VI) plume in groundwater for remediation: A case study at Kanpur, Uttar Pradesh. *Journal of the Geological Society of India*, 74, 49–57, https://doi.org/10.1007/s12594-009-0103-z.

Sloof, R. (1990). Towards Healthier Water Resources Management. *Waterlines*, 9, 2, https://doi.org/10.3362/0262-8104.1990.030.

Smedley, P.L., and Kinniburgh, D.G. (2002). A review of the source, behavior and distribution of arsenic in natural waters. *Applied Geochemistry*, 17, 517–569. https://doi.org/10.1016/S0883-2927(02)00018-5.

Smith, T. D., and Pilbrow, J. R. (1981). Recent developments in the studies of molecular oxygen adducts of cobalt (II) compounds and related systems. *Coordination Chemistry Reviews*, 39 (3), 295-383, https://doi.org/10.1016/S0010-8545(00)82006-8.

Sohrabi, M. R., Matbouie, Z., Asgharinezhad, A. A., and Dehghani, A. (2013). Solid phase extraction of Cd (II) and Pb (II) using a magnetic metal-organic framework, and their determination by FAAS. *Microchimica Acta*, 180 (7-8), 589-597, https://doi.org/10.1007/s00604-013-0952-4.

Som-Aum, W., Li, H., Liu, J., and Lin, J. M. (2008). Determination of arsenate by sorption pre-concentration on polystyrene beads packed in a microfluidic device with chemiluminescence detection. *Analyst*, 133 (9), 1169-1175, https://doi.org/10.1039/B801608A.

Som-Aum, W., Threeprom, J., Li, H., and Lin, J. M. (2007). Determination of chromium (III) and total chromium using dual channels on glass chip with

chemiluminescence detection. *Talanta*, 71 (5), 2062-2068, https://doi.org/10.1016/j.talanta.2006.09.017.

Sreevani, I., Reddy, P.R., and Reddy, V.K. (2013). A rapid and simple spectrophotometric determination of traces of chromium (VI) in waste water samples and in soil samples by using 2-hydroxy, 3-methoxy benzaldehyde thiosemicarbazone (HMBATSC). *Journal of Applied Physics*, 3, 40–45.

Sridhar, S. G. D., Sakthivel, A. M., Sangunathan, U., Balasubramanian, M., Jenefer, S., Rafik, M. M., and Kanagaraj, G. (2017). Heavy metal concentration in groundwater from Besant Nagar to Sathankuppam, South Chennai, Tamil Nadu, India. *Applied Water Science*, 7(8), 4651-4662, https://doi.org/10.1007/s13201-017-0628-z.

Steinmaus, C. M., George, C. M., Kalman, D. A., and Smith, A. H. (2006). Evaluation of two new arsenic field test kits capable of detecting arsenic water concentrations close to 10 μg/L. *Environmental science & technology*, 40(10), 3362-3366, https://doi.org/10.1021/es060015i..

Sun, H., Li, W., Dong, Z. Z., Hu, C., Leung, C. H., Ma, D. L., and Ren, K. (2018). A suspending-droplet mode paper-based microfluidic platform for low-cost, rapid, and convenient detection of lead (II) ions in liquid solution. *Biosensors and Bioelectronics*, 99, 361-367, https://doi.org/10.1016/j.bios.2017.07.073.

Sun, J., Xianyu, Y., and Jiang, X. (2014). Point-of-care biochemical assays using gold nanoparticle-implemented microfluidics. *Chemical Society Reviews*, 43 (17), 6239-6253, https://doi.org/10.1039/C4CS00125G.

Sun, X., Li, B., Qi, A., Tian, C., Han, J., Shi, Y., and Chen, L. (2018). Improved assessment of accuracy and performance using a rotational paper-based device for multiplexed detection of heavy metals. *Talanta*, 178, 426–431, https://doi.org/10.1016/j.talanta.2017.09.059.

Sung, J. H., and Shuler, M. L. (2009). Prevention of air bubble formation in a microfluidic perfusion cell culture system using a microscale bubble trap. *Biomedical microdevices*, 11(4), 731-738, https://doi.org/10.1007/s10544-009-9286-8.

Sungur, S., and Ozkan, A. (2017). Characterization of wastewaters obtained from Hatay tanneries. *Natural and Engineering Sciences*, 2 (2) , 111-118, https://doi.org/10.28978/nesciences.330599.

Sunil, A., and Rao, S.J. (2015). Photometric and fluorimetric determination of chromium(VI) using metal-oxo mediated reaction of 1-(2-hydroxyphenyl)thiourea in micellar medium. *Journal Analytical. Chemistry*, 70, 159–165, https://doi.org/10.1134/S1061934815020185.

Swietlik, R. (1998). Speciation analysis of chromium in waters. *Polish Journal of Environmental Studies, 7*, 257–266.

Tabassum, R., and Gupta. (2016). Simultaneous estimation of vitamin K1 and heparin with low limit of detection using cascaded channels fiber optic surface plasmon resonance. *Biosensors and Bioelectronics*, 86, 48 –55, https://doi.org/10.1016/j.bios.2016.06.030.

Tchounwou, P. B., Yedjou, C. G., Patlolla, A. K., and Sutton, D. J. (2012). Heavy metal toxicity and the environment. *Molecular, Clinical and Environmental Toxicology*, 133–164, https://doi.org/10.1007/978-3-7643-8340-4_6.

Teh, H. B., Li, H., and Yau Li, S. F. (2014). Highly sensitive and selective detection of Pb2+ions using a novel and simple DNAzyme-based quartz crystal microbalance with dissipation biosensor. *The Analyst,* 139 (20), 5170–5175, https://doi.org/10.1039/C4AN00922C.

Toner, P., Bowman, J., Clabby, K., Lucey, J., McGarrigle, M., Concannon, C., Clenaghan, P. Cunningham, J. Delaney, S. O'Boyle, MacGarthaigh, M. (2005). Water quality in Ireland. Environmental Protection Agency, Co. Wexford, Ireland.

Tu, J., Gan, Y., Liang, T., Wan, H., and Wang, P. (2018). A miniaturized electrochemical system for high sensitive determination of chromium(VI) by screen-printed carbon electrode with gold nanoparticles modification. *Sensors and Actuators B: Chemistry,* 272, 582–588, https://doi.org/10.1016/j.snb.2018.06.006.

United Nations International Children's Emergency Fund (UNICEF). *The State of the World's Children 2009: Maternal and Newborn Health*, 9, UNICEF: New York, NY, USA, 2008, ISBN 9280643185, 9789280643183.

Tuzen, M., Saygi, K. O., Karaman, I., and Soylak, M. (2010). Selective speciation and determination of inorganic arsenic in water, food and biological samples. *Food and chemical toxicology*, 48(1), 41-46.

van Hullebusch, E., Zandvoort, M., and Lens, P. (2003). Metal immobilisation by biofilms: Mechanisms and analytical tools. *Reviews in Environmental Science and Biotechnology*, 2, 9-33, https://doi.org/10.1023/B:RESB.0000022995.48330.55.

Ullah, N., Mansha, M., Khan, I., and Qurashi, A. (2018). Nanomaterial-based optical chemical sensors for the detection of heavy metals in water: Recent advances and challenges. *TrAC Trends in Analytical Chemistry, 100,* 155-166, https://doi.org/10.1016/j.trac.2018.01.002.

Vilar, M., Barciela, J., García-Martín, S., Pena, R. M., and Herrero, C. (2007). Comparison of different permanent chemical modifiers for lead determination in Orujo spirits by electrothermal atomic absorption spectrometry. *Talanta*, 71 (4), 1629-1636, https://doi.org/10.1016/j.talanta.2006.07.045.

Vinutha, K., Jahagirdar, A.A., Veena Devi, B., and Nanda, N. (2007). Removal of chromium from industrial wastewater. Proceedings of International Conference on Integrated Water Resource Management, Bangalore, p. 287.

Wackerlig, J., Lieberzeit, P. A. (2015). Molecularly imprinted polymer in nanoparticles in chemical sensing-synthesis, characterization and application. *Sensors and Actuators* B: *Chemical*, 207, 144–157, https://doi.org/10.1016/j.snb.2014.09.094.

Waheed, A., Mansha, M., and Ullah, N. (2018). Nanomaterials-based electrochemical detection of heavy metals in water: current status, challenges and future direction. *TrAC Trends in Analytical Chemistry*, *105*, 37-51, https://doi.org/10.1016/j.trac.2018.04.012.

Walsh, C. L., Babin, B. M., Kasinskas, R. W., Foster, J. A., McGarry, M. J., and Forbes, N. S. (2009). A multipurpose microfluidic device designed to mimic microenvironment gradients and develop targeted cancer therapeutics. *Lab on a chip*, *9* (4), 545-554, https://doi.org/10.1039/B810571E.

Wang, J. (2002). Portable electrochemical systems. *TrAC Trends in Analytical Chemistry*, 21(4), 226-232, https://doi.org/10.1016/S0165-9936(02)00402-8.

Wang, M., Meng, G., Huang, Q., and Qian, Y. (2011). Electrospun 1, 4-DHAQ-doped cellulose nanofiber films for reusable fluorescence detection of trace Cu2+ and further for Cr3+. *Environmental science & technology*, 46(1), 367-373, https://doi.org/10.1021/es202137c.

Wang, S. H., Shen, C. Y., Lin, Y. M., and Du, J. C. (2016). Piezoelectric sensor for sensitive determination of metal ions based on the phosphate-modified dendrimer. *Smart Materials and Structures*, 25 (8), 085018.

Wang, W., Mai, Z., Chen, Y., Wang, J., Li, L., Su, Q., Li, X., and Hong, X. (2017). A label-free fiber optic SPR biosensor for specific detection of C-reactive protein. *Scientific reports*, 7 (1), 16904, https://doi.org/10.1038/s41598-017-17276-3.

Wang, X., Wei, Y., Wang, S., and Chen, L. (2015). Red-to-blue colorimetric detection of chromium via Cr (III)-citrate chelating based on Tween 20-stabilized gold nanoparticles. *Colloids and Surfaces A: Physicochemical and Engineering Aspects*, 472, 57–62, https://doi.org/10.1016/j.colsurfa.2015.02.033.

Wasserman, G.A., Liu, X., Parvez, F., Ahsan, H., Levy, D., Factor-Litvak, P., Kline, J., van Geen, A., Slavkovich, V., Lolacono, N. J., Levy, D., Cheng, Z., and Graziano, H. J. (2006). Water manganese exposure and children's intellectual function in Araihazar, Bangladesh. *Environmental Health Perspectives*, 114, 124–129, https://doi.org/10.1289/ehp.8030.

Wei, X., Tian, T., Jia, S., Zhu, Z., Ma, Y., Sun, J., Lin, Z., and Yang, C. J. (2015). Target-responsive DNA hydrogel mediated “stop-flow” microfluidic paper-based analytic device for rapid, portable and visual detection of multiple targets. *Analytical chemistry*, 87 (8), 4275-4282, https://doi.org/10.1021/acs.analchem.5b00532.

Welch, A.H., and Lico, M.S. (1998). Factors controlling As and U in shallow ground water, southern Carson Desert, Nevada. *Applied Geochemistry*, *13*, 521–539, https://doi.org/10.1016/S0883-2927(97)00083-8.

Whitesides, G. M. (2006). The origins and the future of microfluidics. *Nature*, 442 (7101), 368, https://doi.org/10.1038/nature05058.

WHO (2003). Chromium in drinking-water. Background document for development of WHO Guidelines for Drinking-water Quality, Geneva, Switzerland, WHO/SDE/WSH/03.04/04.

WHO (2003). Iron in drinking water. Background document for development of WHO Guidelines for Drinking-water Quality, World Health Organization, Geneva, Switzerland, WHO/SDE/WSH/03.04/08.

WHO (2003). Mercury in drinking water. Background document for development of WHO Guidelines for Drinking-water Quality, Geneva, Switzerland, WHO/SDE/WSH/03.04/10.

WHO (2003). Nickel in drinking water. Background document for development of WHO Guidelines for Drinking-water Quality, World Health Organization, Geneva, Switzerland, WHO/SDE/WSH/05.08/55.

WHO (2004). Cadmium in drinking-water. Background document for development of WHO Guidelines for Drinking-water Quality. Geneva, Switzerland, WHO/SDE/WSH/03.04/80.

WHO (2004). Copper in drinking-water. Background document for development of WHO Guidelines for Drinking-water Quality. Geneva, Switzerland, WHO/SDE/WSH/03.04/88.

WHO (2008). Guidelines for drinking-water quality, 3rd edition incorporating 1st and 2nd addenda. Vol. 1. Recommendations. Geneva, World Health Organization, 392–394.

WHO (1996). Chromium in Drinking-Water. Background Document for Development of WHO Guidelines for Drinking-Water Quality, World Health Organization: Geneva, Switzerland.

Williams, L., Schoof, R. A., Yager, J. W., and Goodrich-Mahoney, J. W. (2006). Arsenic bioaccumulation in freshwater fishes. Human and Ecological Risk Assessment, 12 (5), 904-923, https://doi.org/10.1080/10807030600826821.

Wongkaew, N., He, P., Kurth, V., Surareungchai, W., and Baeumner, A. J. (2013). Multi-channel PMMA microfluidic biosensor with integrated IDUAs for electrochemical detection. *Analytical and bioanalytical chemistry*, 405(18), 5965-5974, https://doi.org/10.1007/s00216-013-7020-0.

Wu, J., Cao, W., Wen, W., Chang, D. C., and Sheng, P. (2009). Polydimethylsiloxane microfluidic chip with integrated microheater and thermal sensor. *Biomicrofluidics*, 3 (1), 12005. https://doi.org/10.1063/1.3058587.

Wu, H., Liang, J., and Han, H. (2008). A novel method for the determination of Pb 2+ based on the quenching of the fluorescence of CdTe quantum dots. *Microchimica Acta*, 161(1-2), 81-86, https://doi.org/10.1007/s00604-007-0801-4.

Wu, T., Zhao, L., Faye, D., Lefevre, J. P., Delaire, J., and Leray, I. (2012). Determination of lead in water by combining precolumn adsorption and fluorimetric detection in a microfluidic device. *Analytical Methods*, 4 (4), 989-994,
https://doi.org/10.1039/C2AY05677A.

Wu, Y., Zhan, S., Xu, L., Shi, W., Xi, T., Zhan, X., and Zhou, P. (2011). A simple and label-free sensor for mercury (II) detection in aqueous solution by malachite green based on a resonance scattering spectral assay. *Chemical Communications*, 47(21), 6027-6029, https://doi.org/10.1039/C1CC10563A.

Wurster, S., Kratz, E., Lachenmeier, D.W., and Mildau, G. (2012). Spectrophotometric quantification of toxicologically relevant concentrations of chromium (VI) in cosmetic pigments and eyeshadow using synthetic lachrymal fluid extraction. *International Journal of Spectroscopy*, 985131, http://dx.doi.org/10.1155/2012/985131.

Xiang, Y., Tong, A., Jin, P., and Ju, Y. (2006). New fluorescent rhodamine hydrazone chemosensor for Cu (II) with high selectivity and sensitivity. *Organic Letters*, 8 (13), 2863-2866, https://doi.org/10.1021/ol0610340.

Xie, W. Y., Huang, W. T., Zhang, J. R., Luo, H. Q., and Li, N. B. (2012). A triple-channel optical signal probe for Hg II detection based on acridine orange and aptamer-wrapped gold nanoparticles. *Journal of Materials Chemistry*, 22(23), 11479-11482, https://doi.org/10.1039/C2JM31280H.

Xing, W., and Liu, G. (2011). Iron biogeochemistry and its environmental impacts in freshwater lakes. *Fresenius Environmental Bulletin*, *20*(6), 1339-1345.

Xing, S., Xu, H., Chen, J., Shi, G., and Jin, L. (2011). Nafion stabilized silver nanoparticles modified electrode and its application to Cr (VI) detection. *Journal of Electroanalytical Chemistry*, 652, 60–65, https://doi.org/10.1016/j.jelechem.2010.03.035.

Xu, L., Xu, Y., Zhu, W., Sun, X., Xu, Z., and Qian, X. (2012). Modulating the selectivity by switching sensing media: a bifunctional chemosensor selectivity for Cd 2+ and Pb 2+ in different aqueous solutions. *RSC Advances*, 2 (15), 6323-6328, https://doi.org/10.1039/C2RA20840G.

Xue, X., Wang, F. and Liu, X. (2008). One-step, room temperature, colorimetric detection of mercury (Hg2+) using DNA/nanoparticle conjugates. *Journal of the American Chemical Society*, 130 (11), 3244-3245, https://doi.org/10.1021/ja076716c.

Yang, G., Yan, W., Wang, J., and Yang, H. (2014). Fabrication and formation mechanism of Mn 2 O 3 hollow nanofibers by single-spinneret electrospinning. *CrystEngComm*, 16 (30), 6907-6913, https://doi.org/10.1039/C4CE00521J.

Yang, H., and Gijs, M. A. (2018). Micro-optics for microfluidic analytical applications. *Chemical Society Reviews*, *47* (4), 1391-1458, https://doi.org/10.1039/c5cs00649j.

Yeh, P., Yeh, N., Lee, C. H., and Ding, T. J. (2017). Applications of LEDs in optical sensors and chemical sensing device for detection of biochemicals, heavy metals, and environmental nutrients. *Renewable and Sustainable Energy Reviews*, 75, 461-468, https://doi.org/10.1016/j.rser.2016.11.011.

Yogarajah, N., and Tsai, S.S. (2015). Detection of trace arsenic in drinking water: Challenges and opportunities for microfluidics. *Environmental Science: Water Research and Technology 1*, 426–447, https://doi.org/10.1039/C5EW00099H.

Yu, H., Wang, J., Fang, W., Yuan, J., and Yang, Z. (2006). Cadmium accumulation in different rice cultivars and screening for pollution-safe cultivars of rice. *Science of the total environment*, 370 (2-3), 302-309, https://doi.org/10.1016/j.scitotenv.2006.06.013.

Yu, Y., Lin, L.-R., Yang, K.-B., Zhong, X., Huang, R.-B., and Zheng, L.S. (2006). p-Dimethylaminobenzaldehyde thiosemicarbazone: A simple novel selective and sensitive fluorescent sensor for Mercury(II) in aqueous solution. *Talanta*, 69, 103–106, https://doi.org/10.1016/j.talanta.2005.09.015.

Zeng, W., Jacobi, I., Beck, D. J., Li, S., and Stone, H. A. (2015). Characterization of syringe-pump-driven induced pressure fluctuations in elastic microchannels. *Lab on a Chip*, 15 (4), 1110–1115, https://doi.org/10.1039/C4LC01347F.

Zhang, G., Liu, D., and He, P. (1995). Effects of manganese on learning abilities in school children. *Chinese journal of preventive medicine*, 29 (3), 156-158.

Zhang, H., Faye, D., Lefèvre, J. P., Delaire, J. A., and Leray, I. (2013). Selective fluorimetric detection of cadmium in a microfluidic device. *Microchemical Journal*, 106, 167-173, https://doi.org/10.1016/j.microc.2012.06.005.

Zhang, L., Li, Y., Zhang, L., Li, D. W., Karpuzov, D., and Long, Y. T. (2011). Electrocatalytic oxidation of NADH on graphene oxide and reduced graphene oxide modified screen-printed electrode. *International Journal of Electrochemical Science*, 6(3), 819-829.

Zhang, Q., Zhang, X., Zhang, X., Jiang, L., Yin, J., Zhang, P., Han, S., Wang, Y., and Zheng, G. (2019). A feedback-controlling digital microfluidic fluorimetric sensor device for simple and rapid detection of mercury (II) in costal seawater. *Marine Pollution Bulletin*, 144, 20-27, https://doi.org/10.1016/j.marpolbul.2019.04.063.

Zhao, L., Wu, T., Lefevre, J. P., Leray, I., and Delaire, J. A. (2009). Fluorimetric lead detection in a microfluidic device. *Lab on a Chip*, 9 (19), 2818-2823, https://doi.org/10.1039/B904641K.

Zhao, X. M., Yao, L. A., Ma, Q. L., Zhou, G. J., Wang, L., Fang, Q. L., and Xu, Z. C. (2018). Distribution and ecological risk assessment of cadmium in water and sediment in Longjiang River, China: Implication on water quality management after pollution accident. *Chemosphere*, 194, 107-116, https://doi.org/10.1016/j.chemosphere.2017.11.127.

Zhu, Y. G., Williams, P. N., and Meharg, A. A. (2008). Exposure to inorganic arsenic from rice: a global health issue? *Environmental pollution*, 154 (2), 169-171, https://doi.org/ 10.1016/j.envpol.2008.03.015.

Zietz, B. P., Dieter, H. H., Lakomek, M., Schneider, H., Kesler-Gaedtke, B., and Dunkelberg, H. (2003). Epidemiological investigation on chronic copper toxicity to children exposed via the public drinking water supply. *Science of the Total Environment*, 302 (1-3), 127-144, https://doi.org/10.1016/S0048-9697(02)00399-6.

Zou, Z., Jang, A., MacKnight, E., Wu, P. M., Do, J., Bishop, P. L., and Ahn, C. H. (2008). Environmentally friendly disposable sensors with microfabricated on-chip planar bismuth electrode for *in situ* heavy metal ions measurement. *Sensors and Actuators B: Chemical*, 134 (1), 18-24, https://doi.org/10.1016/j.snb.2008.04.005.

Zukauskas A, Shur MS, Gaska R. (2002). Introduction to solid-state lighting. Hoboken, John Wiley & Sons:New Jersey,USA.

Chapter 9

Appendices

Appendix A

Table 2. Absorbance values for arsenic samples (0.01-01 mg L^{-1}) analysed using variamine blue method.

Conc (mg L^{-1})	Abs	Abs	Abs	Abs	Abs	Average	SD	% RSD
0.01	-0.003	-0.056	-0.023	-0.003	-0.021	-0.021	0.022	-101.933
0.02	-0.04	-0.023	-0.051	-0.058	-0.043	-0.021	0.022	-101.933
0.04	0.002	-0.06	-0.01	0.12	0.013	-0.043	0.013	-30.721
0.06	0.012	0.004	0.025	0.019	0.008	0.013	0.066	507.751
0.1	0.038	0.04	0.036	0.023	0.034	0.034	0.007	19.408

Table 3. Absorbance values for arsenic samples (0.1-1 mg L^{-1}) analysed using variamine blue method.

Conc (mg L^{-1})	Abs	Abs	Abs	Abs	Abs	Average	SD	% RSD
0.1	0.038	0.04	0.036	0.023	0.03425	0.034	0.007	19.408
0.2	0.041	0.03	0.034	0.045	0.037	0.037	0.006	15.659
0.4	0.057	0.057	0.058	0.055	0.049	0.055	0.004	6.582
0.6	0.072	0.065	0.064	0.071	0.077	0.070	0.005	7.675
1	0.096	0.103	0.077	0.092	0.085	0.091	0.010	11.054

Table 4. Absorbance values for arsenic samples (1-10 mg L^{-1}) analysed using variamine blue method.

Conc (mg L^{-1})	Abs	Abs	Abs	Abs	Abs	Average	SD	% RSD
1	0.096	0.103	0.077	0.092	0.085	0.091	0.010	11.054
2	0.159	0.141	0.149	0.162	0.137	0.150	0.011	7.286
4	0.229	0.241	0.233	0.224	0.217	0.229	0.009	3.963
6	0.289	0.298	0.297	0.278	0.284	0.289	0.009	2.948
10	0.335	0.324	0.327	0.333	0.337	0.331	0.005	1.659

Table 5. Absorbance values for arsenic samples (10-100 mg L^{-1}) analysed using variamine blue method**.**

Conc (mg L^{-1})	Abs	Abs	Abs	Abs	Abs	Average	SD	% RSD
10	0.335	0.324	0.327	0.333	0.337	0.331	0.005	1.659
20	0.441	0.313	0.334	0.445	0.437	0.394	0.065	16.458
40	0.447	0.491	0.408	0.465	0.395	0.441	0.040	9.007
60	0.546	0.54	0.593	0.584	0.574	0.567	0.023	4.117
100	0.602	0.633	0.695	0.591	0.658	0.636	0.042	6.652

Table 6. Absorbance values for arsenic samples (0.01-10 mg L^{-1}) analysed using molybdenum blue method.

Conc (mg L^{-1})	Abs	Abs	Abs	Abs	Abs	Abs	Average	SD	% RSD
0.01	-0.02	0.001	0.012	0.004	0.02	-0.04	-0.004	0.022	-580.144
0.02	0.012	0.005	0.002	0.003	0.01	0.015	0.008	0.005	67.269
0.04	0.001	0.012	0.01	0.008	0.007	0.013	0.009	0.004	50.875
0.06	0.013	0.028	0.03	0.024	0.026	0.019	0.023	0.006	27.060
0.1	0.047	0.035	0.039	0.041	0.044	0.037	0.041	0.004	11.015

Table 7. Absorbance values for arsenic samples (0.1-1 mg L^{-1}) analysed using molybdenum blue method.

Conc (mg L^{-1})	Abs	Abs	Abs	Abs	Average	SD	% RSD
0.1	0.047	0.035	0.039	0.041	0.041	0.005	12.346
0.2	0.055	0.048	0.056	0.061	0.055	0.005	9.735
0.4	0.073	0.068	0.062	0.063	0.067	0.005	7.618
0.6	0.066	0.086	0.072	0.094	0.080	0.013	16.092
1	0.077	0.097	0.119	0.064	0.089	0.024	26.928

Table 8. Absorbance values for arsenic samples (0.1-1 mg L^{-1}) analysed using molybdenum blue method.

Conc (mg L^{-1})	Abs	Abs	Abs	Average	SD	% RSD
0.1	0.044	0.037	0.034	0.038	0.005	13.387
0.2	0.066	0.052	0.047	0.055	0.010	17.907
0.4	0.069	0.062	0.079	0.070	0.009	12.206
0.6	0.082	0.088	0.084	0.085	0.003	3.608
1	0.096	0.107	0.079	0.094	0.014	15.007

Table 9. Absorbance values for arsenic samples (1-10 mg L^{-1}) analysed using molybdenum blue method.

Conc (mg L^{-1})	Abs	Abs	Abs	Abs	Average	SD	% RSD
1	0.077	0.097	0.119	0.064	0.089	0.024	26.928
2	0.119	0.124	0.136	0.149	0.132	0.013	10.145
4	0.181	0.178	0.152	0.159	0.168	0.014	8.478
6	0.216	0.186	0.172	0.204	0.195	0.019	9.983
10	0.236	0.214	0.281	0.284	0.254	0.034	13.562

Table 10. Absorbance values for arsenic samples (1-10 mg L^{-1}) analysed using molybdenum blue method.

Conc (mg L^{-1})	Abs	Abs	Abs	Average	SD	% RSD
1	0.096	0.107	0.079	0.094	0.014	15.007
2	0.166	0.135	0.108	0.136	0.029	21.288
4	0.169	0.142	0.179	0.163	0.019	11.718
6	0.232	0.222	0.178	0.211	0.029	13.637
10	0.273	0.241	0.266	0.260	0.017	6.470

Table 11. Absorbance values for arsenic samples (10-80 mg L^{-1}) analysed using molybdenum blue method.

Conc (mg L^{-1})	Abs	Abs	Abs	Average	SD	% RSD
10	0.236	0.214	0.281	0.244	0.034	14.016
20	0.328	0.354	0.33	0.337	0.014	4.289
40	0.591	0.649	0.715	0.652	0.062	9.521
60	0.665	0.608	0.654	0.642	0.030	4.708
80	0.571	0.733	0.77	0.691	0.106	15.310

Table 12. Absorbance values for arsenic samples (10-80 mg L^{-1}) analysed using molybdenum blue method.

Conc (mg L^{-1})	Abs	Abs	Abs	Average	SD	% RSD
10	0.284	0.273	0.241	0.266	0.022	8.398
20	0.286	0.276	0.387	0.316	0.061	19.411
40	0.692	0.608	0.721	0.674	0.059	8.712
60	1.447	0.906	0.802	1.052	0.346	32.928
80	0.543	0.803	0.632	0.659	0.132	20.041

Table 13. Absorbance measurements of 1 mg L^{-1} arsenic sample over time analysed with variamine blue method.

Time (min)	Abs	Abs	Abs	Average	SD
0	0.079	0.085	0.081	0.082	0.003
1	0.08	0.084	0.082	0.082	0.002
2	0.082	0.086	0.082	0.083	0.002
3	0.084	0.086	0.082	0.084	0.002
4	0.083	0.085	0.082	0.083	0.002
5	0.084	0.086	0.083	0.084	0.002
6	0.085	0.086	0.084	0.085	0.001
7	0.085	0.087	0.084	0.085	0.002
8	0.086	0.086	0.083	0.085	0.002
9	0.087	0.086	0.084	0.086	0.002
10	0.085	0.086	0.084	0.085	0.001
11	0.084	0.085	0.084	0.084	0.001
12	0.083	0.085	0.083	0.084	0.001
13	0.083	0.084	0.084	0.084	0.001
14	0.083	0.084	0.083	0.083	0.001
15	0.084	0.084	0.083	0.084	0.001
16	0.084	0.083	0.083	0.083	0.001
17	0.084	0.083	0.083	0.083	0.001
18	0.083	0.082	0.083	0.083	0.001
19	0.083	0.082	0.083	0.083	0.001
20	0.083	0.082	0.083	0.083	0.001
21	0.083	0.082	0.083	0.083	0.001

22	0.084	0.082	0.084	0.083	0.001
23	0.083	0.081	0.084	0.083	0.002
24	0.083	0.082	0.083	0.083	0.001
25	0.083	0.082	0.083	0.083	0.001
26	0.084	0.083	0.083	0.083	0.001
27	0.085	0.083	0.084	0.084	0.001
28	0.085	0.084	0.084	0.084	0.001
29	0.086	0.084	0.084	0.085	0.001
30	0.087	0.084	0.085	0.085	0.002
31	0.087	0.084	0.085	0.085	0.002
32	0.086	0.083	0.085	0.085	0.002
33	0.085	0.083	0.085	0.084	0.001
34	0.085	0.083	0.085	0.084	0.001
35	0.084	0.083	0.085	0.084	0.001
36	0.083	0.082	0.085	0.083	0.002
37	0.082	0.082	0.084	0.083	0.001
38	0.082	0.081	0.083	0.082	0.001
39	0.082	0.081	0.082	0.082	0.001
40	0.082	0.081	0.081	0.081	0.001
41	0.081	0.08	0.081	0.081	0.001
42	0.081	0.08	0.08	0.080	0.001
43	0.08	0.079	0.079	0.079	0.001
44	0.08	0.079	0.079	0.079	0.001
45	0.08	0.079	0.078	0.079	0.001
46	0.079	0.079	0.077	0.078	0.001
47	0.079	0.078	0.077	0.078	0.001
48	0.079	0.078	0.077	0.078	0.001
49	0.079	0.078	0.076	0.078	0.002
50	0.078	0.078	0.076	0.077	0.001
51	0.078	0.077	0.075	0.077	0.002
52	0.078	0.077	0.075	0.077	0.002
53	0.077	0.077	0.075	0.076	0.001
54	0.077	0.076	0.074	0.076	0.002
55	0.077	0.076	0.074	0.076	0.002
56	0.076	0.075	0.074	0.075	0.001
57	0.075	0.074	0.073	0.074	0.001
58	0.075	0.074	0.072	0.074	0.002
59	0.074	0.073	0.071	0.073	0.002
60	0.073	0.072	0.07	0.072	0.002

Table 14. Absorbance measurements of 1 mg L^{-1} arsenic sample over time analysed with molybdenum blue method.

Time (min)	Abs	Abs	Abs	Average	SD
0	0.01	0.025	0.021	0.019	0.008
5	0.081	0.094	0.072	0.082	0.011
10	0.102	0.109	0.095	0.102	0.007
15	0.115	0.124	0.115	0.118	0.005
20	0.123	0.127	0.125	0.125	0.002
25	0.127	0.13	0.128	0.128	0.002
30	0.134	0.132	0.135	0.134	0.002
35	0.136	0.135	0.138	0.136	0.002
40	0.139	0.137	0.141	0.139	0.002
45	0.141	0.139	0.142	0.141	0.002
50	0.143	0.141	0.143	0.142	0.001
55	0.144	0.143	0.144	0.144	0.001
60	0.145	0.144	0.144	0.144	0.001
65	0.145	0.145	0.145	0.145	0.000
70	0.147	0.145	0.146	0.146	0.001
75	0.149	0.146	0.148	0.148	0.002
80	0.151	0.148	0.149	0.149	0.002
85	0.152	0.15	0.151	0.151	0.001
90	0.154	0.152	0.152	0.153	0.001
95	0.155	0.153	0.154	0.154	0.001
100	0.157	0.155	0.156	0.156	0.001
105	0.158	0.156	0.158	0.157	0.001
110	0.158	0.156	0.159	0.158	0.002
115	0.158	0.157	0.159	0.158	0.001
120	0.158	0.157	0.159	0.158	0.001
125	0.158	0.157	0.159	0.158	0.001
130	0.158	0.157	0.159	0.158	0.001
135	0.158	0.158	0.16	0.159	0.001
140	0.159	0.158	0.16	0.159	0.001
145	0.159	0.158	0.16	0.159	0.001
150	0.159	0.159	0.16	0.159	0.001
155	0.16	0.159	0.16	0.160	0.001
160	0.16	0.159	0.161	0.160	0.001
165	0.16	0.159	0.161	0.160	0.001
170	0.161	0.16	0.163	0.161	0.002
175	0.161	0.16	0.164	0.162	0.002
180	0.162	0.16	0.164	0.162	0.002

Table 15. Absorbance values of arsenic samples (1–10 mg L^{-1}) analysed using 0.2 M HCl.

Conc (mg L^{-1})	Abs	Abs	Abs	Abs	Abs	Abs	Average	SD
1	0.059	0.089	0.092	0.051	0.041	0.058	0.065	0.021
2	0.143	0.133	0.179	0.155	0.108	0.106	0.137	0.028
4	0.188	0.219	0.234	0.204	0.212	0.305	0.227	0.041
6	0.391	0.337	0.307	0.408	0.465	0.395	0.384	0.056
10	0.776	0.754	0.693	0.784	0.774	0.851	0.772	0.051

Table 16. Absorbance values of arsenic samples (1–10 mg L^{-1}) analysed using 0.4 M HCl.

Conc (mg L^{-1})	Abs	Abs	Abs	Abs	Abs	Abs	Average	SD
1	0.059	0.029	0.032	0.051	0.034	0.034	0.040	0.012
2	0.083	0.068	0.088	0.079	0.061	0.065	0.074	0.011
4	0.188	0.219	0.234	0.204	0.212	0.305	0.227	0.041
6	0.391	0.337	0.307	0.408	0.465	0.395	0.384	0.056
10	0.776	0.754	0.693	0.784	0.774	0.851	0.772	0.051

Table 17. Absorbance values of arsenic samples (1–10 mg L^{-1}) analysed using 0.6 M HCl.

Conc (mg L^{-1})	Abs	Abs	Abs	Abs	Abs	Abs	Abs	Average	SD
1	0.084	0.12	0.126	0.14	0.096	0.073	0.121	0.109	0.025
2	0.228	0.202	0.206	0.143	0.155	0.213	0.212	0.194	0.032
4	0.242	0.235	0.237	0.233	0.311	0.264	0.277	0.257	0.029
6	0.31	0.304	0.334	0.29	0.32	0.357	0.333	0.321	0.022
10	0.385	0.39	0.395	0.421	0.338	0.372	0.428	0.390	0.030

Table 18. Absorbance values of arsenic samples (1–10 mg L^{-1}) analysed using 1 M HCl.

Conc (mg L^{-1})	Abs	Abs	Abs	Abs	Average	SD	% RSD
1	0.186	0.158	0.172	0.197	0.178	0.017	9.503
2	0.324	0.271	0.259	0.338	0.298	0.039	13.034
4	0.338	0.38	0.338	0.437	0.373	0.047	12.561
6	0.467	0.44	0.434	0.447	0.447	0.014	3.211
10	0.565	0.541	0.536	0.668	0.578	0.062	10.675

Table 19. Absorbance values of arsenic samples (1–10 mg L^{-1}) analysed using 1 M HCl.

Conc (mg L^{-1})	Abs	Abs	Abs	Abs	Abs	Average	SD	% RSD
1	0.201	0.233	0.152	0.172	0.198	0.191	0.031	16.109
2	0.264	0.322	0.302	0.242	0.265	0.279	0.032	11.570
4	0.417	0.401	0.426	0.401	0.408	0.411	0.011	2.638
6	0.457	0.487	0.482	0.432	0.47	0.466	0.022	4.741
10	0.603	0.51	0.514	0.54	0.515	0.536	0.039	7.283

Table 20. Absorbance values for arsenic samples (1–10 mg L^{-1}) analysed with variamine blue method and measured in 1 mm quartz cuvettes.

Conc (mg L^{-1})	Abs	Abs	Abs	Average	SD	% RSD
1	0.005	0.009	0.006	0.007	0.002	31.225
3	0.011	0.008	0.013	0.011	0.003	23.593
5	0.019	0.016	0.017	0.017	0.002	8.813
7	0.025	0.028	0.033	0.029	0.004	14.098
10	0.033	0.04	0.035	0.036	0.004	10.015

Table 21. Absorbance values for arsenic samples (1–10 mg L^{-1}) analysed with variamine blue method and measured in 1 mm quartz cuvettes.

Conc (mg L^{-1})	Abs	Abs	Abs	Abs	Abs	Average	SD	% RSD
1	0.008	0.008	0.006	0.005	0.004	0.006	0.002	28.852
3	0.009	0.008	0.01	0.011	0.014	0.010	0.002	22.136
5	0.015	0.011	0.017	0.016	0.016	0.015	0.002	15.635
7	0.038	0.039	0.027	0.021	0.024	0.030	0.008	27.611
10	0.042	0.049	0.029	0.029	0.03	0.036	0.009	25.707

Table 22. Absorbance values for arsenic samples (1–10 mg L^{-1}) analysed with molybdenum blue method and measured in 1 mm quartz cuvettes.

Conc (mg L^{-1})	Abs	Abs	Abs	Average	SD	%RSD
1	0.011	0.016	0.014	0.014	0.003	18.414
2	0.015	0.012	0.021	0.016	0.005	28.641
4	0.023	0.018	0.016	0.019	0.004	18.977
6	0.017	0.024	0.022	0.021	0.004	17.169
10	0.025	0.033	0.032	0.030	0.004	14.530

Table 23. Absorbance values for arsenic samples (1–10 mg L^{-1}) analysed with molybdenum blue method and measured in 1 mm quartz cuvettes.

Conc (mg L^{-1})	Abs	Abs	Abs	Average	SD	%RSD
1	0.008	0.013	0.005	0.009	0.004	46.632
2	0.013	0.017	0.02	0.017	0.004	21.071
4	0.023	0.018	0.026	0.022	0.004	18.096
6	0.025	0.028	0.021	0.025	0.004	14.237
10	0.033	0.029	0.032	0.031	0.002	6.644

Table 19. Absorbance values for arsenic samples (1–6 mg L^{-1}) analysed with 0.04 % potassium iodate concentration.

Conc (mg L^{-1})	Abs	Abs	Abs	Average	SD	% RSD
1	0.094	0.102	0.097	0.0977	0.0040	4.094
4	0.154	0.147	0.142	0.1477	0.0060	4.062
6	0.196	0.191	0.188	0.1917	0.0040	2.087

Table 20. Absorbance values for arsenic samples (1–6 mg L^{-1}) analysed with 0.05 % potassium iodate concentration.

Conc (mg L^{-1})	Abs	Abs	Abs	Average	SD	%RSD
1	0.112	0.108	0.103	0.108	0.005	4.629
4	0.167	0.159	0.162	0.163	0.004	2.454
6	0.227	0.235	0.232	0.231	0.004	1.732

Table 21. Absorbance values for arsenic samples (1–6 mg L^{-1}) analysed with 0.05 % potassium iodate concentration.

Conc mg L^{-1})	Abs	Abs	Abs	Average	SD	% RSD
1	0.153	0.162	0.157	0.157	0.005	3.185
4	0.215	0.205	0.2	0.207	0.008	3.865
6	0.238	0.227	0.233	0.233	0.006	2.575

Table 22. Absorbance values for arsenic samples (1–6 mg L^{-1}) analysed with 0.15 % potassium iodate concentration.

Conc (mg L^{-1})	Abs	Abs	Abs	Average	SD	% RSD
1	0.219	0.226	0.215	0.220	0.006	2.727
4	0.413	0.421	0.418	0.417	0.004	3.837
6	0.52	0.518	0.514	0.517	0.003	0.580

Table 23. Absorbance values for arsenic samples (1–6 mg L^{-1}) analysed with 0.1 % potassium iodate concentration.

Conc (mg L^{-1})	Abs	Abs	Abs	Average	SD	% RSD
1	0.151	0.144	0.142	0.146	0.005	3.425
4	0.215	0.207	0.213	0.212	0.004	1.888
6	0.235	0.234	0.239	0.236	0.003	1.271

Table 24. Absorbance values for arsenic samples (1–6 mg L^{-1}) analysed with 0.04 % potassium iodate concentration.

Conc (mg L^{-1})	Abs	Abs	Abs	Average	SD	% RSD
1	0.092	0.101	0.085	0.093	0.008	8.656
4	0.143	0.154	0.159	0.152	0.008	5.385
6	0.191	0.184	0.199	0.191	0.008	3.923

Table 25. Absorbance values for arsenic samples (1–6 mg L^{-1}) analysed with 0.05 % potassium iodate concentration.

Conc (mg L^{-1})	Abs	Abs	Abs	Average	SD	% RSD
1	0.091	0.097	0.108	0.099	0.009	8.738
4	0.139	0.168	0.154	0.154	0.015	9.438
6	0.224	0.238	0.243	0.235	0.010	4.191

Table 26. Absorbance values for arsenic samples (1–6 mg L^{-1}) analysed with 0.1 % potassium iodate concentration.

Conc (mg L^{-1})	Abs	Abs	Abs	Average	SD	% RSD
1	0.165	0.172	0.155	0.164	0.009	2.559
4	0.237	0.222	0.211	0.223	0.013	2.737
6	0.248	0.259	0.235	0.247	0.012	2.967

Table 27. Absorbance values for arsenic samples (1–6 mg L^{-1}) analysed with 0.15 % potassium iodate concentration.

Conc (mg L^{-1})	Abs	Abs	Abs	Average	SD	% RSD
1	0.236	0.22	0.243	0.233	0.012	2.559
4	0.435	0.448	0.455	0.446	0.010	2.737
6	0.524	0.517	0.532	0.524	0.008	2.967

Table 28. Absorbance values for arsenic samples (1–6 mg L^{-1}) analysed with 0.2 % potassium iodate concentration.

Conc (mg L^{-1})	Abs	Abs	Abs	Average	SD	% RSD
1	0.153	0.164	0.172	0.163	0.010	2.559
4	0.224	0.235	0.248	0.236	0.012	2.737
6	0.251	0.262	0.267	0.260	0.008	2.967

Table 29. Absorbance values of arsenic samples (1–10 mg L^{-1}) analysed at pH 3 using variamine blue method.

Conc (mg L^{-1})	Abs	Abs	Abs	Abs	Abs	Abs	Abs	Abs	Average	SD
1	0.137	0.222	0.095	0.161	0.105	0.152	0.112	0.102	0.136	0.046
2	0.32	0.308	0.154	0.38	0.099	0.303	0.146	0.031	0.218	0.128
4	0.319	0.313	0.285	0.495	0.214	0.259	0.265	0.288	0.305	0.090
6	0.38	0.439	0.35	0.585	0.254	0.286	0.254	0.317	0.358	0.120
10	0.453	0.56	0.482	0.687	0.689	0.489	0.46	0.476	0.537	0.100

Table 30. Absorbance values of arsenic samples (1–10 mg L^{-1}) analysed at pH 3.5 using variamine blue method.

Conc(mg L^{-1})	Abs	Abs	Abs	Average	SD
1	0.157	0.144	0.127	0.143	0.015
2	0.253	0.242	0.232	0.242	0.011
4	0.283	0.271	0.288	0.281	0.009
6	0.277	0.286	0.259	0.282	0.014
10	0.362	0.374	0.355	0.364	0.01

Table 31. Absorbance values of arsenic samples (1–10 mg L^{-1}) analysed at pH 4 using variamine blue method.

Conc (mg L^{-1})	Abs	Abs	Abs	Abs	Abs	Abs	Abs	Average	SD
1	0.126	0.017	0.079	0.075	0.056	0.048	0.252	0.093	0.078
2	0.198	0.072	0.184	0.169	0.111	0.144	0.161	0.148	0.044
4	0.274	0.109	0.182	0.157	0.139	0.162	0.206	0.176	0.053
6	0.302	0.131	0.209	0.197	0.311	0.341	0.342	0.262	0.082
10	0.354	0.361	0.234	0.314	0.326	0.349	0.396	0.333	0.051

Table 32. Absorbance values of arsenic samples (1–10 mg L^{-1}) analysed at pH 4.5 using variamine blue method.

Conc (mg L^{-1})	Abs	Abs	Abs	Abs	Abs	Average	SD	% RSD
1	0.204	0.151	0.007	0.297	0.108	0.153	0.108	70.423
2	0.191	0.175	0.189	0.0187	0.269	0.169	0.092	54.306
4	0.161	0.1	0.148	0.09	0.704	0.241	0.261	108.402
6	0.217	0.154	0.265	0.279	0.249	0.233	0.050	21.362
10	0.241	0.155	0.276	0.344	0.43	0.289	0.104	35.991

Table 33. Absorbance values of arsenic samples (1–10 mg L^{-1}) analysed at pH 4.5 using variamine blue method.

Conc (mg L^{-1})	Abs	Abs	Abs	Abs	Average	SD	% RSD
1	0.072	0.252	0.237	0.16	0.180	0.083	45.857
2	0.27	0.144	0.221	0.198	0.208	0.052	25.118
4	0.57	0.073	0.055	0.109	0.202	0.247	122.193
6	0.265	0.146	0.342	0.481	0.309	0.140	45.526
10	0.361	0.344	0.396	0.133	0.309	0.119	38.569

Table 34. Absorbance values of arsenic samples (1–10 mg L^{-1}) analysed at pH 5 using variamine blue method.

Conc (mg L^{-1})	Abs	Abs	Abs	Abs	Abs	Average	SD	% RSD
1	0.051	0.085	0.086	0.101	0.112	0.087	0.023	26.474
2	0.164	0.156	0.146	0.216	0.133	0.163	0.032	19.517
4	0.175	0.218	0.191	0.195	0.211	0.198	0.017	8.586
6	0.231	0.255	0.262	0.273	0.262	0.257	0.016	6.116
10	0.308	0.287	0.395	0.324	0.336	0.330	0.041	12.337

Table 35. Absorbance values of arsenic samples (1–10 mg L^{-1}) analysed at pH 5 using variamine blue method.

Conc (mg L^{-1})	Abs	Abs	Abs	Abs	Abs	Average	SD	% RSD
1	0.076	0.078	0.091	0.076	0.109	0.086	0.014	16.628
2	0.131	0.133	0.152	0.118	0.153	0.137	0.015	10.876
4	0.172	0.168	0.185	0.193	0.171	0.178	0.011	6.024
6	0.228	0.265	0.235	0.206	0.216	0.230	0.023	9.785
10	0.375	0.329	0.376	0.276	0.321	0.335	0.042	12.467

Table 36. Absorbance values of arsenic samples (1–10 mg L^{-1}) analysed at pH 5.5 using variamine blue method.

Conc (mg L^{-1})	Abs	Abs	Abs	Abs	Abs	Average	SD	% RSD
1	0.076	0.133	0.131	0.019	0.08	0.088	0.047	53.551
2	0.153	0.166	0.101	0.109	0.186	0.143	0.037	25.689
4	0.132	0.152	0.203	0.155	0.078	0.144	0.045	31.377
6	0.296	0.301	0.225	0.235	0.245	0.260	0.036	13.647
10	0.363	0.308	0.372	0.229	0.333	0.321	0.057	17.856

Table 37. Absorbance values of arsenic samples (1–10 mg L^{-1}) analysed at pH 5.5 using variamine blue method.

Conc	Abs	Abs	Abs	Abs	Abs	Average	SD	% RSD
1	0.08	0.08	0.07	0.117	0.075	0.084	0.019	22.144
2	0.186	0.08	0.171	0.17	0.117	0.145	0.045	30.867
4	0.078	0.234	0.246	0.228	0.229	0.203	0.070	34.602
6	0.245	0.255	0.201	0.279	0.302	0.256	0.038	14.840
10	0.333	0.315	0.416	0.403	0.35	0.363	0.044	12.137

Table 38. Absorbance values of arsenic samples (1–10 mg L^{-1}) analysed at pH 2.5 using molybdenum blue method.

Conc (mg L^{-1})	Abs	Abs	Abs	Average	SD	% RSD
1	0.015	0.006	0.014	0.012	0.005	41.666
3	0.025	0.028	0.028	0.027	0.002	7.407
5	0.045	0.056	0.073	0.058	0.014	24.138
7	0.113	0.081	0.103	0.099	0.016	16.162
10	0.168	0.147	0.147	0.154	0.012	7.782

Table 39. Absorbance values of arsenic samples (1–10 mg L^{-1}) analysed at pH 3 using molybdenum blue method.

Conc (mg L^{-1})	Abs	Abs	Abs	Average	SD	% RSD
1	0.024	0.02	0.032	0.025	0.006	24.000
3	0.034	0.029	0.04	0.034	0.006	17.647
5	0.044	0.062	0.041	0.049	0.011	22.449
7	0.077	0.069	0.071	0.072	0.004	5.555
10	0.117	0.126	0.122	0.122	0.005	4.098

Table 40. Absorbance values of arsenic samples (1–10 mg L^{-1}) analysed at pH 3.5 using molybdenum blue method.

Conc (mg L^{-1})	Abs	Abs	Abs	Average	SD	% RSD
1	0.02	0.022	0.019	0.020	0.002	10.000
3	0.058	0.062	0.061	0.060	0.002	3.333
5	0.145	0.132	0.148	0.142	0.009	6.338
7	0.205	0.201	0.195	0.200	0.005	2.500
10	0.387	0.413	0.392	0.397	0.014	3.526

Table 41. Absorbance values of arsenic samples (1–10 mg L^{-1}) analysed at pH 4 using molybdenum blue method.

Conc (mg L^{-1})	Abs	Abs	Abs	Average	SD	% RSD
1	0.039	0.031	0.037	0.036	0.004	11.111
3	0.111	0.12	0.118	0.116	0.005	4.545
5	0.199	0.203	0.212	0.205	0.007	3.415
7	0.243	0.247	0.238	0.243	0.005	2.058
10	0.326	0.318	0.314	0.319	0.006	1.881

Table 42. Absorbance values of arsenic samples (1–10 mg L^{-1}) analysed at pH 4.5 using molybdenum blue method.

Conc (mg L^{-1})	Abs	Abs	Abs	Average	SD	% RSD
1	0.109	0.115	0.119	0.114	0.005	4.386
3	0.258	0.239	0.251	0.249	0.010	4.016
5	0.353	0.362	0.358	0.358	0.005	1.397
7	0.415	0.423	0.404	0.414	0.010	2.415
10	0.524	0.527	0.511	0.521	0.009	1.727

Table 43. Absorbance values of arsenic samples (1–10 mg L^{-1}) analysed at pH 5 using molybdenum blue method.

Conc (mg L^{-1})	Abs	Abs	Abs	SD	Average	% RSD
1	0.008	0.005	0.001	0.004	0.005	80.00
3	0.143	0.148	0.154	0.006	0.148	4.054
5	0.306	0.31	0.295	0.008	0.304	2.632
7	0.394	0.385	0.431	0.024	0.403	5.955
10	0.538	0.542	0.534	0.004	0.538	1.741

Table 44. Absorbance values of arsenic samples (1–10 mg L^{-1}) analysed at pH 5.5 using molybdenum blue method.

Conc (mg L^{-1})	Abs	Abs	Abs	Average	SD	% RSD
1	0.029	0.035	0.043	0.036	0.007	19.444
3	0.13	0.125	0.136	0.130	0.006	4.615
5	0.287	0.292	0.309	0.296	0.012	4.054
7	0.352	0.39	0.39	0.377	0.022	5.835
10	0.423	0.434	0.462	0.440	0.020	4.545

Table 45. Absorbance values of arsenic samples (1–10 mg L^{-1}) analysed at pH 2.5 using molybdenum blue method.

Conc (mg L^{-1})	Abs	Abs	Abs	Average	SD	% RSD
1	0.003	0.006	0.014	0.008	0.006	74.168
3	0.026	0.036	0.022	0.028	0.007	25.754
5	0.041	0.059	0.078	0.059	0.019	31.184
7	0.119	0.092	0.103	0.105	0.014	12.972
10	0.176	0.138	0.164	0.159	0.019	12.191

Table 46. Absorbance values of arsenic samples (1–10 mg L^{-1}) analysed at pH 3 using molybdenum blue method.

Conc (mg L^{-1})	Abs	Abs	Abs	Average	SD	% RSD
1	0.017	0.014	0.022	0.018	0.004	22.876
3	0.028	0.046	0.035	0.036	0.009	24.974
5	0.052	0.06	0.068	0.060	0.008	13.333
7	0.086	0.072	0.095	0.084	0.012	13.743
10	0.114	0.125	0.111	0.117	0.007	6.318

Table 47. Absorbance values of arsenic samples (1–10 mg L^{-1}) analysed at pH 3.5 using molybdenum blue method.

Conc (mg L^{-1})	Abs	Abs	Abs	Average	SD	% RSD
1	0.025	0.034	0.031	0.030	0.005	15.275
3	0.05	0.068	0.073	0.064	0.012	19.000
5	0.155	0.0138	0.142	0.104	0.078	75.328
7	0.215	0.218	0.226	0.220	0.006	2.589
10	0.391	0.14	0.417	0.316	0.153	48.409

Table 48. Absorbance values of arsenic samples (1–10 mg L^{-1}) analysed at pH 4 using molybdenum blue method.

Conc (mg L^{-1})	Abs	Abs	Abs	Average	SD	% RSD
1	0.027	0.038	0.034	0.0330	0.0056	16.8720
3	0.122	0.134	0.119	0.1250	0.0079	6.3498
5	0.205	0.214	0.22	0.2130	0.0075	3.5445
7	0.256	0.244	0.261	0.2537	0.0087	3.4442
10	0.332	0.342	0.333	0.3357	0.0055	1.6408

Table 49. Absorbance values of arsenic samples (1–10 mg L^{-1}) analysed at pH 4.5 using molybdenum blue method.

Conc (mg L^{-1})	Abs	Abs	Abs	Average	SD	% RSD
1	0.111	0.126	0.117	0.118	0.008	6.398
3	0.264	0.273	0.28	0.272	0.008	2.945
5	0.362	0.35	0.341	0.351	0.011	3.002
7	0.419	0.43	0.435	0.428	0.008	1.912
10	0.53	0.542	0.557	0.543	0.014	2.491

Table 50. Absorbance values of arsenic samples (1–10 mg L^{-1}) analysed at pH 5 using molybdenum blue method.

Conc (mg L^{-1})	Abs	Abs	Abs	Average	SD	% RSD
1	0.005	0.002	0.01	0.006	0.004	71.320
3	0.15	0.138	0.165	0.151	0.014	8.959
5	0.32	0.328	0.334	0.327	0.007	2.146
7	0.402	0.414	0.295	0.370	0.066	17.691
10	0.547	0.536	0.552	0.545	0.008	1.502

Table 51. Absorbance values of arsenic samples (1–10 mg L^{-1}) analysed at pH 5.5 using molybdenum blue method.

Conc (mg L^{-1})	Abs	Abs	Abs	Average	SD	% RSD
1	0.038	0.043	0.047	0.043	0.005	10.569
3	0.141	0.153	0.133	0.130	0.010	7.743
5	0.296	0.305	0.301	0.296	0.005	1.523
7	0.368	0.377	0.382	0.377	0.007	1.882
10	0.446	0.432	0.451	0.440	0.010	2.238

Table 52. Absorbance values of arsenic samples (1–10 mg L^{-1}) analysed using 18°C using variamine blue method.

Conc (mg L^{-1})	Abs	Abs	Abs	Average	SD	% RSD
1	0.062	0.09	0.128	0.093	0.033	35.483
3	0.133	0.158	0.169	0.153	0.018	11.745
5	0.206	0.209	0.267	0.227	0.034	14.978
7	0.232	0.252	0.332	0.272	0.053	19.485
10	0.28	0.318	0.376	0.325	0.048	14.769

Table 53. Absorbance values of arsenic samples (1–10 mg L^{-1}) analysed using 30°C using variamine blue method.

Conc (mg L^{-1})	Abs	Abs	Abs	Average	SD	% RSD
1	0.095	0.104	0.104	0.101	0.005	4.95
3	0.274	0.304	0.285	0.288	0.015	5.208
5	0.446	0.448	0.456	0.450	0.005	1.111
7	0.571	0.573	0.567	0.570	0.003	5.263
10	0.646	0.699	0.71	0.685	0.034	4.963

Table 54. Absorbance values of arsenic samples (1–10 mg L^{-1}) analysed using 50°C using variamine blue method.

Conc (mg L^{-1})	Abs	Abs	Abs	Abs	Average	SD	% RSD
1	0.269	0.274	0.282	0.263	0.272	0.008	2.941
3	0.348	0.319	0.335	0.343	0.336	0.013	3.869
5	0.396	0.45	0.401	0.382	0.407	0.030	7.371
7	0.481	0.492	0.439	0.444	0.464	0.026	5.603
10	0.543	0.531	0.519	0.534	0.532	0.010	1.88

Table 55. Absorbance values of arsenic samples (1–10 mg L^{-1}) analysed using 60°C using variamine blue method.

Conc (mg L^{-1})	Abs	Abs	Abs	Average	SD	% RSD
1	0.146	0.141	0.092	0.126	0.030	23.809
3	0.291	0.271	0.284	0.282	0.010	3.546
5	0.419	0.391	0.371	0.394	0.024	6.091
7	0.46	0.453	0.445	0.453	0.008	1.861
10	0.5	0.491	0.696	0.562	0.116	20.64

Table 56. Absorbance values of arsenic samples (1–10 mg L^{-1}) analysed using 70°C using variamine blue method.

Conc (mg L^{-1})	Abs	Abs	Abs	Average	SD	% RSD
1	0.137	0.148	0.132	0.139	0.008	5.756
3	0.286	0.304	0.287	0.292	0.010	3.425
5	0.356	0.383	0.356	0.365	0.016	4.384
7	0.428	0.409	0.563	0.467	0.084	17.987
10	0.362	0.338	0.37	0.357	0.017	4.761

Table 57. Absorbance values of arsenic samples (1–10 mg L^{-1}) analysed using 18°C using variamine blue method.

Conc (mg L^{-1})	Abs	Abs	Abs	Average	SD	% RSD
1	0.071	0.08	0.074	0.075	0.005	6.110
3	0.145	0.152	0.138	0.145	0.007	4.828
5	0.194	0.206	0.086	0.162	0.066	40.797
7	0.233	0.246	0.242	0.240	0.007	2.770
10	0.301	0.322	0.314	0.312	0.011	3.393

Table 58. Absorbance values of arsenic samples (1–10 mg L^{-1}) analysed using 30°C using variamine blue method.

Conc (mg L^{-1})	Abs	Abs	Abs	Average	SD	% RSD
1	0.11	0.094	0.117	0.107	0.012	11.019
3	0.272	0.283	0.264	0.273	0.010	3.494
5	0.561	0.555	0.574	0.563	0.010	1.724
7	0.593	0.985	0.977	0.852	0.224	26.307
10	0.728	0.741	0.719	0.729	0.011	1.517

Table 59. Absorbance values of arsenic samples (1–10 mg L^{-1}) analysed using 50°C using variamine blue method.

Conc (mg L^{-1})	Abs	Abs	Abs	Average	SD	% RSD
1	0.245	0.229	0.261	0.245	0.016	6.531
3	0.322	0.341	0.337	0.333	0.010	3.005
5	0.398	0.438	0.423	0.420	0.020	4.815
7	0.462	0.455	0.477	0.465	0.011	2.419
10	0.558	0.563	0.58	0.567	0.012	2.034

Table 60. Absorbance values of arsenic samples (1–10 mg L^{-1}) analysed using 60°C using variamine blue method.

Conc (mg L^{-1})	Abs	Abs	Abs	Average	SD	% RSD
1	0.146	0.141	0.092	0.126	0.030	23.619
3	0.291	0.271	0.284	0.282	0.010	3.599
5	0.419	0.391	0.371	0.394	0.024	6.125
7	0.46	0.453	0.445	0.453	0.008	1.658
10	0.5	0.491	0.696	0.562	0.116	20.601

Table 61. Absorbance values of arsenic samples (1–10 mg L^{-1}) analysed using 70°C using variamine blue method.

Conc (mg L^{-1})	Abs	Abs	Abs	Average	SD	% RSD
1	0.138	0.152	0.143	0.144	0.007	4.915
3	0.297	0.283	0.306	0.295	0.012	3.924
5	0.378	0.394	0.368	0.380	0.013	3.451
7	0.446	0.482	0.452	0.460	0.019	4.193
10	0.51	0.481	0.472	0.488	0.020	4.072

Table 62. Absorbance values of arsenic samples (1–10 mg L^{-1}) analysed using 18°C using molybdenum blue method.

Conc (mg L^{-1})	Abs	Abs	Abs	Abs	Abs	Average	SD	% RSD
1	0.157	0.074	0.09	0.083	0.111	0.103	0.033	32.164
2	0.16	0.22	0.18	0.18	0.21	0.190	0.024	12.892
4	0.198	0.107	0.186	0.147	0.211	0.170	0.042	25.019
6	0.206	0.134	0.169	0.217	0.191	0.183	0.033	17.971
10	0.328	0.33	0.24	0.35	0.286	0.307	0.044	14.346

Table 63. Absorbance values of arsenic samples (1–10 mg L^{-1}) analysed using 25°C using variamine blue method.

Conc (mg L^{-1})	Abs	Abs	Abs	Abs	Average	SD	% RSD
1	0.135	0.155	0.169	0.209	0.167	0.031	18.563
2	0.172	0.16	0.136	0.212	0.170	0.032	18.824
4	0.21	0.196	0.188	0.182	0.194	0.012	6.186
6	0.165	0.198	0.232	0.196	0.198	0.027	13.637
10	0.208	0.249	0.299	0.222	0.245	0.040	16.327

Table 64. Absorbance values of arsenic samples (1–10 mg L^{-1}) analysed using 30°C using variamine blue method.

Conc (mg L^{-1})	Abs	Abs	Abs	Abs	Average	SD	% RSD
1	0.164	0.19	0.168	0.181	0.176	0.012	6.818
2	0.321	0.298	0.307	0.325	0.313	0.013	4.153
4	0.384	0.411	0.379	0.419	0.398	0.020	5.025
6	0.478	0.489	0.477	0.466	0.478	0.009	1.883
10	0.54	0.562	0.557	0.548	0.552	0.010	1.88

Table 65. Absorbance values of arsenic samples (1–10 mg L^{-1}) analysed using 40°C using variamine blue method.

Conc (mg L^{-1})	Abs	Abs	Abs	Abs	Average	SD	% RSD
1	0.033	0.038	0.027	0.029	0.032	0.005	15.625
2	0.058	0.065	0.071	0.061	0.064	0.006	9.375
4	0.238	0.198	0.211	0.224	0.218	0.017	7.798
6	0.234	0.258	0.253	0.229	0.244	0.014	5.738
10	0.463	0.434	0.420	0.479	0.449	0.027	6.013

Table 66. Absorbance values of arsenic samples (1–10 mg L^{-1}) analysed using 50°C using variamine blue method.

Conc (mg L^{-1})	Abs	Abs	Abs	Abs	Average	SD	% RSD
1	0.243	0.289	0.254	0.247	0.258	0.021	8.139
2	0.274	0.266	0.306	0.300	0.287	0.019	6.620
4	0.513	0.546	0.475	0.64	0.544	0.071	13.051
6	0.67	0.539	0.649	0.678	0.634	0.065	10.252
10	0.59	0.601	0.61	0.622	0.606	0.014	2.310

Appendix B

Table 1. Absorbance values for arsenic samples (0.001-0.01 mg L^{-1}) analysed using LMG method.

Conc (mg L^{-1})	Abs	Abs	Abs	Average	SD	%RSD
0.001	0.001	0.003	0	0.001	0.002	114.564
0.003	0.001	0.003	0.005	0.003	0.002	66.667
0.005	0.004	0.001	0.002	0.002	0.002	65.465
0.007	0.002	0.005	0.003	0.003	0.002	45.826
0.01	0.003	0.006	0.002	0.004	0.002	56.773

Table 2. Absorbance values for arsenic samples (0.01-0.1 mg L^{-1}) analysed using LMG method.

Conc (mg L^{-1})	Abs	Abs	Abs	Average	SD	%RSD
0.01	0.003	0.006	0.002	0.004	0.002	56.773
0.03	0.008	0.007	0.008	0.008	0.001	7.531
0.05	0.018	0.01	0.018	0.015	0.005	30.123
0.07	0.03	0.029	0.02	0.026	0.006	20.915
0.1	0.035	0.036	0.037	0.036	0.001	2.778

Table 3. Absorbance values for arsenic samples (0.1-1 mg L^{-1}) analysed using LMG method.

Conc (mg L^{-1})	Abs	Abs	Abs	Average	SD	%RSD
0.1	0.035	0.036	0.037	0.036	0.001	2.778
0.3	0.065	0.067	0.067	0.066	0.001	1.741
0.5	0.125	0.134	0.137	0.132	0.006	4.731
0.7	0.189	0.192	0.194	0.192	0.003	1.313
1	0.255	0.257	0.249	0.254	0.004	1.641

Table 4. Absorbance values for arsenic samples (1-10 mg L^{-1}) analysed using LMG method.

Conc (mg L^{-1})	Abs	Abs	Abs	Average	SD	% RSD
1	0.255	0.257	0.249	0.254	0.004	1.641
3	0.862	0.858	0.851	0.857	0.006	0.650
5	1.409	1.423	1.432	1.421	0.012	0.815
7	1.989	1.948	1.968	1.968	0.021	1.042
10	2.872	2.668	2.532	2.691	0.171	6.360

Table 5. Absorbance measurements of 1 mg L^{-1} arsenic sample over time analysed with LMG method.

Time (min)	Abs 1	Abs 2	Abs 3	Average	SD
0	0.09	0.088	0.089	0.089	0.001
5	0.147	0.184	0.134	0.155	0.021
10	0.168	0.194	0.143	0.168	0.021
15	0.165	0.2	0.146	0.170	0.022
20	0.168	0.203	0.149	0.173	0.022
25	0.171	0.208	0.151	0.177	0.024
30	0.173	0.208	0.151	0.177	0.023
35	0.175	0.209	0.151	0.178	0.024
40	0.175	0.211	0.152	0.179	0.024
45	0.176	0.211	0.152	0.180	0.024
50	0.177	0.211	0.152	0.180	0.024
55	0.178	0.212	0.152	0.181	0.025
60	0.178	0.212	0.152	0.181	0.025
65	0.179	0.212	0.152	0.181	0.025
70	0.18	0.212	0.152	0.181	0.025
75	0.181	0.212	0.152	0.182	0.024
80	0.181	0.213	0.152	0.182	0.025
85	0.181	0.213	0.152	0.182	0.025
90	0.181	0.213	0.152	0.182	0.025
95	0.181	0.213	0.152	0.182	0.025
100	0.181	0.213	0.152	0.182	0.025
105	0.181	0.213	0.152	0.182	0.025
110	0.181	0.213	0.152	0.182	0.025

115	0.181	0.214	0.152	0.182	0.025
120	0.18	0.214	0.152	0.182	0.025
125	0.18	0.214	0.152	0.182	0.025
130	0.18	0.214	0.152	0.182	0.025
135	0.18	0.214	0.151	0.182	0.026
140	0.18	0.214	0.151	0.182	0.026
145	0.18	0.214	0.151	0.182	0.026
150	0.18	0.214	0.151	0.182	0.026
155	0.18	0.214	0.151	0.182	0.026
160	0.18	0.214	0.151	0.182	0.026
165	0.18	0.214	0.151	0.182	0.026
170	0.18	0.214	0.151	0.182	0.026
175	0.18	0.215	0.151	0.182	0.026
180	0.18	0.216	0.151	0.182	0.027
185	0.18	0.216	0.151	0.182	0.027
190	0.18	0.216	0.151	0.182	0.027
195	0.18	0.217	0.151	0.183	0.027
200	0.18	0.217	0.151	0.183	0.027
205	0.18	0.217	0.151	0.183	0.027
210	0.18	0.217	0.151	0.183	0.027
215	0.18	0.217	0.151	0.183	0.027
220	0.18	0.218	0.151	0.183	0.027
225	0.18	0.218	0.151	0.183	0.027
230	0.18	0.218	0.151	0.183	0.027
235	0.18	0.218	0.151	0.183	0.027
240	0.18	0.218	0.151	0.183	0.027
245	0.18	0.218	0.15	0.183	0.028
250	0.18	0.218	0.15	0.183	0.028
255	0.18	0.218	0.15	0.183	0.028
260	0.18	0.218	0.15	0.183	0.028
265	0.18	0.218	0.15	0.183	0.028
270	0.18	0.218	0.15	0.183	0.028
275	0.179	0.218	0.15	0.182	0.028
280	0.179	0.219	0.15	0.183	0.028
285	0.179	0.219	0.15	0.183	0.028
290	0.179	0.22	0.15	0.183	0.029
295	0.179	0.22	0.15	0.183	0.029
300	0.179	0.221	0.15	0.183	0.029
305	0.179	0.221	0.15	0.183	0.029
310	0.179	0.221	0.15	0.183	0.029
315	0.179	0.221	0.15	0.183	0.029
320	0.179	0.221	0.15	0.183	0.029
325	0.179	0.221	0.15	0.183	0.029
330	0.179	0.221	0.15	0.183	0.029

335	0.179	0.221	0.15	0.183	0.029
340	0.179	0.221	0.15	0.183	0.029
345	0.179	0.222	0.15	0.184	0.030
350	0.179	0.222	0.15	0.184	0.030
355	0.179	0.222	0.15	0.184	0.030
360	0.179	0.222	0.15	0.184	0.030
365	0.179	0.223	0.15	0.184	0.030
370	0.179	0.223	0.15	0.184	0.030
375	0.179	0.223	0.15	0.184	0.030
380	0.179	0.222	0.15	0.184	0.030
385	0.179	0.222	0.15	0.184	0.030
390	0.179	0.223	0.15	0.184	0.030
395	0.179	0.223	0.15	0.184	0.030
400	0.179	0.223	0.15	0.184	0.030
405	0.179	0.223	0.15	0.184	0.030
410	0.179	0.224	0.15	0.184	0.030
415	0.179	0.224	0.15	0.184	0.030
420	0.179	0.224	0.15	0.184	0.030
425	0.179	0.224	0.149	0.184	0.031
430	0.178	0.225	0.149	0.184	0.031
435	0.178	0.225	0.149	0.184	0.031
440	0.178	0.225	0.149	0.184	0.031
445	0.178	0.225	0.149	0.184	0.031
450	0.178	0.225	0.149	0.184	0.031
455	0.178	0.225	0.149	0.184	0.031
460	0.178	0.225	0.149	0.184	0.031
465	0.178	0.225	0.149	0.184	0.031
470	0.178	0.225	0.149	0.184	0.031
475	0.178	0.225	0.149	0.184	0.031
480	0.178	0.225	0.149	0.184	0.031
485	0.178	0.225	0.149	0.184	0.031
490	0.178	0.225	0.149	0.184	0.031
495	0.178	0.225	0.149	0.184	0.031
500	0.178	0.225	0.149	0.184	0.031
505	0.178	0.225	0.149	0.184	0.031
510	0.178	0.225	0.149	0.184	0.031
515	0.178	0.225	0.149	0.184	0.031
520	0.178	0.225	0.149	0.184	0.031
525	0.178	0.225	0.149	0.184	0.031
530	0.178	0.225	0.149	0.184	0.031
535	0.178	0.225	0.149	0.184	0.031
540	0.178	0.225	0.149	0.184	0.031
545	0.178	0.225	0.149	0.184	0.031
550	0.178	0.225	0.149	0.184	0.031

555	0.178	0.224	0.149	0.184	0.031
560	0.178	0.224	0.149	0.184	0.031
565	0.178	0.224	0.149	0.184	0.031
570	0.178	0.224	0.149	0.184	0.031
575	0.178	0.223	0.149	0.183	0.030
580	0.177	0.223	0.149	0.183	0.031
585	0.177	0.223	0.149	0.183	0.031
590	0.177	0.221	0.149	0.182	0.030
595	0.177	0.221	0.148	0.182	0.030
600	0.177	0.22	0.147	0.181	0.030

Table 6. Absorbance values of arsenic samples (0.1–1 mg L^{-1}) analysed in groundwater with LMG method.

Conc (mg L^{-1})	Abs	Abs	Abs	Average	SD	% RSD
0.1	0.013	0.012	0.014	0.013	0.001	7.692
0.3	0.037	0.034	0.041	0.037	0.004	9.407
0.5	0.068	0.064	0.067	0.066	0.002	3.138
0.7	0.076	0.074	0.08	0.077	0.003	3.985
1	0.145	0.134	0.137	0.139	0.006	4.101

Table 7. Absorbance values of arsenic samples (0.1–1 mg L^{-1}) analysed in bog water with LMG method.

Conc (mg L^{-1})	Abs	Abs	Abs	Average	SD	% RSD
0.1	0.001	0.001	0.002	0.001	0.001	0.058
0.3	0.001	0.004	0.004	0.003	0.002	0.173
0.5	0.01	0.006	0.012	0.009	0.003	0.306
0.7	0.025	0.024	0.024	0.024	0.001	0.058
1	0.049	0.054	0.046	0.050	0.004	0.404

Table 8. Absorbance values of arsenic samples (0.1–1 mg L^{-1}) analysed in river water (Killeshin) with LMG method.

Conc (mg L^{-1})	Abs	Abs	Abs	Average	SD	% RSD
0.1	0.026	0.03	0.026	0.027	0.002	0.231
0.3	0.048	0.043	0.036	0.042	0.006	0.603
0.5	0.062	0.059	0.063	0.061	0.002	0.208
0.7	0.09	0.081	0.089	0.087	0.005	0.493
1	0.139	0.125	0.129	0.131	0.007	0.721

Table 9. Absorbance values of arsenic samples (0.1–1 mg L^{-1}) analysed in river water (Barrow) with LMG method.

Conc (mg L^{-1})	Abs	Abs	Abs	Average	SD	% RSD
0.1	0.004	0.007	0.006	0.006	0.002	0.153
0.3	0.026	0.03	0.026	0.027	0.002	0.231
0.5	0.048	0.043	0.036	0.042	0.006	0.603
0.7	0.062	0.059	0.063	0.061	0.002	0.208
1	0.117	0.12	0.126	0.121	0.005	0.458

Table 10. Absorbance values of arsenic samples (0.1–1 mg L^{-1}) analysed in river water (Barrow) with LMG method.

Conc (mg L^{-1})	Abs	Abs	Abs	Average	SD	% RSD
0.1	0.026	0.029	0.026	0.027	0.002	0.173
0.3	0.066	0.07	0.068	0.068	0.002	0.200
0.5	0.092	0.098	0.093	0.094	0.003	0.321
0.7	0.136	0.135	0.133	0.135	0.002	0.153
1	0.165	0.163	0.161	0.163	0.002	0.200

Table 11. Absorbance values of arsenic samples (0.1–1 mg L^{-1}) analysed in groundwater with LMG method.

Conc (mg L^{-1})	Abs	Abs	Abs	Average	SD	% RSD
0.1	0.016	0.029	0.016	0.020	0.008	36.913
0.3	0.056	0.07	0.068	0.065	0.008	11.709
0.5	0.092	0.098	0.085	0.092	0.007	7.098
0.7	0.096	0.135	0.133	0.121	0.022	18.101
1	0.165	0.183	0.173	0.174	0.009	5.193

Table 12. Absorbance values of arsenic samples (0.1–1 mg L^{-1}) analysed in bog water with LMG method.

Conc (mg L^{-})	Abs	Abs	Abs	Average	SD	% RSD
0.1	-0.001	-0.003	0.002	-0.001	0.003	-377.49
0.3	0.001	0.003	0.001	0.002	0.001	69.28
0.5	0.01	0.011	0.008	0.010	0.002	15.80
0.7	0.027	0.022	0.025	0.025	0.003	10.20
1	0.038	0.044	0.047	0.043	0.005	10.66

Table 13. Absorbance values of arsenic samples (0.1–1 mg L^{-1}) analysed in river water (Barrow) with LMG method.

Conc (mg L^{-})	Abs	Abs	Abs	Average	SD	% RSD
0.1	0.016	0.029	0.016	0.020	0.008	36.913
0.3	0.056	0.07	0.068	0.065	0.008	11.709
0.5	0.092	0.098	0.085	0.092	0.007	7.098
0.7	0.096	0.135	0.133	0.121	0.022	18.101
1	0.165	0.183	0.173	0.174	0.009	5.193

Table 14. Absorbance values of arsenic samples (0.1–1 mg L^{-1}) analysed in river water (Barrow) the LMG method.

Conc (mg L^{-1})	Abs	Abs	Abs	Average	SD	% RSD
0.1	0.025	0.031	0.029	0.028	0.003	10.783
0.3	0.043	0.046	0.038	0.042	0.004	9.547
0.5	0.06	0.059	0.068	0.062	0.005	7.914
0.7	0.092	0.094	0.087	0.091	0.004	3.962
1	0.147	0.155	0.142	0.148	0.007	4.431

Table 15. Absorbance values of arsenic samples (0.1–1 mg L^{-1}) analysed in river water (Killeshin) with LMG method.

Conc (mg L^{-1})	Abs	Abs	Abs	Average	SD	% RSD
0.1	0.032	0.034	0.037	0.034	0.003	7.330
0.3	0.065	0.059	0.068	0.064	0.005	7.160
0.5	0.073	0.077	0.081	0.077	0.004	5.195
0.7	0.094	0.105	0.109	0.103	0.008	7.566
1	0.148	0.153	0.156	0.152	0.004	2.653

Table 16. Absorbance values of arsenic samples (0.2–1 mg L^{-1}) analysed at 4°C using LMG method.

Conc (mg L^{-1})	Abs	Abs	Abs	Average	SD
0.2	0.023	0.03	0.02	0.024	0.005
0.4	0.032	0.039	0.031	0.034	0.004
0.6	0.055	0.048	0.045	0.049	0.005
0.8	0.068	0.072	0.076	0.072	0.004
1	0.082	0.095	0.102	0.093	0.010

Table 17. Absorbance values of arsenic samples (0.2–1 mg L^{-1}) analysed at 4°using LMG method.

Conc (mg L^{-1})	Abs	Abs	Average	SD
0.2	0.02	0.023	0.022	0.002
0.4	0.064	0.074	0.069	0.007
0.6	0.094	0.119	0.107	0.018
0.8	0.117	0.149	0.133	0.023
1	0.194	0.201	0.198	0.005

Table 18. Absorbance values of arsenic samples (0.2–1 mg L^{-1}) analysed at 18°C using LMG method.

Conc (mg L^{-1})	Abs	Abs	Abs	Average	SD
0.2	0.031	0.029	0.03	0.030	0.001
0.4	0.074	0.072	0.073	0.073	0.001
0.6	0.106	0.104	0.102	0.104	0.002
0.8	0.138	0.134	0.135	0.136	0.002
1	0.168	0.166	0.168	0.167	0.001

Table 19. Absorbance values of arsenic samples (0.2–1 mg L^{-1}) analysed at 30°C using LMG method.

Conc (mg L^{-1}	Abs	Abs	Abs	Average	SD
0.2	0.048	0.057	0.05	0.052	0.005
0.4	0.11	0.104	0.107	0.107	0.003
0.6	0.154	0.156	0.161	0.157	0.004
0.8	0.195	0.189	0.189	0.191	0.003
1	0.247	0.246	0.245	0.246	0.001

Table 20. Absorbance values of arsenic samples (0.2–1 mg L^{-1}) analysed at 40°C using LMG method.

Conc (mg L^{-1})	Abs	Abs	Abs	Average	SD
0.2	0.053	0.057	0.058	0.056	0.003
0.4	0.106	0.107	0.107	0.107	0.001
0.6	0.161	0.157	0.159	0.159	0.002
0.8	0.203	0.204	0.205	0.204	0.001
1	0.255	0.253	0.255	0.254	0.001

Table 21.Absorbance values of arsenic samples (0.2–1 mg L^{-1}) analysed at 50°C using LMG method.

Conc (mg L^{-1})	Abs	Abs	Abs	Average	SD
0.2	0.061	0.066	0.061	0.063	0.003
0.4	0.112	0.113	0.114	0.113	0.001
0.6	0.171	0.167	0.168	0.169	0.002
0.8	0.219	0.216	0.216	0.217	0.002
1	0.28	0.279	0.278	0.279	0.001

Table 22. Absorbance values of arsenic samples (0.2–1 mg L^{-1}) analysed at 60°C using LMG method.

Conc (mg L^{-1})	Abs	Abs	Abs	Average	SD
0.2	0.042	0.047	0.045	0.045	0.003
0.4	0.1	0.099	0.099	0.099	0.001
0.6	0.16	0.156	0.155	0.157	0.003
0.8	0.219	0.22	0.222	0.220	0.002
1	0.263	0.26	0.261	0.261	0.002

Table 23. Absorbance values of arsenic samples (0.2–1 mg L^{-1}) analysed at pH 3.5 using LMG method.

Conc (mg L^{-1})	Abs	Abs	Abs	Average	SD	% RSD
0.2	0.039	0.037	0.034	0.037	0.003	6.863
0.4	0.071	0.067	0.067	0.068	0.002	3.380
0.6	0.088	0.083	0.085	0.085	0.003	2.949
0.8	0.11	0.106	0.112	0.109	0.003	2.794
1	0.13	0.13	0.128	0.129	0.001	0.893

Table 24. Absorbance values of arsenic samples (0.2–1 mg L^{-1}) analysed at pH 3.9 using LMG method.

Conc (mg L^{-1})	Abs	Abs	Abs	Average	SD	% RSD
0.2	0.037	0.039	0.04	0.039	0.002	3.950
0.4	0.072	0.075	0.074	0.074	0.002	2.074
0.6	0.101	0.103	0.103	0.102	0.001	1.128
0.8	0.125	0.127	0.128	0.127	0.002	1.206
1	0.155	0.158	0.159	0.157	0.002	1.323

Table 25. Absorbance values of arsenic samples (0.2–1 mg L^{-1}) analysed at pH 4 using LMG method.

Conc (mg L^{-1})	Abs	Abs	Abs	Average	SD	% RSD
0.2	0.045	0.061	0.065	0.057	0.011	18.567
0.4	0.086	0.088	0.089	0.088	0.002	1.742
0.6	0.117	0.121	0.123	0.120	0.003	2.539
0.8	0.144	0.15	0.152	0.149	0.004	2.800
1	0.17	0.177	0.175	0.174	0.004	2.072

Table 26. Absorbance values of arsenic samples (0.2–1 mg L^{-1}) analysed at pH 4.7 using LMG method.

Conc (mg L^{-1})	Abs	Abs	Abs	Average	SD	% RSD
0.2	0.053	0.045	0.047	0.048	0.004	8.614
0.4	0.109	0.107	0.107	0.108	0.001	1.072
0.6	0.133	0.126	0.132	0.130	0.004	2.905
0.8	0.158	0.154	0.151	0.154	0.004	2.276
1	0.206	0.188	0.194	0.196	0.009	4.676

Table 27. Absorbance values of arsenic samples (0.2–1 mg L^{-1}) analysed at pH 5 using LMG method.

Conc (mg L^{-1})	Abs	Abs	Abs	Average	SD	% RSD
0.2	0.046	0.05	0.049	0.048	0.002	4.307
0.4	0.102	0.094	0.095	0.097	0.004	4.494
0.6	0.142	0.139	0.132	0.138	0.005	3.728
0.8	0.169	0.169	0.165	0.168	0.002	1.377
1	0.202	0.201	0.2	0.201	0.001	0.498

Table 28. Absorbance values of arsenic samples (0.2–1 mg L^{-1}) analysed at pH 5.5 using LMG method.

Conc (mg L^{-1})	Abs	Abs	Abs	Average	SD	% RSD
0.2	0.055	0.06	0.057	0.057	0.003	4.389
0.4	0.107	0.107	0.105	0.106	0.001	2.014
0.6	0.161	0.16	0.161	0.161	0.001	0.543
0.8	0.204	0.203	0.207	0.205	0.002	1.296
1	0.258	0.255	0.25	0.254	0.004	1.975

Table 29. Absorbance values of arsenic samples (0.2–1 mg L^{-1}) analysed at pH 5.8 using LMG method.

Conc (mg L^{-1})	Abs	Abs	Abs	Average	SD	% RSD
0.2	0.047	0.045	0.051	0.048	0.003	6.409
0.4	0.089	0.078	0.083	0.083	0.006	6.609
0.6	0.128	0.126	0.122	0.125	0.003	2.438
0.8	0.16	0.155	0.151	0.155	0.005	2.903
1	0.195	0.19	0.186	0.190	0.005	2.369

Table 30. Absorbance values of arsenic samples (0.2–1 mg L^{-1}) analysed pH 6 using LMG method.

Conc (mg L^{-1})	Abs	Abs	Abs	Average	SD	% RSD
0.2	0.039	0.041	0.035	0.038	0.003	7.970
0.4	0.081	0.082	0.088	0.084	0.004	4.525
0.6	0.119	0.12	0.11	0.116	0.006	4.734
0.8	0.16	0.156	0.153	0.156	0.004	2.246
1	0.187	0.185	0.184	0.185	0.002	0.824

Table 31. Absorbance values of arsenic samples (0.2–1 mg L^{-1}) analysed using reagent ratio E using LMG method.

Conc (mg L^{-1})	Abs	Abs	Abs	Average	SD	%RSD
0.2	0.054	0.066	0.046	0.056	0.010	18.463
0.4	0.085	0.099	0.083	0.089	0.008	9.422
0.6	0.119	0.134	0.124	0.126	0.008	6.193
0.8	0.167	0.153	0.165	0.162	0.007	4.588
1	0.179	0.175	0.204	0.186	0.016	8.497

Table 32. Absorbance values of arsenic samples (0.2–1 mg L^{-1}) analysed using reagent ratio D using LMG method.

Conc (mg L^{-1})	Abs	Abs	Abs	Average	SD	% RSD
0.2	0.0525	0.036	0.0405	0.043	0.009	19.836
0.4	0.093	0.066	0.0525	0.071	0.021	29.044
0.6	0.1275	0.1035	0.0795	0.104	0.024	23.077
0.8	0.1215	0.105	0.114	0.114	0.008	7.247
1	0.156	0.123	0.126	0.135	0.018	13.517

Table 33. Absorbance values of arsenic samples (0.2–1 mg L^{-1}) analysed using reagent ratio C using LMG method.

Conc (mg L^{-1})	Abs	Abs	Abs	Average	SD	% RSD
0.2	0.05	0.048	0.036	0.045	0.008	16.952
0.4	0.085	0.079	0.078	0.081	0.004	4.693
0.6	0.141	0.131	0.124	0.132	0.009	6.473
0.8	0.174	0.173	0.156	0.168	0.010	6.033
1	0.204	0.199	0.199	0.201	0.003	1.439

Table 34. Absorbance values of arsenic samples (0.2–1 mg L^{-1}) analysed using reagent ratio B using LMG method.

Conc (mg L^{-1})	Abs	Abs	Abs	Average	SD	% RSD
0.2	0.047	0.055	0.053	0.052	0.004	8.058
0.4	0.096	0.108	0.1	0.101	0.006	6.030
0.6	0.116	0.119	0.1	0.112	0.010	9.147
0.8	0.138	0.142	0.131	0.137	0.006	4.064
1	0.175	0.176	0.165	0.172	0.006	3.536

Table 35. Absorbance values of arsenic samples (0.2–1 mg L^{-1}) using LMG method analysed using reagent ratio A using LMG method.

Conc (mg L^{-1})	Abs	Abs	Abs	Average	SD	% RSD
0.2	0.056	0.055	0.048	0.053	0.004	8.224
0.4	0.086	0.095	0.099	0.093	0.007	7.134
0.6	0.154	0.142	0.149	0.148	0.006	4.064
0.8	0.178	0.174	0.185	0.179	0.006	3.110
1	0.248	0.236	0.241	0.242	0.006	2.494

Table 36. Absorbance values for arsenic samples (0.2–1 mg L^{-1}) using LMG method analysed on day 0 with the same potassium iodate and hydrochloric acid mix.

Conc (mg L^{-1})	Abs	Abs	Abs	Average	SD	% RSD
0.2	0.088	0.085	0.093	0.089	0.003	2.838
0.4	0.148	0.147	0.142	0.146	0.003	2.207
0.6	0.185	0.182	0.186	0.184	0.002	1.129
0.8	0.22	0.224	0.225	0.223	0.003	1.186
1	0.24	0.242	0.249	0.244	0.005	1.939

Table 37. Absorbance values for arsenic samples (0.2–1 mg L^{-1}) using LMG method analysed on day 1 with the same potassium iodate and hydrochloric acid mix.

Conc (mg L^{-1})	Abs	Abs	Abs	Average	SD	% RSD
0.2	0.049	0.053	0.057	0.053	0.003	5.764
0.4	0.103	0.109	0.105	0.106	0.003	2.839
0.6	0.147	0.151	0.144	0.147	0.004	2.384
0.8	0.184	0.19	0.188	0.187	0.003	1.631
1	0.225	0.231	0.229	0.228	0.003	1.338

Table 38. Absorbance values for arsenic samples (0.2–1 mg L^{-1}) using LMG method analysed on day 2 with the same potassium iodate and hydrochloric acid mix.

Conc (mg L^{-1})	Abs	Abs	Abs	Average	SD	% RSD
0.2	0.048	0.06	0.056	0.055	0.006	11.177
0.4	0.103	0.109	0.105	0.106	0.003	2.891
0.6	0.146	0.155	0.152	0.151	0.005	3.035
0.8	0.185	0.191	0.188	0.188	0.003	1.596
1	0.221	0.217	0.226	0.221	0.005	2.037

Table 39. Absorbance values for arsenic samples (0.2–1 mg L^{-1}) using LMG method analysed on day 3 with the same potassium iodate and hydrochloric acid mix.

Conc (mg L^{-1})	Abs	Abs	Abs	Average	SD	% RSD
0.2	0.049	0.053	0.057	0.053	0.004	7.547
0.4	0.083	0.109	0.091	0.094	0.013	14.117
0.6	0.143	0.154	0.146	0.148	0.006	3.851
0.8	0.182	0.18	0.176	0.179	0.003	1.704
1	0.246	0.235	0.239	0.240	0.006	2.320

Table 40. Absorbance values for arsenic samples (0.2–1 mg L^{-1}) using LMG method analysed on day 4 with the same potassium iodate and hydrochloric acid mix.

Conc (mg L^{-1})	Abs	Abs	Abs	Average	SD	% RSD
0.2	0.055	0.048	0.051	0.051	0.004	6.841
0.4	0.101	0.106	0.111	0.106	0.005	4.717
0.6	0.138	0.146	0.141	0.142	0.004	2.853
0.8	0.174	0.176	0.176	0.175	0.001	0.659
1	0.217	0.213	0.223	0.218	0.005	2.312

Table 41. Absorbance values for arsenic samples (0.2–1 mg L^{-1}) using LMG method analysed on day 5 with the same potassium iodate and hydrochloric acid mix.

Conc (mg L^{-1})	Abs	Abs	Abs	Average	SD	% RSD
0.2	0.035	0.033	0.041	0.036	0.004	11.459
0.4	0.066	0.06	0.061	0.062	0.003	5.157
0.6	0.103	0.095	0.097	0.098	0.004	4.234
0.8	0.132	0.128	0.135	0.132	0.004	2.667
1	0.196	0.198	0.195	0.196	0.002	0.778

Table 42. Absorbance values for arsenic samples (0.2–1 mg L^{-1}) using LMG method analysed on day 0 with the same buffer and dye mix.

Conc (mg L^{-1})	Abs	Abs	Abs	Average	SD	% RSD
0.2	0.059	0.051	0.054	0.055	0.004	7.393
0.4	0.102	0.101	0.106	0.103	0.003	2.569
0.6	0.146	0.152	0.1566	0.152	0.005	3.508
0.8	0.182	0.195	0.188	0.188	0.007	3.455
1	0.225	0.224	0.216	0.222	0.005	2.225

Table 43. Absorbance values for arsenic samples (0.2–1 mg L^{-1}) using LMG method analysed on day 1 with the same buffer and dye mix.

Conc (mg L^{-1})	Abs	Abs	Abs	Average	SD	% RSD
0.2	0.055	0.047	0.052	0.051	0.004	7.873
0.4	0.095	0.102	0.098	0.098	0.004	3.571
0.6	0.137	0.139	0.134	0.137	0.003	1.841
0.8	0.177	0.168	0.175	0.173	0.005	2.726
1	0.207	0.21	0.195	0.204	0.008	3.891

Table 44. Absorbance values for arsenic samples (0.2–1 mg L^{-1}) using LMG method analysed on day 2 with the same buffer and dye mix.

Conc (mg L^{-1})	Abs	Abs	Abs	Average	SD	% RSD
0.2	0.06	0.059	0.058	0.059	0.001	1.695
0.4	0.101	0.094	0.087	0.094	0.007	7.447
0.6	0.137	0.142	0.131	0.137	0.006	4.030
0.8	0.168	0.174	0.162	0.168	0.006	3.571
1	0.198	0.203	0.201	0.201	0.003	1.254

Table 45. Absorbance values for arsenic samples (0.2–1 mg L^{-1}) using LMG method analysed on day 3 with the same buffer and dye mix.

Conc (mg L^{-1})	Abs	Abs	Abs	Average	SD	% RSD
0.2	0.039	0.042	0.037	0.039	0.003	6.398
0.4	0.08	0.075	0.089	0.081	0.007	8.723
0.6	0.118	0.121	0.112	0.117	0.005	3.917
0.8	0.144	0.154	0.148	0.149	0.005	3.386
1	0.169	0.164	0.177	0.170	0.007	3.857

Table 46. Absorbance values for arsenic samples (0.2–1 mg L^{-1}) using LMG method analysed on day 5 with the same buffer and dye mix.

Conc (mg L^{-1})	Abs	Abs	Abs	Average	SD	% RSD
0.2	0.042	0.043	0.048	0.044	0.003	7.251
0.4	0.072	0.076	0.077	0.075	0.003	3.528
0.6	0.111	0.115	0.118	0.115	0.004	3.063
0.8	0.134	0.137	0.143	0.138	0.005	3.321
1	0.171	0.174	0.176	0.174	0.003	1.449

Table 47. Absorbance values for arsenic samples (1–10 mg L^{-1}) measured in quartz cuvettes with 1 mm path length using LMG method.

Conc (mg L^{-1})	Abs	Abs	Abs	Average	SD	% RSD
1	0.004	0.005	0.003	0.004	0.001	25.000
3	0.007	0.008	0.006	0.007	0.001	14.286
5	0.012	0.014	0.012	0.013	0.001	9.116
7	0.018	0.016	0.015	0.016	0.002	9.352
10	0.022	0.023	0.019	0.021	0.002	9.758

Table 48. Absorbance values for arsenic samples (1–10 mg L^{-1}) measured in quartz cuvettes with 10 mm path length using LMG method.

Conc (mg L^{-1})	Abs	Abs	Abs	Average	SD	% RSD
0.2	0.064	0.058	0.066	0.063	0.004	6.644
4	0.100	0.109	0.099	0.103	0.006	5.365
0.6	0.147	0.142	0.153	0.147	0.006	3.738
0.8	0.178	0.174	0.186	0.179	0.006	3.407
1	0.214	0.216	0.107	0.179	0.062	34.839

Table 49. Absorbance values for arsenic samples (1–10 mg L^{-1}) measured in poly methyl methacrylate cuvettes using LMG method.

Conc (mg L^{-1})	Abs	Abs	Abs	Average	SD	% RSD
0.2	0.067	0.059	0.062	0.063	0.004	6.449
0.4	0.105	0.093	0.098	0.099	0.006	6.109
0.6	0.14	0.148	0.114	0.134	0.018	13.266
0.8	0.166	0.17	0.176	0.171	0.005	2.949
1	0.208	0.195	0.197	0.200	0.007	3.500

Table 50. Absorbance values for arsenic samples (1–10 mg L^{-1}) measured in polystyrene cuvettes using LMG method.

Conc (mg L^{-1})	Abs	Abs	Abs	Average	SD	% RSD
0.2	0.054	0.054	0.056	0.055	0.001	2.112
0.4	0.095	0.097	0.098	0.097	0.002	1.580
0.6	0.136	0.142	0.137	0.138	0.003	2.324
0.8	0.177	0.178	0.178	0.178	0.001	0.325
1	0.202	0.2	0.201	0.201	0.001	0.498

Appenidx C

Table 1. Absorbance values for chromium samples (0.001-0.01 mg L^{-1}) analysed using DPC method.

Conc (mg L^{-1})	Abs	Abs	Abs	Average	SD	%RSD
0.001	0.001	0.001	0.002	0.001	0.001	0.058
0.003	0.001	0.003	0.002	0.002	0.001	0.100
0.005	0.002	0.001	0.002	0.002	0.001	0.058
0.007	0.002	0.005	0.003	0.003	0.002	0.153
0.01	0.003	0.004	0.004	0.004	0.001	0.058

Table 2. Absorbance values for chromium samples (0.01-0.1 mg L^{-1}) analysed using DPC method.

Conc (mg L^{-1})	Abs	Abs	Abs	Average	SD	%RSD
0.01	0.003	0.004	0.004	0.004	0.001	0.058
0.03	0.008	0.007	0.008	0.008	0.001	0.058
0.05	0.018	0.018	0.018	0.018	0.000	0.000
0.07	0.03	0.029	0.02	0.026	0.006	0.551
0.1	0.035	0.036	0.037	0.036	0.001	0.100

Table 3. Absorbance values for chromium samples (0.1-1 mg L^{-1}) analysed using DPC method.

Conc (mg L^{-1})	Abs	Abs	Abs	Average	SD	% RSD
0.1	0.035	0.036	0.037	0.036	0.001	0.100
0.3	0.065	0.067	0.067	0.066	0.001	1.515
0.5	0.125	0.134	0.137	0.132	0.006	0.624
0.7	0.189	0.192	0.194	0.192	0.003	0.252
1	0.255	0.257	0.249	0.254	0.004	0.416

Table 4. Absorbance values for chromium samples (1-10 mg L^{-1}) analysed using DPC method.

Conc (mg L^{-1})	Abs	Abs	Abs	Average	SD	% RSD
1	0.255	0.257	0.249	0.254	0.004	0.416
3	0.85	0.858	0.851	0.853	0.004	0.436
5	1.409	1.413	1.432	1.418	0.012	1.229
7	1.96	1.948	1.968	1.959	0.01	1.007
10	2.672	2.668	2.532	2.624	0.08	7.97

Table 5. Absorbance values for chromium samples (0.1-1 mg L^{-1}) analysed using DPC method.

Conc (mg L^{-1})	Abs	Abs	Abs	Average	SD	%RSD
0.1	0.027	0.025	0.024	0.025	0.002	6.030
0.3	0.065	0.067	0.067	0.066	0.001	0.115
0.5	0.125	0.134	0.137	0.132	0.006	0.624
0.7	0.189	0.192	0.194	0.192	0.003	0.252
1	0.255	0.257	0.249	0.254	0.004	0.416

Table 6. Absorbance values for chromium samples (0.1-1 mg L^{-1}) analysed using DPC method.

Conc (mg L^{-1})	Abs	Abs	Abs	Average	SD	% RSD
0.1	0.054	0.058	0.057	0.056	0.002	0.208
0.3	0.082	0.101	0.087	0.090	0.010	0.985
0.5	0.112	0.137	0.135	0.128	0.014	1.389
0.7	0.163	0.114	0.149	0.142	0.025	2.524
1	0.188	0.193	0.281	0.221	0.052	5.231

Table 7. Absorbance values for chromium samples (0.1-1 mg L^{-1}) analysed using DPC method in 1 to 1 ratio.

Conc (mg L^{-1})	Abs	Abs	Abs	Average	SD	%RSD
0.1	0.039	0.039	0.04	0.039	0.001	0.058
0.3	0.116	0.119	0.129	0.121	0.007	0.681
0.5	0.197	0.194	0.205	0.199	0.006	0.569
0.7	0.277	0.293	0.284	0.285	0.008	0.802
1	0.386	0.396	0.384	0.389	0.006	0.643

Table 8. Absorbance values for chromium samples (0.1-1 mg L^{-1}) analysed using DPC method and measured in 10 mm quartz cuvettes. .

Conc (mg L^{-1})	Abs	Abs	Abs	Average	SD	%RSD
0.1	0.039	0.039	0.040	0.039	0.001	0.058
0.3	0.116	0.119	0.129	0.121	0.007	0.681
0.5	0.197	0.194	0.205	0.199	0.006	0.569
0.7	0.277	0.293	0.284	0.285	0.008	0.802
1	0.386	0.396	0.384	0.389	0.006	0.643

Table 9. Absorbance values for chromium samples (0.1-1 mg L^{-1}) analysed using DPC method measured in 1 mm quartz cuvettes.

Conc (mg L^{-1})	Abs	Abs	Abs	Average	SD	% RSD
0.1	0.001	-0.003	-0.006	-0.003	0.004	-131.696
0.3	-0.002	0.001	0	0.000	0.002	-458.258
0.5	0.011	0.008	0.012	0.010	0.002	20.145
0.7	0.018	0.016	0.018	0.017	0.001	6.662
1	0.021	0.017	0.018	0.019	0.002	11.152

Table 10. Absorbance values for chromium samples (0.1–1 mg L^{-1}) using DPC method analysed on day 0 with the same dye.

Conc (mg L^{-1})	Abs	Abs	Abs	Average	SD	%RSD
0.1	0.007	0.005	0.007	0.006	0.001	0.115
0.3	0.065	0.067	0.067	0.066	0.001	0.115
0.5	0.125	0.134	0.137	0.132	0.006	0.624
0.7	0.189	0.192	0.194	0.192	0.003	0.252
1	0.255	0.257	0.249	0.254	0.004	0.416

Table 11.Absorbance values for chromium samples (0.1–1 mg L^{-1}) using DPC method analysed on day 7 with the same dye.

Conc (mg L^{-1})	Abs	Abs	Abs	Average	SD	%RSD
0.1	0.035	0.038	0.043	0.04	0.00	0.40
0.3	0.102	0.152	0.101	0.12	0.03	2.92
0.5	0.165	0.187	0.146	0.17	0.02	2.05
0.7	0.206	0.203	0.199	0.20	0.00	0.35
1	0.279	0.263	0.286	0.28	0.01	1.18

Table 12. Absorbance values for chromium samples (0.1–1 mg L^{-1}) using DPC method analysed on day 14 with the same dye.

Conc (mg L^{-1})	Abs	Abs	Abs	Average	SD	%RSD
0.1	0.023	0.024	0.026	0.024	0.002	0.153
0.3	0.07	0.077	0.08	0.076	0.005	0.513
0.5	0.135	0.148	0.177	0.153	0.022	2.150
0.7	0.23	0.22	0.196	0.215	0.017	1.747
1	0.283	0.286	0.316	0.295	0.018	1.825

Table 13. Absorbance values for chromium samples (0.1–1 mg L^{-1}) using DPC method analysed on day 21 with the same dye.

Conc (mg L^{-1})	Abs	Abs	Abs	Average	SD	%RSD
0.1	0.045	0.032	0.037	0.038	0.007	0.656
0.3	0.077	0.071	0.07	0.073	0.004	0.379
0.5	0.123	0.117	0.126	0.122	0.005	0.458
0.7	0.154	0.182	0.184	0.173	0.017	1.677
1	0.225	0.217	0.216	0.219	0.005	0.493

Table 14. Absorbance values for chromium samples (0.1–1 mg L^{-1}) using DPC method analysed on day 28 with the same dye.

Conc (mg L^{-1})	Abs	Abs	Abs	Average	SD	%RSD
0.1	0.033	0.032	0.02	0.028	0.007	0.723
0.3	0.075	0.07	0.073	0.073	0.003	0.252
0.5	0.108	0.106	0.116	0.110	0.005	0.529
0.7	0.168	0.18	0.197	0.182	0.015	1.457
1	0.237	0.22	0.203	0.220	0.017	1.700

Table 24. Absorbance values for chromium samples (0.1–1 mg L^{-1}) using DPC method analysed on day 0 with dye and sulfuric acid combined reagent.

Conc (mg L^{-1})	Abs	Abs	Abs	Average	SD	% RSD
0.1	0.027	0.032	0.032	0.030	0.003	0.289
0.3	0.081	0.112	0.119	0.104	0.020	2.022
0.5	0.181	0.188	0.198	0.189	0.009	0.854
0.7	0.262	0.254	0.268	0.261	0.007	0.702
1	0.382	0.375	0.402	0.386	0.014	1.401

Table16. Absorbance values for chromium samples (0.1–1 mg L^{-1}) using DPC method analysed on day 7 with dye and sulfuric acid combined reagent.

Conc (mg L^{-1})	Abs	Abs	Abs	Average	SD	%RSD
0.1	0.058	0.062	0.062	0.061	0.002	0.231
0.3	0.116	0.125	0.118	0.120	0.005	0.473
0.5	0.235	0.231	0.242	0.236	0.006	0.557
0.7	0.273	0.279	0.289	0.280	0.008	0.808
1	0.378	0.387	0.409	0.391	0.016	1.595

Table17. Absorbance values for chromium samples (0.1–1 mg L^{-1}) using DPC method analysed on day 14 with dye and sulfuric acid combined reagent.

Conc (mg L^{-1})	Abs	Abs	Abs	Average	SD	% RSD
0.1	0.038	0.041	0.043	0.041	0.003	0.252
0.3	0.115	0.115	0.118	0.116	0.002	0.173
0.5	0.204	0.209	0.203	0.205	0.003	0.321
0.7	0.269	0.245	0.268	0.261	0.014	1.358
1	0.363	0.363	0.377	0.368	0.008	0.808

Table 18. Absorbance values for chromium samples (0.1–1 mg L^{-1}) using DPC method analysed on day 21 with dye and sulfuric acid combined reagent.

Conc (mg L^{-1})	Abs	Abs	Abs	Average	SD	%RSD
0.1	0.033	0.031	0.032	0.032	0.001	0.100
0.3	0.091	0.09	0.096	0.092	0.003	0.321
0.5	0.163	0.184	0.167	0.171	0.011	1.115
0.7	0.243	0.245	0.245	0.244	0.001	0.115
1	0.346	0.336	0.36	0.347	0.012	1.206

Table 19. Absorbance values for chromium samples (0.1–1 mg L^{-1}) using DPC method analysed on day 28 with dye and sulfuric acid combined reagent.

Conc (mg L^{-1})	Abs	Abs	Abs	Average	SD	% RSD
0.1	0.024	0.027	0.031	0.027	0.004	12.848
0.3	0.068	0.071	0.067	0.069	0.010	14.780
0.5	0.121	0.128	0.124	0.124	0.005	3.801
0.7	0.185	0.188	0.183	0.185	0.003	1.358
1	0.328	0.307	0.318	0.318	0.010	3.100

Table 20. Absorbance values of chromium samples (0.1–1 mg L^{-1}) analysed at pH 1.5 using DPC method.

Conc (mg L^{-1})	Abs	Abs	Abs	Average	SD	% RSD
0.1	0.01	0.012	0.012	0.011	0.001	10.189
0.3	0.043	0.041	0.04	0.041	0.002	3.696
0.5	0.075	0.071	0.072	0.073	0.002	2.865
0.7	0.1621	0.1617	0.1619	0.162	0.000	0.124
1	0.2198	0.223	0.221	0.221	0.002	0.733

Table 21. Absorbance values of chromium samples (0.1–1 mg L^{-1}) analysed at pH 1.8 using DPC method.

Conc (mg L^{-1})	Abs	Abs	Abs	Average	SD	% RSD
0.1	0.053	0.057	0.059	0.056	0.003	5.423
0.3	0.088	0.093	0.091	0.090	0.003	2.796
0.5	0.128	0.126	0.131	0.128	0.003	1.961
0.7	0.155	0.152	0.154	0.154	0.002	0.994
1	0.239	0.244	0.241	0.241	0.003	1.043

Table 22. Absorbance values of chromium samples (0.1–1 mg L^{-1}) analysed at pH 2 using DPC method.

Conc (mg L^{-1})	Abs	Abs	Abs	Average	SD	% RSD
0.1	0.013	0.016	0.019	0.040	0.003	7.563
0.3	0.063	0.042	0.041	0.049	0.012	25.527
0.5	0.086	0.096	0.105	0.096	0.010	9.935
0.7	0.157	0.144	0.163	0.155	0.010	6.280
1	0.218	0.241	0.225	0.228	0.012	5.171

Table 23. Absorbance values of chromium samples (0.1–1 mg L^{-1}) analysed at pH 2.2 using DPC method.

Conc (mg L^{-1})	Abs	Abs	Abs	Average	SD	% RSD
0.1	0.029	0.035	0.031	0.032	0.003	9.547
0.3	0.065	0.066	0.066	0.066	0.001	0.879
0.5	0.108	0.123	0.122	0.118	0.008	7.127
0.7	0.21	0.192	0.186	0.196	0.012	6.372
1	0.278	0.256	0.279	0.271	0.013	4.797

Table 24. Absorbance values of chromium samples (0.1–1 mg L^{-1}) analysed at pH 2.4 using DPC method.

Conc (mg L^{-1})	Abs	Abs	Abs	Average	SD	% RSD
0.1	-0.006	-0.003	-0.014	-0.008	0.006	-74.168
0.3	0.037	0.046	0.05	0.044	0.007	15.019
0.5	0.105	0.097	0.096	0.099	0.005	4.966
0.7	0.182	0.212	0.184	0.193	0.017	8.706
1	0.252	0.257	0.261	0.257	0.005	1.757

Table 25. Absorbance values of chromium samples (0.1–1 mg L^{-1}) analysed at pH 2.8 using DPC method.

Conc (mg L^{-1})	Abs	Abs	Abs	Average	SD	% RSD
0.1	0.027	0.026	0.028	0.027	0.001	3.704
0.3	0.072	0.072	0.075	0.073	0.002	2.373
0.5	0.132	0.112	0.126	0.123	0.010	8.322
0.7	0.157	0.153	0.152	0.154	0.003	1.718
1	0.231	0.247	0.239	0.239	0.008	3.347

Table 26. Absorbance measurements of 1 mg L^{-1} chromium sample over time analysed with DPC method.

Time	Abs	Abs	Abs	SD	Average
0	0.361	0.359	0.383	0.013	0.368
5	0.363	0.334	0.384	0.025	0.360
10	0.361	0.319	0.384	0.033	0.355
15	0.36	0.311	0.384	0.037	0.352
20	0.357	0.308	0.384	0.039	0.350
25	0.357	0.306	0.384	0.040	0.349
30	0.356	0.304	0.384	0.041	0.348
35	0.355	0.303	0.384	0.041	0.347
40	0.353	0.303	0.384	0.041	0.347
45	0.352	0.306	0.384	0.039	0.347
50	0.351	0.308	0.384	0.038	0.348
55	0.349	0.311	0.383	0.036	0.348
60	0.347	0.312	0.383	0.036	0.347
65	0.346	0.315	0.383	0.034	0.348
70	0.344	0.316	0.383	0.034	0.348
75	0.343	0.317	0.383	0.033	0.348
80	0.342	0.317	0.383	0.033	0.347
85	0.34	0.318	0.382	0.033	0.347
90	0.339	0.318	0.382	0.033	0.346
95	0.339	0.319	0.382	0.032	0.347
100	0.337	0.319	0.382	0.032	0.346
105	0.334	0.319	0.381	0.032	0.345
110	0.332	0.319	0.38	0.032	0.344
115	0.331	0.319	0.379	0.032	0.343
120	0.33	0.319	0.378	0.031	0.342
125	0.328	0.318	0.378	0.032	0.341
130	0.328	0.318	0.378	0.032	0.341

135	0.326	0.318	0.378	0.033	0.341
140	0.325	0.32	0.378	0.032	0.341
145	0.325	0.32	0.378	0.032	0.341
150	0.323	0.32	0.378	0.033	0.340
155	0.322	0.32	0.378	0.033	0.340
160	0.321	0.32	0.377	0.033	0.339
165	0.32	0.32	0.375	0.032	0.338
170	0.319	0.32	0.373	0.031	0.337
175	0.318	0.32	0.372	0.031	0.337
180	0.317	0.32	0.371	0.030	0.336
185	0.317	0.32	0.371	0.030	0.336
190	0.316	0.32	0.371	0.031	0.336
195	0.315	0.32	0.37	0.030	0.335
200	0.314	0.32	0.37	0.031	0.335
205	0.313	0.321	0.37	0.031	0.335
210	0.313	0.321	0.37	0.031	0.335
215	0.313	0.321	0.37	0.031	0.335
220	0.313	0.321	0.37	0.031	0.335
225	0.312	0.321	0.369	0.031	0.334
230	0.311	0.321	0.369	0.031	0.334
235	0.31	0.321	0.368	0.031	0.333
240	0.309	0.321	0.368	0.031	0.333
245	0.308	0.321	0.367	0.031	0.332
250	0.308	0.321	0.367	0.031	0.332
255	0.307	0.321	0.367	0.031	0.332
260	0.306	0.321	0.367	0.032	0.331
265	0.305	0.321	0.366	0.032	0.331
270	0.304	0.321	0.366	0.032	0.330
275	0.304	0.321	0.365	0.031	0.330
280	0.303	0.321	0.365	0.032	0.330
285	0.303	0.322	0.365	0.032	0.330
290	0.303	0.322	0.364	0.031	0.330
295	0.302	0.322	0.364	0.032	0.329
300	0.302	0.322	0.364	0.032	0.329
305	0.302	0.322	0.364	0.032	0.329
310	0.301	0.333	0.363	0.031	0.332
315	0.301	0.332	0.363	0.031	0.332
320	0.301	0.332	0.363	0.031	0.332
325	0.301	0.332	0.362	0.031	0.332
330	0.301	0.332	0.362	0.031	0.332
335	0.301	0.332	0.361	0.030	0.331
340	0.301	0.332	0.361	0.030	0.331
345	0.301	0.332	0.361	0.030	0.331
350	0.301	0.332	0.36	0.030	0.331

355	0.3	0.332	0.36	0.030	0.331
360	0.3	0.332	0.36	0.030	0.331
365	0.3	0.332	0.359	0.030	0.330
370	0.3	0.331	0.359	0.030	0.330
375	0.3	0.331	0.358	0.029	0.330
380	0.299	0.331	0.358	0.030	0.329
385	0.299	0.333	0.357	0.029	0.330
390	0.299	0.333	0.356	0.029	0.329
395	0.299	0.333	0.355	0.028	0.329
400	0.299	0.333	0.355	0.028	0.329
405	0.298	0.333	0.354	0.028	0.328
410	0.297	0.329	0.353	0.028	0.326
415	0.296	0.329	0.353	0.029	0.326
420	0.296	0.329	0.352	0.028	0.326
425	0.295	0.328	0.352	0.029	0.325
430	0.294	0.328	0.352	0.029	0.325
435	0.293	0.327	0.352	0.030	0.324
440	0.293	0.328	0.352	0.030	0.324
445	0.292	0.326	0.352	0.030	0.323
450	0.292	0.326	0.352	0.030	0.323
455	0.291	0.325	0.351	0.030	0.322
460	0.291	0.324	0.351	0.030	0.322
465	0.291	0.323	0.35	0.030	0.321
470	0.29	0.323	0.349	0.030	0.321
475	0.29	0.32	0.348	0.029	0.319
480	0.29	0.321	0.347	0.029	0.319
485	0.289	0.32	0.347	0.029	0.319
490	0.289	0.319	0.346	0.029	0.318
495	0.288	0.317	0.345	0.029	0.317
500	0.288	0.316	0.345	0.029	0.316
505	0.288	0.316	0.343	0.028	0.316
510	0.287	0.314	0.343	0.028	0.315
515	0.286	0.313	0.342	0.028	0.314
520	0.286	0.312	0.341	0.028	0.313
525	0.286	0.311	0.34	0.027	0.312
530	0.285	0.31	0.34	0.028	0.312
535	0.285	0.309	0.339	0.027	0.311
540	0.284	0.309	0.338	0.027	0.310
545	0.283	0.308	0.337	0.027	0.309
550	0.283	0.308	0.336	0.027	0.309
555	0.282	0.307	0.335	0.027	0.308
560	0.281	0.306	0.334	0.027	0.307
565	0.28	0.305	0.333	0.027	0.306
570	0.279	0.304	0.332	0.027	0.305

575	0.278	0.304	0.331	0.027	0.304
580	0.277	0.303	0.33	0.027	0.303
585	0.276	0.302	0.329	0.027	0.302
590	0.275	0.301	0.328	0.027	0.301
595	0.274	0.3	0.327	0.027	0.300
600	0.274	0.299	0.326	0.026	0.300

Table 27. Absorbance values of chromium samples (0.1–1 mg L^{-1}) analysed with 0.025 M sulfuric acid.

Conc (mg L^{-1})	Abs	Abs	Abs	Average	SD	% RSD
0.1	0.07	0.051	0.012	0.044	0.030	2.957
0.3	0.065	0.06	0.031	0.052	0.018	1.836
0.5	0.065	0.06	0.053	0.059	0.006	0.603
0.7	0.143	0.141	0.139	0.141	0.002	0.200
1	0.191	0.167	0.187	0.182	0.013	1.286

Table 28. Absorbance values of chromium samples (0.1–1 mg L^{-1}) analysed with 0.05 M sulfuric acid.

Conc (mg L^{-1})	Abs	Abs	Abs	Average	SD	% RSD
0.1	0.018	0.037	0.032	0.029	0.010	0.985
0.3	0.102	0.105	0.109	0.105	0.004	0.351
0.5	0.165	0.153	0.155	0.158	0.006	0.643
0.7	0.192	0.193	0.189	0.191	0.002	0.208
1	0.269	0.273	0.263	0.268	0.005	0.503

Table 29. Absorbance values of chromium samples (0.1–1 mg L^{-1}) analysed with 0.1 M sulfuric acid.

Conc (mg L^{-1})	Abs	Abs	Abs	Average	SD	% RSD
0.1	0.01	0.006	0.08	0.032	0.042	4.162
0.3	0.045	0.038	0.041	0.041	0.004	0.351
0.5	0.077	0.069	0.073	0.073	0.004	0.400
0.7	0.164	0.133	0.164	0.154	0.018	1.790
1	0.241	0.245	0.237	0.241	0.004	0.400

Table 30. Absorbance values of chromium samples (0.1–1 mg L^{-1}) analysed with 0.1 M sulfuric acid.

Conc (mg L^{-1})	Abs	Abs	Abs	Average	SD	% RSD
0.1	0.036	0.047	0.054	0.046	0.009	0.907
0.3	0.087	0.068	0.073	0.076	0.010	0.985
0.5	0.092	0.116	0.142	0.117	0.025	2.501
0.7	0.172	0.167	0.164	0.168	0.004	0.404
1	0.225	0.217	0.218	0.220	0.004	0.436

Table 31. Absorbance values of chromium samples (0.1–1 mg L^{-1}) analysed with 0.4 M sulfuric acid.

Conc (mg L^{-1})	Abs	Abs	Abs	Average	SD	% RSD
0.1	0.012	0.015	0.033	0.020	0.011	1.136
0.3	0.06	0.098	0.093	0.084	0.021	2.065
0.5	0.16	0.156	0.153	0.156	0.004	0.351
0.7	0.193	0.196	0.237	0.209	0.025	2.458
1	0.286	0.27	0.271	0.276	0.009	0.896

Table 32. Absorbance values of chromium samples (0.1–1 mg L−1) analysed with 0.6 M sulfuric acid.

Conc (mg L^{-1})	Abs	Abs	Abs	Average	SD	% RSD
0.1	0.019	0.045	0.026	0.030	0.013	1.345
0.3	0.052	0.09	0.07	0.071	0.019	1.901
0.5	0.082	0.109	0.108	0.100	0.015	1.531
0.7	0.128	0.175	0.147	0.150	0.024	2.364
1	0.207	0.208	0.227	0.214	0.011	1.127

Table 33. Absorbance values of chromium samples (0.1–1 mg L^{-1}) analysed with 0.8 M sulfuric acid.

Conc (mg L^{-1})	Abs	Abs	Abs	Average	SD	% RSD
0.1	0.09	0.01	0.06	0.053	0.040	4.041
0.3	0.048	0.065	0.058	0.057	0.009	0.854
0.5	0.1	0.108	0.084	0.097	0.012	1.222
0.7	0.155	0.145	0.164	0.155	0.010	0.950
1	0.287	0.225	0.24	0.251	0.032	3.235

Table 34. Absorbance values of chromium samples (0.1–1 mg L^{-1}) analysed with 1.0 M sulfuric acid.

Conc (mg L^{-1})	Abs	Abs	Abs	Average	SD	% RSD
0.1	0.01	0.006	0.08	0.032	0.042	4.162
0.3	0.045	0.038	0.041	0.041	0.004	0.351
0.5	0.077	0.069	0.073	0.073	0.004	0.400
0.7	0.164	0.133	0.164	0.154	0.018	1.790
1	0.241	0.245	0.237	0.241	0.004	0.400

Table 35. Absorbance values of chromium samples (0.1–1 mg L^{-1}) analysed in double deionized water with DPC method.

Conc (mg L^{-1})	Abs	Abs	Abs	Average	SD	%RSD
0.1	0.039	0.039	0.04	0.039	0.001	0.058
0.3	0.116	0.119	0.129	0.121	0.007	0.681
0.5	0.197	0.194	0.205	0.199	0.006	0.569
0.7	0.277	0.293	0.284	0.285	0.008	0.802
1	0.356	0.376	0.364	0.365	0.010	2.755

Table 36. Absorbance values of chromium samples (0.1–1 mg L^{-1}) analysed in double deionized water with DPC method.

Conc (mg L^{-1})	Abs	Abs	Abs	Average	SD	% RSD
0.1	0.039	0.039	0.038	0.039	0.001	1.577
0.3	0.137	0.127	0.099	0.121	0.020	16.433
0.5	0.235	0.198	0.162	0.199	0.037	18.387
0.7	0.263	0.351	0.237	0.284	0.060	21.169
1	0.387	0.430	0.340	0.386	0.045	11.678

Table 37. Absorbance values of chromium samples (0.1–1 mg L^{-1}) analysed in ground water with DPC method.

Conc (mg L^{-1})	Abs	Abs	Abs	Average	SD	% RSD
0.1	0.049	0.044	0.051	0.048	0.003	6.133
0.3	0.098	0.096	0.098	0.097	0.001	0.969
0.5	0.163	0.178	0.177	0.173	0.007	3.966
0.7	0.299	0.293	0.285	0.292	0.006	1.962
1	0.325	0.377	0.344	0.349	0.021	6.162

Table 38. Absorbance values of chromium samples (0.1–1 mg L^{-1}) analysed in ground water with DPC method.

Conc (mg L^{-1})	Abs	Abs	Abs	Average	SD	% RSD
0.1	0.039	0.045	0.039	0.041	0.003	8.449
0.3	0.078	0.089	0.091	0.086	0.007	8.140
0.5	0.163	0.178	0.177	0.173	0.008	4.857
0.7	0.301	0.295	0.278	0.291	0.012	4.095
1	0.337	0.345	0.351	0.344	0.007	2.040

Table 39. Absorbance values of chromium samples (0.1–1 mg L^{-1}) analysed in bog water with DPC method.

Conc (mg L^{-1})	Abs	Abs	Abs	Average	SD	% RSD
0.1	0.094	0.093	0.0901	0.092	0.002	2.193
0.3	0.166	0.162	0.163	0.164	0.002	1.272
0.5	0.235	0.235	0.231	0.234	0.002	0.988
0.7	0.315	0.337	0.328	0.327	0.011	3.386
1	0.45	0.459	0.4732	0.461	0.012	2.539

Table 40. Absorbance values of chromium samples (0.1–1 mg L^{-1}) analysed in bog water with DPC method.

Conc (mg L^{-1})	Abs	Abs	Abs	Average	SD	% RSD
0.1	0.059	0.052	0.604	0.238	0.317	132.902
0.3	0.111	0.105	0.105	0.107	0.003	3.237
0.5	0.167	0.154	0.135	0.152	0.016	10.588
0.7	0.294	0.285	0.298	0.292	0.007	2.278
1	0.417	0.406	0.418	0.414	0.007	1.610

Table 41. Absorbance values of chromium samples (0.1–1 mg L^{-1}) analysed in river water (Barrow) with DPC method.

Conc (mg L^{-1})	Abs	Abs	Abs	Average	SD	% RSD
0.1	0.008	0.008	0.009	0.008	0.000	5.010
0.3	0.016	0.020	0.018	0.018	0.002	10.318
0.5	0.101	0.090	0.078	0.090	0.012	13.333
0.7	0.209	0.210	0.161	0.194	0.028	14.476
1	0.324	0.322	0.300	0.315	0.013	4.241

Table 42. Absorbance values of chromium samples (0.1–1 mg L^{-1}) analysed in river water (Barrow) with DPC method.

Conc (mg L^{-1})	Abs	Abs	Abs	Average	SD	%RSD
0.1	0.011	0.011	0.0016	0.0079	0.0054	68.9885
0.3	0.044	0.046	0.048	0.0460	0.0020	4.3478
0.5	0.142	0.153	0.131	0.1420	0.0110	7.7465
0.7	0.214	0.259	0.206	0.2263	0.0286	12.6237
1	0.293	0.292	0.31	0.2983	0.0101	3.3908

Table 43. Absorbance values of chromium samples (0.1–1 mg L^{-1}) analysed in river water (River Barrow from St. Mullins site) with DPC method.

Conc (mg L^{-1})	Abs	Abs	Abs	Average	SD	% RSD
0.1	0.013	0.017	0.014	0.015	0.002	11.665
0.3	0.067	0.110	0.088	0.088	0.021	24.138
0.5	0.179	0.175	0.183	0.179	0.004	2.242
0.7	0.216	0.213	0.202	0.210	0.008	3.577
1	0.320	0.302	0.299	0.307	0.011	3.727

Table 44. Absorbance values of chromium samples (0.1–1 mg L^{-1}) analysed in river water (River Barrow from St. Mullins site) with DPC method.

Conc (mg L^{-1})	Abs	Abs	Abs	Average	SD	% RSD
0.1	0.012	0.015	0.033	0.0200	0.0114	1.1358
0.3	0.06	0.098	0.093	0.0837	0.0206	2.0648
0.5	0.16	0.156	0.153	0.1563	0.0035	0.3512
0.7	0.193	0.196	0.237	0.2087	0.0246	2.4583
1	0.286	0.27	0.271	0.2757	0.0090	0.8963

Table 45. Absorbance values of chromium samples (0.1–1 mg L^{-1}) analysed in river water (Killeshin) with DPC method.

Conc (mg L^{-1})	Abs	Abs	Abs	Average	SD	% RSD
0.1	0.009	0.009	0.007	0.008	0.001	9.148
0.3	0.019	0.020	0.019	0.019	0.001	4.253
0.5	0.100	0.095	0.085	0.093	0.007	8.669
0.7	0.150	0.151	0.140	0.147	0.006	4.860
1	0.293	0.280	0.272	0.282	0.022	7.350

Table 46. Absorbance values of chromium samples (0.1–1 mg L^{-1}) analysed in river water (Killeshin) with DPC method.

Conc (mg L^{-1})	Abs	Abs	Abs	Average	SD	% RSD
0.1	0.008	0.009	0.010	0.009	0.001	9.075
0.3	0.018	0.019	0.024	0.020	0.003	15.091
0.5	0.089	0.084	0.075	0.083	0.007	8.668
0.7	0.139	0.141	0.129	0.126	0.006	4.860
1	0.315	0.280	0.321	0.289	0.022	7.777

Table 47. Absorbance values of chromium samples (0.1–1 mg L^{-1}) measured in 1mm quartz cuvettes analysed using DPC method.

Conc (mg L^{-1})	Abs	Abs	Abs	Average	SD	%RSD
0.01	0.000	0.000	0.000	0.000	0.000	0.000
0.03	0.002	0.000	0.001	0.001	0.001	0.200
0.05	0.001	0.002	0.004	0.002	0.002	65.465
0.07	0.002	0.011	0.010	0.008	0.005	64.342
0.1	0.012	0.001	0.015	0.009	0.007	78.976

Table 48. Absorbance values of chromium samples (0.1–1 mg L^{-1}) measured in 1mm quartz cuvettes analysed using DPC method.

Conc (mg L^{-1})	Abs	Abs	Abs	Average	SD	% RSD
0.1	0.001	-0.002	0	0.000	0.002	0.153
0.3	0.003	0.003	0.004	0.003	0.001	0.058
0.5	0.01	0.009	0.01	0.010	0.001	0.058
0.7	0.017	0.017	0.017	0.017	0.000	0.000
1	0.023	0.024	0.022	0.023	0.001	0.100

Appenidx D

Table 1. Microfluidic chip measurements for arsenic samples ranging from 0.3-2 mg L^{-1}.

Conc (mg L^{-1})	Volt	Abs	Volt2	Abs 2	Average	SD	% RSD
0.3	3.07	0.02	2.98	0.03	0.02	0.01	37.46
0.5	2.91	0.04	2.88	0.04	0.04	0.00	7.75
0.7	2.77	0.06	2.67	0.08	0.07	0.01	16.47
1	2.53	0.10	2.48	0.11	0.10	0.01	6.48
2	1.96	0.21	2.14	0.17	0.19	0.03	14.14

Table 2. Absorbance values of arsenic samples ranging from 0.3-2 mg L^{-1} measuredobtained using microfluidic detection system.

Conc (mg L^{-1})	Abs	Abs	Abs	Average	SD	% RSD
0.3	0.017	0.019	0.014	0.017	0.003	15.252
0.5	0.029	0.032	0.026	0.029	0.003	10.345
0.7	0.047	0.042	0.044	0.044	0.003	5.674
1	0.077	0.076	0.079	0.078	0.002	1.971
2	0.155	0.154	0.158	0.156	0.002	1.334

Table 3. Absorbance values of arsenic samples ranging from 0.3-2 mg L^{-1} measuredobtained using UV-vis spectroscopy.

Conc (mg L^{-1})	Abs	Abs	Abs	Average	SD	% RSD
0.3	0.035	0.033	0.037	0.035	0.002	5.714
0.5	0.053	0.051	0.047	0.05	0.003	6.110
0.7	0.071	0.077	0.076	0.075	0.003	4.286
1	0.098	0.115	0.111	0.108	0.009	8.229
2	0.248	0.256	0.259	0.254	0.006	2.239

Table 4. % difference of results obtained using microfluidic detection system and actual arsenic concentration in samples with various water matrices.

Equation	Sample	Conc calculated (mg L^{-1})	Actual conc (mg L^{-1})	% Difference
y=0.1152x-0.0169	Double deionised water	0.490	0.500	2.000
	Double deionised water	0.800	0.700	-14.286
y=0.0824x+0.0159	Double deionised water	0.290	0.500	42.000
	Double deionised water	0.580	0.700	17.143
y = 0.0899x + 0.01	Double deionised water	0.406	0.500	18.865
	Bog lake	1.362	1.000	-36.198
	Bog lake	0.474	0.500	5.157
	Double deionised water	0.787	0.900	12.594
y = 0.109x + 0.009	Double deionised water	0.344	0.500	31.247
	Bog lake	1.132	1.000	-13.249
	Bog lake	0.400	0.500	19.942
	Double deionised water	0.787	0.900	12.594

Table 5. Microfluidic chip measurements for arsenic samples ranging from 0.3-2 mg L^{-1}.

Conc (mg L^{-1})	Volt	Abs	Volt2	Abs 2	Average	SD	% RSD
0.3	3.07	0.02	2.98	0.03	0.02	0.01	37.46
0.5	2.91	0.04	2.88	0.04	0.04	0.00	7.75
0.7	2.77	0.06	2.67	0.08	0.07	0.01	16.47
1	2.53	0.10	2.48	0.11	0.10	0.01	6.48
2	1.960	0.21	2.14	0.17	0.19	0.03	14.14

Table 6. Microfluidic chip measurements for arsenic samples ranging from 0.3-2 mg L^{-1}.

Conc (mg L^{-1})	Voltage 1	Voltage 2	Abs 1	Abs 2
0.3	1.723	1.719	0.007	0.008
0.7	1.096	1.109	0.204	0.198
1	0.879	0.865	0.299	0.306
2	0.219	0.302	0.902	0.764

Table 7. Microfluidic chip measurements for arsenic samples prepared in various water matrices.

Conc (mg L^{-1})	Volt	Abs	Volt 2	Abs 2	Volt 3	Abs 3
1	2.54	0.09	2.36	0.13	2.45	0.11
0.7	2.64	0.08	2.63	0.08	2.60	0.08
1 river	2.39	0.12	2.47	0.10	2.46	0.11
1 lake	2.31	0.13	2.37	0.12	2.30	0.14
1 repeated	2.36	0.12	2.40	0.12		

Table 8. Microfluidic chip measurements for arsenic samples prepared in various water matrices.

Conc (mg L^{-1})	Volt	Abs	Volt 2	Abs 2	Volt 3	Abs 3
1	2.690	0.112	2.563	0.133	2.666	0.116
0.7	2.885	0.082	2.840	0.088	2.989	0.066
1 river	2.562	0.133	2.633	0.121	2.675	0.114
1 lake	2.500	0.144	2.541	0.137	2.473	0.149
1 repeated	2.600	0.127	2.632	0.121		

Table 9. Microfluidic chip measurements for arsenic samples ranging from 0.3-2 mg L^{-1}.

Conc(mg L^{-1})	Voltage 1	Voltage 2	Abs 1	Abs 2
0.3	1.723	1.720	0.007	0.008
0.7	1.096	1.109	0.204	0.198
1	0.880	0.866	0.299	0.306
2	0.220	0.302	0.902	0.764
Sample (0.5 ppm)	1.472		0.075	

Table 10. Microfluidic chip measurements for arsenic samples ranging from 0.3-2 mg L^{-1}.

Conc (mg L^{-1})	Voltage	Abs	Voltage 2	Abs2
0.3	3.625	0.018	3.512	0.031
0.7	3.250	0.065	3.320	0.056
1	3.068	0.090	3.174	0.075
2	2.453	0.187	2.693	0.147

Table 11. Comparison between concentrations calculated from calibration curves and the true concentration.

Equation	Sample	Cal conc(ppm)	Actual conc(ppm)
y = 0.0983x - 0.0084	0.5 ppm	0.513	5
	river 0.5 ppm	0.602	0.5
y = 0.0683x + 0.0089	0.5 ppm	0.520	0.5
	river 0.5 ppm	0.613	0.5

Table 12. Microfluidic chip measurements for arsenic samples ranging from 0.3-2 mg L^{-1}.

Conc (mg L^{-1})	Voltage	Abs	Voltage 2	Abs 2
0.3	3.299	0.023	3.245	0.030
0.7	2.885	0.082	2.840	0.088
1	2.690	0.112	2.563	0.133
2	2.285	0.183	2.098	0.220

Table 13. % difference of results obtained using microfluidic detection system and actual arsenic concentration in samples with various water matrices.

Equation	Sample	Calculated conc	Actual conc
y = 0.0899x + 0.01	0.5 ppm sample	0.406	0.5
	1 ppm bog lake	1.362	1
	0.5 ppm bog lake	0.474	0.5
	unknown	0.787	0.9
y = 0.109x + 0.009	0.5 ppm sample	0.344	0.5
	1 ppm bog lake	1.132	1
	0.5 ppm bog lake	0.400	0.5
	unknown	0.787	0.9

Table 14. Microfluidic chip measurements for arsenic samples ranging from 0.3-2 mg L^{-1}.

Conc(mg L^{-1})	Voltage	Abs	Voltage2	Abs 2
0.3	3.067	0.017	2.982	0.029
0.7	2.770	0.061	2.670	0.077
1	2.514	0.103	2.456	0.113
2	1.956	0.212	2.138	0.174

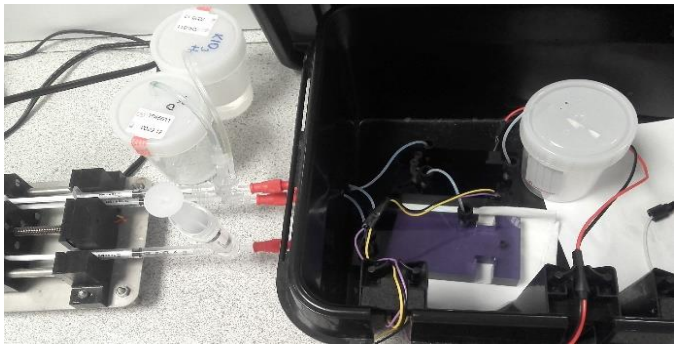

Figure 2. Microfluidic detection system using PMMA detection chips with dimensions 100×45×15 mm and 20 mm.

Figure 3. Food dyes used for microfluidic detection chips mixing assessment.

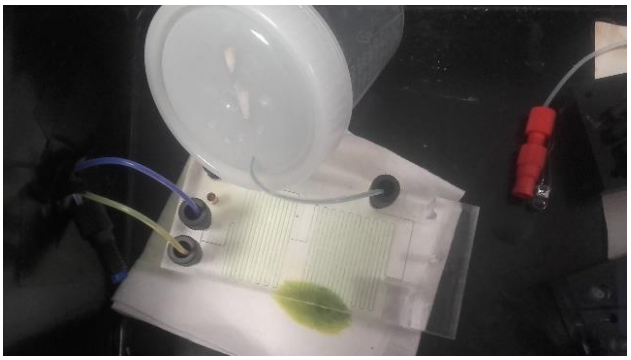

Figure 4. Assessment of mixing on microfluidic detection chip using blue and yellow food dyes.

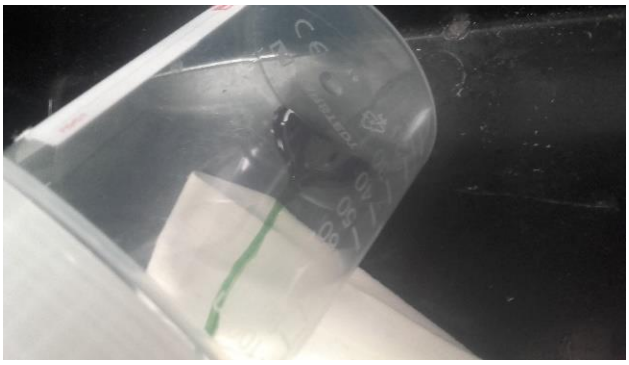

Figure 5. Waste container during mixing assessment using different coloured food dyes.

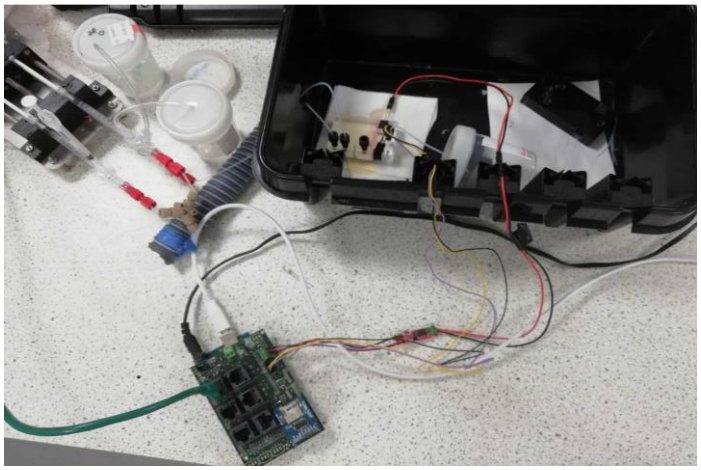

Figure 6. Microfluidic detection system set up using PMMA microfluidic detection chip with dimension 60 × 40 × 16 mm.